2016

ADVANCED MEASUREMENTS OF UNDERSAMPLED GLOBALLY SIGNIFICANT BIOMASS BURNING SOURCES

Chelsea Elizabeth Stockwell

ADVANCED MEASUREMENTS OF UNDERSAMPLED GLOBALLY SIGNIFICANT BIOMASS BURNING SOURCES

By

CHELSEA ELIZABETH STOCKWELL

B.S. Chemistry, Truman State University, Kirksville, MO, 2011

Dissertation

presented in partial fulfillment of the requirements
for the degree of

Doctorate of Philosophy
in Chemistry

The University of Montana
Missoula, MT

May 2016

Approved by:

Scott Whittenburg, Dean of The Graduate School
Graduate School

Dr. Robert Yokelson, Committee Chair
Department of Chemistry

Dr. Christopher Palmer, Committee Member
Department of Chemistry

Dr. Richard Field, Committee Member
Department of Chemistry

Dr. Michael DeGrandpre, Committee Member
Department of Chemistry

Dr. Lloyd Queen, Committee Member
Department Forest Management

Stockwell, Chelsea, PhD, Spring 2016 Chemistry

Advanced measurements of undersampled globally significant biomass burning sources

Advisor: Dr. Robert Yokelson, Department of Chemistry

During the fourth Fire Lab at Missoula Experiment (FLAME-4) laboratory campaign, we burned historically undersampled and globally significant biomass fuels. The open-path Fourier transform infrared (OP-FTIR) spectroscopy system provided new emissions data while measuring gases that overlap with fire emissions measured in numerous field campaigns. Based on the lab-field comparisons, we conclude that our lab-measured emission factors (EFs) for some of the fires can be adjusted to better represent typical open burning. In addition we deployed a high-resolution proton-transfer-reaction time-of-flight mass spectrometer (PTR-TOF-MS) to characterize biomass burning (BB) emissions for the first time. BB is the second largest global atmospheric source of gas-phase non-methane organic compounds (NMOCs) and a significant portion of the higher molecular weight species remains unidentified including intermediate and semi-volatile organic compounds (I/SVOCs). Realistic estimates of I/SVOC emissions from BB sources are vital to advance current understanding of air quality and climate impacts (particularly secondary organic aerosol and photochemical ozone production).Using several approaches we were able to assign the most probable identities to most major exact masses, including I/SVOCs. Approximately 80-96% of the total NMOC mass detected by the PTR-TOF-MS and FTIR was positively or tentatively identified compared to 30-70% in previous large-scale studies. We report data for many rarely measured or previously unmeasured emissions in several compound classes that are likely secondary organic aerosol precursors. The Nepal Ambient Monitoring and Source Testing Experiment (NAMaSTE) campaign targeted source characterization of numerous important but undersampled (and often inefficient) combustion sources that are widespread in the developing world such as brick kilns, wood and dung cooking fires, crop residue and garbage burning, generators, irrigation pumps, and motorcycles. We report the trace gas and aerosol measurements obtained by FTIR spectroscopy, whole air sampling, and photoacoustic extinctiometers based on the NAMaSTE field work. The trace gas measurements are the most comprehensive to date for these sources and the light absorption by both black and brown carbon was important for many sources. The NAMaSTE data will significantly enhance regional-global chemistry and climate modeling.

ACKNOWLEDGEMENTS

My thanks to everyone who has supported me as I pursued my doctoral degree. I am incredibly thankful to my advisor Bob Yokelson for all his time and effort throughout my studies because none of this would be possible without his support and prompt email responses. Thanks to my committee members for their supervision and guidance: Christopher Palmer, Michael DeGrandpre, Dick Field, and Lloyd Queen. I owe thanks to Ted Christian and Sheryl Akagi for their mentoring and guidance. I'd like to acknowledge all the individuals who have provided data or useful discussions throughout the course of graduate school: Patrick Veres, Lindsay Hatch, Thilina Jayarathne, Prakash Bhave, Elizabeth Stone, Peter DeCarlo, Eri Saikawa, Don Blake, Arnico Panday, Dave Griffith, Mark Cochrane, Kevin Ryan, Sonia Kreidenweis, Allen Robinson, Paul DeMott, Kip Carrico, Ryan Sullivan, Jim Reardon, and Gavin McMeeking. I am also thankful for the support on my international campaigns from individuals in the organizations of ICIMOD, MinErgy, and BOS. Thanks to all my friends near and far for their support. I thank my parents and my oma and opa for always encouraging and supporting my higher education. Of course I thank Patrick Barney for being Patrick Barney. And finally I thank Napoleon for his love, comfort, and furry demeanor through the tough times.

TABLE OF CONTENTS

LIST OF FIGURES

LIST OF TABLES

ABBREVIATION INDEX

AAE	Absorption Ångström Exponent
AE33	Aethalometer
AMS	Aerosol Mass Spectrometer
B_{abs}	Absorption coefficient
BB	Biomass Burning
BBCEAS	Broadband Cavity Enhanced Absorption Spectrometer
BBOP	Biomass Burn Observation Project
BC	Black Carbon
B_{ext}	Extinction coefficient
BrC	Brown Carbon
B_{scat}	Scattering coefficient
BTEX	Benzene, Toluene, Ethylbenzene, Xylenes
CCN	Cloud Condensation Nuclei
CCNC	Cloud Condensation Nuclei Counter
CFs	Calibration Factors
CFDC	Continuous-Flow Diffusion Chamber
CMB	Chemical Mass Balance
CMU	Canegie Mellon University
CR	Crop Residue
EC	Elemental Carbon
EFs	Emission Factors
ERs	Emission Ratios
FEP	Fluorinated Ethylene Propylene
FLAME-4	fourth Fire Lab at Missoula Experiment
FMPS	Fast Mobility Particle Sizer
FSL	Fire Sciences Laboratory
FTIR	Fourier Transform Infrared
GB	Garbage Burning
GHGs	Global Greenhouse Gases
HITRAN	HIgh-resolution TRANsmission molecular absorption database
H-TDMA	Hygroscopic Tandem Differential Mobility Analyzer

HR-TOF-AMS	High Resolution Time-of-Flight Aerosol Mass Spectrometer
IC	Ion Chromatography
IGP	Indo-Gangetic Plains
IR	InfraRed
IVE	International Vehicle Emissions
IVOCs	Intermediate-volatility organic compounds
KNP	Kruger National Park
LAAP-TOF	Laser Ablation Aerosol Particle Time-of-Flight
LA-FTIR	Land-based Fourier Transform Infrared
MAC	Mass Absorption Coefficient
MCE	Modified Combustion Efficiency
MCT	Mercury-Cadmium-Telluride
MRP	Mega Rice Project
MSW	Municipal Solid Waste
ncps	normalized counts per second
NAMaSTE	Nepal Ambient and Source Testing Experiment
NMHCs	Non-Methane Hydrocarbons
NMOCs	Non-Methane Organic Compounds
NPF	New Particle Formation
OA	Organic Aerosol
OC	Organic Carbon
OP-FTIR	Open-Path Fourier Transform Infrared
OVOCs	Oxygenated Volatile Organic Compounds
PAH	Polycyclic Aromatic Hydrocarbons
PAS	Photoacoustic Aerosol Absorption Spectrometer
PAX	Photoacoustic Extinctiometer
PILS/MOUDI	Particle-into-liquid sampler micro-orifice uniform-deposit impactor
$PM_{2.5}$	Particulate Matter with Aerodynamic Diameter < 2.5 microns
PNNL	Pacific Northwestern National Laboratories
PTR-QMS	Proton-Transfer-Reaction (Quadrupole) Mass Spectrometer
PTR-TOF-MS	Proton-Transfer-Reaction Time-of-Flight Mass Spectrometry
PVC	Polyvinyl Chloride
RCEI	Reactive Chlorine Emissions Inventory

SEAC^{4}RS	Studies of Emissions, Atmospheric Composition, Clouds and Climate Coupling by Regional Surveys
SEM	Scanning Electron Microscope
SMPS	Scanning Mobility Particle Sizers
SOA	Secondary Organic Aerosols
SP2	Single Particle Soot Photometers
SSA	Single Scattering Albedo
SVOCs	Semi-Volatile Organic Compounds
TEM	Transmission Electron Microscope
THC	Total Hydrocarbon Analyzer
USDA	U.S. Department of Agriculture
USEPA	U.S. Environmental Protection Agency
VMR	Volumetric Mixing Ratio
VOCs	Volatile Organic Compounds
WAS	Whole Air Sampling
2D-GC-TOF-MS	two-dimensional gas chromatography time-of-flight mass spectrometry

Chapter 1 : Introduction

1.1 Biomass burning impacts and background

The combustion of biomass involves the oxidation of organic fuels which can include living or dead vegetation. Biomass burning (BB) can include natural wildfires, prescribed fires, land clearing/crop turnover burns, combustion of waste (trash/tires), and/or biofuel burning (e.g. cooking fires, brick/charcoal making, etc.), all of which are considered important emission sources. Altogether, BB is the largest source of primary, fine carbonaceous particles and the second largest source of total trace gases in the global atmosphere (Bond et al., 2004, 2013; Akagi et al., 2011). Although fire is a naturally occurring process, humans have familiarized it for various purposes including land management, pest control, cooking, heating, lighting, disposal, hunting, and industrial use (Crutzen and Andreae, 1990). The continuously-growing global population contributes to increases in these anthropogenic fire practices. While the detailed chemistry of several major atmospheric sources, including temperate forest biogenic emissions (e.g. Ortega et al., 2014) and developed-world fossil-fuel based emissions (e.g. Ryerson et al., 2013), has been sampled with a wide range of instrumentation; many important emission sources remain undersampled, or rarely sampled, and traditionally ignored by large-scale comprehensive research efforts. Thus, the injection of poorly characterized, gas- and particle-phase emissions from undersampled combustion sources into the atmosphere can have critical climatic, radiative, chemical, and ecological impacts on local to global scales.

BB emits atmospherically significant trace gases, and the primary carbon-containing gases emitted in order of abundance are carbon dioxide (CO_2), carbon monoxide (CO), and methane (CH_4), which includes two major greenhouse gases. Other significant gas-phase primary emissions including nitric oxide (NO), nitrogen dioxide (NO_2) (van der A et al., 2008), and

nitrous acid (HONO) play important roles in the oxidative state of the atmosphere by contributing to both sources and sinks of the hydroxyl radical (OH), a primary atmospheric oxidant (Thompson, 1992). BB is also the largest source of fine particles in our atmosphere and the primary emissions and secondary formation of organic aerosols can affect air quality and also climate directly through scattering and absorption of radiation (Reid et al., 2005a,b) or indirectly by changing the microphysical structure of clouds (Rosenfeld, 1999; Grell et al., 2011).

While BB emissions are recognized as the second largest global atmospheric source of gas-phase non-methane organic compounds (NMOCs) behind biogenic emissions, there remains a significant portion of the higher molecular weight species classified as unidentified (Christian et al., 2003; Warneke et al., 2011; Yokelson et al., 2013a). These NMOCs particularly impact smoke evolution by rapid formation of secondary organic aerosols (SOA) and secondary gases including photochemical ozone (O_3) (Reid et al., 1998; Trentmann et al., 2005; Alvarado and Prinn, 2009; Yokelson et al., 2009; Vakkari et al., 2014). Thus, it is widely accepted that the addition of large amounts of these highly reactive species into the atmosphere alters chemistry on local to global scales (Andreae and Merlet, 2001; Andreae et al., 2001; Karl et al., 2007). The many unknowns and initial variability of gas-phase BB emissions limit our ability to accurately model the atmospheric impacts of fire at all scales (Trentmann et al., 2005; Mason et al., 2006; Alvarado and Prinn, 2009; Alvarado et al., 2009; Wiedinmyer et al., 2011). Estimating or modeling the potential of smoke photochemistry to generate secondary aerosols or O_3 requires realistic estimates of NMOC emissions in fresh smoke and knowledge of the chemical processing environment. Measurements capable of identifying and quantifying rarely measured and presently unidentified emissions of NMOCs, in particular the chemically complex low-volatility fraction, are vital to advance current understanding of the BB impacts on air quality

and climate. Further, the characterization of the smoke emissions (both gases and particles) that result from fires burning a wide range of globally significant and historically undersampled fuels is essential to model the initial impact and evolution of the emissions and their influence on local to global atmospheric chemistry.

1.2 Motivation and goals

The overarching goal of this dissertation is to burn both historically undersampled and well-studied fuels while adding new instrumentation and experimental methods to provide previously unavailable information on smoke composition, properties, and evolution. A critical objective of our laboratory campaign was to acquire this new information under conditions where the lab results can be confidently used to better understand real-world fires.

Another major goal focuses on the identification and quantification of highly reactive NMOCs in order to: (1) better characterize the overall chemical and physical properties of fresh BB emissions, (2) better understand the distribution of emitted carbon across a range of volatilities in fresh smoke, and (3) improve the capability of current photochemical models to simulate the climatic, radiative, chemical, and ecological impacts of smoke on local to global scales.

Although emissions characterization in a laboratory offers several advantages, it is important to go into the real-world and measure authentic combustion emissions. South Asia is a major pollution generating region that remains rarely sampled. The poorly characterized emission sources in South Asia include many diverse and loosely-regulated combustion sources that are greatly undersampled relative to their proportion of global emissions (Akagi et al., 2011). The field component of this dissertation was a highly collaborative effort with several goals: (1) to measure the first detailed trace gas chemistry and aerosol optical properties for many

undersampled BB sources and other combustion sources in developing countries (2) using the new data to expand and update emissions inventories (3) support a source apportionment for Kathmandu Nepal and, in turn, inform mitigation strategies, and (4) enhance regional air quality and climate modeling.

1.3 Outline of thesis

Section 1.4 provides a brief synopsis of how atmospheric processes are influenced by BB emissions and then a brief review of the literature regarding gaseous and particulate emissions from BB sources, their post-emission evolution, and the major atmospheric implications.

Chapter 2 contains background information on common BB terms and common calculations used to quantify BB emissions including emission ratios (ERs), emission factors (EFs), and modified combustion efficiency (MCE).

Chapter 3 introduces and provides a brief overview of the fourth Fire Lab at Missoula Experiment (FLAME-4) that took place from October to November 2012 at the Missoula Fire Science Laboratory. This chapter details the laboratory configurations utilized during two stages of the campaign, the fuels burned, and the suite of instrumentation deployed.

In Chapter 4 I focus on the detailed description of the trace gas measurements by the open-path Fourier transform infrared (OP-FTIR) spectrometer. I present the major findings by OP-FTIR and compare lab and field data to inform the use of emissions data from the OP-FTIR and the extensive suit of other instruments deployed during the FLAME-4 burns.

In Chapter 5 I focus on the detailed description of NMOC measurements by proton-transfer-reaction time-of-flight mass spectrometry (PTR-TOF-MS). I describe the first deployment of this technology in well-mixed laboratory smoke and present the first detailed NMOC characterization of gases emitted by BB sources during the FLAME-4 campaign.

Chapter 6 presents a brief overview of the The Nepal Air Monitoring and Source Testing Experiment (NAMaSTE) campaign (site descriptions, source types, instrumentation) that took place in April 2015. I then focus on the detailed description of trace gases measured using a mobile Fourier transform infrared (FTIR) system, whole air sampling (WAS) collection and optical properties measured by two photoacoustic extinctiometers (PAX). I present the major findings for the source characterization of numerous important but undersampled combustion sources that are widespread in the developing world such as cooking with a variety of stoves and solid fuels, brick kilns, open burning of garbage, crop-residue burning, generators, irrigation pumps, and motorcycles.

1.4 Literature review

1.4.1 Atmospheric processes and gaseous biomass burning emissions

The absorption of solar radiation by molecules drives many important chemical reactions in the atmosphere. The absorbing molecules become electronically excited and can subsequently dissociate or react directly with other molecules to form more stable species or free radicals that drive several important atmospheric oxidation cycles that substantially influence the composition of the atmosphere. Ultimately photochemical reactions can yield trace gases and aerosols that influence visibility, climate, and air quality. The atmospheric lifetimes of species emitted by BB can vary greatly (seconds to years), thus only those compounds that are stable and abundant can be measured readily.

As an example of how BB pollutants are processed in the atmosphere, I'll briefly explain the main oxidation pathway of two major fire emissions, carbon monoxide and nitric oxide. The most common fate of CO in the atmosphere is oxidation by a hydroxyl radical (OH), which consists of OH-addition followed by decomposition to carbon dioxide and an H atom. Since the

atmosphere is ~20% oxygen, O_2 readily recombines with H to generate a highly reactive peroxyradical (HO_2). HO_2 will then react with the co-emitted NO and convert it to nitrogen dioxide while regenerating OH (the primary atmospheric oxidant). NO_2 can then photolyze yielding an oxygen atom that will ultimately yield ozone. This is a catalytic cycle that oxidizes a major fire pollutant, CO, to form O_3. Several termination steps are possible including nitric acid formation (HNO_3) by NO_2 oxidation. HNO_3 then reacts with BB-emitted ammonia (NH_3) to make solid ammonium nitrate. Alternatively, oxidation products or oxygenated species directly emitted by BB -each with its own pathway and branching pattern- can yield products of new gases including peroxyacyl nitrate (PAN) and O_3. The atmospheric processing of BB emissions is clearly a highly dynamic process that is heavily dependent on the initial mix of emissions and the subsequent processing environment.

Current source estimates for highly reactive non-methane organic compounds indicate that BB is well ahead of urban emissions and closely behind biogenic emissions as the major atmospheric contributor (Yokelson et al., 2008; Akagi et al., 2011). NMOCs have critical impacts on smoke evolution, particularly by rapid formation of secondary organic aerosols (SOA) and photochemical ozone in the presence of NO_x (Reid et al., 1998; Trentmann et al., 2005; Alvarado and Prinn, 2009; Yokelson et al., 2009; Vakkari et al., 2014). For major fire-types characterized by most available instrumentation the initial amount, evolution, and identity of ~30-70% of the mass of gas-phase NMOCs is attributed to unidentifiable species (Yokelson et al., 2013a). This major knowledge gap leads to large uncertainties in the modeled predictions of the evolution and/or atmospheric burden of these highly reactive species by both bottom-up and top-down approaches (described in Sect. 2.2).

A large portion of the unidentified NMOCs (35-64%; Yokelson et al., 2013a) are likely higher molecular weight semi-volatile organic compounds (SVOCs) that can be oxidized in the atmosphere to form smaller, more volatile organic compounds (VOCs) via a process sometimes referred to as "fragmentation" (involving carbon-carbon bond cleavage) (Chacon-Madrid and Donahue, 2011). Formic and acetic acids are important secondary products of smoke photochemistry and can be a major carbon-reservoir in plumes. Although secondary formation can be highly variable, Yokelson et al. (2003a) observed the ratio of acetic acid (CH_3COOH) to CO to grow up to 9% in under an hour in an African smoke plume (Timbavati, Figure 1.1). Often there is greater production of these secondary products than can be explained by the "known" precursors. Additionally, the oxidation of NMOCs in the presence of NO_x can lead to variable O_3 formation rates (Hobbs et al., 2003; Yokelson et al., 2003a; Pfister et al., 2006; 2008; Akgai et al., 2013a; Figure 1.2) or rapid formation of peroxyacetyl nitrate, a major NO_x reservoir (Akagi et al., 2012). Ozone production can affect air quality and is especially important in the tropics, where BB can be the predominant source of ozone precursors (Andreae and Merlet, 2001). At present, models are unable to replicate observed O_3 formation in BB plumes based on known gas-phase NMOCs; however, by assuming more initial SVOCs the models better simulate this rapid formation (Trentmann et al., 2005; Mason et al., 2006; Alvarado and Prinn. 2009; Alvarado et al., 2009).

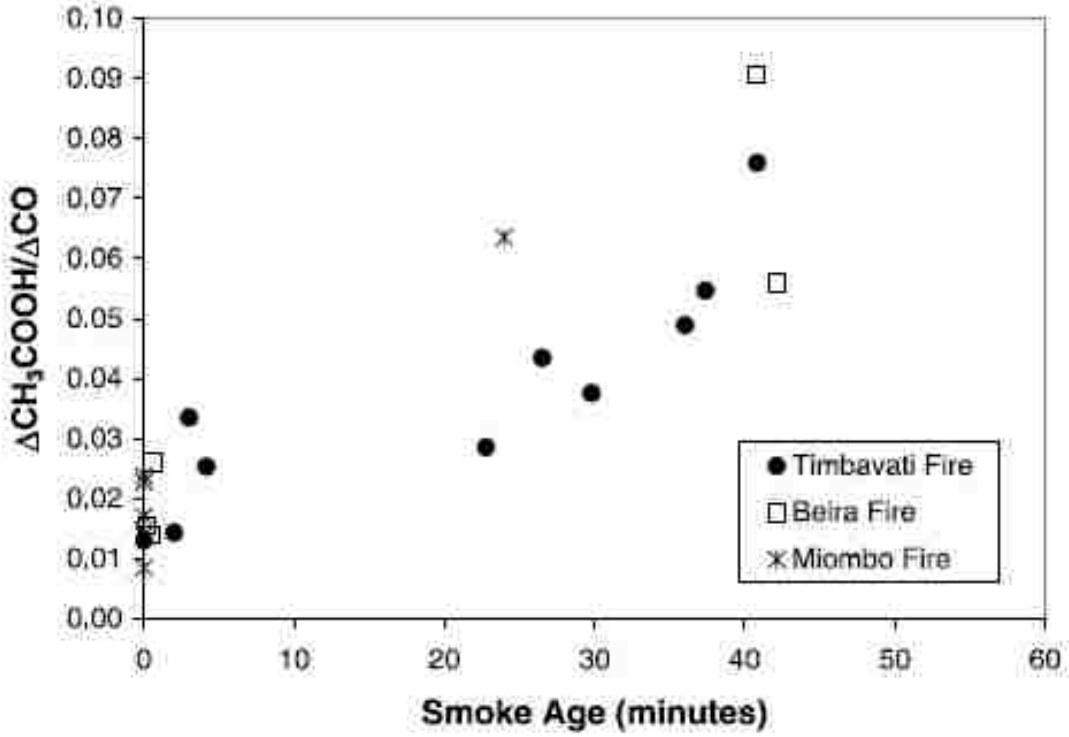

Figure 1.1.The increasing of ratios of excess acetic acid to excess CO as a function of smoke age. Figure taken from Yokelson et al. (2003a) Figure 5.

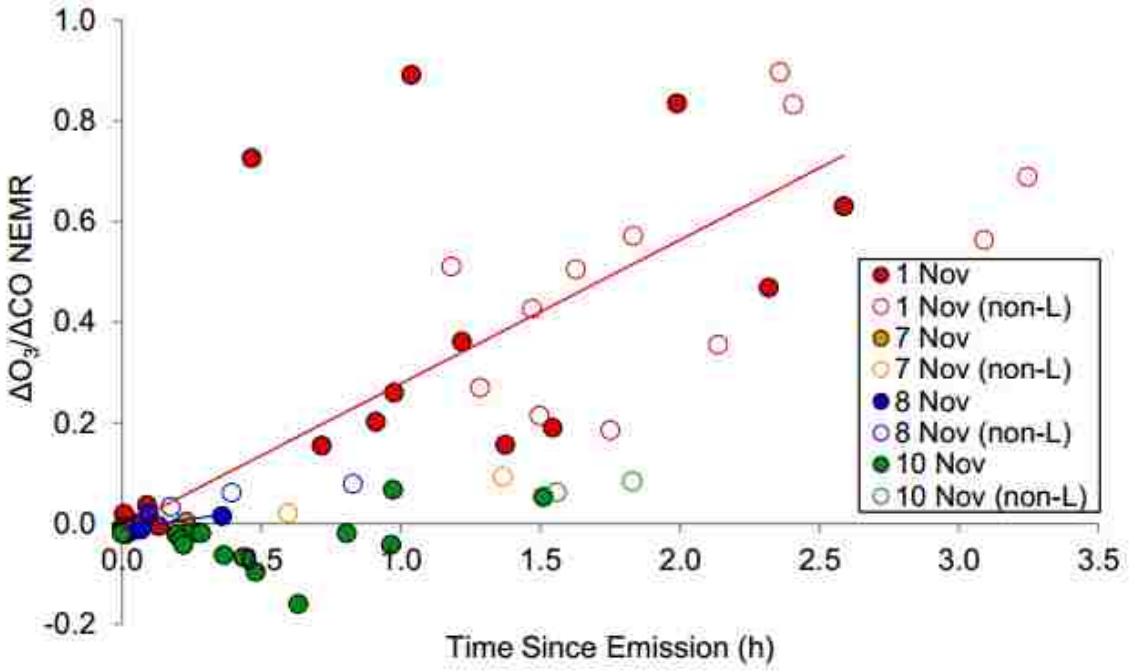

Figure 1.2. The variable formation rate of O_3 illustrated by showing the excess mixing ratio of ozone normalized to that of non-reactive CO to account for dilution and plotted versus time since emission. Figure taken from Akagi et al. (2013) Figure 12.

Conversely, primary SVOCs can be oxidized to form larger molecules with lower vapor pressures that can condense into the aerosol phase, thus contributing to organic aerosol growth by "functionalization" (addition of functional groups with no change in carbon number) (Chacon-Madrid and Donahue, 2011). As an example, the organic aerosol (OA) to CO ratio has been shown to increase by a factor of 2-4 in field smoke-plume studies and chamber simulations (Yokelson et al., 2009; Grieshop et al., 2009). It is not clear what variables control these outcomes (Yokelson et al., 2009; Grieshop et al., 2009; Capes et al., 2009; Cubison et al., 2011), yet these processes significantly influence atmospheric composition. The ratio of ΔOA/ΔCO on a short timescale is shown in Figure 1.3 for a number of studies including BB sources and fossil fuel emissions (DeCarlo et al., 2010). Recent modeling suggests heterogeneous chemistry and

unidentified organic species may also contribute to the rapid formation of O_3 and SOA in young smoke plumes where previously underestimated (Trentmann et al., 2005; Mason et al., 2006; Alvarado and Prinn, 2009; Alvarado et al., 2009).

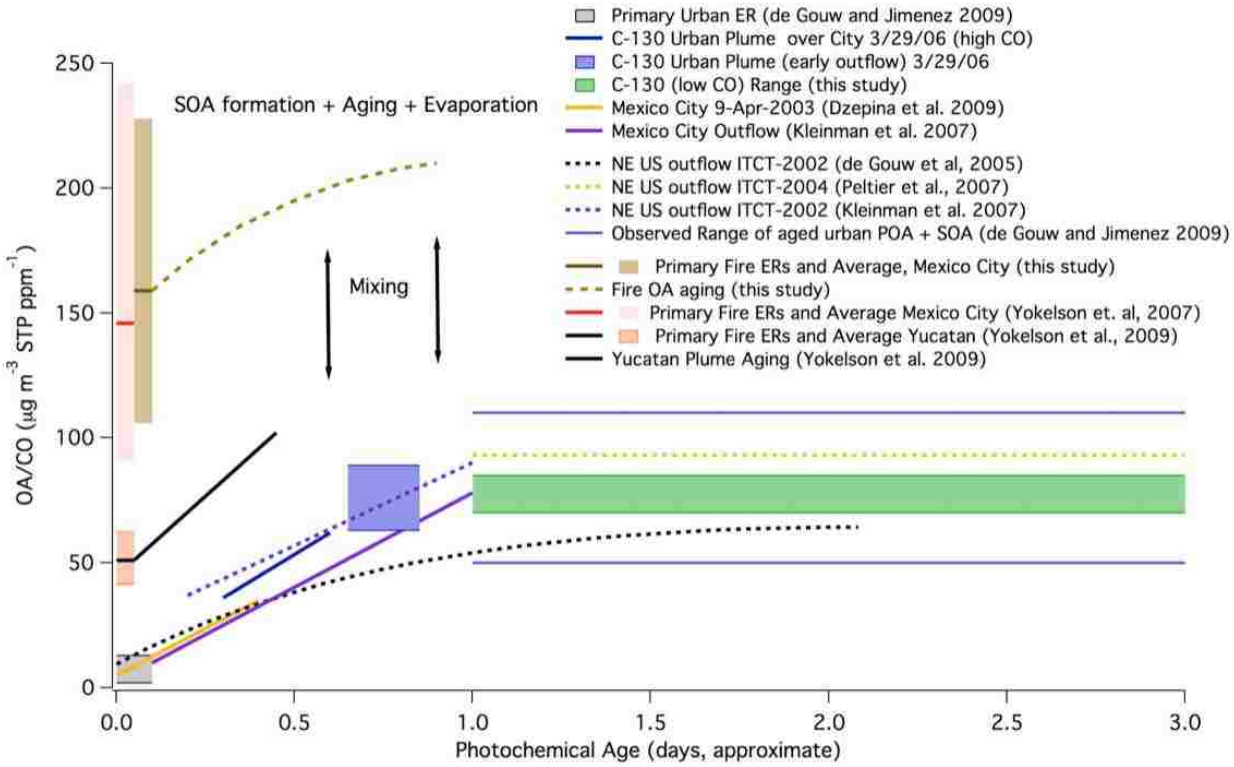

Figure 1.3. The ΔOA to ΔCO ratios for multiple field measurements including fossil fuel and biomass burning emissions. The ΔOA/ΔCO ratios were larger for biomass burning emissions but were highly variable. Figure taken from DeCarlo et al. (2010) Figure 3.

1.4.2 Light absorption and scattering by aerosols

Biomass burning is the largest source of primary, fine (i.e. sub-micron diameter) carbonaceous particles (Crutzen and Andreae, 1990; Bond et al., 2004; 2013), though an amount of fine particles similar to BB initial emissions may also form via secondary processes, including gas to particle conversion as discussed above. Atmospheric aerosols can be both anthropogenic and natural and they have critical impacts on air quality, health, and climate. The radiative effects of these particles depend on their size and optical properties, which are in turn linked to chemical

composition. Global estimates of the direct radiative forcing due to BB aerosol vary significantly (ranging from net warming to net cooling) depending on the assumptions about the aerosol optical properties (Reid et al., 2005a). Thus the optical properties of BB aerosols need to be better constrained to correctly model the climate forcing from BB events. Generally, aerosols can affect climate directly by scattering and absorption of solar radiation (Bond and Bergstrom, 2006) in the atmosphere and by influencing surface albedo; or indirectly by affecting cloud microphysical properties (optical properties, precipitation behavior, cloud droplet size, albedo etc.) (Hobbs and Radke, 1969; Crutzen and Andreae, 1990).

The composition of BB particles varies greatly but generally consists of a mixture of black carbon (pure "soot"), organic compounds, salts, and trace elements including metals (Reid et al., 2005a). Black carbon (BC) is formed by the incomplete combustion of carbon-containing fuels and is a primary component of particulate matter (Moosmüller et al., 2009). BC can make up a large fraction of primary aerosols emitted by BB and strongly absorbs solar radiation over a broad range of wavelengths (Bond and Bergstrom, 2006) making it the second most important warming agent in the atmosphere after CO_2 (Bond et al., 2013). BC mass concentrations in the atmosphere are dependent on emissions, aging, transport, and removal processes and the optical properties depend on size, morphology, refractive indices, and mixing state (Levoni et al., 1997). After emission, BC can be coated by various substances due to processes such as condensation or collisions with other particles (a.k.a coagulation) (Liu et al., 2013). The coating alters what is known as the internal mixing state. The coating can enhance absorption (Bond and Bergstrom, 2006) if non-absorbing material refracts light toward the BC "core" (Toon and Ackerman, 1981). However, if the coating material is soluble, the removal rate from the atmosphere is enhanced. Generally, the atmospheric removal of BC occurs over several days to weeks by both

precipitation (wet deposition) and dry deposition onto surfaces. Fast mixing effects have been observed in a fresh plume <1 hr (Akagi et al., 2012), and therefore it is also important to include co-emitted species (soluble organics, sulfates, aerosol precursors, NO_x) in order to assess BC effects, which could vary dramatically by source (Akagi et al., 2012; Lack and Corbett, 2012). These enhanced absorptions may contribute to underestimates in BC burdens by factors of 1.75-4 in Africa, South Asia, Southeast Asia, Latin America, and the Pacific region (Bond et al., 2013).

BB aerosol also has a high content of organic matter with the carbon portion of that matter known as organic carbon (OC). OC was traditionally considered a scattering-only aerosol (Chung et al., 2012), and because OC/BC ratios in BB aerosol are often in the range 3-10, the net direct effect of BB aerosol was estimated to be cooling. However, more recent studies indicate a fraction of BB-OC can absorb light in the UV range and is now referred to as brown carbon (BrC) for its brownish/yellowish appearance (Kirchstetter et al., 2004; Andreae and Gelencser, 2006; Chen and Bond, 2010). BB is the main global source of BrC, but BrC has widely varying optical properties and poorly constrained emission sources. Thus, a better representation of BrC in emissions inventories and more measurements of its optical properties (and lifetime) are critically needed in climate models.

Open (landscape scale) BB generates ~40% of the global emissions of sub-micron BC aerosol and ~65% of primary sub-micron OC (Bond et al., 2013). The combination of open BB and industrial and domestic consumption of biofuel accounts for an even larger fraction of global BC and OC emissions, but this is poorly constrained with much of the biofuel emissions occurring in little studied regions of Asia and Africa (Akagi et al., 2011). There is limited data concerning the amount of biofuel and biomass combusted and the technology involved in these processes (e.g. amount of fuel consumed, cookstove efficiency) as well as the optical properties of OC emitted

by these combustion sources (Kirchstetter et al., 2004; Hecobian et al., 2010; Chen and Bond, 2010; Arola et al., 2011).

In summary, the role of BC and OC (particularly BrC) must be better assessed in order to mitigate climate effects by controlling anthropogenic output (biofuel consumption for heating/cooking, industrial processes, diesel engines, etc.). For mitigation strategies it is important to assess radiative forcing due to the individual effects of specific emission sectors.

Aerosol optical properties can be described by several parameters. Firstly, scattering and absorption coefficients are necessary to model radiative transfer (Clarke et al., 1987). A scattering coefficient is a measure of efficiency of the scattering of light by particles, while an absorption coefficient is a measure of photons absorbed (both per unit distance of the light path). The aerosol extinction coefficient (B_{ext}) is the sum of scattering (B_{scat}) and absorption (B_{abs}) coefficients ($B_{ext} = B_{scat} + B_{abs}$). The single scattering albedo (SSA) is the ratio of the scattering coefficient to total extinction:

$$SSA = \frac{B_{scat}}{B_{ext}} \quad (1)$$

where a value of 1 implies all extinction is due to scattering. Generally an SSA below ~0.9 contributes net warming (Praveen et al., 2012). Light-absorbing aerosols including BC and BrC have wavelength-dependent absorptions (Andreae and Gelenscer, 2006), where BrC absorption is more significant at shorter wavelengths (blue to UV-range). The absorption Ångström exponent (AAE) is a parameter describing the empirical relationship between light absorbed at different wavelengths and is defined as:

$$AAE(\lambda_1\lambda_2) = -\frac{\log\left(B_{abs,\lambda_1} / B_{abs,\lambda_2}\right)}{\log\left(\lambda_1 / \lambda_2\right)} \quad (2)$$

where a pure black carbon AAE value of 1 is commonly assumed as a community standard (Lack and Langridge, 2013) and an AAE value greater than 1.6 is often considered a threshold for significant amounts of brown carbon (Lack and Cappa, 2010). Even larger AAE values have been observed for some BB aerosol (i.e. 2-10) and indicate increasingly significant absorption that would be missed by traditional measurements of BC only.

Chapter 2 : Biomass burning measurements

2.1 Emission ratios, emission factors, and modified combustion efficiency

Emission ratios (ERs) are calculated for gas-phase species and can be taken as the mixing ratio above background of species X relative to a relatively non-reactive, co-emitted reference species, most commonly CO or CO_2. In fresh smoke, molar emission ratios to CO ($\Delta X/\Delta CO$) can be calculated for gases and aerosols and are used to derive emission factors (EFs) in units of grams of species X emitted per kilogram of dry biomass burned by the carbon mass balance method (CMB), which assumes all of the burned carbon is volatilized and that all of the major carbon-containing species have been measured (Ward and Radke, 1993; Yokelson et al., 1996, 1999; Burling et al., 2010):

$$EF(X)\left(g\,kg^{-1}\right) = F_C \times 1000 \times \frac{MM_x}{AM_C} \times \frac{\frac{\Delta X}{\Delta CO}}{\sum_{j=1}^{n}\left(NC_j \times \frac{\Delta C_j}{\Delta CO}\right)} \quad (3)$$

where F_C is the measured carbon mass fraction of the fuel; MM_x is the molar mass of species X; AM_C is the atomic mass of carbon (12 g mol-1); NC_j is the number of carbon atoms in species j; ΔC_j or ΔX referenced to ΔCO are the fire-average molar emission ratios for the respective species. The denominator of the last term in Eq. (3) estimates total carbon.

Emissions from fires are highly variable due in part to the naturally changing combustion processes; chiefly flaming and smoldering, which depend on many factors such as fuel geometry, moisture and environmental variables (Bertschi et al., 2003b; Yokelson et al., 2011). Combustion efficiency, or the fraction of fuel carbon converted to carbon as CO_2, is highly variable and can change from point to point during a fire. Flaming combustion involves the reaction of O_2 with gas and results in oxidized forms of C, H, N and S while generating black carbon particles. Smoldering combustion consists of pyrolysis and gasification where pyrolysis is the thermal breakdown of solids into gases and gasification (glowing) is surface oxidation. To estimate the relative amount of smoldering and flaming combustion that occurs over the course of a fire, the modified combustion efficiency (MCE) for each fire is calculated by (Yokelson et al., 1996):

$$MCE = \frac{\Delta CO_2}{\Delta CO_2 + \Delta CO} = \frac{1}{\left(1 + \left(\frac{\Delta CO}{\Delta CO_2}\right)\right)} \quad (4)$$

Though flaming and smoldering combustion often occur simultaneously, a higher MCE value designates relatively more flaming combustion (more complete oxidation) and lower MCE designates more smoldering combustion. “Pure” flaming combustion has an MCE of ~0.99 while pure smoldering typically has an MCE of ~0.8 (usual range 0.75-0.84). Thus, for example, an MCE of ~0.9 represents roughly equal amounts of flaming and smoldering. MCE can also be

calculated for any point, or group of points, of special interest during a fire or as a time series (Yokelson et al., 1996).

The emissions of individual gas- and condensed-phase species fluctuate widely depending on a myriad of interactive factors including fuel properties (elemental content, degree of decomposition, seasonal chemistry, moisture, size, loading); external environmental parameters (wind speed, temperature, relative humidity, dilution); and the relative contribution of the before-mentioned combustion processes (Yokelson et al., 1996, 2011; Andreae and Merlet, 2001; Keene et al., 2006). Many of these factors influencing emissions are extremely heterogeneous both temporally and spatially in the natural environment, they can be modified by the fire itself, and they are rarely measured.

2.2 Emission inventories

Several approaches are viable to estimate the amount of material BB sources inject into the atmosphere. Bottom-up modeling of the local to global atmosphere requires emissions inventories that incorporate measurements of the amount of a trace gas or aerosol species emitted per unit fuel consumption (EFs). The mass of fuel burned at various scales (a.k.a "activity data") is multiplied by EFs to generate estimates of initial emissions, which can then be transported and aged in models to estimate impacts. Sampling the smoke before most of the photochemical processing occurs is important as these are the initial values included in existing models. As mentioned earlier, the identity of approximately 30-70% of initially emitted NMOC mass is unknown (Yokelson et al., 2013a). This major knowledge gap introduces large uncertainty into bottom-up modeling approaches, and this uncertainty is magnified as it propagates through the modeled predictions.

Top-down modeling uses known EFs to constrain total fuel consumption at various geographic scales. The top-down emission estimates are inferred from the amount required to reproduce the observed loading. While top-down approaches typically start with a limited number of species measured by satellite or other global networks, they rely heavily on traditional smoke characterization to estimate other important smoke constituents. Further, they need a-priori estimates, which are generally the bottom-up inventory.

Constructing comprehensive inventories for models requires emissions data for a variety of important fuel (ecosystem) types (Randerson et al., 2005; van der Werf et al., 2010; Akagi et al., 2011; Wiedinmyer et al., 2011). The complete characterization of the smoke emissions that result from fires burning a wide range of globally significant fuels is ideal to model the initial impact and evolution of the emissions and their influence on local to global atmospheric chemistry. Fire-type specific EFs are also important to any projection of how changes in BB (land-use changes, global warming, etc.) can impact atmospheric chemistry and climate. Thus, progress in global atmospheric science is partially dependent upon investigation of undersampled fire types and the development and deployment of improved technologies that can better characterize initial emissions and subsequent evolution of NMOCs.

2.3 Sampling considerations: ground, airborne, laboratory

Many different approaches are useful for characterizing initial BB emissions and subsequent aging. Field studies based on airborne or ground-based platforms characterize authentic fires burning in the complex, natural environment.However, much of the smoke routinely goes un-sampled, which could cause emissions to be over- or under-estimated (Yokelson et al., 2008). Airborne platforms are ideal for representative sampling of most open fires and smoke aging, while ground-based sampling can characterize initially un-lofted smoke produced by residual

smoldering combustion, which is important during some fires (e.g. smoldering peat) (Bertschi et al., 2003a, 2003b; Akagi et al., 2012, 2013, 2014; Yokelson et al., 2013a). More specifically, airborne platforms are ideal for measuring the emissions in well-mixed, lofted plumes and may provide insight into post-emission plume evolution (Akagi et al., 2012, 2013; Yokelson et al., 2013b); however, the contribution of un-lofted smoke over the course of the fire is sometimes uncertain (Akagi et al., 2014). Uncertainty can also arise during ground-based sampling when smoke is aggressively lofted or as unpredictable spread rates limit sampling accessibility. Notably for this work, ground-based sampling is the only practical option for characterizing most domestic and industrial biofuel use. A third approach, burning biomass fuels in a laboratory has also been a useful way to characterize BB smoke (Yokelson et al., 1996, 2008, 2013a; Goode et al., 1999; Christian et al., 2003; McMeeking et al., 2009; Petters et al., 2009; Levin et al., 2010). Benefits typically include better fuel characterization, the opportunity to sample all the smoke from a fire, and quantification of more species/properties due to a more extensive suite of instrumentation.

While laboratory-based measurements lead to highly accurate emissions characterization in general, it should be recognized that laboratory fires can sometimes differ from the fires that actually impact the atmosphere on a large scale. In particular, laboratory fires sometimes burn with higher MCE (higher flaming/smoldering) than observed in the field but have similar ERs of species co-emitted during related combustion processes while also exhibiting a similar EF dependence on MCE as is observed in the field (Christian et al., 2003; Yokelson et al., 2013a). In general, lab and field data should be compared (as will be discussed in Chapter 4) and the comparison can inform the use of laboratory data. While laboratory measurements offer many

advantages, it is important for researchers to go into the real-world and measure authentic BB emissions.

Chapter 3 : The fourth Fire Lab at Missoula Experiment (FLAME-4)

3.1 FLAME-4 introduction

During the fourth Fire Lab at Missoula Experiment (October-November 2012), a large variety of regionally and globally significant biomass fuels was burned at the US Forest Service Fire Sciences Laboratory in Missoula, Montana. Over 40 scientists were involved to better characterize particulate and gaseous emissions using an extensive suite of instrumentation. The primary goal of the campaign involved burning historically undersampled fuels alongside more traditionally studied fuels to get more detailed information on smoke composition, properties, and evolution. This large-scale laboratory experiment to better characterize the initial properties of gas- and particle-phase emissions was performed under conditions where the lab results could be confidently used to better understand real-world fires. Thus, during FLAME-4, advanced lab measurements were combined with a lab-field comparison to enhance our understanding of important aspects of BB including: (1) the effect of fuel type and fuel chemistry on the initial emissions; (2) the distribution of the emitted carbon among pools of various volatility in fresh and aged smoke with special attention to the large pool of unidentified semi-volatile organic gases identified in previous work (Yokelson et al., 2013a); and (3) the factors influencing the evolution of smoke's chemical, physical, and cloud-nucleating properties. This chapter provides a brief overview of the FLAME-4 experiment (configurations used, fuels burned, and instruments deployed).

3.2 FLAME-4 configurations

3.2.1 US Forest Service Fire Sciences Laboratory

The US Forest Service Fire Sciences Laboratory (FSL) in Missoula, Montana houses a large indoor combustion room described in greater detail elsewhere (Christian et al., 2003; Burling et al., 2010). The room is 12.5 m × 12.5 m × 22 m high with a 1.6 m diameter exhaust stack joined to a 3.6 m diameter inverted funnel opening ~2 m above a continuously weighed fuel bed (Figure 3.1). The room is slightly pressurized with conditioned, outdoor air to generate a large flow that entrains the fire emissions and vents them up through the stack. A sampling platform surrounding the stack stands 17 m above the fuel bed where emissions are drawn into sampling lines fixed to the stack. The room temperature and relative humidity were documented for each burn.

A set of twin smog chambers was deployed by Carnegie Mellon University (CMU) on the combustion room floor to investigate smoke aging with a focus on atmospheric processes leading to O_3 and SOA formation. The chambers consisted of fluorinated ethylene propylene (FEP) Teflon bags with UV lights affixed to the walls to initiate photochemical aging (Hennigan et al., 2011). Fresh BB smoke was drawn from the platform height in heated passivated sampling lines and introduced into the chambers after dilution to typical ambient levels using Dekati injectors. The smoke was then monitored for up to 8 hours by a large suite of instruments to examine initial and photochemically processed gas and aerosol concentrations and composition. The monitoring instruments included those in the CMU mobile lab, which was deployed just outside the building. We used the open-path Fourier transform infrared (OP-FTIR) spectrometer to measure the pre-dilution smoke that filled the chambers, but we did not monitor the subsequently-diluted chamber contents via FTIR.

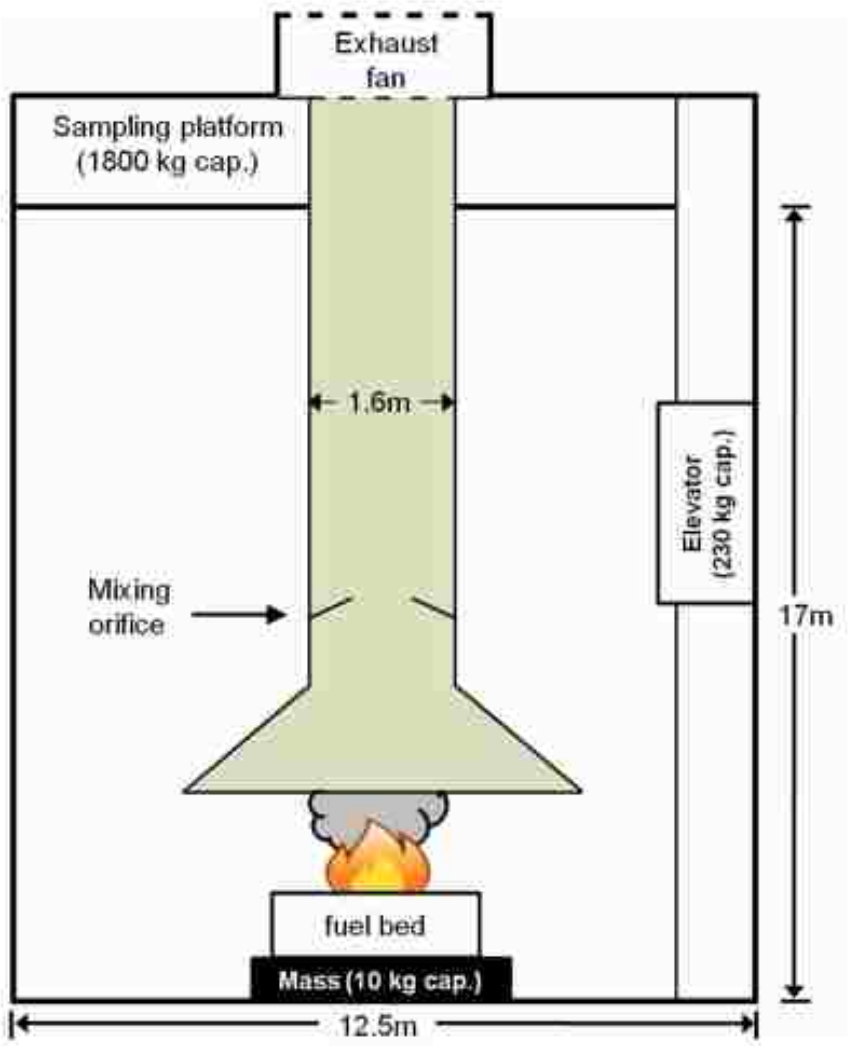

Figure 3.1. Schematic of combustion chamber at the Missoula Fire Sciences Laboratory. Taken from Burling et al. (2010) Figure 1.

3.2.2 Stack burn configuration

Experiments were conducted using two primary laboratory configurations. In the first configuration (hereafter "stack" burns), most of the instrumentation was stationed on the platform at 17 m while the remaining instruments were located in adjacent rooms with sampling lines pulling from ports at the sampling platform height. The stack burn fires lasting ~2-30 min were situated on a fuel bed located directly below the combustion stack described above.

Emissions traveled upward through the stack at a constant flow rate while the instruments sampled continuously at the platform height. The smoke was well mixed and had aged approximately 5 s by the time it reached the sampling height. Previous studies found that the temperature and mixing ratios are constant across the width of the stack at the platform height, confirming well-mixed emissions that can be monitored representatively by many different sample lines throughout the fire (Christian et al., 2004).

3.2.3 Room burn configuration

In the second configuration, referred to hereafter as "room" burns, much of the instrumentation was relocated to other rooms immediately adjacent to the combustion room and air samples were drawn from lines projecting well into the combustion room. The combustion room was sealed and the fuels burned for several minutes. Within ~15-20 minutes the fresh smoke was well-mixed throughout the entire combustion room and was monitored while being "stored" in low-light conditions for several hours. O_3 and PAN remained below the sub-ppbv detection limits of the OP-FTIR during this storage period. Smoke emissions from room burns were also diluted into the smog chambers shortly after they became well mixed for further perturbation and analysis. These room burns were conducted primarily to allow more time-consuming analyses of the optical and ice-nucleating properties of smoke, which is described in greater detail elsewhere (Levin et al., 2014). Figure 3.2 shows temporal profiles for CO and CO_2 excess mixing ratios during each configuration of the experiment and during distinct fuel-specific burns.

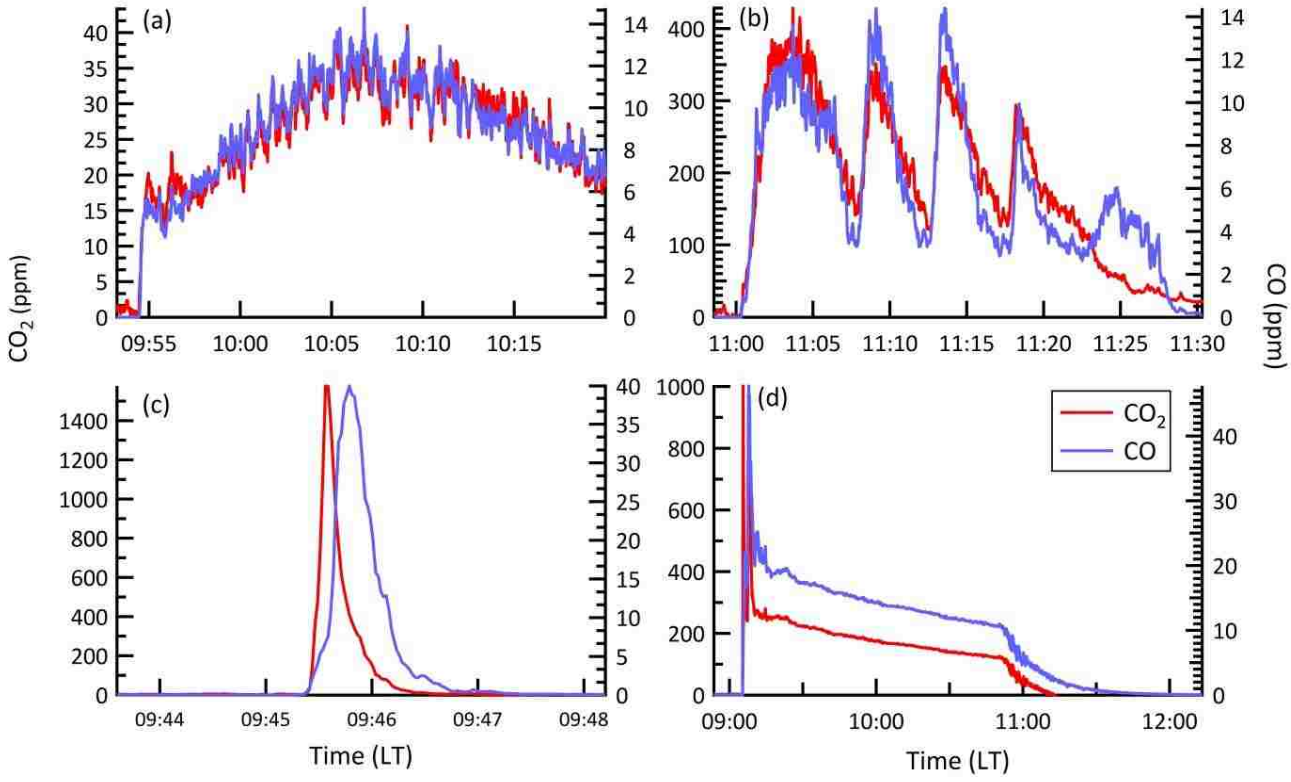

Figure 3.2. Excess mixing ratios of CO and CO2 versus time for a (a) typical peat "stack" burn, (b) open cookstove "stack" burn (feeding fire), (c) grass "stack" burn, and (d) "room" burn.

3.3 Fuels overview

This section summarizes the significance and authenticity of the fuels burned during FLAME-4. Selected properties are presented in Table 3.1, which includes the sampling location and dry weight percentage of carbon, nitrogen, and ash measured using a commercial CHN analyzer. Fuel chlorine and/or sulfur content are shown for selected fuels (Midwest Microlab LLC; ALS Environmental). Fuel loadings varied by fuel but were chosen to simulate real-world values, typically in the range of 0.1-5 kg m^{-2} (Akagi et al., 2011). Global estimates of biomass consumption for several major fuel types investigated here are shown in Table 4 of Akagi et al. (2011). The fuels were primarily ignited with electric resistively heated coils, but for cooking

fires and occasionally other fires, a propane or butane torch was used and small amounts of alcohol were sometimes required.

Table 3.1. Summary of fuels burned and fuel elemental analysis

Fuel	Stack Exp.	Room Exp.	Environmental Chamber Exp.	Fuel Type	Sampling Location (s)	C-Content (%)	N-Content (%)	Cl / S-Content (%)	Ash
African grass (tall)	11	1	0	Savanna/Sourveld/Tall grass	Kruger National Park, R.S.A.	43.56 - 43.82	0.21 - 0.32	bdl / 0.063	4.7
African grass (short)	8	0	0	Savanna/Sweetveld/Short grass	Kruger National Park, R.S.A.	43.56 - 44.56	0.47 - 0.70	0.19 / 0.21	3.5 - 5.4
Giant Cutgrass	5	3	2	Marsh	Jasper Co., SC	44.84	2.03	0.34 / 0.21	2.3
Sawgrass	12	1	0	Marsh	Jasper Co., SC	45.83	0.93	0.77 / 0.16	3.5
Wiregrass	7	2	1	Pine forest understory	Chesterfield Co., SC	46.70	0.61	bdl	-
Peat (CAN)	3	0	0	Boreal Peat	Ontario & Alberta, CAN	44.05 - 46.74	0.93 - 1.22	nm	7.6 - 9.2
Peat (NC)	2	1	0	Temperate Peat	Green Swamp & Alligator River NWR, NC	25.79 - 51.12	0.63 - 1.26	nm / 0.12	14.7 - 58.4
Peat (IN)	2	1	1	Indonesian Peat	South Kalimantan	53.83 – 59.71	2.03 - 2.50	nm / 0.12	1.4 – 3.8
Organic Alfalfa	3	0	0	Crop residue	Fort Collins, CO	42.28	2.91	nm / 0.29	4.4
Organic Hay	6	2	1	Crop residue	Fort Collins, CO	41.39	1.99	1.13 / 0.22	7.7
Organic Wheat Straw	6	2	0	Crop residue	Fort Collins, CO	43.32	0.40	0.32 / 0.085	3.7
Conventional Wheat Straw	2	0	0	Crop residue	Maryland	43.53	0.39	2.57	3.4
Conventional Wheat Straw	2	1	0	Crop residue	Walla Walla Co., WA	40.20	0.69	bdl	10.4
Sugar Cane	2	1	0	Crop residue	Thibodaux, LA	41.33	0.76	0.4	9.1
Rice Straw	7	4	1	Crop residue	CA, China, Malaysia, Taiwan	37.85 - 42.07	0.88 - 1.30	0.61 / 0.14-0.21	7.7 - 12.2
Millet	3	0	0	Crop residue & Cookstove fuel	Ghana	43.58	0.08	nm	7.4
Red Oak	5	0	0	Cookstove fuel	Commercial lumberyard	46.12	0.09	nm / 0.009	5.9
Douglas Fir	3	0	0	Cookstove fuel	Commercial lumberyard	46.70	bdl	nm	-
Okote	2	0	2	Cookstove fuel	Honduras via Commercial lumberyard	45.09	bdl	nm / 0.011	8.5
Trash	2	0	0	Trash or waste	Missoula, MT	50.29 - 50.83[a]	nm	nm	-
Shredded Tires	2	0	0	Trash or waste	Iowa City, IA	81.98[b]	0.57	nm /1.56[b]	-
Plastic Bags	1	0	0	Trash or waste	Missoula, MT	74.50[c]	nm	nm	-
Juniper	2	0	0	Temperate Forest	Outskirts Missoula, MT	50.73	1.17	nm	4.0
Ponderosa Pine	11	5	10	Temperate Forest	Outskirts Missoula, MT	51.11	1.09	nm	1.5
Black Spruce	5	7	9	Boreal Forest	South of Fairbanks, AK	50.50	0.66	nm / 0.054	3.8
Chamise	7	1	0	Chaparral	San Jacinto Mtns, CA	50.27	1.00	nm / 0.060	-
Manzanita	3	1	0	Chaparral	San Jacinto Mtns, CA	49.89	0.73	nm / 0.049	-
Total	**124**	**33**	**27**						

Note: "nm" indicates not measure,"bdl" indicates below the detection limit

[a] estimated using approach described in *Christian et al.* [2010]

[b] estimated from Table 1 in *Martinez et al.* [2013]

[c] estimated using USEPA (2010)

3.3.1 South African and US grasses

Fire is a natural disturbance factor and valuable ecological management tool in grasslands, which are widespread globally. During the dry season in southern Africa, savannas are burned for reasons ranging from agricultural maintenance to grazing control (Govender et al., 2006). The fires consume aboveground biomass consisting mainly of grass with some litter and woody debris. Savanna fire emissions (mainly in Africa) have been estimated to contribute up to 44% of the total global pyrogenic carbon emissions in some years (van der Werf et al., 2011). A smaller, but significant fraction of the total pyrogenic emissions is attributed to this source by Wiedinmyer et al. (2011).

Savanna fuels burned during FLAME-4 were collected from experimental burn plots in Kruger National Park (KNP) in South Africa, a savanna ecosystem prone to fire that has been the location of a number of ground- and aircraft-based campaigns measuring BB emissions (Sinha et al., 2003; Yokelson et al., 2003a, Wooster et al., 2011). We obtained tall- and short- grass samples from KNP near previous research sites (Shea et al., 1996) toward the peak of the fire season in September 2012. The tall-grass site (Pretoriouskop sourveld) is at an elevation of 560-640 m with an annual precipitation of ~700 mm. The landscape is dominated by tall, coarse grasses densely dispersed in clumps throughout the area with very little tree or leaf litter. The short-grass site (Skukuza sweetveld) is at a lower elevation (400-480 m) with less precipitation (~570 mm) and was covered by much shorter grasses but included a greater amount of leaf litter. In both cases our lab simulations did not include the minor leaf component due to import restrictions.

Other grass samples burned included wiregrass, sawgrass, and giant cutgrass, all of which are common prescribed fire fuels in the southeastern US (Knapp et al., 2009). Wiregrass is frequently a significant component of the forest understory while the other two grasses are the major fuel components in coastal wildlife refuges. Prescribed burning in coastal marshes of the southeastern US is done to improve habitat for waterfowl (Nyman and Chabreck, 1995). All our US grass samples were collected in South Carolina.

3.3.2 Boreal, temperate, and tropical peat samples

Peat deposits are accumulated, partially decomposed vegetation that is highly susceptible to combustion when dry and burns predominately by "creeping" surface or underground smoldering that is difficult to detect from space (Reid et al., 2013). Peat fires are the largest contributor to annual greenhouse gas emissions in Indonesia (Parker and Blodgett, 2008). An estimated 0.19 - 0.23 Gt of carbon was released to the atmosphere from peat combustion during the 1997 El Niño, which was equivalent to ~40% of the mean annual global fossil fuel emissions (Page et al., 2002). These emissions had major regional effects on health (Marlier et al., 2013) and climate (van der Werf et al., 2010).

Indonesian peat was sampled from three sites of the fire-prone area of the Mega Rice Project (MRP); a project that drained peatlands in Kalimantan for conversion to rice production that was subsequently abandoned. The first site had little evidence of ground disturbance with no indication of past burning, while the other sites were in highly degraded peat forest with reports of prior burn and logging events. The samples were collected at a depth of 10-20 cm below the surface and were cut into 10 cm × 10 cm × 10 cm blocks. The samples were dried step-wise in a microwave oven to a burnable moisture content.

Peat and organic soil can be a major fuel component for boreal fires (Turetsky et al., 2011). Our boreal peat samples were sub-humid boreal peat from the Hudson Bay Lowlands of Canada where most fires are caused by lightning. We also burned temperate swamp land peat collected in coastal North Carolina, which is subject to accidental fires and occasional prescribed burning. One North Carolina sample was obtained from the site of the large Pains Bay Fire (http://www.inciweb.org/incident/2218/; Rappold et al., 2011) in Alligator National Wildlife Refuge and the other from Green Swamp Preserve near Wilmington, NC.

3.3.3 Open (three-stone), rocket stove, and gasifier cooking fires

Domestic biofuel use is thought to be the second largest type of global BB (Akagi et al., 2011). Approximately 2.8 billion people worldwide burn solid fuels (primarily biomass) indoors for household cooking and heating (Smith et al., 2013) and the smoke emissions may contribute to an estimated 2 million deaths annually and chronic illness (WHO, 2009). Mitigating cooking fire emissions could alleviate adverse health effects and substantial climate impacts (Kirchstetter et al., 2004; Ramanathan and Carmichael, 2008; Andreae and Ramanathan, 2013).

During FLAME-4, an experienced field researcher (L'Orange et al., 2012a, 2012b) simulated "field" cooking with four cookstove types and for five different fuels starting with the cookstove, pot, and water all at ambient temperature. Traditional three-stone cooking fires are the most widespread globally and are simply a pot positioned on three stones or bricks above a continuously fed fuel center. The Envirofit Rocket G-3300 stove is an example of a common approach to reducing fuel consumption per cooking task. The "rocket" type insulated combustion chamber mixes cool air entering the stove with the heated combustion air and optimizes heat transfer to the pot via a vertical chimney (Bryden et al., 2005; MacCarty et al., 2008). The Ezy stove uses minimal material in a "rocket" type design with a patented inner chamber to focus

heat. The Philips HD4012 “gasifier” type stove improves combustion efficiency with forced-draft air delivered by an internal fan (Roth, 2011).

A recent EPA study focused on the fuel-efficiency of various cooking technology options (Jetter et al., 2012) and FLAME-4 purposely included some similar fuels (red oak) and devices (three-stone, Envirofit G-3300 rocket stove, Philips HD4012 gasifier) to connect that work with our more detailed emissions speciation. The Ezy stove we tested was not included in the EPA study. Overall, fuel types for our cooking fire experiments included red oak, Douglas fir, and okote wood cut into 2 cm × 2 cm × 35.5 cm sticks and millet stalks all at ~5-10 % moisture content. We also measured the emissions from Douglas fir chips burned in the G-3300 rocket stove and Philips HD4012 gasifier stove.

3.3.4 Crop residue fires

Sugarcane is an important crop in some US states (LA, FL, HI) and parts of other countries (Brazil, South Africa, Mexico, etc.). Burning sugar cane before harvesting facilitates harvesting and can also have major regional air quality impacts (Lara et al., 2005). Globally, a broad range of other crop residues are burned post-harvest; often “loose” in the field, or in piles when associated with manual harvesting in the developing world (McCarty et al., 2007; Akagi et al., 2011). The fires enable faster crop rotation with less risk of topsoil loss; reduce weeds, disease, and pests, and returns some nutrients to the soil, but they are not yet well characterized and have a large atmospheric influence (Streets et al., 2003; Yevich and Logan, 2003; Chang and Song, 2010; Lin et al., 2010; Oanh et al., 2010; Yokelson et al., 2011; Sinha et al., 2014). The practice of burning agricultural residues on site is seasonally and regionally dependent and in the US may be unregulated or require permits (Melvin, 2012). The emissions from crop residue (CR) fires are often underestimated because (1) in common with all BB, many of the gases are unidentified or

rarely measured and (2) some algorithms for measuring burned area or active fire detection from space may miss some of the small, short-lived burns characteristic of crop-residue fires. Published space-based estimates of the area burned in crop residue fires in the US range from 0.26 to 1.24 Mha yr^{-1} (McCarty et al., 2009; Randerson et al., 2012). In contrast Melvin (2012) found that ~5 Mha of croplands were burned in the US in 2011 based on state records, which would indicate that these fires account for the most burned area in the US. Better characterization of the emissions from these diverse fuels for various burn conditions will address issue (1) and improve current inventories and models.

We burned various crop materials, which account for much of the agricultural burning in the US (McCarty et al., 2007) including sugar cane, rice straw, wheat straw from both conventional and organic farms, hay, and alfalfa collected from LA, CA, WA and MD, and CO, respectively. The crop materials from CO were sampled from an organic farm near Fort Collins and were burned to investigate the potential effects of agricultural chemicals on emissions of Cl, N, P, or S containing species (Eckhardt et al., 2007; Christian et al., 2010; Becker et al., 2012). Since crop residue fires are globally significant, we also burned authentic samples of millet from Ghana and rice straw from Taiwan, China, and Malaysia.

3.3.5 US shrubland and coniferous canopy fires

Temperate ecosystems in the US and Canada experience both natural wildfires and prescribed fires with the latter used to maintain habitats, reduce wildfire impacts, and open land access (Biswell, 1989; Wade and Lunsford, 1989). The effects of both wild and prescribed fires on air quality can be significant on local and regional scales (Park et al., 2007; Burling et al., 2011), necessitating a greater understanding of the emissions from fires in ecosystems such as chaparral and coniferous forests.

In a previous laboratory fire study, extensive efforts were taken to reproduce complete fuel complexes for US prescribed fires with some success (Yokelson et al., 2013a; Burling et al., 2010). During FLAME-4 we included similar chaparral fuels, but concentrated on just a part of the fuel complex for fires in coniferous forest ecosystems (fresh canopy fuels). Green boughs from MT ponderosa pine and AK black spruce were burned primarily to further investigate previous smog chamber smoke aging results using the same fuels (Hennigan et al., 2011).

3.3.6 Tire fires

As the number of vehicles produced grew 5.1% from 2011 to 2012, the estimated total number of vehicles in use globally surpassed a billion (OICA, 2013). Parallel with this growth, tire disposal is a significant environmental concern because they end up in land-fills (including all non-biodegradable components) or being burned and producing emissions that are unfavorable to humans and the environment. Tires are commonly not accepted at land-fills because whole tires can rise to the top of the fill and serve as a major breeding ground for mosquitos (USEPA, 1991). The shredding equipment necessary to prevent this rising is expensive, with added significant labor and effort necessary stemming from the steel webbing under the tread.

According to the US Scrap Tire Management Summary 2005-2009, 1946 of the 4002 tonnes of scrap tires generated in 2005 were used for fuel (RMA, 2011). Tires are useful as a fuel/coal substitute since the sulfur and nitrogen content is comparable to coal, but they produce more heat energy per unit mass (USEPA, 1997). Although ~48% of US scrap tires are recycled as fuel annually, the remainder, plus tires amassed across decades, are disposed of by alternative means including illegal dumps and informal or accidental fires that are notorious for becoming unmanageable and long-lasting. Tire disposal is also a major concern in developing countries where they may be used as fuel for minimally-regulated enterprises such as brick-kilns (Christian

et al., 2010). To better characterize the emissions from tire fires, we burned shredded tires identical to those involved in a major dump fire near Iowa City, IA.

3.3.7 Trash fires

McCulloch et al. (1999) estimated that 1500 Tg of garbage was produced for a world population of 4.5 billion with significant portions disposed of by open burning or incineration. Scaling to the current global population estimate of 7.05 billion (UNFPA, 2012), 2500 Tg of garbage is produced annually, and the impact of disposal on local and global scales remains under-evaluated due partly to the lack of small burn detection by satellite. During ACE-Asia Simoneit et al. (2004a, b) observed that phthalates and n-alkanes that they attributed to trash burning accounted for ~10% of ambient organic aerosol mass in the central-west Pacific. In the US alone, it is estimated that 12-40% of households in rural areas burn garbage in their backyards (USEPA, 2006) and the airborne emissions could play a critical role in chemical deposition onto crops and soils. Lemieux et al. (1998, 2000, 2003) simulated open burning of household waste and concluded that this is a large US source of carbonyl and polychlorinated dibenzo-p-dioxins and polychlorinated dibenzofuran. Previous work has already established that garbage burning is an important source of black carbon, ozone precursors, hydrogen chloride, particulate chloride and a variety of toxic materials including dioxins, hence better evaluation of this source is crucial (Costner, 2005; Christian et al., 2010; Li et al., 2012; Lei et al., 2013).

We ignited two fires that burned mixed, common waste collected daily at the FSL and another fire to separately measure the emissions from burning plastic shopping bags. The fuels we ignited for the garbage burns were intended to represent common household refuse with the understanding that household waste is highly variable. The overall carbon fraction for waste samples was determined by a procedure described in detail elsewhere (Christian et al., 2010).

Briefly, the mass of each trash component was used to weight the carbon content of each component to calculate overall carbon content (IPCC, 2006; USEPA, 2006) as shown in Table 3.2.

Table 3.2. Estimate of carbon content of trash components burned during FLAME-4

(a)Trash burn 1

Component	Category	Component weight (g)	Mass fraction	Estimated Carbon Fraction
manila packing paper	paper	82	0.21	0.46
PVC pipe	plastic	38.6	0.10	0.74
Sunmaid raisins foil container	metal	6.4	0.02	-
banana peel	organic (food waste)	70	0.18	0.38
soft black foam	plastic	2	0.01	0.74
plastic Coke bottle	plastic	26	0.07	0.74
coffee grounds, wet	organic	114	0.29	0.38
styrofoam meal-to-go container	plastic	6	0.02	0.74
Kozy Shack pudding container	plastic	23	0.06	0.74
rubber trim	rubber	26	0.07	0.76
		394	1.00	0.50

(b)Trash burn 2

Component	Category	Component weight (g)	Mass fraction	Estimated Carbon Fraction
brown paper	paper	123	0.22	0.46
added rubber	rubber	34	0.06	0.76
waxy coffee cups	-	28	0.05	-
styrofoam	plastic	10	0.02	0.74
assorted plastics	plastic	45	0.08	0.74
plastic grocery bags	plastic	17	0.03	0.74
pizza crusts	organic	62	0.11	0.38
aluminum foil	metal	17	0.03	-
bleach bottle	plastic	93	0.17	0.74
coffee grounds	organic	46	0.08	0.38
newspaper	paper	85	0.15	0.46
		560	1.00	0.51

*combined estimates from IPCC (2006) Table 2.4 and USEPA (2007) Annex 3 Tables A-125 to A-130

3.4 Instrument overview

A goal of the FLAME-4 study was to extensively characterize gas and aerosol emissions, therefore, a comprehensive suite of instrumentation was deployed. Here we list our instruments as well as others for which the results are presented elsewhere. Gas-phase emissions were measured by OP-FTIR, a proton-transfer-reaction time-of-flight mass spectrometer (PTR-TOF-MS), two whole air sampling (WAS) systems, cartridge sampling followed by gas chromatography mass spectrometry (GC-MS), cartridge sampling followed by two-dimensional gas chromatography time-of-flight mass spectrometry (2D-GC-TOF-MS), a total hydrocarbon

analyzer (THC), criteria gas monitors, and a proton-transfer-reaction (quadrupole) mass spectrometer (PTR-QMS).

Particle-phase instruments were deployed to measure aerosol chemistry, size distribution, optical properties, and cloud-nucleating properties. Particle chemistry measurements included gravimetric filter sampling of particulate matter with aerodynamic diameter < 2.5 microns ($PM_{2.5}$) followed by elemental carbon (EC) and organic carbon analyses as well as GC-MS and ion chromatography (IC) of extracts; an aethalometer; a high resolution time-of-flight aerosol mass spectrometer (HR-TOF-AMS); laser ablation aerosol particle time-of-flight (LAAP-TOF) single-particle mass spectrometer; and a particle-into-liquid sampler micro-orifice uniform-deposit impactor (PILS/MOUDI) to collect samples for several types of electrospray MS analyses (Bateman et al., 2010). Particle mass was also measured by a tapered element oscillating microbalance (TEOM^{TM} 1405-DF). Chemistry and structure at the microscopic level were probed by collecting grids for scanning electron microscope (SEM) and transmission electron microscope (TEM) analyses.

Optical properties were measured by several single particle soot photometers (SP2); a photoacoustic extinctiometer (PAX); several photo-acoustic aerosol absorption spectrometers (PAS), PASS-3d (ambient/denuded), PASS-UV, the NOAA PAS system; and a broadband cavity enhanced absorption spectrometer (BBCEAS) (Washenfelder et al., 2013).

Size distributions were measured by several scanning mobility particle sizers (SMPS) and a fast mobility particle sizer (FMPS). Cloud nucleating properties of the aerosol were measured by a cloud condensation nuclei counter (CCNC), a continuous-flow diffusion chamber (CFDC) measuring ice nuclei, and a hygroscopic tandem differential mobility analyzer (H-TDMA). Table

3.3 provides a brief description of individual instrument capabilities and results from these instruments are reported elsewhere (e.g. Liu et al., 2014; Saleh et al., 2014; Hatch et al., 2015; Tkacik et al., 2016).

Table 3.3. FLAME-4 instruments and measurement capabilities

FLAME-4 Measurements		
Instrument	**Institution**	**Species Measured**
OP-FTIR	University of Montana	CO2, CO, CH4, C2H2, C2H4, C3H6, H2O, HCHO, HCOOH, CH3OH, CH3COOH, glycolaldehyde, furan, NO, NO2, HONO, NH3, HCN, HCl, SO2
PTR-TOF-MS	University of Montana	High resolution m/z 18-300 VOC & I/SVOC
PTR-QMS	Carnegie Mellon University	Low resolution m/z 18-200 VOC & I/SVOC
Criteria gas monitors	Carnegie Mellon University	O3, NOx, CO2, SO2
THC	Max Planck Institute	Total hydrocarbons
WAS (GC-MS)	University of California, Irvine	CO2,CO, CH4, HC, OVOC, some SVOC, S and Cl- organics
WAS, Cartridges (GC-MS)	University of Miami	CO2,CO, CH4, HC, OVOC, some SVOC, S and Cl- organics
Cartridges (2D-GC/TOFMS)	Portland State University	VOC & I/SVOC
NOx isotope	Brown University	15N
HR-TOF-AMS	Carnegie Mellon University	OA,Cl-, SO2--, NH4+, NO3-
SP2	Carnegie Mellon University	BC: #, mass, size, coating
AET	Carnegie Mellon University	BC mass
SMPS	Carnegie Mellon University	Particle size 10-500 nm
LAAP-TOF	Carnegie Mellon University	Single particle composition 0.1-1 micron
CFDC	Colorado State University	Ice nuclei: #, size, composition
CCNC	Colorado State University	Cloud condensation nuclei
TEOM	Colorado State University	Particle mass
H-TDMA	Colorado State University	Aerosol hygroscopic growth factor
SP2	Colorado State University	BC: #, mass, size, coating
FMPS	Aecom Technology Corporation	Fast particle size distribution
PAX-870	Droplet Measurement Technologies	Particle scattering and absorption at 870 nm
Filters (Teflon/ Quartz)	University of Iowa	PM2.5, EC/OC, IC, GC-MS, HP-PAED
MOUDI	Pacific Northwest National Laboratory	Nano-DESI-HR-MS analysis of high MW PM organics
PILS	Pacific Northwest National Laboratory	ESI-HR-MS analysis of high MW PM organics
SMPS	National Oceanic and Atmospheric Administration	Particle size 10-500 nm
BBCES	National Oceanic and Atmospheric Administration	Aerosol broadband UV extinction
NOAA PAS	University of Wyoming	Aerosol absorption at multiple wavelengths
PASS-3d	Los Alamos National Laboratory	Aerosol Babs and Bsca (405, 532, 781 nm)
PASS-UV	Los Alamos National Laboratory	Aerosol Babs and Bsca (375 nm)
SP2	Los Alamos National Laboratory	BC: #, mass, size, coating
TEM	Los Alamos National Laboratory	Grids for Electron Microscopy
SEM	Los Alamos National Laboratory	Grids for Electron Microscopy

Chapter 4 : OP-FTIR component of FLAME-4

4.1 OP-FTIR introduction

In FLAME-4, the overarching goal was to burn both historically undersampled and well-studied fuels while adding new instrumentation and experimental methods to provide previously unavailable information on smoke composition, properties, and evolution. It was critical to acquire this new information under conditions where the lab results can be confidently used to better understand real-world fires. In this respect the open-path Fourier transform infrared spectroscopy system was especially helpful since it provided new emissions data and also measured many of the major inorganic and organic gaseous products of both flaming and smoldering combustion that overlapped well with the suite of fire emissions measured in numerous field campaigns.

This chapter focuses on a detailed description of the trace gas measurements by OP-FTIR. We present the major findings by OP-FTIR and compare lab and field data to inform the use of emissions data from the OP-FTIR and the extensive suite of other instruments deployed during the FLAME-4 campaign.

4.2 Open-path FTIR experimental

4.2.1 OP-FTIR data collection

The OP-FTIR deployed in FLAME-4 was used to measure the emissions of a suite of trace gases and consisted of a Bruker Matrix-M IR Cube spectrometer with a mercury-cadmium-telluride (MCT) liquid nitrogen cooled detector interfaced to a thermally stable 1.6 m base open-path White cell. The optical path length was 58.0 m and infrared (IR) spectra were collected at a resolution of 0.67 cm^{-1} covering the range 600-3400 cm^{-1}. During stack burns the OP-FTIR was

positioned on the sampling platform so that the open path spanned the width of the stack, allowing the continuously rising emission stream to be directly measured. For stack burns, four interferograms were co-added to give single ppbv detection limits at a time resolution of 1.5 s with a duty cycle greater than 95%. Spectral collection began a few minutes before fire ignition and continued throughout the fire. During the room burns, the OP-FTIR was removed from the stack but remained on the sampling platform in the combustion room. For the slower changing concentrations in this portion of the experiment, we increased the sensitivity by co-adding 16 interferograms (time resolution to 6 s) with continuous collection starting a few minutes before ignition and continuing until all the smoke was exhausted from the room. A pressure transducer and two temperature sensors were located beside the White cell optical path and their outputs were logged and used to calculate mixing ratios from the concentrations determined from the IR absorption signals for both experimental configurations.

Mixing ratios were determined for carbon dioxide (CO_2), carbon monoxide (CO), methane (CH_4), acetylene (C_2H_2), ethene (C_2H_4), propylene (C_3H_6), formaldehyde (HCHO), formic acid (HCOOH), methanol (CH_3OH), acetic acid (CH_3COOH), glycolaldehyde ($C_2H_4O_2$), furan (C_4H_4O), water (H_2O), nitric oxide (NO), nitrogen dioxide (NO_2), nitrous acid (HONO), ammonia (NH_3), hydrogen cyanide (HCN), hydrogen chloride (HCl), and sulfur dioxide (SO_2) by multi-component fits to selected sections of the IR transmission spectra with a synthetic calibration non-linear least-squares method (Griffith, 1996; Yokelson et al., 2007) applying both the HITRAN spectral database and reference spectra recorded at Pacific Northwest National Laboratory (PNNL) (Rothman et al., 2009; Sharpe et al., 2004; Johnson et al., 2006, 2010). The selected spectral windows and hence interfering species depend strongly on resolution, relative humidity, pathlength, and concentration of the smoke. The spectral regions and parameters are

re-optimized for every experiment with current ranges reported in Table 4.1, though we caution against using our settings in other work. Although nitrous oxide (N_2O) is fitted as part of the CO and CO_2 analysis, it is not reported because any enhancements are too small to be resolved confidently at 0.67 cm^{-1} resolution. Even with higher resolution OP-FTIR, significant N_2O enhancements were not observed in smoke confirming it is at most a minor product (Griffith et al., 1991).

Table 4.1. Spectral regions used to retrieve concentrations for the OP-FTIR data reported in this work.

Target Molecular species	HITRAN Species	PNNL species	Spectral Region (cm^{-1})
CO_2, CO, H_2O	H_2O, CO_2, CO, N_2O	-	2050-2280
CH_4	H_2O, CH_4	-	1291.69-1310
C_2H_2	H_2O, CO_2, C_2H_2	-	723-740
C_2H_4, NH_3	H_2O, CO_2, NH_3	C_2H_4	920-980
C_3H_6	H_2O, CO_2, NH_3, C_2H_4	C_3H_6	900-925
CH_3OH	H_2O, CO_2, NH_3	CH_3OH	990-1064
HCHO, HCl	CO_2, CH_4, HCl	HCHO	2730-2800
HCOOH	H_2O, NH_3, HCOOH	-	1098-1114
CH_3COOH	H_2O, NH_3	CH_3COOH, C_3H_8O	1176-1195
FURAN	H_2O, CO_2, C_2H2	FURAN	743.1-763.5
HCN	H_2O, CO_2, C_2H2	HCN	710.2-717
NO	H_2O, NO	-	1896.5-1903.2
NO_2	H_2O, NO_2	-	1595-1599
HONO	H_2O, NH_3	HONO, glycolaldehyde	822-877
SO_2	SO_2	-	2460-2530

OP-FTIR offers several important advantages in the study of complex mixtures such as BB smoke. Each species exhibits a unique pattern of multiple peaks imparting resistance to interference from other species and aiding in explicit identification. The technique has no storage artifacts, it allows flexible sampling volumes that target multiple molecules simultaneously in the same parcel of air, and it provides continuous high temporal resolution data (Yokelson et al.,

1996; Burling et al., 2010). Several million fitted retrievals provided real-time data for all 157 burns. On occasion a few of the target compounds were not present in detectable quantities during the course of certain fires. The uncertainties in the individual mixing ratios vary by spectrum and molecule and are dominated by uncertainty in the reference spectra (1-5%) or the detection limit (0.5-15 ppb), whichever is larger. Comparisons with other techniques and calibration standards are described elsewhere (Goode et al., 1999; Christian et al., 2004; Akagi et al., 2013). Uncertainties in fire-integrated amounts vary by molecule and fire, but are usually near 5% given the ppm-level concentrations.

4.2.2 Emission ratio and emission factor determination

Excess mixing ratios (denoted ΔX for each species "X") for all 20 gas-phase species measured using OP-FTIR were calculated by subtracting the relatively small average background mixing ratio measured before each fire from all the mixing ratios observed during the burn. The molar emission ratio for each species "X" relative to CO (ΔX/ΔCO) is the ratio between the sum of the ΔX over the entire fire relative to the sum of the ΔCO over the entire fire. In early combustion lab experiments the flux of products and smoke temperature varied greatly over the course of the fire and had to be measured and corrected for (Yokelson et al., 1996). However, current experiments have featured an entrainment flow that is much greater than the fire-driven flow so that the total flow and smoke temperature are essentially constant. Because the large entrainment flow ensures a constant total flow, a comparison of the sums is valid, although very small adjustments to these fire-integrated sums were made so they would represent the actual amount of emissions generated given the small changes in the emissions density that resulted from small changes in absolute temperature and pressure over the course of some burns. Molar ER to CO were calculated for all the species measured using OP-FTIR for all 157 burns and were used to

calculate EFs by the carbon mass-balance method (CMB), which assumes all of the burned carbon is volatilized and that all of the major carbon-containing species have been measured (Ward and Radke, 1993; Yokelson et al., 1996, 1999; Burling et al., 2010). The species CO_2, CO, and CH_4, which are all quantified by OP-FTIR, usually comprise 98-99% of the total carbon emissions for most fire types. By ignoring the carbon emissions not measured by OP-FTIR, emission factor estimates based solely on species measured by OP-FTIR are typically inflated by a factor of ~1-2% (Andreae and Merlet, 2001; Yokelson et al., 2013a). Because of EF dependence on assumed total carbon, slightly different EF will appear when including other instruments (Stockwell et al., 2015; Hatch et al., 2015; see Chapter 5). However, these differences are only a few percent (except for peat fires where they are ~5%) and insignificant compared to other uncertainties in global BB.

4.2.3 Measurement strategy

Most BB emissions inventories rely on the average EF obtained at the average MCE observed in airborne measurements, when available, because most of the smoke from most field fires is entrained in a convection column making airborne measurements the most representative (Andreae and Merlet, 2001; Akagi et al., 2011). For fires that may be dominated by poorly lofted emissions, such as peat fires or residual smoldering combustion (Bertschi et al., 2003b), a ground-based MCE could be most representative. Laboratory fire experiments can provide measurements not available from field experiments or significantly increase the amount of sampling for fire-types rarely sampled in the field, but it is important to assess the representativeness of lab fire emission factors. The assessment of lab-derived EFs is not completely straight-forward because BB produces highly variable emissions when field fires burn in a complex and dynamic environment that probably cannot be fully characterized safely.

Fortunately, one parameter that correlates strongly with EFs, MCE, has been measured on most field fires. “Ideal” lab fire simulations would burn with a range of MCE similar to that observed in natural fires. This is sometimes achieved, but is sometimes elusive due to differences in fuel moisture, wind, scale, etc. (Yokelson et al., 2013a). Thus, a second, more readily achieved goal is for the lab fires to burn with a range in MCE that is broad enough to determine the EF dependence on MCE and then use this relationship to predict EFs at the field-average MCE (Christian et al., 2003). In addition, even if lab fires differ from field fires in fire-integrated MCE, the ER to CO for smoldering compounds and the ER to CO_2 for flaming compounds is useful (Akagi et al., 2011). Finally, in the simplest approach, the average ratio of field EF to lab EF can be applied as a correction factor to adjust lab EFs (Yokelson et al., 2008). This approach was also warranted for adjustments to fuel-specific lab EFs reported in Yokelson et al. (2013a) because the results had the lowest error of prediction. When lab EFs are adjusted it is not expected (for instance) that the EF versus MCE relationship will be identical in the lab and field or always be highly correlated, but simply that the adjustment procedure will nudge the EF in the right direction. We can take the level of agreement between the lab-based predictions and the airborne-measured averages (for species measured in both environments) as the most realistic estimate of uncertainty in using lab equations for species not measured in the field.

4.3 OP-FTIR results and discussion

4.3.1 Stack vs. room decay rates

Considerable gas-specific behavioral variability was noteworthy between stack (n = 125) and room (n = 32) burns. Figure 4.1 shows temporal profiles for the excess mixing ratios of the 19 gas-phase compounds we report for a complete stack burn. Figure 4.2 shows the excess mixing ratios of several gas-phase species during a typical room burn and highlights differences in their

temporal behavior. For all gases in the room burn, a rapid rise and peak in concentration following ignition occurs because the OP-FTIR remained at a height of 17 m during room burn sampling. Rapid vertical mixing and then anticipated slow exchange from the combustion room account for the fast and then gradual decline in concentration for non-sticky species as revealed by the stable gases (e.g. CO and CH_4) shown in Figure 4.2. The stickier gases undergo the same mixing processes, but decay at faster rates as illustrated by NH_3, CH_3COOH, HCOOH, and glycolaldehyde (decaying increasingly fast in the order given). These fast decays introduced error into the preliminary emission ratios to CO that were used to calculate provisional fire-integrated emission factors for each fire. We assessed which gases were affected by this artifact by plotting EF vs MCE for each species for all 157 fires. If the room burn EF fell significantly below the general trend we assumed it was due to losses on the lab walls or aerosol surfaces. Supplement Tables S1 and S2 list the average EF/ER for each fuel type along with uncertainties. All the individual stack and room burn EFs/ERs are included in the Supplemental of Stockwell et al. (2014). The fuel type average EF/ER in the tables for "non-sticky" species (namely: CO_2, CO, CH_4, C_2H_2, C_2H_4, C_3H_6, C_4H_4O, NO, NO_2, HONO, HCN, CH_3OH, HCHO) are based on all 157 fires. Since the room burn EF/ER values for stickier species (HCl, NH_3, glycolaldehyde, CH_3COOH, HCOOH, and SO_2) are expected to be lower limit estimates, the average fuel type EF/ER for these species was calculated excluding room burn data. Next, in the sections below we note significant features of the OP-FTIR emission measurements and compare the emissions from each fuel type to field data when possible following the measurement strategy outlined in Sect 4.2.3.

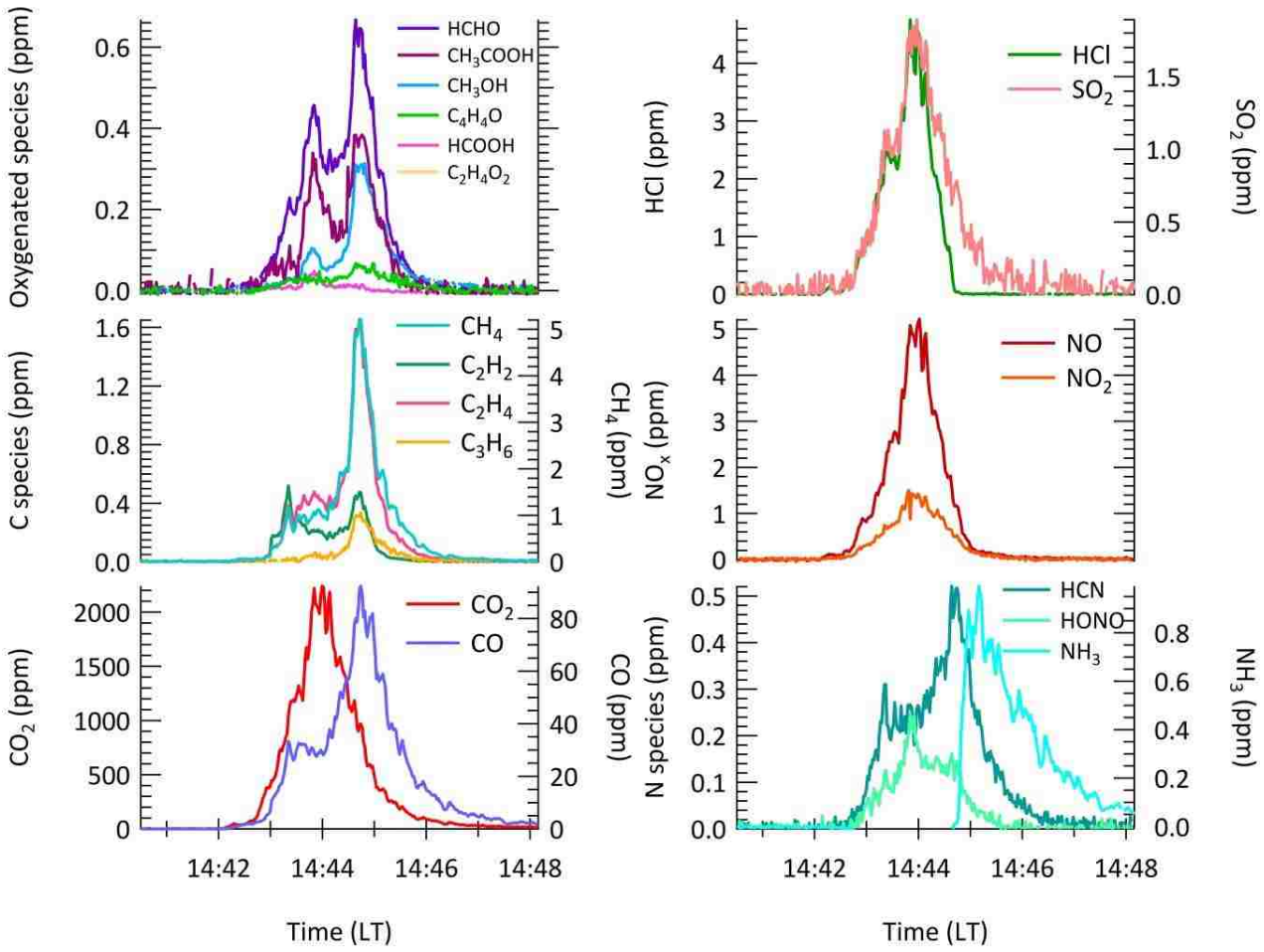

Figure 4.1. Excess mixing ratios of 19 trace gases versus time for a complete sawgrass "stack" burn as measured by OP-FTIR.

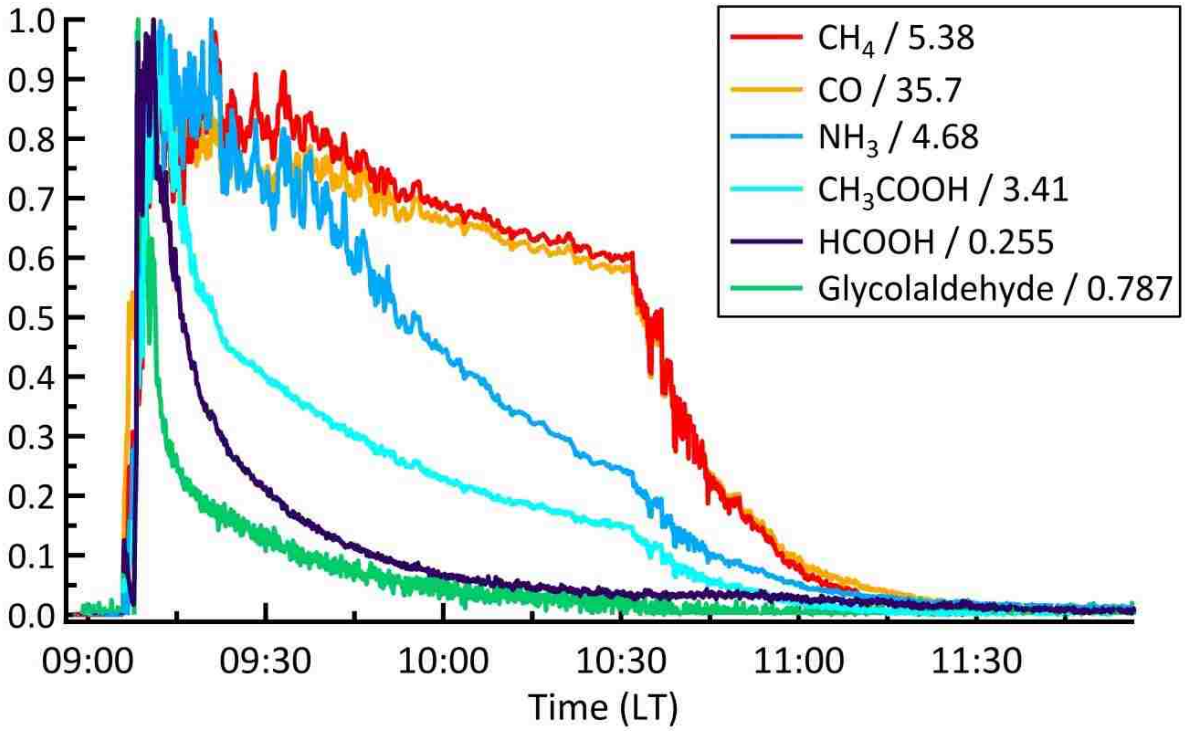

Figure 4.2. Excess mixing ratios of sticky and non-sticky gases normalized by their maximum mixing ratio (shown in legend) to have a maximum value of one during a "room" burn of organic hay. The stable non-sticky species shown are CO and CH_4 while the stickier species include HCl, NH_3, glycolaldehyde, CH_3COOH, and HCOOH: the latter show a faster rate of decay than the stable species CO and CH_4.

4.3.2 Emission from African and US grasses

We measured a range of emissions from 20 African savanna grass fires that includes the first EF for HCl (0.26 ± 0.06 g kg^{-1}) for this fuel type and additional gases rarely measured for savanna fires such as SO_2, HONO, and glycolaldehyde (Ferek et al., 1998; Sinha et al., 2003; Trentmann et al., 2005). We also burned 30 fires with US grasses: giant cutgrass (8), sawgrass (13), and wiregrass (9). Previously, Goode et al. (1999) reported OP-FTIR EF for 13 trace gases from three laboratory fires burning western US bunchgrasses. Thus, our OP-FTIR data and the other anticipated results from FLAME-4 represent a large increase in emissions data for a major fuel component of fires across the US.

We discuss the chlorine emissions from grass fires first. Comprehensive vegetation analyses compiled by Lobert et al. (1999) show that grasses have much higher chlorine content on average than other common vegetative fuels. Thus, grass fires would be expected to emit more chlorine per unit biomass burned. The most studied chlorine-containing compound emitted from BB is methyl chloride, which was considered the largest natural contributor to organic chlorine in the atmosphere in the global reactive chlorine emissions inventory with about 50% contributed by BB (RCEI, Keene et al., 1999). HCl (an inorganic compound) was the Cl-containing gas quantified by OP-FTIR in this study and BB emissions of HCl were not considered in the RCEI. HCl is a "sticky" gas (Webster et al., 1994; Komazaki et al., 2002; Johnson et al., 2003) that readily adheres to surfaces, therefore, open-path optical systems are ideal for measuring primary HCl smoke emissions. In addition, the EFs for HCl for each FLAME-4 fuel type are positively correlated with MCE, and the HCl mixing ratios consistently "track" with CO_2, SO_2, and NO_x as seen in Figure 4.1. This confirms HCl is a flaming compound and since grasses burn primarily by flaming combustion, high HCl emissions would be expected from this fuel. Our lab-average $\Delta HCl/\Delta CO$ ratio for savanna fires (the main global type of grass fire) is ~17 times higher than the $\Delta CH_3Cl/\Delta CO$ reported for savanna fires in Lobert et al. (1999) and still ~5 times higher after adjusting to the field average MCE of savanna grasses (0.938, see below). This indirect comparison suggests that HCl could be a major Cl-containing gas emitted by BB and the emissions could be significant. However, the gas-phase HCl mixing ratios decayed rapidly during our room burn storage periods and Christian et al. (2010) observed high particulate chloride with HCl below detection limits in the fresh emissions from Mexican crop residue fires. At longer time scales, particulate chloride has been observed to decrease as smoke ages (Li et al., 2003; Pratt et al., 2011; Akagi et al., 2012). Thus, both the rate at which HCl is initially

incorporated into the aerosol phase and the possibility that it is slowly reformed in aging plumes via outgassing of chlorine from particles remain to be investigated in detail.

Chlorine emissions from BB can also be affected by deposition of sea-salt, which can increase the Cl concentration of coastal vegetation (McKenzie et al., 1996). The highest average EF(HCl) for a fuel type during the FLAME-4 study was for sawgrass (1.72 ± 0.34 g kg^{-1}). Both, the sawgrass and giant cutgrass were collected in a coastal wildlife refuge that is much closer to the Atlantic coast (~10 km) than the wiregrass sampling location (~165 km). The Cl-content listed in Table 3.1 and the measured EFs for HCl are consistent with the distance from the coast for the US grasses. The African grass EF(HCl) and Cl-content were lower than we measured for the coastal US grasses, but higher than the wiregrass values despite being collected further (225 km) from the coast, confirming that other factors besides distance from the coast effect grass Cl-content.

It is important to compare our FLAME-4 emissions data for African grass fires to field and other laboratory measurements of emissions from African savanna fires. Figure 4.3 shows our EF results with those reported for similar African fuels burned at the FSL during February-March 2001 (Christian el al., 2003), airborne measurements from the SAFARI 2000 campaign (Yokelson et al., 2003a), and ground-based measurements from prescribed savanna fires in KNP (Wooster et al., 2011). We plot EFs for smoldering compounds detected by all three sampling platforms versus MCE, providing an idea of the natural gradient in EFs that result from savanna fuels and the impact measurement approach has on the type of combustion surveyed. The ground-based (long open-path FTIR), airborne (closed-cell FTIR) and laboratory based (open-path FTIR) emission factors can be fit to a single trend. The airborne average EF(NH_3) is within the range of the ground-based EFs for NH_3 at the airborne average MCE, but at the low end

likely due partly to natural variation in fuel nitrogen and partly because the correction for losses in the closed cell in the airborne system was not fully developed until later (Yokelson et al., 2003b). Both field studies observed much lower average MCE than both laboratory studies (likely due to higher fuel moisture, wind, smoldering roots, etc.), but the MCE is shown to correlate with much of the variation in EF.

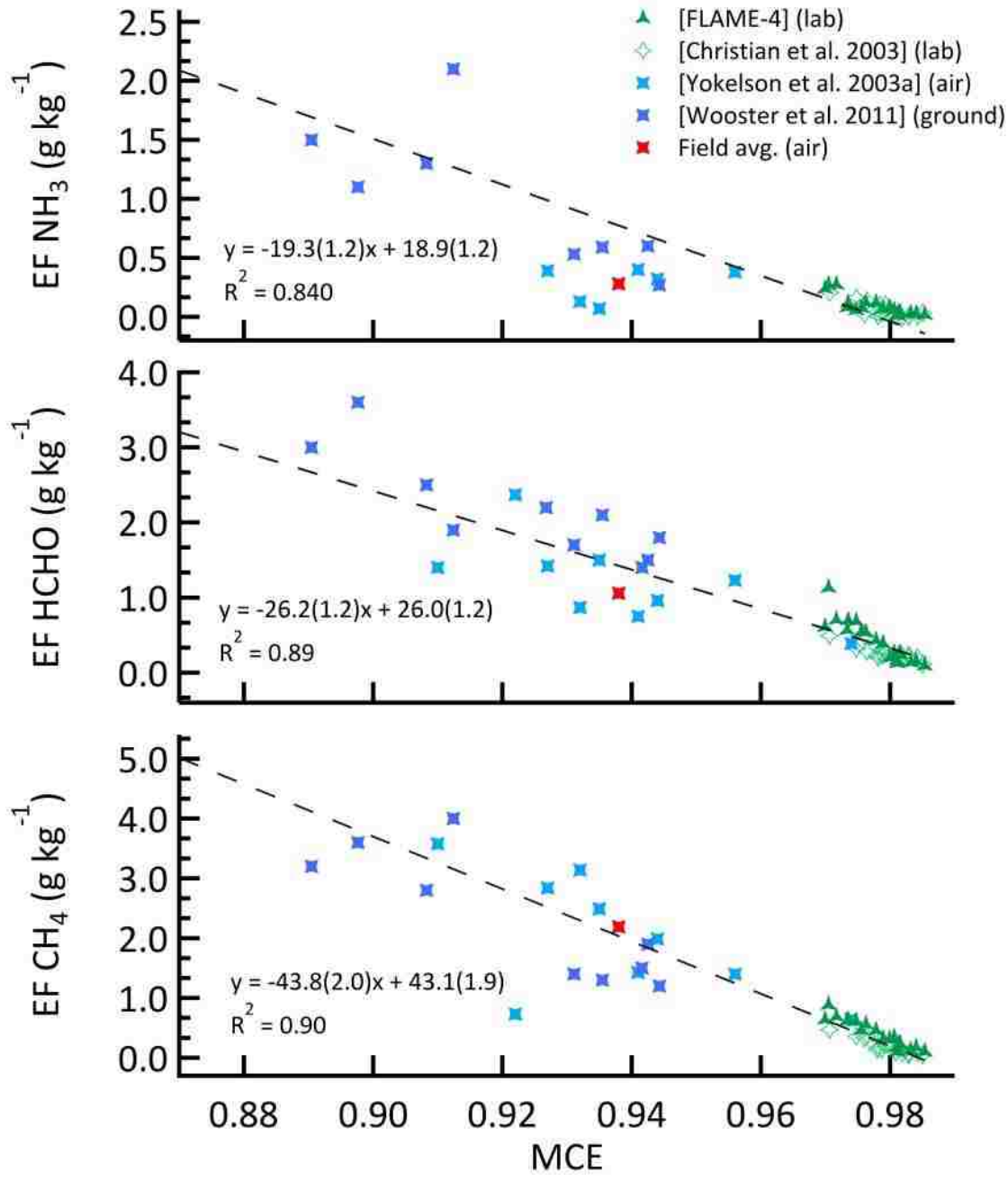

Figure 4.3. Emission factors (g kg-1) of select smoldering species as a function of MCE for FLAME-4 burns of African savanna fuels. Also shown are laboratory data of Christian et al. (2003), ground-based data of Wooster et al. (2011), and airborne data of Yokelson et al. (2003a). The linear fit based on all data is shown.

Next, we exploit the MCE plot-based lab-field EF comparison as described in Sect. 4.2.3 to generate EF from our lab data that are more consistent with field studies. We plot lab and field EFs versus MCE together for African savanna grasses in Figure 4.4 with separate linear fits for comparison. The linear fit from the plot of lab EF versus MCE for each species is used to calculate an EF at the average MCE (0.938) from airborne sampling of authentic African savanna fires reported in Yokelson et al. (2003a). The values shown in Table 4.2 yield lab predicted EFs that are, on average, only 21% different from field values and have even better agreement for hydrocarbon species (±3% including CH_4, C_2H_2, and C_2H_4). The lab-field comparison for nitrogen (N)-containing species has a higher coefficient of variation. Part of the larger variability could be the dependence of N-compound emissions on fuel nitrogen content in addition to MCE (McMeeking et al., 2009; Burling et al., 2010). Better lab-field agreement was obtained in an earlier application (Christian et al., 2003) of this approach for several compounds such as CH_3COOH, but that study featured a broader range of lab MCE that better constrained the fits. However, processing the data by this method improves the representativeness of the FLAME-4 EF across the board.

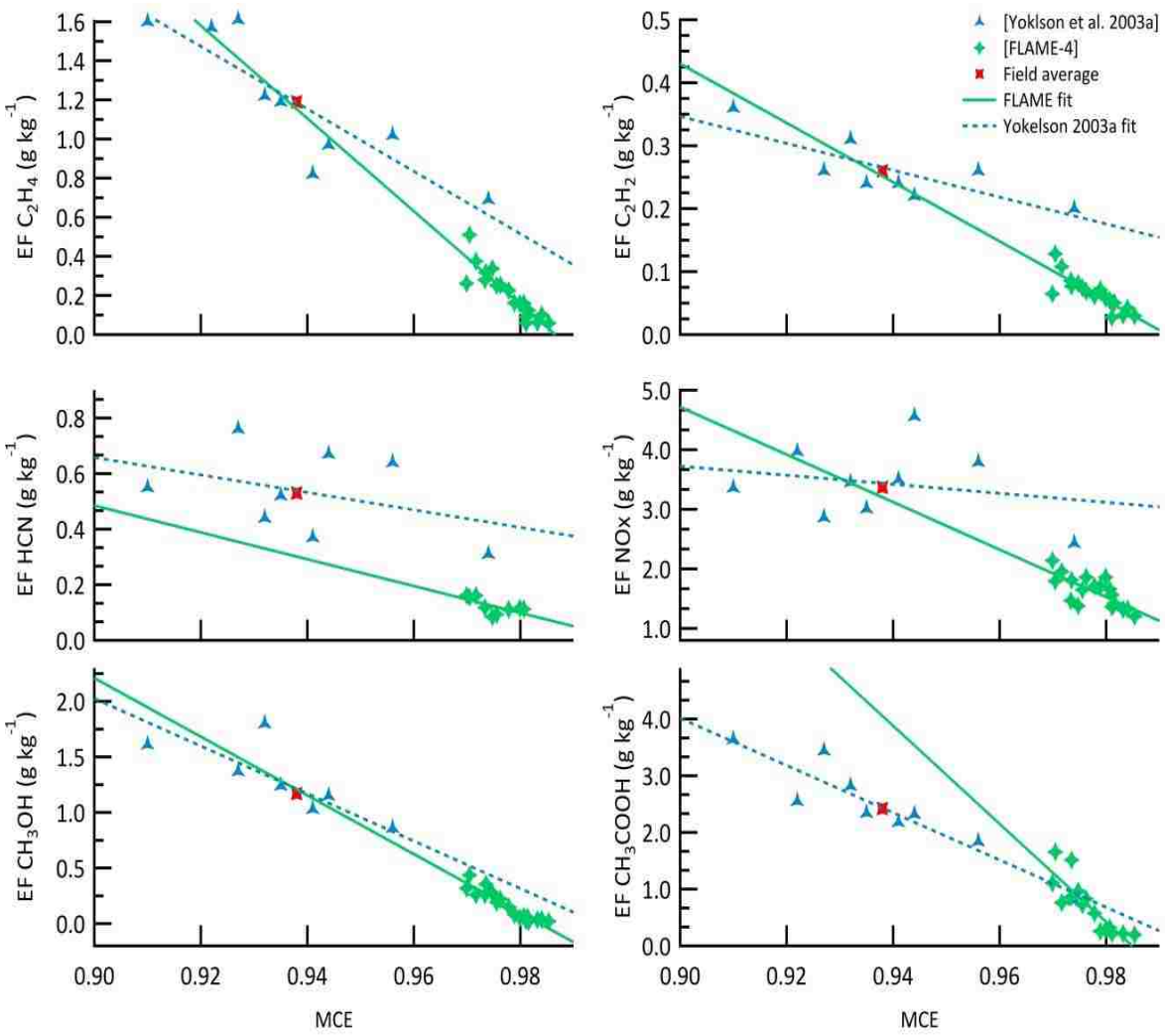

Figure 4.4. Comparison of EF versus MCE between FLAME-4 laboratory African grass fires (green) and airborne field measurements of African savanna fires (blue) for specified hydrocarbons, selected nitrogen containing species, and specified oxygenated species. Lines indicate linear regression of lab-based (green solid line) and airborne (blue dashed line) measurements.

As an alternative to the plot-based analysis, despite the higher MCE of our lab fires, the ERs for smoldering species to CO usually overlap with the field data at the one standard deviation level (Table 4.2, columns 5-7). This is important because most of the compounds emitted by fires are produced during smoldering and the lab ERs can be considered reasonably representative of authentic savanna fires if used this way directly. Some species with "below-average agreement"

using the EF approach do agree well using the ER approach and vice versa. Thus, neither approach is clearly preferred and both are adequate.

A comparison of our EFs for US grasses with field work is not possible due to the lack of the latter type of measurements. However, it is likely that grass fires in the US burn with an average MCE that is lower than our lab average value of 0.961. This should have minimal impact on most of the ERs to CO as discussed above; however, the lab EF versus MCE equations for US grasses could be used to calculate EF for US grasses at the African savanna field MCE (0.938) as shown in the final column of Table 4.2.

Table 4.2. Summary of the comparison of emission factors and emission ratios (to CO) measured in the lab and field for savanna fuels and projected emission factors for US grasses calculated at the savanna grass field average MCE. Values in parentheses are one standard deviation.

	African Savanna grass						US grasses
Species	**Field Yokelson et al. [2003a] (EF)**	**Lab FLAME predict at field avg MCE (EF)**	**Lab EF predict / Field EF avg**	**Field Yokelson et al. [2003a] (ER)**	**Lab FLAME-4 (ER)**	**Field ER avg / Lab ER avg**	**Lab FLAME predict at field avg MCE (EF)**
MCE	0.938	0.938	-	0.938	0.978	-	0.938
Carbon Dioxide (CO_2)	1703	-	-	-	-	-	-
Carbon Monoxide (CO)	71.5	-	-	1	1	1	-
Methane (CH_4)	2.19	2.29	1.04	0.053(0.012)	0.029(0.012)	1.83	2.16
Acetylene (C_2H_2)	0.260	0.251	0.967	0.004(0.001)	0.003(0.001)	1.45	0.448
Ethylene (C_2H_4)	1.19	1.15	0.969	0.017(0.003)	0.008(0.004)	2.01	0.918
Methanol (CH_3OH)	1.17	1.21	1.03	0.014(0.003)	0.005(0.004)	2.77	0.339
Formaldehyde (HCHO)	1.06	2.56	2.41	0.015(0.004)	0.016(0.008)	0.915	0.529
Acetic Acid (CH_3COOH)	2.42	4.05	1.68	0.016(0.002)	0.013(0.007)	1.26	0.873
Formic Acid (HCOOH)	0.270	0.336	1.25	0.003(0.002)	0.002(0.001)	1.55	0.064
Ammonia (NH_3)	0.280	0.691	2.47	0.007(0.004)	0.006(0.004)	1.19	0.709
Hydrogen Cyanide (HCN)	0.530	0.301	0.569	0.009(0.003)	0.005(0.001)	1.70	0.561
Nitrogen Oxides (NO_x as NO)	3.37	3.20	0.950	-	-	-	2.16
Average			1.33(0.65)			1.63(0.54)	
Hydrocarbon avg.			0.994(0.044)			1.76(0.28)	
N-species avg.			1.33(1.00)			1.45(0.36)	
OVOC avg.			1.59(0.61)			1.62(0.80)	

4.3.3 Emissions from Indonesian, Canadian, and North Carolina peat

FLAME-4 OP-FTIR data include the first emissions data for HONO and NO_2 for Indonesian peat fires (Table 4.3). The smoke measurements on three peat samples from Kalimantan represent a significant increase in information given the one previous study of a single laboratory burned sample from Sumatra (Christian et al., 2003). We also report EFs from 4 fires burning extratropical peat that, along with other anticipated FLAME-4 results, adds significantly to the previous laboratory measurements of trace gases emitted by smoldering peat samples that were collected in Alaska and Minnesota (Yokelson et al., 1997). To our knowledge, all detailed chemical characterization of peat fire smoke has been done in the lab.

We discuss/compare the data now available for peat fire emissions from tropical and extratropical ecosystems. The average MCE of our Kalimantan peat fires (0.816) is comparable to the MCE reported for the Sumatran peat (0.838) burned previously by Christian et al. (2003). Figure 4.5 shows the ratio of our Indonesian peat EFs as compiled in the supplementary information (Table S1) to those of Christian et al. (2003) for species reported in both studies. These results display the range of our emissions as well as the study average. The greatest variation within the Indonesian peat fuels was that the single Sumatran peat fire emitted ~14 times more NH_3 per unit biomass combusted than the average of the stack burn Kalimantan samples, even though their MCE and percent nitrogen content were comparable (2.12% for Sumatran peat versus 2.27% for the Kalimantan peat). Comparing extratropical peat between studies, we find that 4.3 times larger NH_3 emission factors were observed for the peat burned by Yokelson et al. (1997) than from our FLAME-4 North Carolina and Canadian stack peat burns. For the extratropical case, only part of the higher levels seen earlier may be due to N-content

differences (0.63-1.28% in FLAME-4 versus 0.78-3.06 % in Yokelson et al. (1997)). We suspect that part of the differences for NH_3 and other species seen in Figure 4.5 (and discussed below) may be due to subtle, compound-specific fuel chemistry differences associated with the fact that the FLAME-4 samples evolved chemically at (and were collected at) greater depths than the samples burned earlier. Mineral content could vary (Table 3.1) and different logging/land-use histories could affect the incorporation of woody material. Another possible cause involves the drying method. In the previous studies the peat was allowed to air dry to a very low moisture content (~5%) before ignition, whereas the FLAME-4 samples were stored wet and cool and then microwaved lightly just before ignition due to new United States Department of Agriculture (USDA) handling/storage restrictions. Drier peat may be consumed relatively more by glowing combustion, which could promote higher NH_3 and CH_4 emissions (Yokelson et al., 1997, Figure 3).

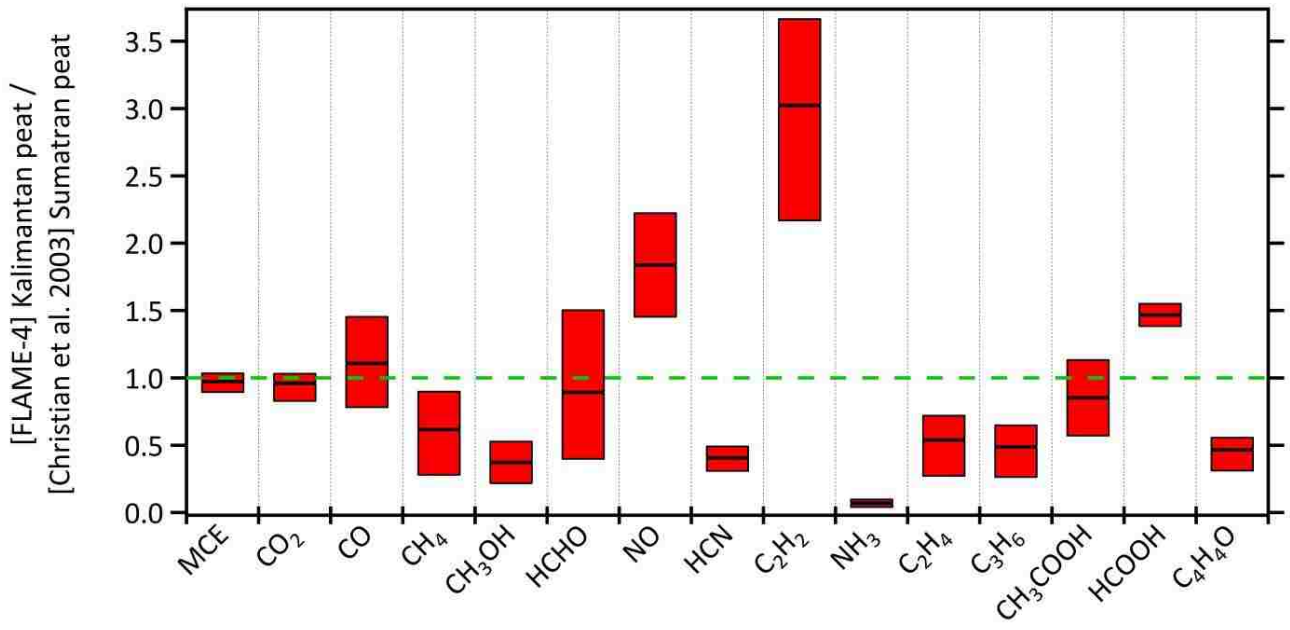

Figure 4.5. The ratio of our Kalimantan peat fire EF to the EF from the single Sumatran peat fire of Christian et al. (2003). The upper and lower bounds of the bars represent ratios based on the range of our data, while the lines inside the bars represent the FLAME-4 study-average EF.

The emissions also differed between the FLAME-4 Kalimantan peat and the earlier Sumatran peat study for N-containing gases that we measured other than NH_3 as shown in Figure 4.6, namely HCN and NO_x. The FLAME-4 Kalimantan peat fire NO_x emissions are 4.2 times higher than previously reported for Sumatran peat, which could impact the predictions of chemical transport models since NO_x emissions strongly influence O_3 and SOA production in aging BB plumes (Trentmann et al., 2005; Alvarado and Prinn, 2009; Grieshop et al., 2009). Larger emissions of NO_x from the Kalimantan peat samples likely occurred because two of the Kalimantan peat samples briefly supported spontaneous surface flaming whereas the Sumatran peat sample was completely burned by smoldering combustion and NO_x is primarily produced during flaming combustion. The large range in EF(HCN) observed (1.38 – 7.76 g kg^{-1}) when considering all peat-burning studies adds uncertainty to any use of this compound as a tracer for

peat fires (Akagi et al., 2011). Although there are noticeable differences between the Kalimantan and Sumatran laboratory fires, with this study we have quadrupled the amount of data available on Indonesian peat, which likely means the new overall averages presented in Table 4.3 are closer to the regional averages than the limited earlier data despite the high variability.

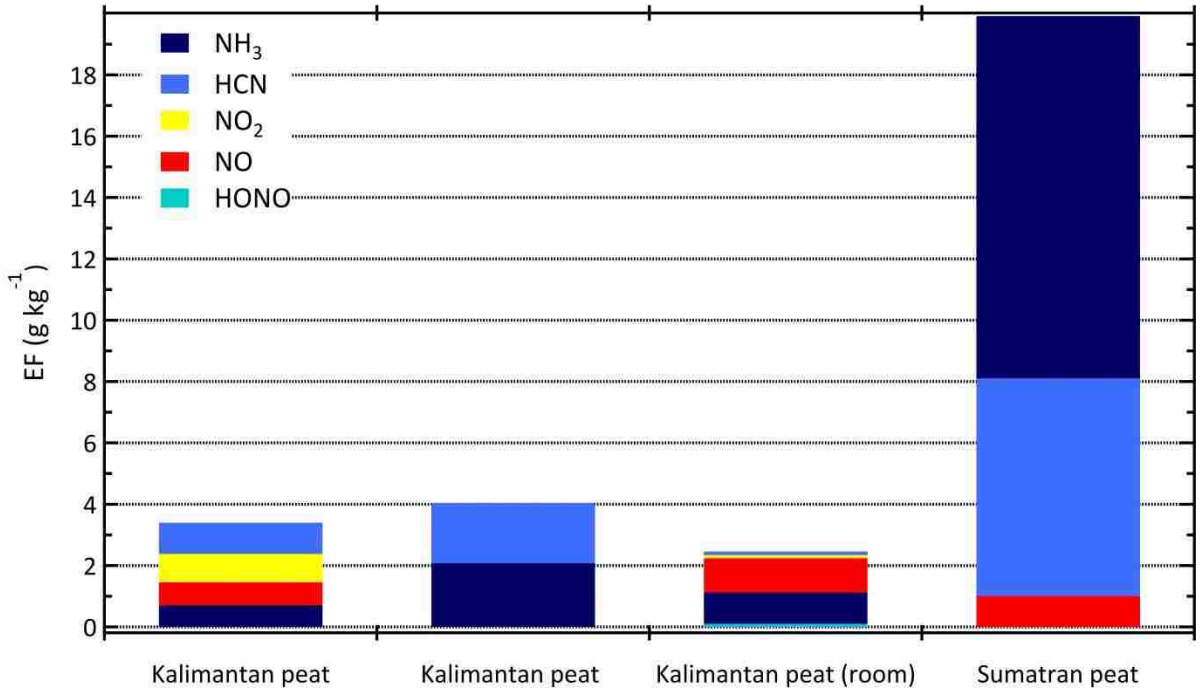

Figure 4.6. Emission factors (g kg-1) for all nitrogen-containing species measured in current Kalimantan and past Sumatran laboratory peat fires (Christian et al., 2003). The Kalimantan peat room burn includes NH3, a sticky species, thus the value should be considered a lower limit estimate.

Sulfur emissions are also variable between peat fire studies. The lack of observed SO_2 emissions from our Kalimantan peat fires is noteworthy since earlier studies of Kalimantan smoke attributed heterogeneous aerosol growth to SO_2 emitted from peat fires with support by unpublished laboratory data (Gras et al., 1999). We did detect small amounts of SO_2 from one of three NC peat fires, but, despite a careful search, no OCS was detected, which was the only

sulfur containing compound detected in previous extratropical peat fire studies (Yokelson et al., 1997).

The emissions of CH_4 from biomass fires make a significant contribution to the global levels of this greenhouse gas (Simpson et al., 2006). The EFs for CH_4 measured for BB studies in general exhibit high variability with higher emissions at lower MCE (Burling et al., 2010). We observed high variability in EFs for CH_4 at similar MCEs for our Kalimantan peat samples (range 5.72 - 18.83 kg^{-1}) with our upper end comparable to the EFs for CH_4 previously reported for the Sumatran peat sample (20.8 g kg^{-1}). Sumatran peat may burn with high variability, but with only one sample there is no probe of this. Emission factors for CH_4 from extratropical peat are also consistently high (4.7 - 15.2 g kg^{-1}). Taken together, all the FLAME-4 results, earlier measurements of EFs for CH_4 for peat, and field measurements of fuel consumption by peat fires (Page et al., 2002; Ballhorn et al., 2009) suggest that peat fires are a significant source of CH_4, an important infrared absorber in our atmosphere (Forster et al., 2007; Worden et al., 2013).

Table 4.3. Comparison of emission factors (g kg^{-1}) for three laboratory peat studies including Yokelson et al. (1997), Christian et al. (2003), and FLAME-4. The average and one standard deviation are shown for each peat type during the study and an overall regional EF is shown for extratropical and Indonesian peat. Values in parentheses are one standard deviation.

Species	Peat Emissions						
	Peat Canadian	**Peat NC**	**Peat AK & MN[a]**	**Overall Extratropical Peat**	**Kalimantan peat**	**Sumatran peat[b]**	**Overall Indonesian Peat**
MCE	0.805(0.009)	0.726(0.067)	0.809(0.327)	0.766(0.061)	0.816(0.065)	0.838	0.821(0.054)
Carbon Dioxide (CO_2)	1274(19)	1066(287)	1395(52)	1190(231)	1637(204)	1703	1653(170)
Carbon Monoxide (CO)	197(9)	276(139)	209(68)	238(97)	233(72)	210	227(60)
Methane (CH_4)	6.25(2.17)	10.9(5.3)	6.85(5.66)	8.67(4.27)	12.8(6.6)	20.8	14.8(6.7)
Acetylene (C_2H_2)	0.10(0.00)	0.16(0.08)	0.10(0.00)	0.13(0.06)	0.18(0.05)	0.059	0.15(0.07)
Ethylene (C_2H_4)	0.81(0.29)	1.27(0.77)	1.37(0.51)	1.13(0.56)	1.39(0.62)	2.57	1.68(0.78)
Propylene (C_3H_6)	0.50(0.00)	1.17(0.63)	2.79(0.44)	1.36(0.96)	1.49(0.63)	3.05	1.88(0.94)
Methanol (CH_3OH)	0.75(0.35)	2.83(2.87)	4.04(3.43)	2.34(2.25)	3.24(1.39)	8.69	4.60(2.95)
Formaldehyde (HCHO)	1.43(0.37)	1.41(1.16)	1.99(2.67)	1.51(0.79)	1.25(0.79)	1.40	1.29(0.65)
Furan (C_4H_4O)	0.88(0.04)	1.78(1.84)	-	1.42(1.39)	0.89(0.27)	1.91	1.15(0.56)
Nitrous Acid (HONO)	0.18(0.00)	0.48(0.50)	-	0.38(0.39)	0.10	-	0.10
Nitric Oxide (NO)	-	0.51(0.12)	-	0.51(0.12)	1.85(0.56)	1.00	1.57(0.63)
Nitrogen Dioxide (NO_2)	-	2.31(1.46)	-	2.31(1.46)	2.36(0.03)	-	2.36(0.03)
Hydrogen Cyanide (HCN)	1.77(0.55)	4.45(3.02)	5.09(5.64)	3.66(2.43)	3.30(0.79)	8.11	4.50(2.49)
Acetic Acid (CH_3COOH)	1.86(1.35)	8.46(8.46)	7.29(4.89)	5.59(5.49)	7.65(3.65)	8.97	8.09(2.69)
Formic Acid (HCOOH)	0.40(0.06)	0.44(0.34)	0.89(1.50)	0.51(0.27)	0.55(0.05)	0.38	0.49(0.11)
Glycolaldehyde ($C_2H_4O_2$)	-	-	1.66(2.64)	1.66	-	-	-
Hydrogen Chloride (HCl)	-	7.68E-03	-	7.68E-03	-	-	-
Ammonia (NH_3)	2.21(0.24)	1.87(0.37)	8.76(13.76)	3.38(3.02)	1.39(0.97)	19.9	7.57(10.72)

[a]Source is *Yokelson et al*. [1997]

[b]Source is *Christian et al.* [2003]

4.3.4 Cooking fire emissions

Biofuel combustion efficiency and emissions depend on the stove design, type and size of fuel, moisture, energy content, and each individual's cooking management (e.g. lighting and feeding) (Roden et al., 2008). The fire-averaged emissions of species we measured by OP-FTIR for four types of stoves and five fuel types are reported in Table 4.4 . From the OP-FTIR data alone we report the first EF for HCN for open cooking fires; the first EF for HCN, NO, NO_2, HONO, glycolaldehyde, furan, and SO_2 for rocket stoves; and the first large suite of compounds for gasifier devices.

We begin with a brief discussion of the first HCN measurements for cooking fires. HCN is emitted primarily by BB (Li et al., 2000) and can be used to estimate the contribution of BB in mixed regional pollution, most commonly via HCN/CO ratios (Yokelson et al., 2007; Crounse et al., 2009). HCN was below the detection limit in previous cooking fire studies using an FTIR system with a short (11 m) pathlength leading to speculation that the HCN/CO emission ratio was low for commonly used wood cooking fuels (Akagi et al., 2011). In FLAME-4, the higher sensitivity FTIR and longer pathlength allowed FTIR detection of HCN on a few cooking fires and the HCN/CO emission ratio ($1.72 \times 10^{-3} \pm 4.08 \times 10^{-4}$) is about a factor of 5 lower than most other BB fuels burned in this study; excluding peat, which had anomalously high HCN/CO ratios up to (2.26×10^{-2}). The divergent HCN/CO ratios for these two types of BB should be considered when using HCN to probe pollution sources in areas where one or both types of burning are important (e.g. Mexico, Indonesia).

Since minimizing cooking fire fuel consumption is a paramount concern for global health, air quality, and climate, it is of great interest to compare the FLAME-4 cooking fire results, which are of unprecedented detail, to a major cookstove performance study by Jetter et al. (2012). We

assess the validity of synthesizing results from these two important studies using the handful of gases measured in both studies (CO_2, CO, and CH_4). In Figure 4.7 we have averaged emissions for all fuels for these three species by stove type for the traditional three-stone fires, the Envirofit rocket stove, and the Philips gasifier stove and compared to identical stoves burning red oak fuel in the performance testing reported by Jetter et al. (2012). We show the ratio of our fire-average (ambient start) EF to the EF reported by Jetter et al. (2012) specific to different operating conditions in their tests: i.e. when the cookstove had (1) an ambient temperature start, (2) hot-start, and (3) when water in the cooking pot started from a simmer. The FLAME-4 emissions of CO_2, CO, and CH_4 for the traditional three-stone and Envirofit rocket designs agree very well with the performance-oriented emissions data for ambient- and hot- start conditions. We obtained higher emissions than Jetter et al. (2012) for the Philips gasifier type stove, but the three-stone and rocket designs are much more widely-used than the gasifier globally and, in general, lower performance may have more relevance to real world use (see below). In any case, the comprehensive emissions speciation in FLAME-4 can be combined with the performance testing by Jetter et al. (2012) to better understand the major currently-used global cooking options with reasonable confidence. We note that our focus was comprehensive emissions speciation, but point out that our traditional three-stone fires took the longest time to reach a steady state, consumed the most fuel, and produced higher mixing ratios of pollutants for their respective fuel types as shown in Figure 4.8.

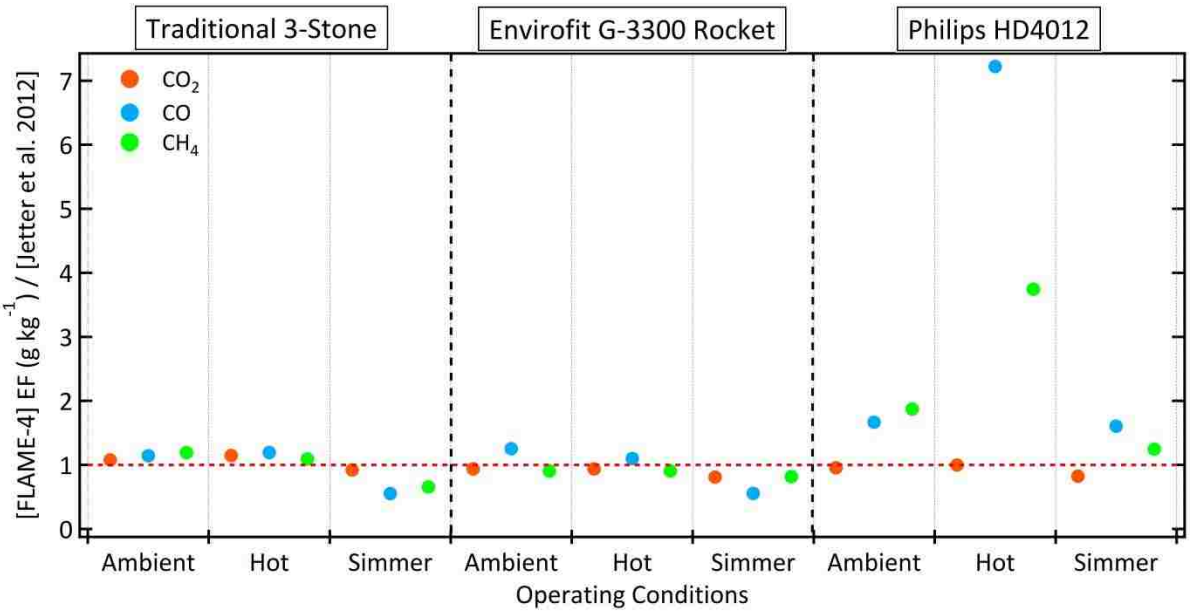

Figure 4.7. Comparison of FLAME-4 3-stone, Envirofit G-3300 Rocket, and Philips HD4012 cookstove EF to EF reported during performance testing by Jetter et al. (2012). The Ezy stove was not tested by Jetter et al. (2012). Each circle represents the FLAME-4 fire average EF of all fuel types measured with all components starting at ambient temperatures compared to the Jetter et al (2012) data collected under regulated operating conditions.

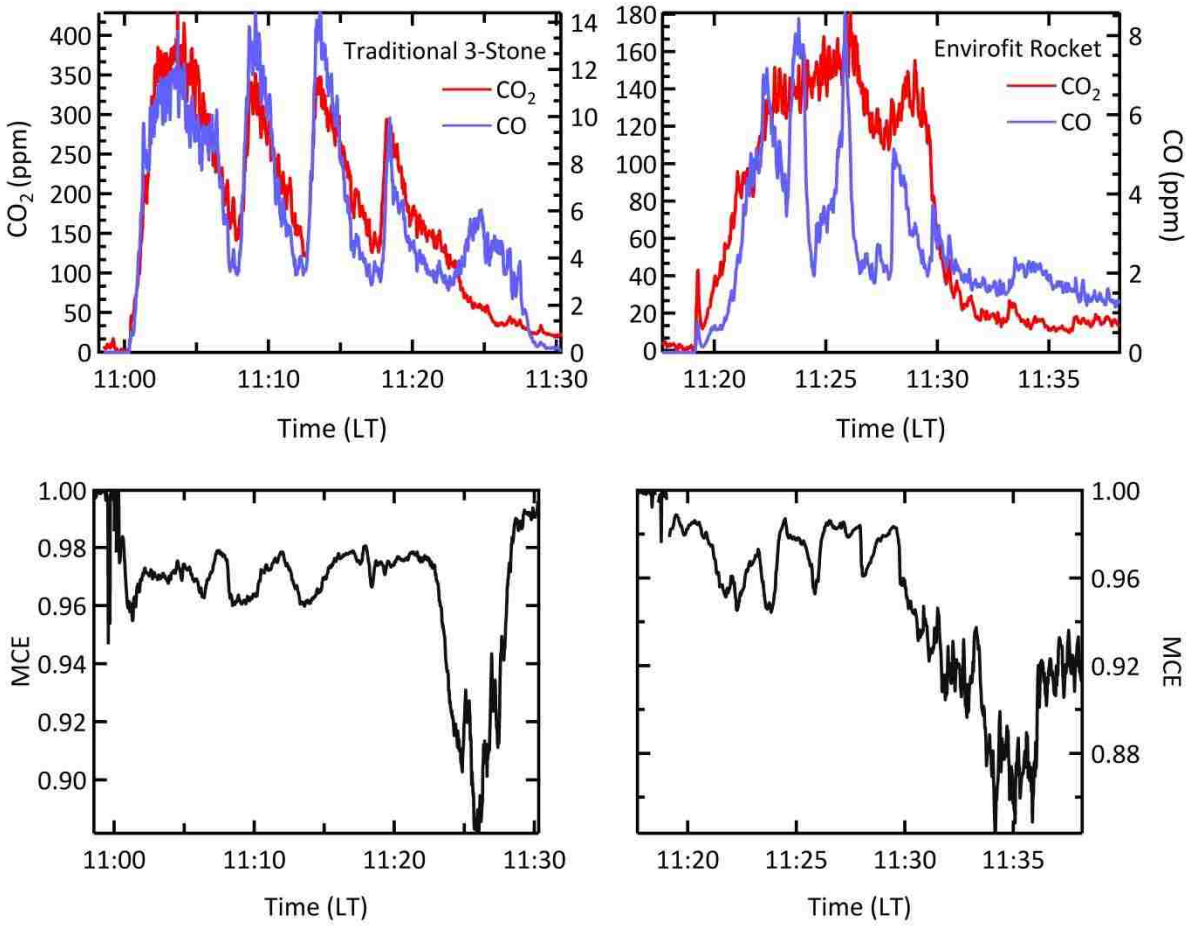

Figure 4.8. Excess mixing ratio profiles of CO and CO_2 for both a traditional 3-stone cooking fire (104) and a more advanced "rocket" design stove (115) showing cleaner combustion and shorter time to reach a steady-state in the stove. The profiles of MCE versus time are included for both stove types.

We now compare our FLAME-4 OP-FTIR-based open cooking fire EFs to field measurements of the EFs from three-stone cooking fires for the few trace gases measured fairly widely in the field (essentially CO_2, CO, and CH_4). Figure 4.9 shows study-average EFs for CH_4 versus MCE for a number of studies including: field data from Zambia (Bertschi et al., 2003a), Mexico (Johnson et al., 2008; Christian et al., 2010), and China (Zhang et al., 2000); laboratory data from FLAME-4 and Jetter et al. (2012); and recommended global averages (Andreae and Merlet 2001; Yevich and Logan, 2003; Akagi et al., 2011). The range of MCE demonstrates the natural

variability of cooking fire combustion conditions. We observe a strong negative correlation of EF(CH_4) with MCE (R^2 = 0.87) that includes all the studies. However, the Jetter et al. (2012) study and especially FLAME-4 are offset to higher MCE than the field average. As discussed earlier, this may reflect more efficient stove use sometimes observed in lab studies. More representative lab EFs can readily be calculated from the MCE plot-based comparison (described in Sect 4.2.3 The FLAME-4 EFs agree well with the field data after adjustment by this approach and we use it to project EF for species not measured in the field: namely HCN (0.071 g kg^{-1}) and HONO (0.170 g kg^{-1}), which we report for the first time, to our knowledge, for open cooking. The $\Delta HONO/\Delta NO_x$ is ~13% confirming that HONO is an important part of the cooking fire NO_x budget. As noted above for other BB types, the lab ERs of smoldering compounds to CO are also fairly representative and included for open cooking in .

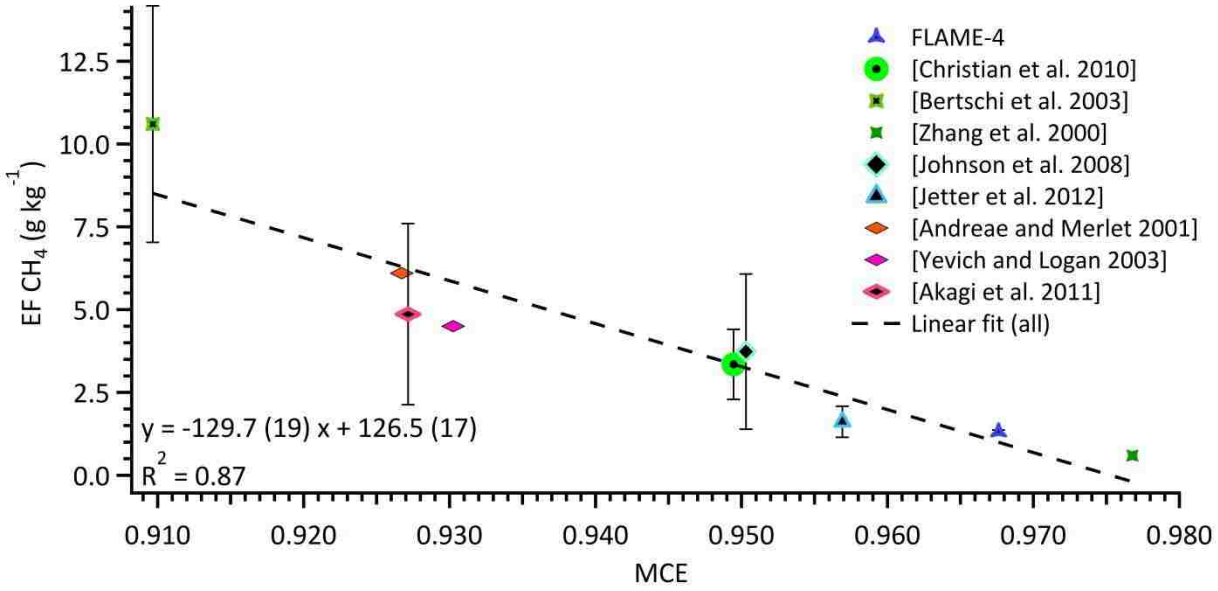

Figure 4.9. Open cooking fire fire-averaged emission factors of CH_4 as a function of MCE for current and past laboratory and field measurements together with the recommended global averages. Error bars indicate the one standard deviation of EF for each study where available.

We also compare with the limited field measurements of rocket stove emissions. The FLAME-4 EFs of species available for comparison generally agree within one standard deviation of the Christian et al. (2010) field Patsari cookstove data. Thus, despite the small sample size, we conclude that the FLAME-4 ERs, EFs, and measurements to be presented elsewhere (such as aerosol optical properties) for these advanced cookstoves can likely be used directly with some confidence to assess the atmospheric impact of using these stoves.

Table 4.4 Fire-average emission factors (g kg^{-1}) for cookstoves. The average emission ratios to CO for smoldering compounds are also shown for three-stone traditional cooking fires.

Species	Traditional and Advanced Cooking stoves									
	3 stone (EF)				Envirofit G3300 Rocket (EF)			Ezy stove (EF)		Philips HD4012(EF)
	Doug Fir	Okote	Red Oak	ER avg (stdev)	Doug Fir	Okote	Red Oak	Millet	Red Oak	Doug Fir
MCE	0.963	0.968	0.972	0.968(0.004)	0.974	0.966	0.985	0.950	0.985	0.984
Carbon Dioxide (CO_2)	1640	1589	1628	-	1662	1586	1661	1503	1656	1682
Carbon Monoxide (CO)	39.8	33.5	30.2	-	28.1	35.8	15.9	49.9	16.3	17.3
Methane (CH_4)	1.27	1.37	1.29	0.067(0.010)	0.90	1.32	0.23	2.64	0.41	0.37
Acetylene (C_2H_2)	0.41	1.07	0.41	0.020(0.013)	0.055	1.26	0.052	0.42	0.23	0.16
Ethylene (C_2H_4)	0.39	1.03	0.37	0.018(0.012)	0.11	0.83	0.063	0.84	0.21	0.16
Propylene (C_3H_6)	bdl	0.11	0.058	0.002(0.001)	bdl	bdl	bdl	bdl	0.012	0.006
Water (H_2O)	0.10	0.14	0.15	0.006(0.002)	0.15	0.14	0.14	0.089	0.19	0.23
Methanol (CH_3OH)	0.70	0.057	0.90	0.014(0.012)	0.56	0.066	0.43	0.77	0.81	0.087
Formaldehyde (HCHO)	0.63	0.24	0.50	0.012(0.005)	0.51	0.25	0.21	0.82	0.40	0.21
Formic Acid (HCOOH)	0.14	0.037	0.32	0.003(0.003)	0.17	0.038	0.15	0.13	0.24	0.050
Acetic Acid (CH_3COOH)	0.63	bdl	4.16	0.036(0.040)	0.72	bdl	1.74	1.98	2.99	0.076
Furan (C_4H_4O)	0.087	bdl	0.087	0.001(0.000)	bdl	bdl	bdl	bdl	0.016	bdl
Glycolaldehyde ($C_2H_4O_2$)	0.094	bdl	0.15	0.002(0.001)	0.18	bdl	bdl	bdl	0.11	0.26
Nitric Oxide (NO)	0.34	0.24	0.42	-	0.48	0.29	0.65	1.03	0.57	0.61
Nitrogen Dioxide (NO_2)	1.04	0.94	1.49	-	1.14	bdl	0.98	bdl	1.57	1.66
Hydrogen Cyanide (HCN)	bdl	0.061	0.059	0.002(0.000)	bdl	0.043	bdl	bdl	bdl	bdl
Nitrous Acid (HONO)	0.18	0.51	0.22	0.005(0.003)	bdl	0.66	bdl	bdl	bdl	bdl
Ammonia (NH_3)	0.019	bdl	0.023	0.001(0.000)	0.021	7.09E-04	0.022	0.23	0.018	0.011
Hydrogen chloride (HCl)	bdl	bdl	bdl	-	bdl	bdl	bdl	bdl	bdl	bdl
Sulfur Dioxide (SO_2)	bdl	0.52	bdl	-	bdl	bdl	bdl	bdl	bdl	bdl

Note: "bdl" indicates mixing ratio was below detection limit

4.3.5 Emission from crop residue fires

FLAME-4 provides the first comprehensive emissions data for burning US crop residue and greatly expands the emissions characterization for global agricultural fires. The EFs and ERs for all the crop residue fuels burned during FLAME-4 are compiled in Tables S1 and S2 in the Supplement. Upon initial assessment of these data, a distinction between two groups emerges. To illustrate this, the EF dependence on MCE for NH_3 emitted by burning CR fuels is illustrated in Figure 4.10. The EFs for NH_3 from alfalfa and organic hay are much larger than for the other crops at all MCE, which makes sense as these crops are high in N (Table 3.1) and are grown partly to meet the high protein needs of large livestock. The EF(NH_3) for millet was smaller than for the other CR fuels. The millet EF could differ because of inherent low N content (Table 3.1) or possible N losses since the samples were collected a year prior to burning. Alfalfa, hay, and millet were also outliers in the EF versus MCE plots made for other trace gases. The remaining fuels, sugar cane and especially rice straw and wheat straw are associated with important crops grown for human nutrition and these three were grouped together to compare laboratory CR fire emissions to the limited available field data as detailed later. Since emissions can readily be grouped as "feed" fuels and "food" fuels, it became apparent that a high degree of fuel specificity may not be necessary for implementation of CR emissions into models.

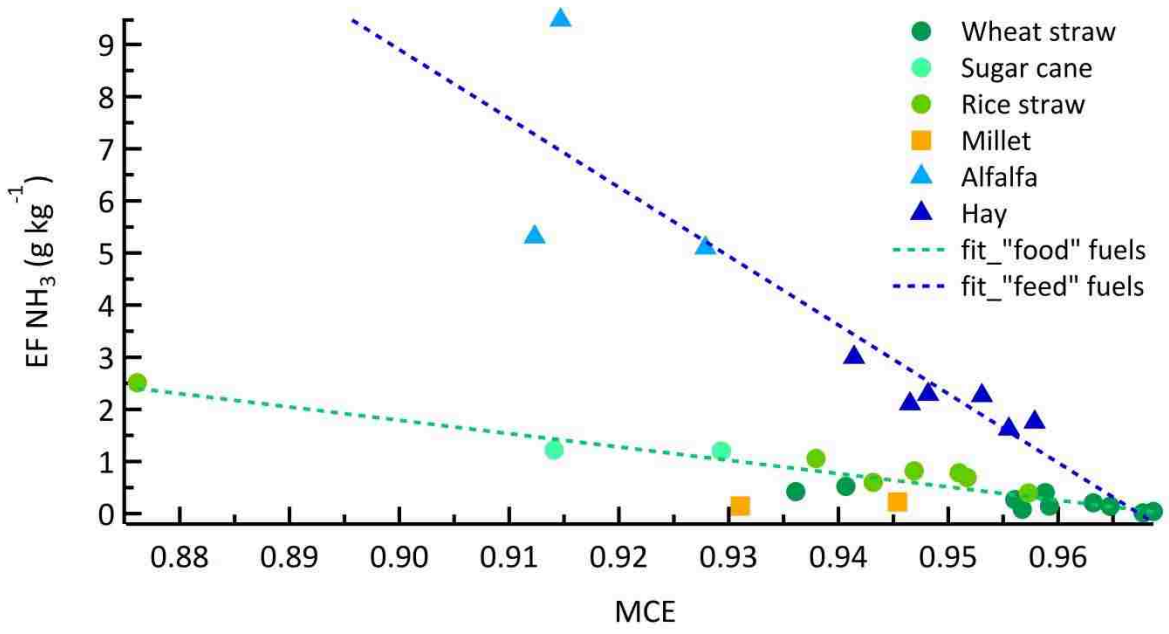

Figure 4.10. Emission factors of NH_3 as a function of MCE for "feed" crop residue fuels (triangles), "food" crop residue fuels (circles), and older millet samples (squares). Also shown are the lines of best fit from "food" fuels (green) and "feed" fuels (blue).

Crops are domesticated "grasses" that would be expected to have high Cl content. The use of agricultural chemicals could further increase Cl content and/or Cl emissions. HCl is the Cl-containing species we could measure with OP-FTIR and its emissions are correlated with flaming combustion as noted earlier. The highest CR EF(HCl) (0.923 g kg^{-1}) was observed for the CR (Maryland wheat straw) with the highest Cl content (2.57%). As seen in Table 3.1, the Cl content of the two conventional wheat straw samples varied significantly with the sample from the east shore of MD being much higher than the inland sample from WA. However, even though the organic wheat straw from Colorado had much lower Cl content than the conventional wheat straw from MD it was significantly higher in Cl than the conventional wheat straw from WA that was also sampled closer to the coast. This confirms our earlier statement that Cl content can depend on more than the distance from the coast for similar vegetation. In addition, the high variability in Cl indicates that measuring the extent to which agricultural chemicals may

contribute to vegetation Cl content and/or Cl emissions would require a more precise experiment where only the applied chemical regime varies. Nevertheless, we confirm above average initial emissions of HCl for this fuel type.

Other notable features of the CR fire emissions are discussed next. Of all our FLAME-4 fuels, sugarcane fires had the highest average EF for formaldehyde, glycolaldehyde, acetic acid, and formic acid. Glycolaldehyde is considered the simplest "sugar-like" molecule; it has been reported as a direct BB emission in laboratory-, ground-, and aircraft-based measurements by FTIR and its atmospheric chemistry (including as an isoprene oxidation product) has been discussed there-in (Yokelson et al., 1997; Ortiz-Montalvo et al., 2012; Akagi et al., 2013; Johnson et al., 2013). In Figure 4.11, we show the EFs for glycolaldehyde as a function of MCE for our FLAME-4 CR fires, all remaining FLAME-4 fuels, a series of airborne measurements from US field campaigns (in 2009-2011) (Johnson et al., 2013), and older laboratory measurements of smoldering rice straw (Christian et al., 2003). The FLAME-4 CR fires have significantly higher EFs than the pine-forest understory and shrubland fires discussed in Johnson et al. (2013), but rice straw fire measurements by Christian et al. (2003) adjusted to reflect the new PNNL reference spectrum have even higher EFs for both glycolaldehyde and acetic acid in comparison to our current sugarcane measurements. The higher EFs in the previous lab study are consistent with the lower MCE that resulted from burning the rice straw in dense piles similar to those observed in Indonesia where manual harvesting is common (Christian et al., 2003).

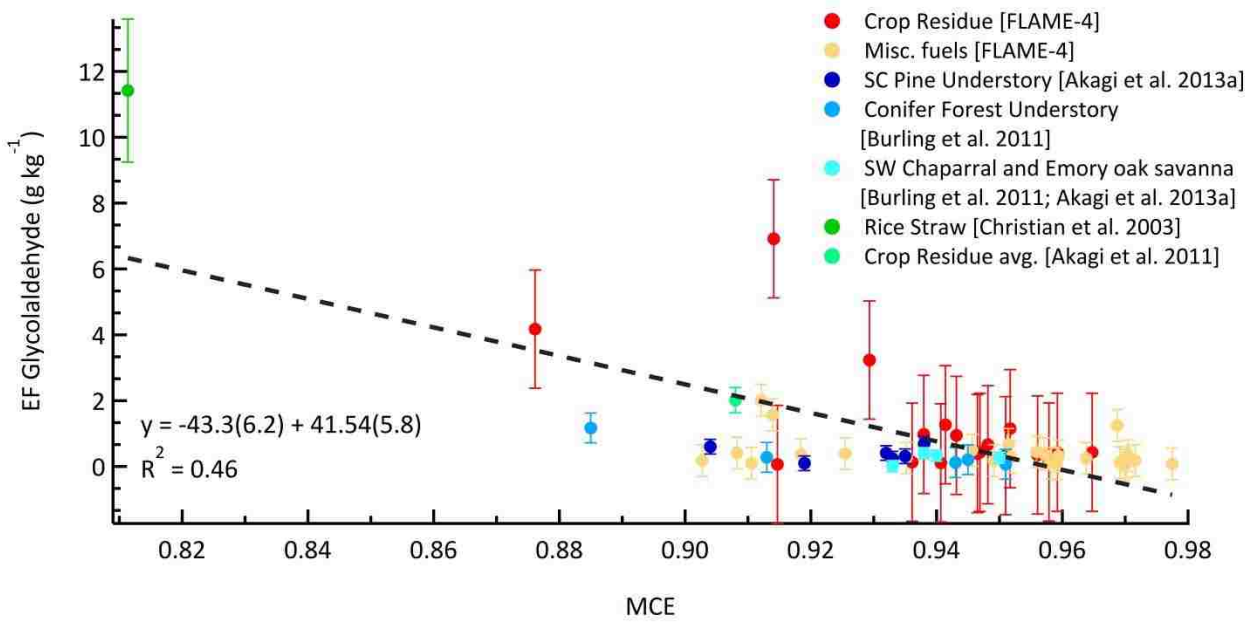

Figure 4.11. Glycolaldehyde EF as a function of MCE shown for current FLAME-4 CR, all remaining FLAME-4 fuels, a series of airborne measurements from US field campaigns, and laboratory rice straw measurements with error bars representing one standard deviation of EF where available.

Next we compare the FLAME-4 CR fire EFs to the limited field data available. Although CR fire emissions are undoubtedly affected by crop type and burning method (loosely packed and mostly flaming versus piled and mostly smoldering), this type of specificity has not been implemented in atmospheric models to our knowledge. All available ground-based and airborne field measurements of CR fire EFs were averaged into a single set of EFs for burning crop residue in the field by Akagi et al. (2011) in their supplementary Table 13. The average ratio of our FLAME-4 MCE plot-based EF predictions for 13 overlapping species to the field EF is close to one, with the good agreement reflecting some cancellation of positive and negative offsets (Table 4.5). The lab and field ERs are also shown to agree very well. The mostly small differences that do occur between the FLAME-4 lab-predicted EFs and the field studies could be due to differences in fuel, burning conditions, and sampling regions. The field CR fire EFs are all from Mexico (Yokelson et al., 2009, 2011; Christian et al., 2010) while FLAME-4 measured EFs for a

variety of fuels from Colorado, Washington, California, Louisiana, China, Taiwan, and Malaysia. Data from recent airborne campaigns sampling US CR fires including SEAC^{4}RS (Studies of Emissions, Atmospheric Composition, Clouds and Climate Coupling by Regional Surveys, www.nasa.gov/mission_pages/seac4rs/index.html) and BBOP (Biomass Burn Observation Project, www.bnl.gov/envsci/ARM/bbop) will provide valuable comparisons to our FLAME-4 CR fire EFs at a later date.

Table 4.5. Summary of the comparison of emission factors and emission ratios (to CO) measured in the lab and field for crop residue fuels. Values in parentheses are one standard deviation.

	Crop Residue					
Species	**Field Akagi et al. [2011][a] (EF)**	**Lab FLAME-4[b] predict at field avg MCE (EF)**	**Lab EF predict / Field EF avg**	**Field Akagi et al. [2011] (ER)**	**Lab FLAME-4 (ER)**	**Field ER avg / Lab ER avg**
MCE	0.925	0.925	-	0.925	0.946	-
Carbon Dioxide (CO_2)	1664	-	-	-	-	-
Carbon Monoxide (CO)	85.6	-	-	-	-	-
Methane (CH_4)	5.01	3.66	0.730	0.102(0.051)	0.072(0.018)	1.42
Acetylene (C_2H_2)	0.230	0.346	1.50	0.003(0.001)	0.005(0.003)	0.542
Ethylene (C_2H_4)	1.16	1.40	1.21	0.014(0.007)	0.017(0.006)	0.787
Propylene (C_3H_6)	0.496	0.605	1.22	0.004(0.002)	0.004(0.002)	0.920
Methanol (CH_3OH)	2.67	1.97	0.738	0.027(0.014)	0.017(0.008)	1.60
Formaldehyde (HCHO)	1.85	2.02	1.10	0.020(0.010)	0.024(0.011)	0.840
Acetic Acid (CH_3COOH)	4.52	4.07	0.901	0.025(0.012)	0.019(0.013)	1.32
Formic Acid (HCOOH)	1.00	0.669	0.669	0.007(0.004)	0.003(0.003)	2.36
Nitric Oxide (NO)	2.06	1.49	0.721	-	-	-
Nitrogen Dioxide (NO_2)	3.48	1.71	0.491	-	-	-
Nitrogen Oxides (NO_x as NO)	3.64	2.08	0.572	-	-	-
Ammonia (NH_3)	1.76	1.15	0.654	0.034(0.017)	0.016(0.011)	2.07
Hydrogen Cyanide (HCN)	0.160	0.399	2.49	0.002(0.001)	0.005(0.002)	0.421
Absolute average			1.00(0.54)			1.23(0.64)
Hydrocarbon avg.			1.17(0.32)			0.918(0.370)
N-species avg.			0.986(0.847)			1.24(1.16)
OVOC avg.			0.851(0.191)			1.53(0.64)

[a] Supplementary Table 13 in Akagi et al. [2011]

[b] Fuels grouped as food sources as detailed in Sect. 4.3.5

4.3.6 Emission from US shrubland and coniferous canopy fires

We burned fresh boughs from the following coniferous vegetation that is widespread in the western US and Canada: ponderosa pine, black spruce, and juniper. The canopy of these trees/shrubs is sometimes consumed in prescribed burns, but that is more commonly the case in wildfires, especially crown fires. However, these fuels were not burned to simulate real, complete wildfire fuel complexes: rather they were of interest as an extension of FLAME-3 smog chamber experiments investigating organic aerosol transformations (Hennigan et al., 2011). In FLAME-3 black spruce produced the most secondary organic aerosol upon aging while ponderosa pine produced the least SOA. The SOA results for these and other fuels from FLAME-4 will be reported separately (Tkacik et al., 2016). The OP-FTIR data is of value to characterize the starting conditions in the smog chambers. For instance, in FLAME-4 the ponderosa pine burns were characterized by a lower MCE (0.917 ± 0.032 , range 0.839-0.952), hence more smoldering-dominated burns than the black spruce burns (MCE 0.951 ± 0.012, range 0.933 - 0.970). Both ponderosa pine and spruce boughs were also burned in the lab fire study of Yokelson et al. (2013a) and, collectively with the FLAME-4 measurements, we now have more detailed information on the initial emissions from these fuels than was available during the FLAME-3 campaign.

There are just a few published field measurements of emissions from chaparral fires, which include: (1) Airborne measurements of EFs reported by Burling et al. (2011) for 16 of the trace-gas species also measured in this work for five California chaparral fires and (2) a limited number of trace gases reported by Radke et al. (1991) and Hardy et al. (1996) for prescribed chaparral burns. For these published field studies as a group the average EF is 0.935 ± 0.011.We combined the seven chamise and three manzanita burns from FLAME-4 to represent chaparral

fuels and obtained a slightly lower lab-average MCE of 0.929 ± 0.017 (spanning a range of 0.903-0.954). The lab MCE and EFs agree well with the MCE and EFs from field measurements, which suggests that FLAME-4 measurements can be used directly and confidently including for species and properties not yet measured in the field. The emissions data from recent field studies of wildfires (SEAC^{4}RS, BBOP) that burned some coniferous canopy and chaparral fuels can be compared with our FLAME-4 EFs in the future.

4.3.7 Emission from tire fires

To our knowledge, FLAME-4 presents the first comprehensive emissions data for burning tires. Emissions are affected by fuel composition and tires are composed of natural and synthetic rubber, carbon black, fabric, reinforcing textile cords, steel-wired fibers and a number of chemical accelerators and fillers added during the manufacturing process (Mastral et al., 2000). One such additive is sulfur which is essential during the vulcanization process in creating rigid and heat resistant tires. The sulfur could be emitted during combustion of tires in various forms including SO_2, which is a monitored, criteria air pollutant chiefly because atmospheric oxidation of SO_2 results in acid rain and sulfate aerosol particles that are a major climate forcing agent with adverse effects on human health (Schimel et al., 1996; Lehmann and Gay, 2011; Rohr and Wyzga, 2012). For the two tire burns conducted during FLAME-4 the average MCE was 0.963; burns dominated by flaming combustion. SO_2 is a product of flaming combustion (see Figure 4.1 or Lobert et al., 1991) and our tire samples likely contained high amounts of S that was efficiently converted to SO_2 by the high MCE burns resulting in a very high average EF(SO_2) of 26.2 ± 2.2 g kg^{-1}. To put this in perspective, our second largest EF(SO_2) arose from giant cutgrass (3.2 g kg^{-1}), which was about three times the typical FLAME-4 EF(SO_2) of ~1 g kg^{-1}. About ~48% of the scrap tires generated in the US in 2005 (RMA, 2011) were used as fuel (coal

substitute) and this was the fate of ~20% of the scrap tires in Canada in 2004 (Pehlken and Essadiqi, 2005). However, our calculations suggest that tire combustion only contributed ~0.5% of SO_2 emissions for the US and Canada in 2005 (Smith et al., 2011). Meanwhile, combustion of fossil fuels, specifically coal, was estimated to account for 56% of the world SO_2 emissions in 1990 (Smith et al., 2001). Despite the low total global significance compared to coal it is quite possible for the SO_2 and other combustion products from tire burning to have important local effects (http://thegazette.com/2012/06/01/how-is-iowa-city-landfill-fire-affecting-air-quality/).

Many species including HONO, NO_2, HCN, CH_3COOH, HCOOH, and furan were quantified for the first tire burn (~500 g) but fell below the detection limit during the second smaller fire (~50 g). For one such species, gas-phase nitrous acid (HONO), tire burning produced the largest EF (1.51 g kg^{-1}) of the entire study. Daytime photolysis of HONO serves to form NO and the atmospheric oxidant OH on a timescale of 10-20 min (Schiller et al., 2001). To normalize for differences in the nitrogen content of fuels shown in Table 3.1, it is useful to compare ΔHONO to ΔNO_x. The ER($\Delta HONO/\Delta NO_x$) for tire burns (19%) is incidentally within the typical range of ~3-30% for BB studies compiled in Akagi et al. (2011). The EF of HONO (1.51g kg^{-1}) and NO_x as NO (3.90 g kg^{-1}) were among the largest for this study while the EF(HCN) was small (0.36 g kg^{-1}) and NH_3 remained below the detection limit even in the bigger tire fire. These results suggest that much of the fuel nitrogen is converted to NO_x and HONO and that the mid-range N-content estimated for tires by Martinez et al. (2013) shown in Table 3.1 (0.57%) is large enough to support the observed EF.

4.3.8 Emission from burning trash and plastic bags

Published measurements of trash burning emissions are rare. The FLAME-4 measurements are the first to report EF for glycolaldehyde for trash burning. Since it is difficult to be confident

about waste simulation, we first assess the relevance of the FLAME-4 trash fire simulations by comparison to the limited previous data. The emissions from burning simulated military waste were evaluated in two previous studies for a number of species not measured by OP-FTIR including polycyclic aromatic hydrocarbons, particulate matter, several volatile organic compounds, polychlorinated or brominated dibenzodioxins, and furans (Aurell et al., 2012; Woodall et al., 2012). These two studies are not discussed further here. In Table 4.6 we show the EFs from the two trash burns in FLAME-4 and "overlapping" previously-published garbage burning EF including those from 72 spot field measurements of fires in authentic Mexican landfills reported by Christian et al. (2010), an airborne campaign that sampled a single dump fire in Mexico (Yokelson et al. 2011), and a single previous laboratory simulation (Yokelson et al., 2013a).

The first FLAME-4 trash fire simulation had much higher HCl, HCHO, and glycolaldehyde and lower NO_x, NH_3, and SO_2 than the second simulation. The average of the two FLAME-4 burns and most of the trash fire EF we measured in FLAME-4 are well within the range observed in the field for hydrocarbons and the oxygenated organic compounds except for acetic acid which had mixing ratios below the detection limit in FLAME-4. The increase in estimated carbon content between studies accounts for the considerable increase in EF(CO_2) for the FLAME-4 burns. The EFs reported in Table 4.6 for field data assumed an overall carbon fraction of 40% while an estimated value of ~50% was calculated for FLAME-4 waste (see Table 3.2). There were significantly lower emissions of N-containing compounds and HCl in the FLAME-4 trash burn simulations compared to the Mexican landfill fires. The single laboratory trash fire EF(HCl) reported by Yokelson et al. (2013a) (10.1 g kg^{-1}) and the higher of two EF(HCl) from FLAME-4 (1.52 g kg^{-1}) lie close to the upper and lower end of the actual Mexican landfill fire results (1.65-

9.8 g kg^{-1}). Based on the EF(HCl) of pure polyvinyl chloride (PVC) reported in Christian et al. (2010) we expected a higher EF(HCl) correlated to the high PVC mass percentage (9.8%) in our simulated trash sample that contained PVC. The EF(HCl) is affected by the combustion factor of the PVC itself and the actual percent burned may have been low during our simulation. The differences between the emissions of Mexican landfill fires and our laboratory garbage fires likely reflect the general difficulty of simulating real-world landfill content; in particular we likely underrepresented a nitrogen source such as food waste in lab simulations. While a more realistic representation of complex, real-world waste would have been ideal, the FLAME-4 data should be useful for enhancing our knowledge of the emissions from some components of this globally important, but under-sampled source.

We burned one trash component separately in one fire: namely plastic shopping bags. Much of the plastic produced globally ends up in landfills with alternative means of disposal including incineration, open burning, or use as an alternative household fuel in developing countries. It has been estimated that 6.6 Tg CO_2 was generated from the incineration of plastics in waste in 2011 in the US and that incineration is the disposal method for 7-19 percent of waste in the US generating an estimated 12 Tg CO_2 annually (USEPA, 2013). Shopping bags primarily consist of high and low density polyethylene (HDPE, LDPE) with a carbon content of 86%, the highest value in this study (USEPA, 2010). The EF(CO_2) of 3127 g kg^{-1} is slightly larger than that from shredded tires (2882 g kg^{-1}). During the single burn of "pure" plastic bags, flaming combustion dominated more than in any other FLAME-4 fire, as can be seen in the high MCE (0.994), the steady high ratio of $\Delta CO_2/\Delta CO$ (Figure 4.12) and by the fact that many smoldering combustion species remained below the OP-FTIR detection limit. In this respect, plastic bags are higher quality fuel than biomass although less-controlled combustion of mixed refuse, or a mix of

plastics and biomass, would likely result in less efficiency and greater EFs for smoldering species.

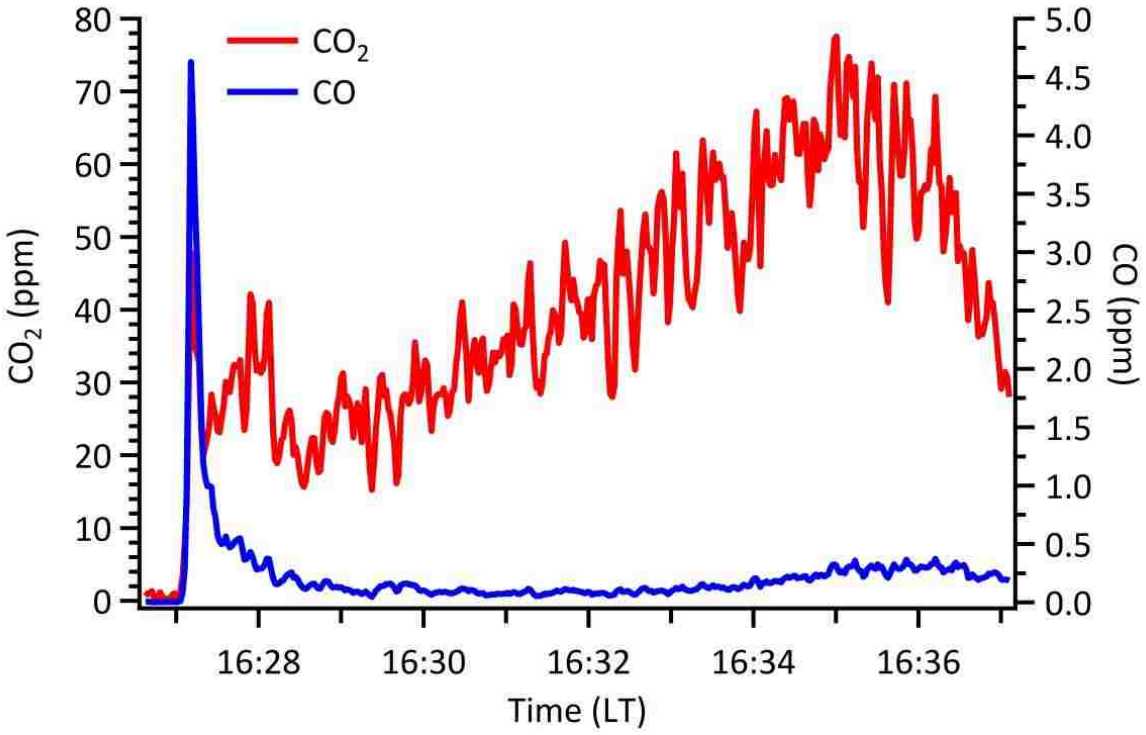

Figure 4.12. Excess mixing ratio profiles of CO and CO_2 for the FLAME-4 plastic bag burn characterized by a large long-lived ratio of $\Delta CO_2/\Delta CO$ corresponding to strong flaming combustion.

Table 4.6. Emission factors (g/kg dry fuel) for previously published garbage burns and current FLAME-4 burns

Species	Trash Burning							
	EF Christian et al. [2010]				EF Yokelson et al. [2011]	EF Yokelson et al. [2013]	EF FLAME-4	
	ground				airborne	laboratory	laboratory	
MCE	0.964	0.911	0.958	0.968	0.974	0.967	0.969	0.977
Carbon Dioxide (CO_2)	1404	1270	1385	1409	1538	1341	1773	1813
Carbon Monoxide (CO)	33.8	79.1	38.7	29.6	26.1	28.7	36.4	26.6
Methane (CH_4)	1.16	10.3	2.18	1.14	0.77	0.31	0.94	0.66
Ethylene (C_2H_4)	0.82	4.75	2.2	0.99	0.32	1.74	1.02	0.95
Acetylene (C_2H_2)	0.14	0.72	0.53	0.2	bdl	0.44	0.40	0.25
Propylene (C_3H_6)	0.36	3.34	0.97	0.36	bdl	0.85	0.68	0.61
Formaldehyde (HCHO)	0.56	0.48	0.68	0.76	bdl	0.76	1.26	0.59
Methanol (CH_3OH)	0.31	2.81	0.4	0.26	bdl	0.14	0.23	0.11
Acetic Acid (CH_3COOH)	0.58	7.4	0.92	0.78	bdl	0.55	bdl	bdl
Formic Acid (HCOOH)	0.05	0.14	0.34	0.19	bdl	0.18	0.02	0.07
Glycolaldehyde ($C_2H_4O_2$)	nm	nm	nm	nm	nm	nm	1.25	0.08
Furan (C_4H_4O)	nm	nm	nm	nm	nm	0.05	bdl	0.08
Nitric Oxide (NO)	bdl	bdl	bdl	bdl	bdl	0.42	0.46	0.58
Nitrogen Dioxide (NO_2)	bdl	bdl	bdl	bdl	6.87	0.70	0.49	1.05
Nitrogen Oxides (NO_x as NO)	bdl	bdl	bdl	bdl	4.48	0.73	0.62	1.06
Ammonia (NH_3)	0.46	2.52	0.39	bdl	0.77	bdl	bdl	0.06
Hydrogen Cyanide (HCN)	bdl	bdl	bdl	bdl	0.47	0.12	0.10	0.01
Nitrous Acid (HONO)	nm	nm	nm	nm	nm	0.05	0.33	0.15
Hydrogen chloride (HCl)	1.65	bdl	9.8	3.02	bdl	10.1	1.52	0.09
Sulfur Dioxide (SO_2)	nm	nm	nm	nm	nm	0.77	bdl	0.90

Note: "nm" indicates not measured, "bdl" indicates mixing ratio was below detection limit

4.4 Conclusions

We used an open-path FTIR to measure the emissions of 20 of the most abundant trace gases produced by laboratory burning of a suite of locally to globally significant fuels including: African savanna and US grasses; crop-residue; temperate, boreal, and Indonesian peat; traditional cooking fires and cooking fires in advanced stoves; US coniferous and shrubland fuels; shredded tires; and trash. We report fire-integrated emission ratios (ER) to CO and emission factors (EF, grams of compound emitted per kilogram of fuel burned) for each burn.

The fire-type average EF and ER for sticky species (HCl, NH_3, HCOOH, CH_3COOH, glycolaldehyde, SO_2) are computed without the data from the room burns (due to losses on aerosol or lab surfaces) as shown in Tables S1 and S2 in the Supplement.

Many of the fire-types simulated have large global significance, but were not sampled extensively in the past. The fire types simulated that have been subject to extensive past study were sampled with new instrumental techniques in FLAME-4. In either case it is necessary to establish the relevance of the lab simulations by comparison to field data when available. The emissions from field fires depend on a large number of fuel and environmental variables and are therefore highly variable. Laboratory BB can sometimes occur with a different average ratio of flaming to smoldering combustion than is observed for field fires in similar fuels. Smoldering combustion produces the great majority of measured emitted species and we find that our ER to CO for smoldering compounds are normally similar to field results. Based on lab/field comparisons, we conclude that our lab-measured EF for some of the fires can be adjusted to better represent typical open burning. We describe a straight forward procedure for making these adjustments when warranted. For some fuels there is only lab emissions data available (e.g. peat and tires) and we must rely solely on that. In other cases (e.g. rocket stoves and chaparral) both the lab ER and EF can be used directly to supplement field data. For some fuels (e.g. African grasses and crop residue) the ER can be used directly and we provide a procedure to adjust the lab EF that is based on analysis of the overlap species and has a characterized uncertainty. Thus, all the FLAME-4 results for various species and properties, especially those yet unmeasured in field studies, should be useful to enhance the understanding of global BB. As mentioned above, this is important in part because the smoke characterization in FLAME-4 featured the first use of

many instruments, the first sampling with some instruments for certain fuels, and the first use of dual smog chambers to characterize the chemical evolution of smoke during simulated aging.

For tropical peat (a major global fuel type) there is very little data even after we quadrupled the number of samples burned as part of FLAME-4. Significant differences in EF between FLAME-4 Kalimantan peat and Sumatran peat from Christian et al. (2003) include ~14 times greater NH_3 emission from the Sumatran peat even though each study reported similar nitrogen contents (2.12% and 2.27%). Other emissions were also variable from Canadian, North Carolina, and Indonesian peat. These variable emissions could reflect differences in sampling depth; chemical, microbial, and physical weathering; drying and ignition methods, and land-use history. This highlights the need for field measurements and underscores the challenge of developing robust emissions data for this fuel type. Despite the high variability, the large increase in sampling should increase confidence in the mean emission factors for this fuel type. In addition, in all the lab peat fires studied, the emissions of HCN, NH_3, and CH_4 were elevated in comparison to the average for other types of BB.

Emissions were quantified for open-cooking fires and several improved cooking stoves. We obtained good agreement for the few species that were also measured in a major cook-stove performance study indicating that our far more detailed emissions characterization in FLAME-4 can be closely linked to the performance results. This should enable a more comprehensive assessment of the economic and air quality issues associated with cooking technology options. Some of the gas-phase species (HONO, HCN, NO_x, glycolaldehyde, furan, and SO_2) are reported for "rocket" stoves (a common type of improved stove) for the first time and this emission data can be used directly without an adjustment procedure. A large set of EF for gasifier type stoves is also reported for the first time. We report the first $\Delta HCN/\Delta CO$ ER for open cooking fires, which

dominate global biofuel use. The low HCN/CO ER from cooking fires and the high HCN/CO ER from peat fires should be factored into any source apportionment based on using HCN as a tracer in regions featuring one or both types of burning.

We report the first extensive set of trace gas EF for US crop residue fires, which account for the largest burned area in the US. We report detailed EF for burning rice straw from the US and several Asian countries where this is a major pollution source. Burning food crop residues produced clearly different emissions from feed crop residues. Feed crop residues had high N-content and burning alfalfa produced the highest NH_3 emissions of any FLAME-4 fire. Burning sugarcane produced the highest emissions of glycolaldehyde and several other oxygenated organic compounds, possibly related to high sugar content. Increased knowledge of agricultural fire emissions should improve atmospheric modeling at local to global scales.

In general, for a wide variety of biomass fuels, the emissions of HCl are positively correlated with fuel Cl-content and MCE and larger than assumed in previous inventories. The HCl emissions are large enough that it could be the main chlorine-containing gas in very fresh smoke, but partitioning to the aerosol could be rapid. The emission factors of HCl and SO_2 for most crop residue and grass fires were elevated above the study average for these two gases consistent with their generally higher fuel Cl/S and tendency to burn by flaming combustion. The linkage observed between fuel chemistry or specific crops and the resulting emissions illustrates one advantage of lab-based emissions research. In contrast, our laboratory simulation of garbage burning in FLAME-4 returned an EF(HCl) (1.52 g kg^{-1}) near the lower end of actual landfill fire measurements (1.65 g kg^{-1}), possibly because a large fraction of the added polyvinyl chloride did not burn. Lower N-emissions from lab garbage burning than in Mexican landfills could be linked to missing N in our waste simulation, but we don't have nitrogen analysis of authentic waste to

verify this. The average SO_2 EF from burning shredded tires was by far the highest for all FLAME-4 fuels at 26.2 g kg^{-1}. High SO_2 emissions together with high EF for NO_x and HONO are consistent with high sulfur and nitrogen content of tires and a tendency to burn by flaming combustion. Finally, we note that this paper gives an overview of the FLAME-4 experiment and the trace gas results from OP-FTIR alone. Much more data on emissions and smoke properties will be reported separately.

Chapter 5 : PTR-TOF-MS component of FLAME-4

5.1 Introduction PTR-TOF-MS

The large number of unknown NMOCs emitted by BB sources severely limits our ability to accurately model atmospheric impacts. Measurements capable of identifying and quantifying rarely measured and presently unidentified emissions of NMOCs are vital for advancing current understanding of the BB impact on air quality and climate.

Proton-transfer-reaction time-of-flight mass spectrometry (PTR-TOF-MS) is an emerging technique that simultaneously detects most NMOCs present in air samples including: oxygenated organics, aromatics, alkenes, and nitrogen-containing species at parts per trillion detection limits (pptv) (Jordan et al., 2009; Graus et al., 2010). The instrument uses H_3O^+ reagent ions to ionize NMOCs via proton-transfer-reactions to obtain high resolution mass spectra of protonated NMOCs with a low degree of molecular fragmentation at a mass accuracy sufficient enough to determine molecular formulas ($C_wH_xN_yO_z$).

Although there are many advantages to PTR-TOF-MS over conventional PTR quadrupole mass spectrometers (increased mass range, high measurement frequency, and high mass resolution) there remain several difficulties involving PTR technology including (1) detection is limited to molecules with a proton affinity greater than water, (2) complicated spectra due to parent ion fragmentation or cluster ion formation, and (3) the inability of the method to isolate isomers. Despite the limitations of this technology, PTR-TOF-MS is ideal for studying complex gaseous mixtures such as those present in BB smoke.

A major target of FLAME-4 was the identification and quantification of highly reactive NMOCs for a number of fuel and fire-types including undersampled sources. In doing so we will better

understand the distribution of emitted carbon across a range of volatilities in fresh smoke. The collected EFs for the range of fire-types could improve and update the capability of current photochemical models to simulate the climatic, radiative, chemical, and ecological impacts of smoke on local to global scales. As discussed in the previous chapter, FLAME-4 emissions were compared extensively to field measurements of fire emissions and they were shown to be representative of "real-world" BB either as is or after straightforward adjustment procedures detailed therein. In this chapter, we describe the first application (to our knowledge) of PTR-TOF-MS technology to laboratory BB smoke to characterize emissions from a variety of authentic globally significant fuels. We report on several new or rarely measured gases and present a large set of useful emission ratios and emission factors for major fuel types that can inform/update current atmospheric models.

5.2 PTR-TOF-MS experimental

5.2.1 PTR-TOF-MS data collection

Real-time analysis of NMOCs was performed using a commercial PTR-TOF-MS 8000 instrument from Ionicon Analytik GmbH (Innsbruck, Austria) that is described in detail by Jordan et al. (2009). The PTR-TOF-MS sampled continuously at a frequency of 0.2 Hz through heated PEEK tubing (0.0003 m o.d., 80°C) positioned facing upward to limit particulate uptake. The instrument was configured with a mass resolution ($m/\Delta m$) in the range of 4000 to 5000 at *m/z* 21 and a typical mass range from *m/z* 10-600. The drift tube was operated at 600 V with a pressure of 2.30 mbar at 80 °C (E/N ~ 136Td, with E as the electric field strength and N as the concentration of neutral gas; 1 Td=10^{-17} V cm^2). A dynamic dilution system was set up to reduce the concentration of sampled smoke and minimize reagent ion depletion. Mass calibration was performed by permeating 1,3-diiodobenzene (protonated parent mass at *m/z* 330.85; fragments at

m/z 203.94 and 204.94) into a 1 mm section of Teflon tubing used in the inlet flow system. The high mass accuracy of the data allowed for the determination of the atomic composition of protonated NMOC signals where peaks were clearly resolved. The post-acquisition data analysis to retrieve counts per second based on peak analysis was performed according to procedures described in detail elsewhere (Müller et al., 2010, 2011, 2013). An initial selection of ions (~68 masses up to *m/z* ~143) was chosen based upon incidence and abundance for post-acquisition analysis. In select cases (nominally one fire of each fuel type), additional compounds (~50 masses) were analyzed and are reported. A reasonable estimation procedure showed that the peaks selected for analysis accounted for >99% of the NMOC mass up to *m/z* 165 in our PTR-TOF-MS spectra. An earlier BB study (Yokelson et al., 2013a) using mass scans to *m/z* 214 found that ~1.5% of NMOC mass was present at *m/z* > 165.

5.2.2 PTR-TOF-MS Calibration

Calibration of the PTR-TOF-MS was performed every few days at the FSL using a bottle gas standard (Apel-Riemer Environmental). Calibrations were performed by adding a known quantity of calibration gas directly to the end of the PTR-TOF-MS sample inlet. The calibration mixture included: formaldehyde (HCHO); methanol (CH_3OH); acetonitrile (CH_3CN); acetaldehyde (CH_3CHO); acetone (C_3H_6O); dimethyl sulfide (C_2H_6S); isoprene (C_5H_8); methyl vinyl ketone (C_4H_6O); methyl ethyl ketone (C_4H_8O); benzene (C_6H_6); toluene ($C_6H_5CH_3$); p-xylene (C_8H_{10}); 1,3,5-trimethylbenzene (C_9H_{12}); and α-pinene ($C_{10}H_{16}$).

The normalized sensitivity of the instrument (ncps/ppbv) was determined for calibrated compounds based on the slope of the linear fit of signal intensities (normalized to the H_3O^+ signal, ~10^6 cps) versus a range of volumetric mixing ratios (VMR). Multi-point calibration curves varied due to instrumental drift and dilution adjustments, accordingly, and average

calibration factors (CFs, ncps/ppbv) were determined throughout the field campaign as described by Warneke et al. (2011) and were used to calculate concentrations.

Quantification of the remaining species was performed using calculated mass-dependent calibration factors based on the measured calibration factors. Figure 5.1a shows the spread in the normalized response of compounds versus mass (labeled by compound name) overlaid with the linearly fitted mass-dependent, transmission curve (black markers and dotted line). It is clear from Figure 5.1a that the oxygenated species (blue labels) and the hydrocarbon species (green labels) exhibit a slightly different mass dependent behavior, however, both groups show a linear increase with mass that is similar to that observed for the transmission efficiency (Figure 5.1b and c). To reduce bias, mass dependent calibration factors were determined using a linear approximation for oxygenated and hydrocarbon species separately (Figure 5.1b and 1c). α-Pinene was not included in the linear approximation for hydrocarbons as this compound is well-known to be susceptible to substantial fragmentation in the drift tube. Sulfur and nitrogen-containing compounds were considered collectively and together they more closely follow the trend of the oxygenated species. Thus, in cases where a compound contains a non-oxygen heteroatom (such as methanethiol), the mass dependent calibration factor was determined using the relationship established using the oxygenated species. Calibration factors were then determined according to the exact mass for all peaks where the chemical formula has been determined. Our approach does not yet account for the potential for ions to fragment and/or cluster, however, we expect this impacts less than 30% of NMOC and usually to a small degree for any individual species. These latter issues change the mass distribution of observed carbon, but should not have a large effect on the total observed carbon.

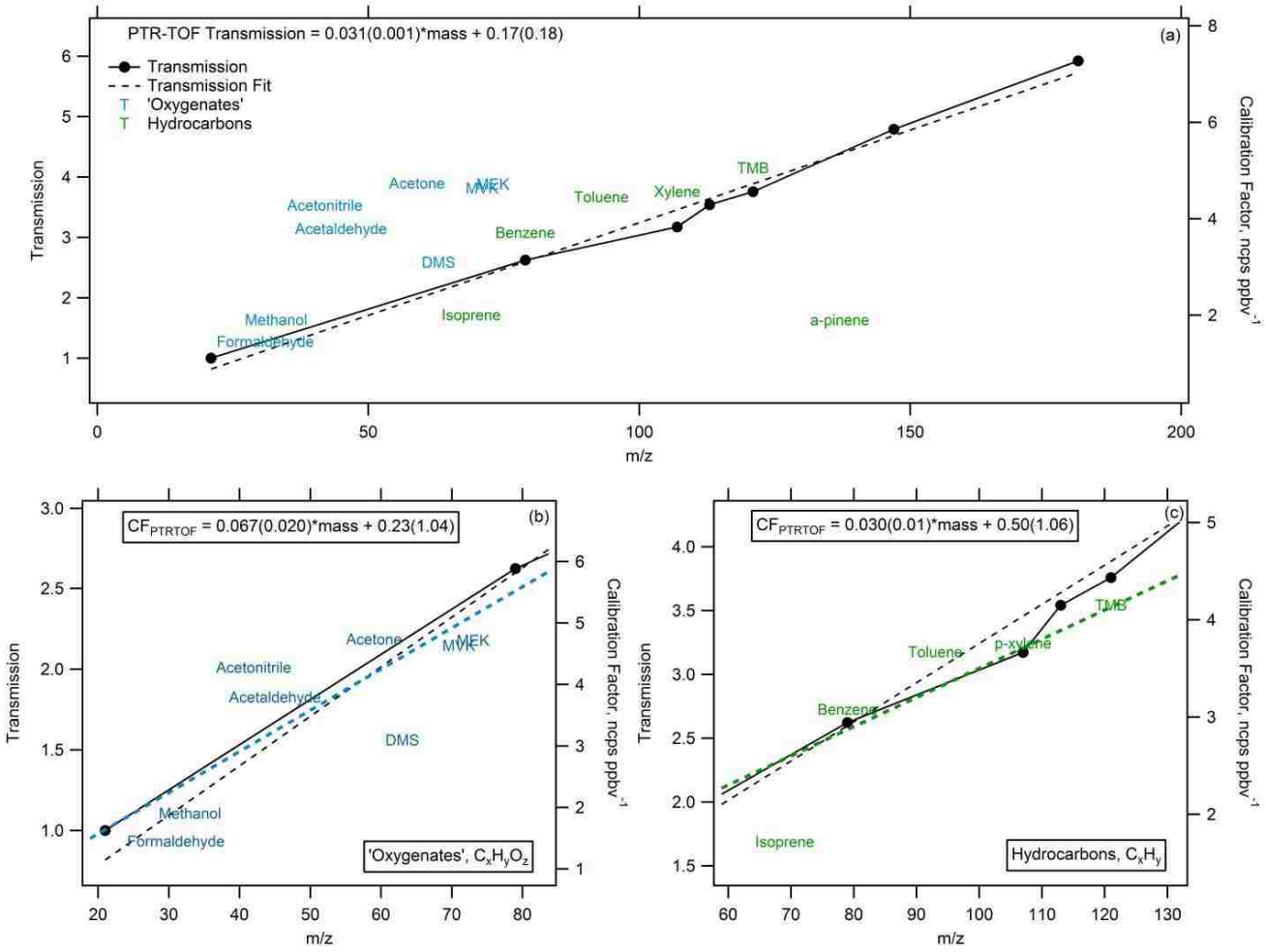

Figure 5.1. (a) The normalized response of calibration factors ("CF," ncps/ppbv) versus mass (calibrated species labeled by name) overlaid with the linearly fitted mass-dependent transmission curve (black markers and dotted line). Separate linear approximations (b) oxygenated (blue) and (c) hydrocarbon (green) species used to calculate approximate calibration factors for all observed masses where explicit calibrations were not available.

It is difficult to assess the overall error introduced using this method of calibration factor approximation, as only a limited number of comparable measurements of calibration factors are available. The deviation of measured calibration factors for species contained in the gas standard from the linear approximation yields a range of errors (21 ± 19%) with a maximum of 50% observed in all cases (excluding α-pinene, for reasons detailed above). While PTR-TOF-MS is typically known as a soft ionization method, fragmentation is common among higher molecular

weight species and therefore needs to be considered as a limitation of this technique. For the individual species identified it would be misleading to give a set error based on this limited analysis, however, in the absence of any known molecular fragmentation a maximum error of 50% is prescribed, but with larger errors possible for compounds with N and S heteroatoms. Better methods for the calculation of mass dependent calibration factors by compound class should be developed in the near future to improve the accuracy of VOC measurements using PTR-TOF-MS.

5.2.3 Intercomparison

The OP-FTIR system had the highest time resolution with no sampling line, storage, fragmentation, or clustering artifacts; thus, for species in common with PTR-TOF-MS, the OP-FTIR data was used as the primary data. The results from the intercomparison (for methanol) of OP-FTIR and PTR-TOF-MS show excellent agreement using an orthogonal distance regression to determine slope (0.995 ± 0.008) and the R^2 coefficient (0.789). This result is consistent with the good agreement for several species measured by both PTR-MS and OP-FTIR observed in numerous past studies of laboratory BB emissions (Christian et al., 2004; Karl et al., 2007; Veres et al. 2010; Warneke et al., 2011).

5.2.4 Emission ratio and emission factor determination

Excess mixing ratios (denoted ΔX for each species "X") were calculated by applying an interpolated background correction (determined from the pre and post fire concentrations). The molar emission ratio (ER) for each species "X" relative to CH_3OH ($\Delta X/\Delta CH_3OH$) is the ratio between the integral of ΔX over the entire fire relative to the integral of ΔCH_3OH over the entire fire. We selected CH_3OH as the species in common with the OP-FTIR to serve as an internal standard for the calculation of the fire-integrated ERs of each species X to CO. We do this by

multiplying the MS-derived ER ($\Delta X/\Delta CH_3OH$) by the FTIR-derived ER ($\Delta CH_3OH/\Delta CO$), which minimizes error due to occasional reagent ion depletion or the different sampling frequencies between instruments that would impact calculating ΔX to ΔCO directly. Several fires have been excluded from this calculation as data was either not collected by OP-FTIR and/or PTR-TOF-MS or alternatively, methanol data could not be applied for the conversion because (1) the mixing ratios remained below the detection limit or (2) methanol was used to assist ignition purposes during a few fires. In the case of the tire fires only, the latter issue with CH_3OH was circumvented by using HCOOH (*m/z* 47) as a suitable, alternative internal standard. As discussed in Sect. 5.2.1, ~50 additional masses were analyzed for selected fires and the ERs (to CO) for these fires are included in the bottom panels of Table S1 in Stockwell et al. (2015). The combined ERs to CO from the FTIR and PTR-TOF were then used to calculate emission factors (g kg^{-1} dry biomass burned) by the carbon mass-balance method (CMB), based on the assumption that all of the burned carbon is volatilized and that all of the major carbon-containing species have been measured (Ward and Radke, 1993; Yokelson et al., 1996, 1999; Burling et al., 2010). EFs were previously calculated solely from FLAME-4 OP-FTIR data as described in Stockwell et al. (2014) (see Chapter 3) and a new larger set of EFs, which include more carbon-containing species quantified by PTR-TOF-MS, are now shown in Supplement Table S3. With the additional carbon compounds quantified by PTR-TOF-MS, the EFs calculated by CMB decreased ~1-2% for most major fuels with respect to the previous EFs reported in Stockwell et al. (2014). In the case of peat and sugar cane fires, the OP-FTIR derived EFs are now reduced by a range of ~2-5% and 3.5-7.5%, respectively. Along with these small reductions, this work now provides EFs for many additional species that were unavailable in Stockwell et al. (2014). Finally, the EFs reported in Supplement Table S4 were adjusted (when needed) according to

procedures established in Stockwell et al. (2014) and Sect. 4.2.3 to improve laboratory representation of real-world BB emissions. This table contains the EF we recommend other workers use. In addition to the comparisons considered in Stockwell et al. (2014), we find that our EFs in Table S4 are consistent (for the limited number of overlap species) with additional, recent field studies including Kudo et al. (2014) for Chinese crop residue fires and Geron and Hays (2013) for NC peat fires.

5.3 PTR-TOF-MS Results

5.3.1 Peak assignment

As exemplified by a typical PTR-TOF-MS spectrum of diluted smoke (Figure 5.2a), the complexity of BB smoke emissions presents challenges to mass spectral interpretation and ultimately emissions characterization. Figure 5.2b shows a smaller mass range of the smoke sample shown in Figure 5.2a on a linear scale to illustrate the typical relative importance of the masses (note the intensity of acetaldehyde (*m/z* 45) and acetic acid plus glycolaldehyde (*m/z* 61), which together account for almost 25% of the total signal). Although the spectra are very complex, systematic treatment of the burn data, assisted at some *m/z* by extensive published "off-line" analyses can generate reasonable assignments for many major peaks and result in useful emissions quantification.

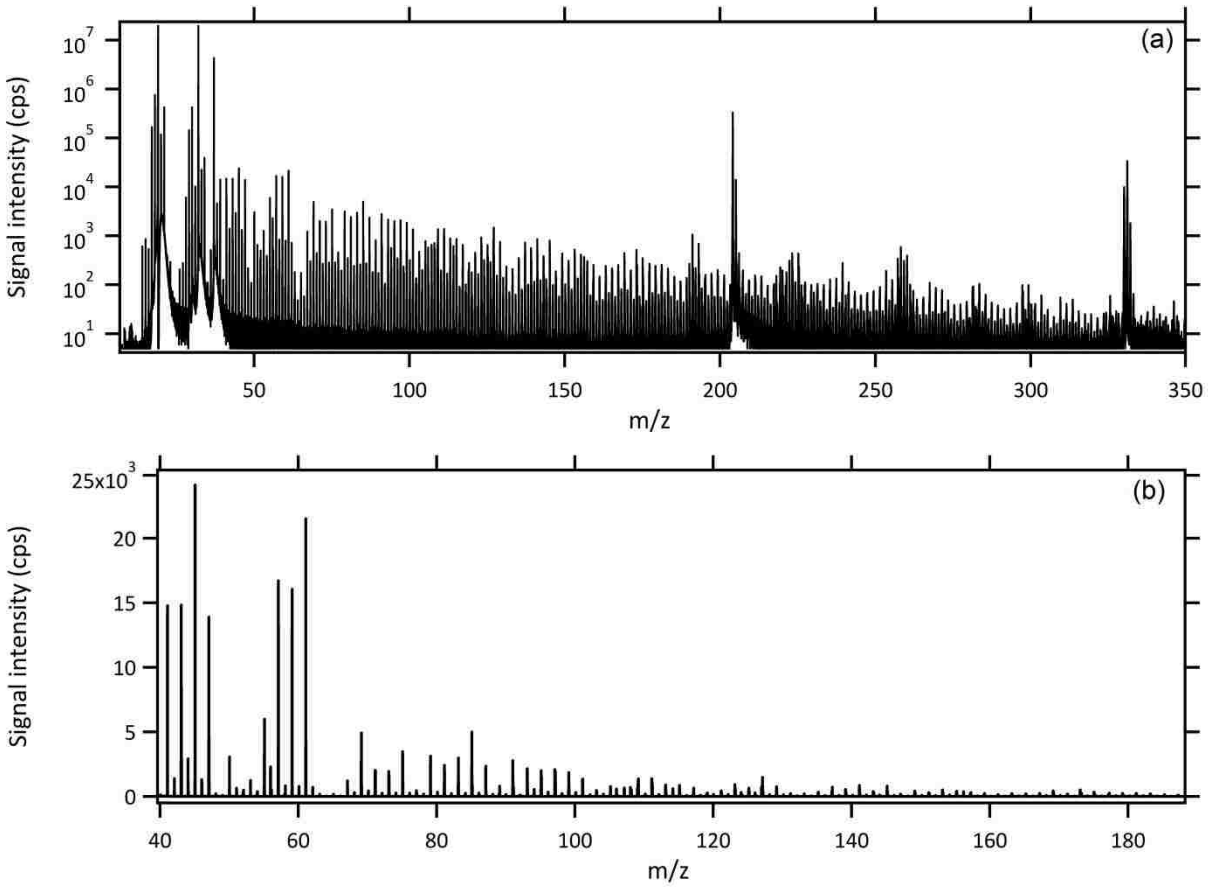

Figure 5.2. A typical full mass scan of biomass burning smoke from the PTR-TOF-MS on a logarithmic (a) and a smaller range linear (b) scale. The internal standard (1,3-diiodobenzene) accounts for the major peaks ~*m/z* 331 and fragments at peaks near *m/z* 204 and 205.

As described earlier, the PTR-TOF-MS scans have sufficiently high resolution to assign molecular formulas ($C_wH_xN_yO_z$) to specific ion peaks by matching the measured exact mass with possible formula candidates for the protonated compound. Specific compound identification for formula candidates can be unambiguous if only one species is structurally plausible or explicit identification of the compound had previously been confirmed by BB smoke analysis (Akagi et al., 2011; Yokelson et al., 2013a, etc.). Supplement Table S5 lists every mass and formula assignment for observable peaks up to *m/z* 165 and categorizes each mass as a confirmed identity, a tentative (most likely) species assignment, or an unknown compound. For several confirmed identities, the most abundant species at that exact mass is listed with likely

contributions to the total signal from the secondary species listed in column 5. Most of the tentatively identified species have, to our knowledge, typically not been directly observed in BB smoke, but have been frequently verified with off-line techniques as major products in the extensive literature describing biomass pyrolysis experiments of various fuel types (Liu et al., 2012; Pittman Jr. et al., 2012; Li et al., 2013; more citations in Table S5). Several tentative assignments are supported by off-line analyses being published elsewhere (Hatch et al., 2015), for example, simultaneous grab samples analyzed by two dimensional gas chromatography (2D-GC) support tentative assignments for furan methanol, salicylaldehyde, and benzofuran. In the case of nitrogen-containing formulas, the suggested compounds have been observed in the atmosphere, tobacco smoke, or lab fire smoke at moderate levels (Lobert, 1991; Ge et al., 2011; etc.). Select studies supporting these assignments are referenced in the mass table with alternative possibilities also listed. An exhaustive list of all the many papers supporting the assignments is beyond the scope of this work. Several remaining compounds are also classified as tentative assignments as the identities designated are thought to be the most structurally likely. We anticipate that some or even many of the tentative assignments (and a few of the confirmed assignments) will be refined in future years as the results of more studies become available. We offer the tentative assignments here as a realistic starting point that improves model input compared to an approach in which these species are simply ignored.

5.3.2 Unidentified compounds

The identities of several compounds remain unknown, especially at increasing mass where numerous structural and functional combinations are feasible. However, compared to earlier work at unit mass resolution (Warneke et al., 2011; Yokelson et al., 2013a), the high-resolution capability of the PTR-TOF-MS has enhanced our ability to assign mass peaks while always

identifying atomic composition. With unit mass resolution spectrometers, FTIR, and GC-MS grab samples, Yokelson et al. (2013) estimated that ~31% to ~72% of the gas-phase NMOC mass remained unidentified for several fuel types. For similar, commonly burned biomass fuels (chaparral, grasses, crop residue, etc.), considering a PTR-TOF range up to *m/z* 165, we estimate that ~7% of the detected NMOC mass remains unidentified, while ~12% is tentatively assigned using selection criteria described in Sect. 5.3.1. The compounds considered in this study cover a smaller mass range (up to *m/z* 165 rather than *m/z* 214) than in the earlier study, but in that earlier study, the compounds in the range *m/z* 165-214 accounted for only ~1.5% of the NMOC mass (Yokelson et al., 2013a). Thus, the molecular formula assignments from the PTR-TOF aided in positive and tentative identification and quantification resulting in a reduction of the estimate of unidentified NMOCs from ~31% down to ~7%.

Calculations of unidentified and tentatively assigned emissions relative to overall NMOC emissions (including FTIR species) for several lumped fuel groups are summarized in Table 5.1. Estimates of total intermediate and semivolatile gas-phase organic compounds (IVOC + SVOC, estimated as the sum of species at or above the mass of toluene) are also included as these less volatile compounds are likely to generate SOA via oxidation and/or cooling. Similar to previous organic soil fire data, the percentages of unidentified and tentatively identified NMOCs for peat burns are significantly larger than for other fuel types (sum ~37%) and they could be a major source of impacts and uncertainty during El-Niño years when peat combustion is a major global emission source (Page et al., 2002; Akagi et al., 2011).

Table 5.1. Quantities for various categories of compounds (g kg^{-1}) and calculation of mass ratios and/or percentages for several fuel types.

Quantity or Ratio	Chaparral	Coniferous Canopy	Peat	Grasses	Cooking Fires	Crop Residue	Trash
Σ NMOCs	13.1	23.9	40.5	5.17	8.16	29.6	7.13
Σ I/SVOCs	3.49	7.13	14.6	1.38	1.33	7.21	1.83
Σ Tentatively assigned NMOCs	1.43	2.77	7.01	0.72	0.72	4.38	0.51
Σ Unidentified NMOCs	1.23	1.79	7.50	0.39	0.33	2.10	0.41
Σ (I/SVOCs) / Σ NMOC	0.21	0.28	0.37	0.26	0.15	0.24	0.26
Percent NMOCs Tentatively assigned	8.35	9.74	17.5	13.9	8.19	14.0	7.20
Percent NMOCs Unidentified	7.24	6.75	19.5	7.19	3.77	6.90	5.75
Percent NMOCs Tentatively + Unidentified	16	16	37	21	12	21	13

5.4 Discussion

For all fuel types, there is noticeable variability concerning which compounds have the most significant emissions. Figure 5.3 includes both FTIR and PTR emissions grouped into the following categories: non-methane hydrocarbons, oxygenates containing only one oxygen, oxygenates containing two oxygen atoms, and oxygenates containing three oxygen atoms. Within these categories, the contributions from aromatics, phenolic compounds, and furans are further indicated. As shown in Figure 5.3, oxygenated compounds account for the majority of the emissions for all biomass and biomass-containing fuels (i.e. tires and plastic bags are excluded). Oxygenated compounds containing only a single oxygen atom accounted for ~ 50% of the total raw mass signal (> *m/z* 28, excluding *m/z* 37) on average and normally had greater emissions than oxygenated compounds containing two oxygen atoms or hydrocarbons. Sugar cane has the highest emissions of oxygenated compounds as was noted earlier in the FTIR data (Stockwell et al., 2014; Sect. 4.3.5) and is one of the few fuels where the emissions of compounds containing two oxygens are the largest. To facilitate discussion we grouped many of the assigned (or tentatively assigned) mass peak features into categories including: aromatic hydrocarbons; phenolic compounds; furans; nitrogen-containing compounds; and sulfur-containing compounds

These categories do not account for the majority of the emitted NMOC mass, but account for most of the rarely-measured species reported in this work. We then also discuss miscellaneous compounds at increasing *m/z*.

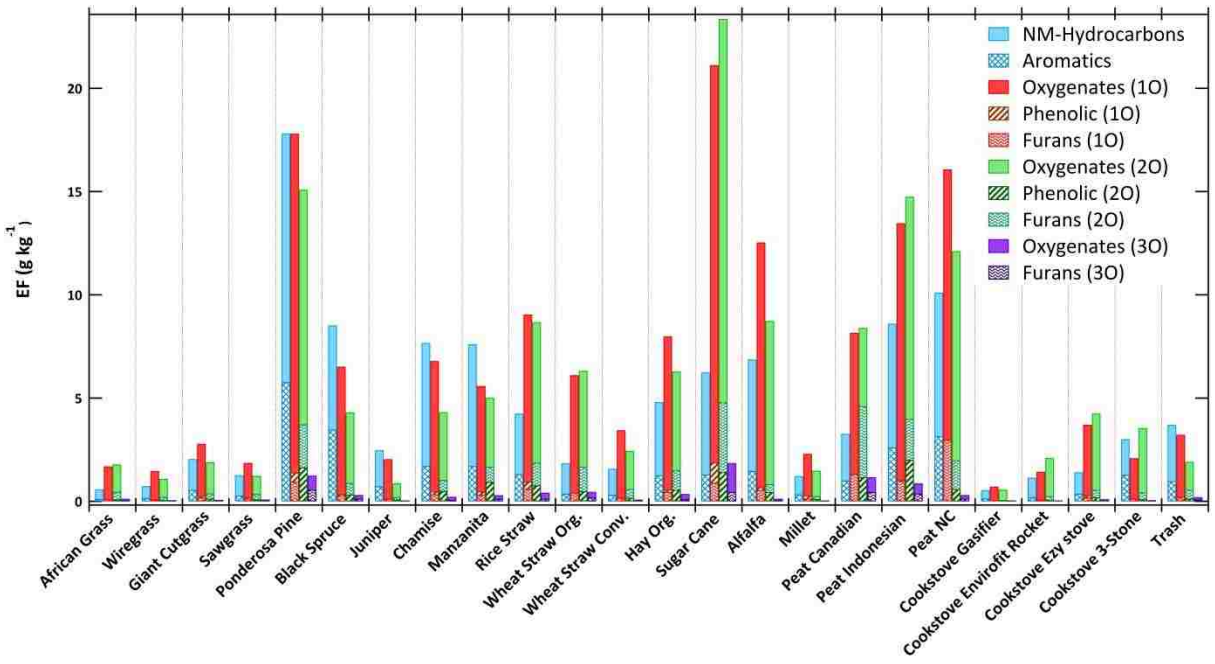

Figure 5.3. The emission factors (g kg-1) of total observed hydrocarbons and total observed species oxygenated to different degrees averaged for each fire type based on a synthesis of PTR-TOF-MS and OP-FTIR data. The patterned sections indicate the contribution to each of the above categories by selected functionalities discussed in the text (aromatic hydrocarbons, phenolics, furans). The parenthetical expressions indicate how many oxygen atoms are present.

5.4.1 Aromatic hydrocarbons

Aromatic hydrocarbons contributed most significantly to the emissions for several major fuel types including ponderosa pine, peat, and black spruce. The identities of these ringed structures are more confidently assigned due to the small H to C ratio at high masses. The aromatics confidently identified in this study include benzene (*m/z* 79), toluene (*m/z* 93), phenylacetylene (*m/z* 103), styrene (*m/z* 105), xylenes/ethylbenzene (*m/z* 107),1,3,5-trimethylbenzene (*m/z* 121), and naphthalene (*m/z* 129), while masses more tentatively assigned include dihydronaphthalene

(*m/z* 131), p-cymene (*m/z* 135), and methylnaphthalenes (*m/z* 143). All masses are likely to have minor contributions from other hydrocarbon species. The EFs for aromatic species quantified during all fires are averaged by fuel type and shown in Figure 5.4a. The EF for p-cymene was only calculated for select burns and has been included in Figure 5.4a for comprehensiveness.

Aromatic structures are susceptible to multiple oxidation pathways and readily drive complex chemical reactions in the atmosphere that are highly dependent on hydroxyl radical (OH) reactivity (Phousongphouang and Arey, 2002; Ziemann and Atkinson, 2012). Ultimately these gas-phase aromatic species have high yields for SOA as their physical and chemical evolution lead to lower volatility species that condense into the particle phase. SOA yields from these parent aromatic HCs have been shown to strongly vary depending on environmental parameters including relative humidity, temperature, aerosol mass concentration, and particularly the level of nitrogen oxides (NO_x) and availability of RO_2 radicals, further adding to the complexity in modeling the behavior and fate of these compounds (Ng et al., 2007; Song et al., 2007; Henze et al., 2008; Chhabra et al., 2010, 2011; Im et al., 2014).

Domestic biofuel burning and open BB together comprise the largest global atmospheric source of benzene (Andreae and Merlet, 2001; Henze et al., 2008), thus not surprisingly benzene is a significant aromatic in our dataset. The ERs relative to benzene for the aromatics listed above are shown in Table 5.2 and are positively correlated with benzene as demonstrated by Figure 5.4b. Henze et al. (2008) outline how ERs to CO of major aromatics (benzene, xylene, and toluene) can be implemented as a part of a model to predict SOA formation. An identical or similar approach that incorporates the additional aromatics detected by PTR-TOF-MS in this work may be useful to predict the contribution of aromatics from BB to global SOA by various reaction pathways.

Toluene, another major emission, often serves as a model compound to study the formation of SOA from other small ringed volatile organic compounds (Hildebrandt et al., 2009). Black spruce yielded the greatest toluene ER (to benzene) during FLAME-4 (3.24 ± 0.42) and has been linked to significant OA enhancement during chamber photo-oxidation aging experiments investigating open BB emissions during FLAME-III, though toluene was not significant enough to account for all of the observed SOA (Hennigan et al., 2011).

Naphthalene is the simplest species in a class of carcinogenic and neurotoxic compounds known as polycyclic aromatic hydrocarbons (PAH) and was detected from all fuels. The rapid rate of photo-oxidation of these smaller-ringed gas-phase PAHs (including naphthalene and methylnaphthalenes) can have important impacts on the amount and properties of SOA formed and yields significantly more SOA over shorter timespans in comparison to lighter aromatics (Chan et al., 2009). Under low-NO_x conditions (BB events generate NO_x though at lower ratios to NMOC and/or CO than those present in urban environments) the SOA yield for benzene, toluene, and *m*-xylene was ~ 30% (Ng et al., 2007), while naphthalene yielded enhancements as great as 73% (Chan et al., 2009).

In summary, many of the species identified and detected during FLAME-4 are associated with aerosol formation under diverse ambient conditions (Fisseha et al., 2004; Na et al., 2006; Ng et al., 2007; Chan et al., 2009). We present here initial emissions for a variety of aromatics from major global fuels. A more focused study to probe the extent and significance of SOA formation in BB plumes by these aromatic precursors was performed by chamber oxidation during the FLAME-4 campaign and will be presented in Tkacik et al. (2016).

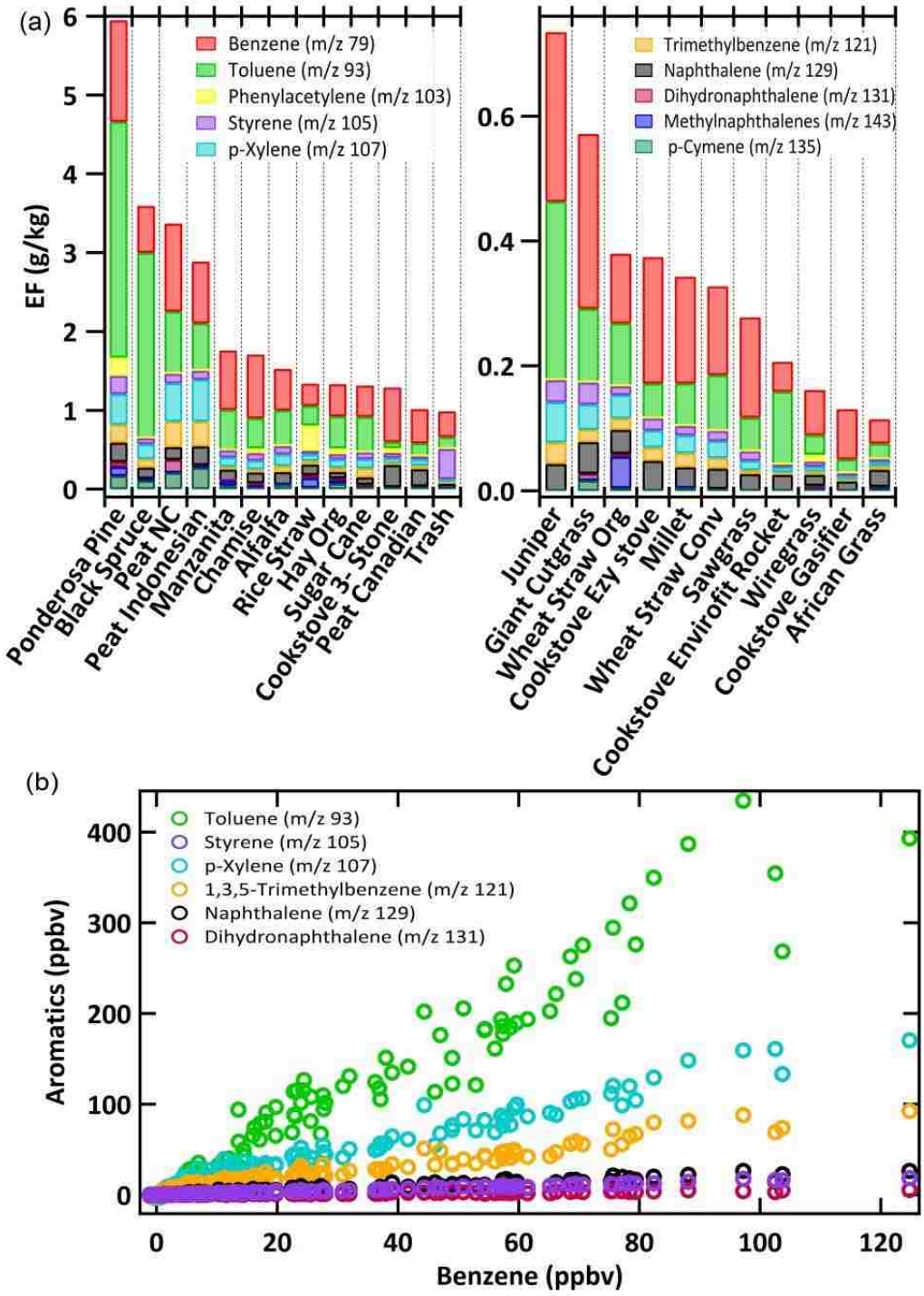

Figure 5.4. (a) The EFs of the aromatics analyzed in all fires averaged and shown by fuel type. Individual contributions from benzene and other aromatics are indicated by color. The EFs for p-Cymene are only calculated for select fires and should not be considered a true average. (b) The correlation plots of selected aromatics with benzene during a black spruce fire (Fire 74). Similar behavior was observed for all other fuel type

Table 5.2. Emission ratios to benzene, phenol, and furan for aromatic hydrocarbons, phenolic compounds, and substituted furans in lumped fuel-type categories.

	Fuel Type (# burns)	Grasses (42)	Coniferous Canopy (14)	Chaparral (8)	Peat (6)	Crop Residue (food, 19)	Crop Residue (feed, 9)	Open 3-Stone Cooking (3)	Rocket Cookstoves (5)	Gasifier Cookstove (1)	Trash (2)	Tires (1)	Plastic Bags (1)
ER/Benzene	MCE	0.968(0.010)	0.933(0.032)	0.927(0.017)	0.767(0.074)	0.946(0.022)	0.940(0.017)	0.968(0.004)	0.972(0.015)	0.984	0.973(0.006)	0.961	0.994
Toluene	C_7H_8	0.44(0.26)	2.19(0.84)	0.49(0.17)	0.53(0.17)	0.70(0.22)	1.00(0.44)	0.095(0.029)	0.98(1.39)	0.24	0.41(0.20)	0.056	0.69
Phenylacetylene	C_8H_6	0.094(0.022)	0.13	0.067(0.039)	-	0.65(0.45)	0.14(0.09)	0.10(0.05)	-	-	-	0.020	-
Styrene	C_8H_8	0.078(0.025)	0.11(0.02)	0.074(0.020)	0.087(0.027)	0.10(0.03)	0.14(0.05)	0.054(0.021)	0.076(0.023)	0.042	0.86(0.16)	0.064	0.094
p-Xylene	C_8H_{10}	0.102(0.058)	0.21(0.03)	0.12(0.03)	0.32(0.16)	0.20(0.08)	0.24(0.11)	0.052(0.034)	0.10(0.05)	0.048	0.095(0.017)	0.043	0.029
Trimethylbenzene	C_9H_{12}	0.059(0.045)	0.11(0.03)	0.043(0.023)	0.17(0.08)	0.11(0.05)	0.11(0.06)	0.014(0.007)	0.050(0.048)	0.026	0.033(0.016)	0.011	0.047
Naphthalene	$C_{10}H_8$	0.18(0.16)	0.13(0.05)	0.10(0.03)	0.15(0.09)	0.20(0.17)	0.18(0.11)	0.21(0.05)	0.30(0.17)	0.12	0.10	0.19	0.059
Dihydronaphthalene	$C_{10}H_{10}$	0.040(0.030)	0.034(0.016)	0.020(0.010)	0.050(0.019)	0.059(0.028)	0.051(0.021)	0.019(0.006)	-	-	-	9.81E-03	-
p-Cymene[a]	$C_{10}H_{14}$	0.018(0.013)	0.11(0.01)	0.037	0.15(0.12)	0.035(0.019)	0.11(0.03)	4.10E-03	-	nm	0.018	nm	nm
Methyl Naphthalenes	$C_{11}H_{10}$	0.032(0.009)	0.053(0.005)	0.033(0.007)	-	0.19(0.09)	0.057(0.037)	-	-	-	-	0.031	-
ER/Phenol													
Cresols (Methylphenols)[a]	C_7H_8O	0.52(0.19)	0.55(0.07)	0.49	0.29(0.18)	0.57(0.10)	0.61(0.14)	-	0.34(0.28)	nm	nm	nm	nm
Catechol (Benzenediols)[b]	$C_6H_6O_2$	0.73(0.41)	0.76(0.29)	1.72(1.28)	1.58(1.03)	0.93(0.45)	0.67(0.30)	0.74(0.65)	1.86(1.29)	0.49	1.12(0.65)	0.082	0.31
Vinylphenol	C_8H_8O	0.66(0.19)	0.33(0.09)	0.30(0.05)	0.18(0.05)	0.60(0.35)	0.29(0.06)	0.18(0.06)	0.25(0.18)	0.14	0.34(0.02)	0.17	0.33
Salicylaldehyde	$C_7H_6O_2$	0.18(0.06)	0.17(0.04)	0.15(0.04)	0.20(0.13)	0.18(0.08)	0.11(0.04)	0.16(0.06)	0.27(0.15)	0.22	0.28(0.09)	0.17	-
Xylenol (2,5-dimethyl phenol)	$C_8H_{10}O$	0.25(0.09)	0.19(0.06)	0.11(0.06)	0.31(0.09)	0.34(0.07)	0.33(0.07)	0.18(0.09)	0.35(0.11)	0.11	0.23(0.00)	0.026	-
Guaiacol (2-Methoxyphenol)	$C_7H_8O_2$	0.40(0.23)	0.42(0.12)	0.21(0.09)	0.71(0.36)	0.76(0.33)	0.47(0.16)	0.52(0.40)	1.30(0.73)	0.31	0.54(0.32)	0.019	2.02
Creosol (4-Methylguaiacol)[a]	$C_8H_{10}O_2$	0.21(0.16)	0.21(0.09)	0.067	0.12(0.17)	0.19(0.10)	0.24(0.07)	0.46	0.62(0.23)	nm	0.043	nm	nm
3-Methoxycatechol[a]	$C_7H_8O_3$	0.090(0.072)	0.067(0.031)	0.028	0.19(0.04)	0.066(0.037)	0.063(0.035)	0.28	0.44	nm	0.14	nm	nm
4-Vinylguaiacol[a]	$C_9H_{10}O_2$	0.29(0.19)	0.27(0.12)	0.052	0.27(0.04)	0.37(0.19)	0.31(0.11)	0.34	0.35(0.22)	nm	0.054	nm	nm
Syringol[a]	$C_8H_{10}O_3$	0.13(0.07)	0.078(0.029)	0.21(0.12)	0.22(0.07)	0.16(0.10)	0.12(0.02)	0.94	0.92(0.53)	nm	-	nm	nm
ER/Furan													
2-Methylfuran	C_5H_6O	0.53(0.27)	1.02(0.40)	0.77(0.30)	0.34(0.14)	1.50(0.66)	1.36(0.38)	0.95(0.33)	1.66(1.95)	0.55	0.64(0.02)	2.10	2.10
2-Furanone	$C_4H_4O_2$	0.93(0.50)	1.53(0.80)	0.96(0.49)	0.44(0.36)	2.05(1.09)	1.16(0.56)	0.73(0.21)	2.37(3.39)	1.28	1.04(0.49)	3.02	-
2-Furaldehyde (Furfural)	$C_5H_4O_2$	1.61(0.81)	1.82(0.85)	1.35(0.75)	1.34(0.85)	2.78(1.21)	1.69(0.96)	2.47(1.84)	5.69(8.46)	1.26	1.03(0.29)	2.09	0.39
2,5-Dimethylfuran[a]	C_6H_8O	0.27(0.09)	0.58(0.20)	0.615573	0.11(0.01)	0.62(0.77)	0.98(0.14)	-	-	nm	0.2715416	nm	nm
Furfuryl alcohol	$C_5H_6O_2$	0.77(0.49)	1.23(0.57)	0.85(0.44)	0.25(0.21)	1.98(1.21)	1.21(0.55)	0.86(0.25)	1.35	0.00	0.78(0.31)	1.06	1.03
Methylfurfural[b]	$C_6H_6O_2$	0.42(0.24)	1.18(0.89)	1.95(1.49)	0.44(0.35)	0.98(0.52)	0.90(0.42)	0.59(0.20)	1.06(1.32)	0.37	0.38(0.06)	1.33	0.093
Benzofuran	C_8H_6O	0.059(0.028)	0.11(0.05)	0.10(0.05)	0.017(0.010)	0.10(0.04)	0.11(0.05)	0.39(0.57)	0.041(0.030)	0.069	0.058(0.018)	2.79	0.056

Hydroxymethylfurfural	$C_6H_6O_3$	0.21(0.16)	0.64(0.43)	0.28(0.19)	0.18(0.14)	0.49(0.35)	0.27(0.14)	0.20(0.06)	0.44(0.52)	0.30	0.39(0.22)	0.28	-
Methylbenzofuran isom.[a]	C_9H_8O	0.67(0.58)	-	-	-	-	-	-	-	nm	-	nm	nm

Note: "nm" indicates not measured; blank indicates species remained below the detection limits; values in parenthesis indicate one standard deviation

[a] Species were only selected for a few key fires and are not considered the average of each fuel type

[b] Significant contributions from both methylfurfural and catechol reported in pyrolysis reference papers, thus there is no indication which species is the major contributor at this mass

5.4.2 Phenolic compounds

Phenol is detected at *m/z* 95. Earlier studies burning a variety of biomass fuels found that OP-FTIR measurements of phenol accounted for the observed PTR-MS signal at this mass even at unit mass resolution, though small contributions from other species such as vinyl furan were possible, but not detected (Christian et al., 2004). 2D-GC grab samples in FLAME-4 find that other species with the same formula (only vinyl furan) are present at levels less than ~2% of phenol (Hatch et al., 2015). Thus, we assume that within experimental uncertainty *m/*z 95 is a phenol measurement in this study and find that phenol is one of the most abundant oxygenated aromatic compounds detected. Several substituted phenols were speciated for every fire and included catechol (*m/z* 111), vinylphenol (*m/z* 121), salicylaldehyde (*m/z* 123), xylenol (*m/z* 123), and guaiacol (*m/z* 125) (Figure 5.5a). Several additional species were quantified for selected fires and included cresol (*m/z* 109), creosol (*m/z* 139), 3-methoxycatechol (*m/z* 141), 4-vinylguaiacol (*m/z* 151), and syringol (*m/z* 155). The EFs for these additional phenolic compounds were calculated for select burns and are included in Figure 5.5a with the regularly analyzed compounds. Significant emissions of these compounds are reported in Table 5.2 relative to phenol and the selected compounds shown in Figure 5.5b demonstrate the tight correlation between these derivatives and phenol.

Phenol, methoxyphenols (guaiacols), dimethoxyphenols (syringol), and their derivatives are formed during the pyrolysis of lignin (Simoneit et al., 1993) and can readily react with OH radicals leading to SOA formation (Coeur-Tourneur et al, 2010; Lauraguais et al., 2014). Hawthorne et al. (1989,1992) found that phenols and guaiacols accounted for 21% and 45% of aerosol mass from wood smoke, while Yee et al. (2013) noted large SOA yields for phenol (24-

44%), guaiacol (44-50%), and syringol (25-37%) by photo-oxidation chamber experiments under low-NO_x conditions (<10 ppb).

Softwoods are considered lignin-rich and are associated predominately with guaiacyl units (Shafizadeh, 1982). Thus not surprisingly, guaiacol emissions were significant for ponderosa pine. Peat, an accumulation of decomposing vegetation (moss, herbaceous, woody materials), has varying degrees of lignin-content depending on the extent of decomposition, sampling depth, water table levels, etc. (Williams et al., 2003). The peat burns all emitted significant amounts of phenolic compounds, with noticeable compound specific variability between regions (Indonesia, Canada, and North Carolina). It is also noteworthy that sugar cane, which also produced highly oxygenated emissions based on FTIR and PTR-TOF-MS results, had the greatest total emissions of phenolic compounds.

The photochemical formation of nitrophenols and nitroguaiacols by atmospheric oxidation of phenols and substituted phenols via OH radicals in the presence of NO_x is a potential reaction pathway for these compounds (Atkinson et al., 1992; Olariu et al., 2002; Harrison et al., 2005; Lauraguais et al., 2014). Nitration of phenol in either the gas or aerosol phase is anticipated to account for a large portion of nitrophenols in the environment. Higher nitrophenol levels are correlated with increased plant damage (Hinkel et al., 1989; Natangelo et al., 1999) and consequently are linked to forest decline in central Europe and North America (Rippen et al., 1987). Nitrophenols are also important components of brown carbon and can contribute to SOA formation in BB plumes (Kitanovski et al., 2012; Desyaterik et al., 2013; Mohr et al., 2013; Zhang et al., 2013). Nitrated phenols including nitroguaiacols and methyl-nitrocatechols are suggested as suitable BB molecular tracers for secondary BB aerosol considering their reactivity with atmospheric oxidants is limited (Iinuma et al., 2010; Kitanovski et al., 2012; Lauraguais et

al., 2014). The oxidation products from the phenolic compounds detected in fresh smoke here have not been directly examined and would require a more focused study beyond the scope of this paper.

As with the aromatic compounds, the ERs provided in Table 5.2 can be used to estimate initial BB emissions of phenolic species, both rarely measured or previously unmeasured, from a variety of fuels in order to improve atmospheric modeling of SOA and nitrophenol formation.

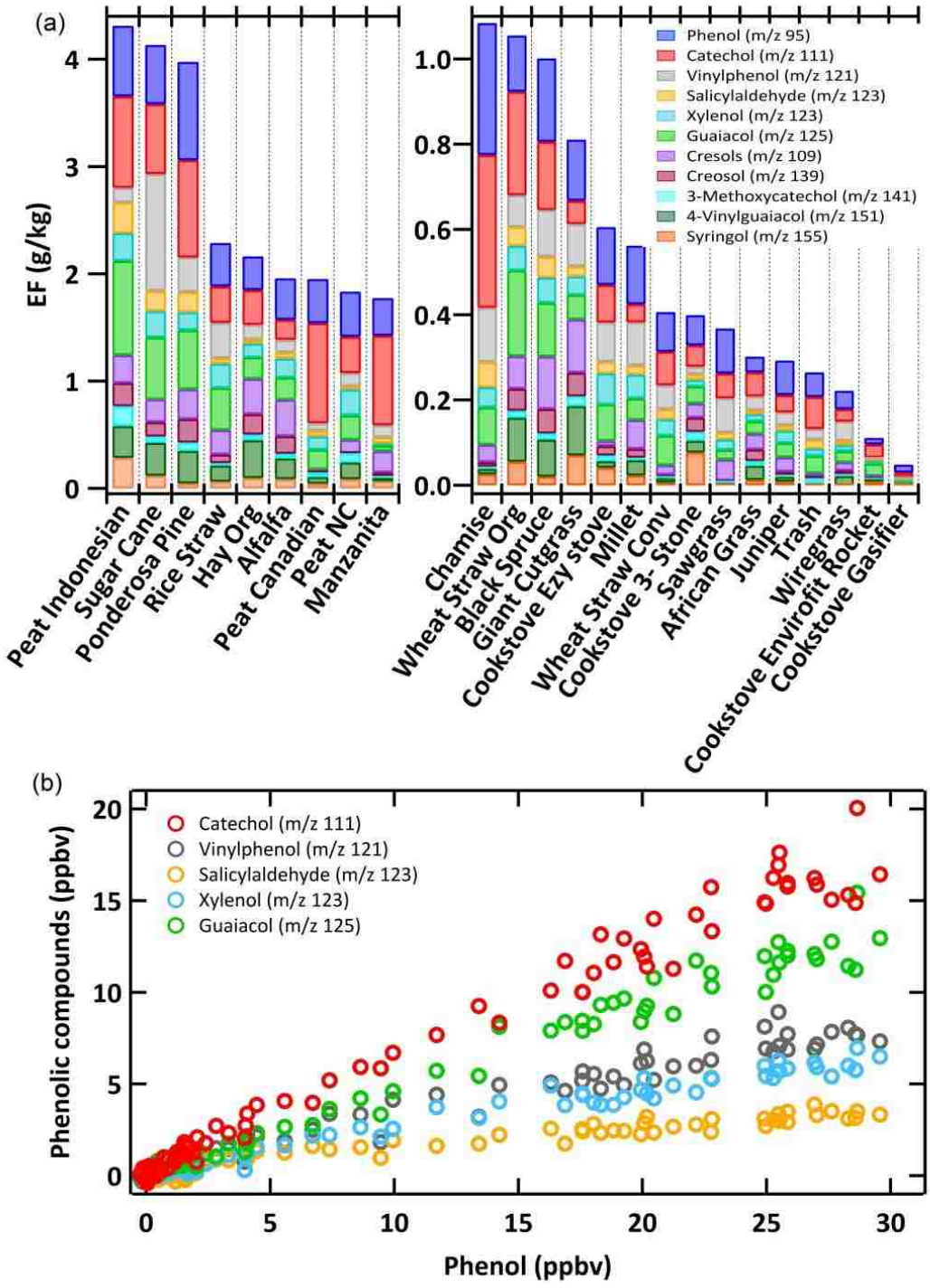

Figure 5.5. (a) The distribution in average fuel EF for several phenolic compounds, where compound specific contributions are indicated by color. The EFs for compounds additionally analyzed a single time for select fires are included but are not a true average.(b) The linear correlation of select phenolic compounds with phenol during an organic hay burn (Fire 119).

5.4.3 Furans

Other significant oxygenated compounds include furan and substituted furans which arise from the pyrolysis of cellulose and hemicellulose. The substituted furans regularly quantified included 2-methylfuran (*m/z* 83), 2-furanone (*m/z* 85), furfural (*m/z* 97), furfuryl alcohol (*m/z* 99), methylfurfural (*m/z* 111), benzofuran (*m/z* 119), and hydroxymethylfurfural (*m/z* 127), while 2,5-dimethylfuran (*m/z* 97) and methylbenzofurans (*m/z* 133) were occasionally quantified. The ERs to furan for these compounds are summarized in Table 5.2 and Figure 5.6a shows the average EF for the regularly quantified masses and the individual fire EFs for the occasionally quantified compounds.

Furan and substituted furans are oxidized in the atmosphere primarily by OH (Bierbach et al., 1995), but also by NO_3 (Berndt et al., 1997) or Cl atoms (Cabañas et al., 2005; Villanueva et al., 2007). Photo-oxidation of furan, 2-methylfuran, and 3- methylfuran produce butenedial, 4-oxo-2-pentenal, and 2-methylbutenedial (Bierbach et al 1994, 1995). These products are highly reactive and can lead to free radical (Wagner et al., 2003), SOA, or O_3 formation. In fact, aerosol formation from photo-oxidation chamber experiments has been observed for furans and their reactive intermediates listed above (Gomez Alvarez et al., 2009; Strollo and Ziemann, 2013). Even less is known concerning SOA yields from furans with oxygenated functional groups, which comprise the majority of the furan emissions in this study. Alvarado and Prinn (2009) added reaction rates for furans based on 2-methylfuran and butenedial values (Bierbach et al., 1994, 1995) to model O_3 formation in an aging savanna smoke plume. Although a slight increase in O_3 was observed after 60 min, it was not large enough to account for the observed O_3 concentrations in the plume. The furan and substituted furan ERs compiled here may help

explain a portion of the SOA and O_3 produced from fires that cannot be accounted for based upon previously implemented precursors (Grieshop et al., 2009).

Furfural was generally the dominant emission in this grouping consistent with concurrent 2D-GC measurements (Hatch et al., 2015) while emissions from 2-furanone and furan also contributed significantly. Friedli et al. (2001) observed that ERs of alkyl furans linearly correlated with furan and concluded that these alkylated compounds likely break down to furan. Our expanded substituted furan list includes a variety of functionality ranging from oxygenated substituents to those fused with benzene rings for diverse fuel types. Similar to the behavior observed for alkylated furans, the emissions of our substituted furans linearly correlate with furan as shown in Figure 5.6b. As noted for phenolic compounds, sugar cane produced the largest emissions of furans excluding Canadian peat, supporting sugar cane as an important emitter of oxygenated compounds. The emissions from furan, phenol, and their derivatives reflect variability in cellulose and lignin composition of different fuel types. Cellulose and hemicellulose compose ~75% of wood while lignin only accounts for ~25% on average (Sjöström, 1993). Accordingly the Σfurans/Σphenols for initially analyzed compounds indicate that furans are dominant in nearly every fuel type.

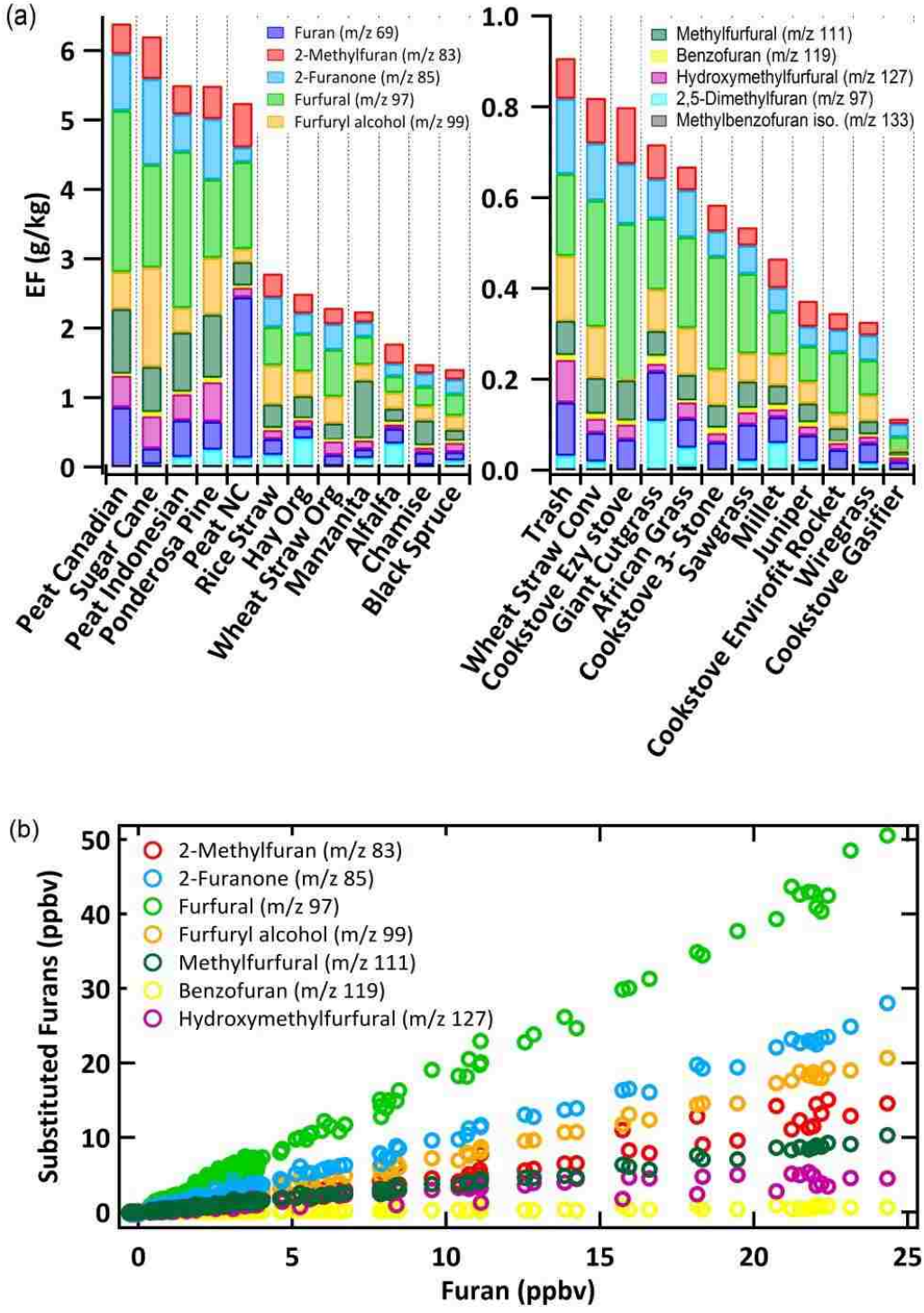

Figure 5.6. (a) The distribution in average fuel EF for furan and substituted furans, where individual contributions are indicated by color. The EFs for substituted furans additionally analyzed a single time are not true averages. (b) The linear correlation of furan with select substituted furans for an African grass fire (Fire 49).

5.4.4 Nitrogen-containing compounds

Many nitrogen (N)-containing peaks were not originally selected for post-acquisition analysis in every fire. However, the additional analysis of selected fires included a suite of N-containing organic compounds to investigate their potential contribution to the N-budget and new particle formation (NPF). Even at our mass resolution of ~5000, the mass peak from N-compounds can sometimes be overlapped by broadened ^{13}C "isotope" peaks of major carbon containing emissions. This interference was not significant for the following species that we were able to quantify in the standard or added analysis: C_2H_3N (acetonitrile, calibrated), C_2H_7N (dimethylamine; ethylamine), C_2H_5NO (acetamide), C_3H_9N (trimethylamine), C_4H_9NO (assorted amides), $C_4H_{11}NO$ (assorted amines), C_7H_5N (benzonitrile). As illustrated by the multiple possibilities for some formulas, several quantified nitrogen-containing species were observed but explicit single identities or relative contributions could not be confirmed. The logical candidates we propose are based upon atmospheric observations and include classes of amines and amides shown in Table S5 (Lobert et al., 1991; Schade and Crutzen, 1995; Ma and Hays et al., 2008; Barnes et al., 2010; Ge et al., 2011). Additional N-containing compounds were clearly observed in the mass spectra such as acrylonitrile, propanenitrile, pyrrole, and pyridine, but they were often overlapped with isotopic peaks of major carbon compounds, thus a time-intensive analysis would be necessary to provide quantitative data. For the species in this category, quantification was possible for select fires by 2D-GC-MS and they are reported by Hatch et al. (2015) for the FLAME-4 campaign.

We present in Table 5.3 the abundance of each N-containing gas quantified by PTR-TOF-MS and FTIR relative to NH_3 for selected fires. The additional nitrogen-containing organic gases detected by PTR-TOF-MS for these 29 fires summed to roughly 22 ± 23% of NH_3 on average

and accounted for a range of 0.1-8.7% of the fuel nitrogen. These compounds contributed most significantly to fuel N for peat and this varied by sampling location. This is not surprising since environmental conditions and field sampling depths varied considerably. Stockwell et al. (2014) reported large differences for N-containing compounds quantified by FTIR between FLAME-4 and earlier laboratory studies of emissions from peat burns. In any case, the additional NMOCs (including N-containing compounds) speciated by PTR-TOF-MS substantially increases the amount of information currently available on peat emissions.

The relevance of the N-containing organics to climate and the N-cycle is briefly summarized next. Aerosol particles acting as cloud condensation nuclei (CCN) critically impact climate by production and modification of clouds and precipitation (Novakov and Penner, 1993). NPF, the formation of new stable nuclei, is suspected to be a major contributor to the amount of CCN in the atmosphere (Kerminen et al., 2005; Laaksonen et al., 2005; Sotiropoulou et al., 2006). Numerous studies have suggested that organic compounds containing nitrogen can play an important role in the formation and growth of new particles (Smith et al., 2008; Kirkby et al., 2011; Yu and Luo, 2014). The primary pathways to new particle formation include (1) reaction of organic compounds with each other or atmospheric oxidants to form higher molecular weight, lower volatility compounds that subsequently partition into the aerosol phase or (2) rapid acid/base reactions forming organic salts. The observation of significant emissions of N-containing organic gases in FLAME-4 could improve understanding of the compounds, properties, and source strengths contributing to new particle formation and enhance model predictions on local to global scales. The identities and amounts of these additional nitrogen containing emissions produced by peat and other BB fuels are also important in rigorous analysis of the atmospheric nitrogen budget.

Table 5.3. Emission ratios to NH_3 for nitrogen-containing species

Assignment	African Grass K1	African Grass S1	African Grass S2	Org. Alfalfa	Org. Alfalfa	Black Spruce	Chamise	3-Stone Red Oak	Envirofit Rocket-Red Oak	Giant Cutgrass	Giant Cutgrass	Org. Hay	Juniper	Manzanita
Fire #	49	82	81	36	65	39	63	102	105	116	120	87	98	10
MCE	0.973	0.978	0.970	0.915	0.912	0.959	0.943	0.972	0.985	0.959	0.956	0.941	0.963	0.933
%N	0.21	0.47	0.70	2.91	2.91	0.66	1.00	0.09	0.09	2.03	2.03	1.99	1.17	0.73
Ammonia (NH_3)	1	1	1	1	1	1	1	1	1	1	1	1	1	1
Hydrogen Cyanide (HCN)	0.950	0.579	0.428	0.102	0.113	0.471	0.162	1.60		0.277	0.625	0.116	8.32E-02	-
Nitric oxide (NO)	7.92	7.94	4.87	0.1371	0.257	3.48	2.84	10.4	16.7	1.74	2.52	0.423	2.66	8.33E-01
Nitrogen dioxide (NO_2)	5.48	2.84	1.93	0.0465	7.41E-02	2.76	0.502	23.8	16.4	0.404	0.743	9.61E-02	0.632	2.60E-03
Nitrous acid (HONO)	0.752	0.449	0.305	0.026	1.73E-02	0.504	0.220	3.47	-	6.41E-02	0.157	3.97E-02	0.135	0.412
Acetonitirile (C_2H_3N)	0.138	0.072	0.089	0.025	6.25E-02	7.28E-02	3.98E-02	0.125	2.62E-03	0.123	9.88E-02	8.13E-02	2.57E-02	-
Dimethylamine; Ethylamine (C_2H_7N)	-	0.032	0.032	6.35E-03	8.79E-03	8.30E-03	1.26E-02	0.221	2.33E-02	-	9.28E-04	2.65E-02	3.76E-03	4.33E-03
Acetamide (C_2H_5NO)	-	-	-	-	-	-	-	0.137	-	-	-	-	-	-
Trimethylamine (C_3H_9N)	0.051	0.004	0.011	1.32E-03	1.94E-03	4.05E-03	1.19E-03	-	-	9.16E-03	4.97E-04	3.16E-02	1.95E-04	1.26E-03
Assorted Amides (C_4H_9NO)	0.032	0.015	0.017	1.53E-03	4.09E-03	-	3.80E-03	0.191	6.56E-02	3.32E-03	-	7.24E-03	1.30E-03	-
Assorted Amines ($C_4H_{11}NO$)	-	3.18E-03	4.28E-03	-	-	-	-	-	-	-	-	-	-	-
Benzonitrile (C_7H_5N)	-	-	-	-	-	0.011	-	-	-	-	1.34E-03	-	-	6.58E-03
NH_3 as fuel N (%)	3.05	2.11	2.78	25.8	14.7	4.27	4.47	2.10	2.01	4.60	1.86	11.8	5.14	9.66
TOF N-species as fuel-N (%)	0.675	0.265	0.425	0.894	1.13	0.411	0.256	1.41	0.184	0.622	0.188	1.73	0.159	0.118

Table 5.3 (continued)

Assignment	Millet	Peat Canadian	Peat Indonesian	Peat Indonesian	Peat NC	Ponderosa Pine	Rice Straw China	Rice Straw Taiwan	Sawgrass	Sugar Cane	Sugar Cane	Wheat Straw Conv	Wheat Straw Org	Wiregrass
Fire #	37	112	114	125	113	35	93	85	55	117	121	75	96	78
MCE	0.931	0.811	0.744	0.872	0.692	0.912	0.938	0.947	0.957	0.914	0.929	0.963	0.965	0.972
%N	0.08	1.22	2.50	2.03	1.26	1.09	1.30	1.09	0.93	0.76	0.76	0.69	0.40	0.61
Ammonia (NH_3)	1	1	1	1	1	1	1	1	1	1	1	1	1	1
Hydrogen Cyanide (HCN)	-	0.571	1.22	3.02	1.47	0.374	0.205	0.299	0.696	0.287	0.210	0.288	0.590	0.891
Nitric oxide (NO)	3.40	-	-	1.16	0.211	1.15	0.843	1.36	5.10	0.456	0.555	3.82	4.71	14.44
Nitrogen dioxide (NO_2)	1.04	-	-	1.24	0.294	1.01	0.516	0.829	1.64	0.487	0.462	1.50	4.03	3.62
Nitrous acid (HONO)	-	-	-	-	-	0.447	0.139	0.116	0.250	0.214	0.171	0.240	0.454	1.29
Acetonitirile (C_2H_3N)	3.71E-02	7.33E-02	0.103	0.465	0.170	6.61E-02	0.092	0.104	0.115	0.103	0.078	4.18E-02	0.124	7.59E-02
Dimethylamine; Ethylamine (C_2H_7N)	3.40E-02	-	-	-	-	0.034	2.20E-02	2.20E-02	-	5.13E-02	8.52E-03	1.41E-02	8.55E-02	-
Acetamide (C_2H_5NO)	-	0.486	0.616	0.364	0.475	-	2.25E-02	-	-	-	-	-	-	-
Trimethylamine (C_3H_9N)	2.84E-03	-	-	-	-	3.74E-03	2.46E-03	2.11E-02	1.26E-02	4.13E-02	3.56E-03	3.92E-03	5.59E-02	2.60E-02
Assorted Amides (C_4H_9NO)	1.73E-02	1.08E-03	2.99E-04	3.82E-02	2.68E-04	1.62E-02	3.57E-03	1.08E-02	3.24E-03	3.16E-02	-	5.91E-03	5.29E-02	2.09E-02
Assorted Amines ($C_4H_{11}NO$)	-	-	-	-	-	-	4.92E-03	2.49E-03	-	8.99E-03	-	-	1.24E-02	-
Benzonitrile (C_7H_5N)	-	-	-	-	-	-	-	-	-	-	0.017	-	-	-
NH_3 as fuel N (%)	14.7	15.4	6.49	2.78	10.1	5.81	6.49	6.08	2.03	12.2	12.6	2.46	2.89	1.04
TOF N-species as fuel-N (%)	1.34	8.66	4.67	2.41	6.52	0.697	0.957	0.978	0.265	2.88	1.35	0.161	0.954	0.127

5.4.5 Sulfur, phosphorous, and chlorine-containing compounds

Sulfur emissions are important for their contribution to acid deposition and climate effects due to aerosol formation. Several S-containing gases have been detected in BB emissions including SO_2, carbonyl sulfide (OCS), dimethylsulfide (DMS), and dimethyl disulfide (DMDS), where DMS is one of the most significant organosulfur compounds emitted by BB and is quantified by PTR-TOF-MS in our primary dataset (Friedli et al., 2001; Meinardi et al., 2003; Akagi et al., 2011; Simpson et al., 2011). The signal at *m/z* 49 had a significant mass defect and is attributed to methanethiol (methyl mercaptan, CH_3SH), which to our knowledge has not been previously reported in real-world BB smoke though it has been observed in cigarette smoke (Dong et al., 2010) and in emissions from pulp and paper plants (Toda et al., 2010). Like DMS, the photochemical oxidation of CH_3SH leads to SO_2 formation (Shon and Kim, 2006), which can be further oxidized to sulfate or sulfuric acid and contribute to the aerosol phase. The emissions of CH_3SH are dependent on the fuel S-content and are negatively-correlated with MCE. The greatest EF(CH_3SH) in our additional analyses arose from organic alfalfa, which had the highest S-content of the selected fuels and also produced significant emissions of SO_2 detected by FTIR.

Other organic gases containing chlorine and phosphorous were expected to be readily detectable because of their large, unique mass defects and possible enhancement by pesticides and fertilizers in crop residue fuels. However, they were not detected in significant amounts by our full mass scans. Fuel P and Cl may have been emitted primarily as aerosol, ash, low proton affinity gases, or as a suite of gases that were evidently below our detection limit.

5.4.6 Miscellaneous (order of increasing m/z)

m/z 41: The assignment of propyne is reinforced by previous observations in BB fires, and it is of some interest as a BB marker even though it has a relatively short lifetime of ~2 days

(Simpson et al., 2011; Akagi et al., 2013; Yokelson et al., 2013a). Considering that propyne was not detected in every fuel type, a level of uncertainty is added to any use of this compound as a BB tracer and in general, the use of multiple tracers is preferred when possible.

m/z 43: The high-resolution capabilities of the PTR-TOF-MS allowed propylene to be distinguished from ketene fragments at *m/z* 43. The propylene concentrations are superseded in our present dataset by FTIR measurements, however, the two techniques agree well.

m/z 45: PTR technology has already been reported as a reliable way to measure acetaldehyde in BB smoke (Holzinger et al., 1999; Christian et al., 2004). Photolysis of acetaldehyde can play an important role in radical formation and is the main precursor of peroxy acetyl nitrate (PAN) (Trentmann et al., 2003). A wide range in EF(acetaldehyde) (0.13-4.3 g kg^{-1}) is observed during FLAME-4 and reflects variability in fuel type. The detailed emissions from a range of fuels in this dataset can aid in modeling and interpretation of PAN formation in aging BB plumes of various regions (Alvarado et al., 2010, 2013). Crop-residue fuels regularly had the greatest emissions of acetaldehyde, which is important considering many crop-residue fires evade detection and are considered both regionally and globally underestimated. Sugar cane burning had the largest acetaldehyde EF (4.3 ± 1.4 g kg^{-1}) and had significant emissions of oxygenated and N-containing compounds, consequently it is likely to form a significant amount of PAN.

m/z 57: The signal at *m/z* 57 using unit-mass resolution GC-PTR-MS was observed to be primarily acrolein with minor contributions from alkenes (Karl et al., 2007). In the PTR-TOF-MS, the two peaks at *m/z* 57 ($C_3H_5O^+$ and $C_4H_9^+$) are clearly distinguished and acrolein is often the dominant peak during the fire with the highest emissions from ponderosa pine and sugar cane.

m/z 69: The high resolution of the PTR-TOF-MS allowed three peaks to be distinguished at *m/z* 69, identities attributed to carbon suboxide (C_3O_2), furan (C_4H_4O), and mostly isoprene (C_5H_8) (Figure 5.7). Distinguishing between isoprene and furan is an important capability of the PTR-TOF-MS. The atmospheric abundance and relevance of carbon suboxide is fairly uncertain and with an atmospheric lifetime of ~10 days (Kessel et al., 2013) the reactivity and transport of C_3O_2 emitted by fires could have critical regional impacts. The emissions of C_3O_2 by BB will be interpreted in detail at a later date (S. Kessel, personal communication, 2014).

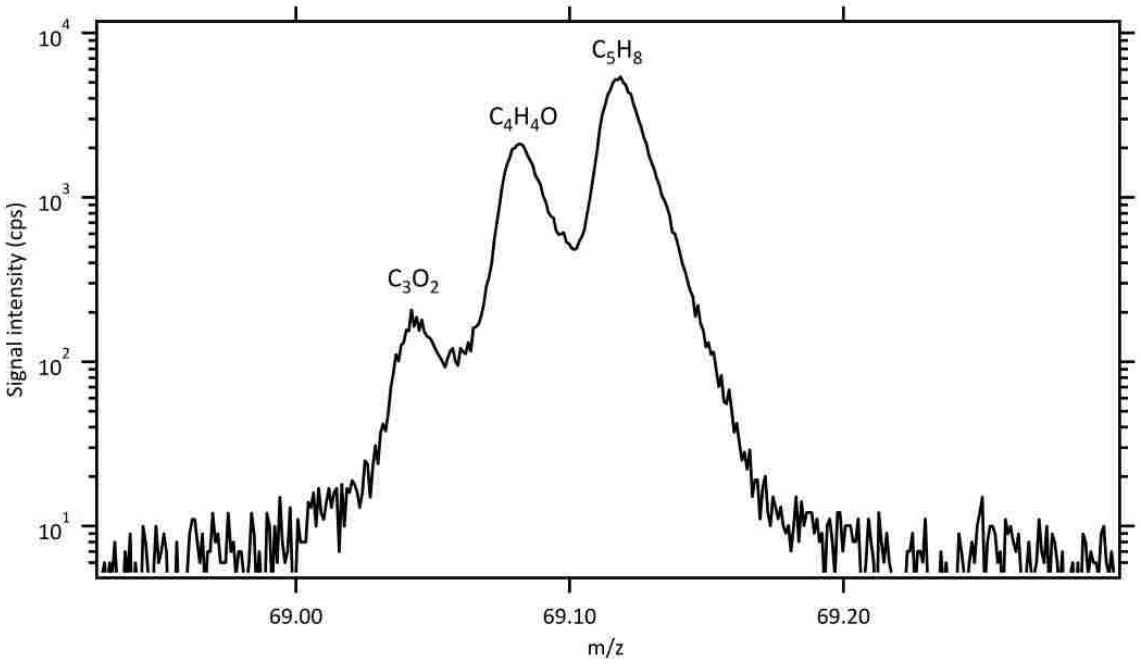

Figure 5.7. Expanded view of the PTR-TOF-MS spectrum at *m/z* 69 demonstrating the advantage over unit mass resolution instruments of distinguishing multiple peaks, in this instance separating carbon suboxide (C_3O_2), furan (C_4H_4O), and mostly isoprene (C_5H_8) in ponderosa pine smoke (fire 70).

m/z 75: Hydroxyacetone emissions have been reported from both field and laboratory fires (Christian et al., 2003; Akagi et al., 2011; Yokelson et al., 2013a; St. Clair et al., 2014). Christian et al. (2003) first reported BB emissions of hydroxyacetone, and noted very large

quantities from burning rice straw. The EF($C_3H_6O_2$) for rice straw was noticeably high (1.10 g kg^{-1}) in the FLAME-4 dataset and only sugar cane had greater emissions.

m/z 85, 87: The largest peak at *m/z* 85 was assigned as pentenone as it was monitored/confirmed by PIT-MS/ GC-MS in an earlier BB study (Yokelson et al., 2013a). Pentenone was a substantial emission from several fuels with ponderosa pine having the greatest EF. By similar evidence the minor peak at *m/z* 87 was assigned to pentanone but was only detected in a few of the fires in the second set of analyses with the most significant emissions arising from Indonesian peat.

m/z 107: Benzaldehyde has the same unit mass as xylenes, but is clearly separated by the TOF-MS. Greenberg et al. (2006) observed benzaldehyde during low temperature pyrolysis experiments with the greatest emissions from ponderosa needles (ponderosa pine produced the greatest EF in our dataset, range 0.10-0.28 g kg^{-1}). Benzaldehyde emissions were additionally quantified by GC-MS during a laboratory BB campaign and produced comparable EF to that of xylenes (Yokelson et al., 2013a). During FLAME-4 the EF(benzaldehyde) was comparable to EF(xylenes calibrated as p-xylene) as seen earlier except for peat burns where xylenes were significantly higher.

m/z 137: At unit mass resolution the peak at *m/z* 137 is commonly recognized as monoterpenes which can further be speciated by GC-MS. However, as shown in Figure 5.8 there can be up to three additional peaks at this mass that presently remain unidentified oxygenated compounds. As anticipated, the hydrocarbon monoterpene peak is significant for coniferous fuels such as ponderosa pine but much smaller for grasses. In this work we calibrated for α-pinene, which has

been reported as a major monoterpene emission from fresh smoke (Simpson et al., 2011; Akagi et al., 2013).

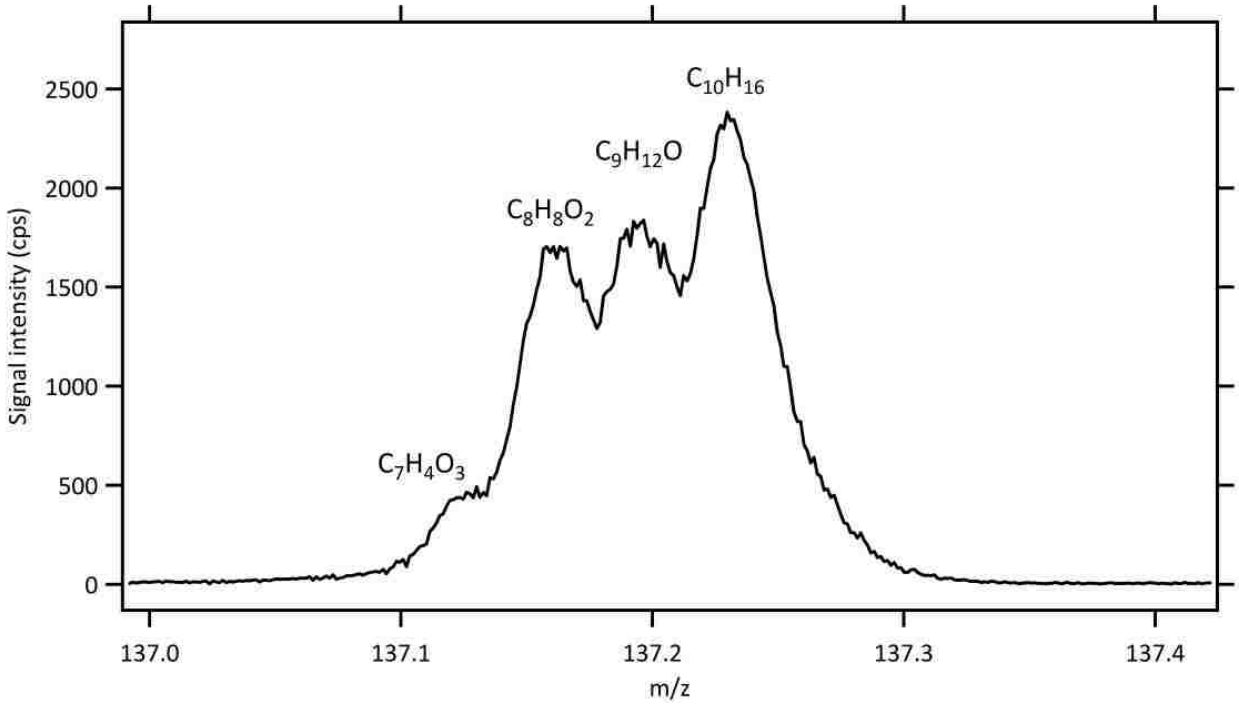

Figure 5.8. Expanded view of the PTR-TOF-MS spectrum of NC peat (fire 61) at m/z 137 showing multiple peaks.

5.1.1 Cookstoves

5.4.7 Cookstoves

Trace gas emissions were measured for four cookstoves including: a traditional 3-stone cooking fire, the most widely used stove design worldwide; two "rocket" type designs (Envirofit G3300 and Ezy stove); and a "gasifier" stove (Philips HD4012). Several studies focus on fuel efficiency of cookstove technology (Jetter et al., 2012), while the detailed emissions of many rarely measured and previously unmeasured gases are reported here and in Stockwell et al. (2014) for FLAME-4 burns. For cooking fires, ~3-6% of the NMOC mass remained unidentified, with the Envirofit rocket stove design generating the smallest percentage in the study. To improve the

representativeness of our laboratory open cooking emissions, the EFs of smoldering compounds reported for 3-stone cooking fires were adjusted by multiplying the mass ratio of each species "X" to CH_4 by the literature-average field EF(CH_4) for open cooking in Akagi et al. (2011). Flaming compounds were adjusted by a similar procedure based on their ratios to CO_2. The preferred values are reported in Table S4. With these adjustments, the emissions of aromatic hydrocarbons (Figure 5.9a), phenolic compounds (Figure 5.9b), and furans (Figure 5.9c) distinctively increased with the primitiveness of design, thus, 3-stone cooking fires produced the greatest emissions. The advancement in emissions characterization for these sources will be used to upgrade models of exposure to household air pollution and the ERs/EFs should be factored in to chemical-transport models to assess atmospheric impacts.

BB is an important source of reactive nitrogen in the atmosphere producing significant emissions of NO_x and NH_3 while non-reactive HCN and CH_3CN are commonly used as BB marker compounds (Yokelson et al., 1996, 2007; Goode et al., 1999; de Gouw et al., 2003). The FTIR used in FLAME-4 provided the first detection of HCN emissions from cooking fires and the HCN/CO ER was about a factor of 5 lower than most other BB fuels burned (Stockwell et al., 2014; Sect. 4.3.4). Similarly, acetonitrile emissions were measured for the first time for cooking fires by PTR-TOF-MS in this study and the CH_3CN/CO ERs from cooking fires are much lower (on average a factor of ~15) than those from other fuels. This should be considered when using CH_3CN/CO ERs to drive source apportionment in areas with substantial emissions from biofuel cooking sources.

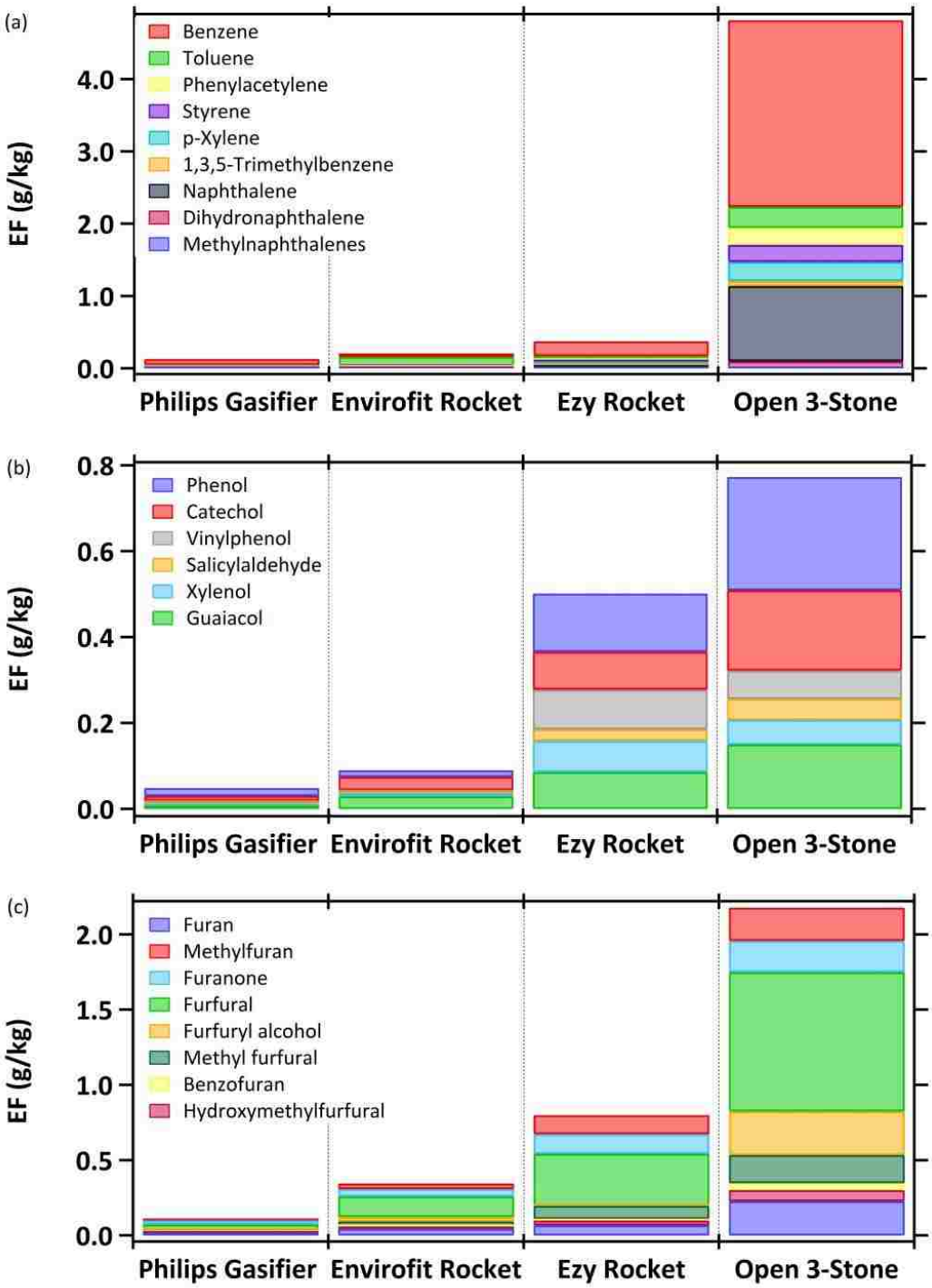

Figure 5.9. Emission factors (g kg-1) of aromatic hydrocarbons (a), phenolic compounds (b), and furans (c), for traditional and advanced cookstoves. The EFs for traditional stoves were adjusted from original lab data (Sect. 5.1.1)

5.5 Conclusions

We investigated the primary BB NMOC emissions from laboratory simulated burns of globally significant fuels using a PTR-TOF-MS instrument. In this first PTR-TOF-MS deployment dedicated to fires we encountered some specific challenges. The fast change in concentration necessitated a fast acquisition rate, which decreases the signal to noise for the emissions above background. The large dynamic concentration range necessitated dilution to minimize reagent ion depletion at peak emissions and the dilution further reduced the signal to noise ratio. Positive identification of some species by co-deployed grab sampling techniques will be explored further in a separate paper, but is challenged by the difficulty of transmitting some important fire emissions through GC columns (Hatch et al., 2015). We attempted to enhance compound identification by switching reagent ions (O_2^+ and NO^+), however, this approach with two broadly sensitive ions in a complex mixture resulted in spectra with complexity whose comparative analysis is beyond the scope of the present effort. Future experiments might consider instead using a less broadly sensitive reagent ion such as NH_3^+ as the alternate reagent ion. We were limited to our pre-chosen calibration mixture based primarily on gases previously observed in smoke. For future experiments we suggest adding more standards to generate more accurate calibration factors, specifically including major species such as furan and phenol and more compounds with S and N heteroatoms. In addition, measuring the fragmentation, if any, of more of the species identified in this work would be of great value. Despite these practical limitations, the experiment produced a great deal of useful new information.

The PTR-TOF-MS obtains full mass scans of NMOCs with high enough resolution to distinguish multiple peaks at the same nominal mass and high enough accuracy to assign chemical formulas from the “exact” masses. This aided in compound identification and more than 100 species were

categorized as a confirmed identity, a tentative (most likely) assignment, or unidentified but with a chemical formula. Chemical identification was aided by observations of compounds reported in smoke emissions, pyrolysis experiments, and those species at relevant concentrations in the atmosphere. This allowed the identification of more masses up to *m/z* 165 than in earlier work at unit mass resolution though an estimated range of 12-37% of the total mass still remains unidentified and tentatively identified. The analysis provides a new set of EFs for ~68 compounds in all fires plus ~50 more in select fires, in addition to species previously quantified by FTIR (Stockwell et al., 2014; Chapter 4) and other techniques during FLAME-4 (Hatch et al., 2015). While significant variability was observed between fuels, oxygenated compounds collectively accounted for the majority of emissions in all fuels with sugar cane producing the highest EF of oxygenated species on average possibly due to its high sugar content.

We also report emission ratios to benzene, phenol, or furan for the aromatic hydrocarbons, phenolic compounds, and substituted furans, respectively. Reporting emissions of previously unmeasured or rarely measured compounds relative to these more regularly measured compounds facilitates adding several new compounds to fire emissions models. To our knowledge this is the first on-line, real-time characterization of several compounds within these "families" for BB. Emissions were observed to vary considerably between fuel types. Several example compounds within each class (i.e. toluene, guaiacol, methylfuran, etc.) have been shown, by chamber experiments, to be highly reactive with atmospheric oxidants and contribute significantly to SOA formation. The EFs characterized by PTR-TOF-MS of fresh BB smoke are presented in Tables S3-S4 and (especially the recommended values in Table S4) should aid model predictions of O_3 and SOA formation in BB smoke and the subsequent effects on air

quality and climate on local-global scales. The EFs and ERs characterized by PTR-TOF-MS for each specific fire are compiled in the Supplementary tables included in Stockwell et al. (2015).

A large number of organic nitrogen-containing species were detected with several identities speculated as amines or amides. These N-containing organic gases may play an important role in new particle formation by physical, chemical, and photochemical processes, though a more focused study is necessary to measure NPF yields from these compounds and processes. The additional N-containing gases detected here account for a range of 1-87% of NH_3 dependent on fuel type with the most significant contribution of additional N-species to fuel N arising from peat burns. The ERs of acetonitrile to CO for cooking fires were significantly lower than other fuels and should be factored into source apportionment models in regions where biofuel use is prevalent if CH_3CN is used as a tracer.

The S-containing compounds detected by PTR-TOF-MS included dimethyl sulfide and methanethiol, where methanethiol was detected for the first time in BB smoke to our knowledge. These compounds may play a role in acid deposition and aerosol formation though to what extent has yet to be extensively studied. Phosphorous- and chlorine-containing organic gases were not readily observed in our dataset, which may reflect that these species were below our detection limit.

Using full mass scans from a high resolution PTR-TOF-MS to characterize fresh smoke has aided in identification of several compounds and provided the chemical formula of other organic trace gases. The additional NMOCs identified in this work are important in understanding fresh BB emissions and will improve our understanding of BB atmospheric impacts. The subsequent oxidation products of these gases are the focus of a companion paper probing BB aging. Taken

together, this work should improve BB representation in atmospheric models, particularly the formation of ozone and secondary organic aerosol at multiple scales.

Chapter 6 : Nepal Ambient and Source Testing Experiment (NAMaSTE)

6.1 NAMaSTE introduction

Several major atmospheric sources such as temperate forest biogenic emissions (e.g. Ortega et al., 2014), developed-world pollution from fossil fuel use (e.g. Ryerson et al., 2013), and laboratory-simulated biomass burning (e.g Stockwell et al., 2014; Chapters 3-5) have been sampled extensively with a wide range of instrumentation; but many important emission sources remain unsampled, or rarely sampled, by reasonably comprehensive efforts (Akagi et al., 2011). As the emissions of greenhouse gases and other air pollutants from developing countries have grown in importance for air quality and regional-global climate studies, the need for a more detailed understanding of these emissions has increased. For example, the diverse and loosely-regulated combustion sources of South Asia are poorly characterized and greatly undersampled relative to their proportion of global emissions (Akagi et al., 2011). These sources include industrial and domestic biofuel use (e.g. cooking fires), brick kilns, poorly-maintained vehicles, open burning of garbage and crop-residue, diesel and gasoline generators, and irrigation pumps.

Approximately 2.8 billion people worldwide burn solid fuels (e.g. wood, dung, charcoal, coal, etc.) for domestic (household) cooking and heating (Smith et al., 2013) with the largest share in Asia. Cooking fires are the largest source of soot in South Asia (Ramanathan and Carmichael, 2008). Industrial solid fuel use (e.g. brick kilns) is ubiquitous, but difficult to quantify in the developing world as it is not highly regulated or adequately-inventoried and can involve a variety of fuels (e.g. coal, sawdust, wood, garbage, tires, crop residue, etc.) (Christian et al., 2010).

Along with industrial and domestic solid fuel use, open burning of agricultural waste and garbage, gasoline and diesel-powered generators, and many examples of high-emitting vehicles are prevalent, but grossly undersampled in the developing world with previous field emissions characterization usually limited to a few trace gases and a few particulate species such as black carbon (BC) mass (Bertschi et al., 2003a; Christian et al., 2010; Akagi et al., 2011; Bond et al., 2013).

Understanding the local through global impacts of these sources is vital to modeling atmospheric chemistry, climate, and, notably, air quality as these sources most commonly occur indoors or near or within population centers. Aerosols directly affect climate through both absorption and scattering of solar radiation and indirectly effect climate by modifying clouds (Bond and Bergstrom, 2006). Therefore, global modeling of radiative forcing requires (among other things) accurate information on the amount and optical properties of aerosol emissions (Reid et al., 2005a,b). BB is a major source of BC in the atmosphere, but it also dominates the global emissions of weakly-absorbing organic aerosol known as brown carbon (BrC). BrC has a contribution to total absorption of BB aerosol that is poorly constrained, but critical to determining whether the net forcing of BB aerosol is positive or negative (Feng et al., 2003; Chen and Bond, 2010). Open burning of biomass and household-level consumption of biofuel account for a majority of BC emissions in important regions including Asia, but data are limited about how much BrC is emitted from biofuel and biomass combustion (Kirchstetter et al., 2004; Chen and Bond, 2010; Hecobian et al., 2010; Arola et al., 2011). In general, there is significant uncertainty in emissions inventories since BrC is rarely tabulated as a separate species though the scattering and absorption of both BC and BrC are necessary to model radiative transfer (Clark et al., 1987).

Additionally, the secondary formation of organic aerosol and ozone as well as the evolution of the BC and BrC optical properties are strongly influenced by the co-emitted gases and particles via processes such as coagulation, evaporation, oxidation, condensation, etc. (Alvarado et al., 2015; May et al., 2015). Near-source measurements of light absorption and scattering by BC and BrC and their emission factors (EFs), along with the suite of co-emitted gas-phase precursors are needed to better estimate the impacts of these undersampled sources on climate, chemistry, and local-global air quality, especially in regions that lack comprehensive sampling.

Current reviews of global BC emissions note that global models likely underestimate BC absorption in several important regions including South Asia (Bond et al., 2013), making this an important region where undersampled emission sources have critical climate and chemistry impacts. BC emissions from South Asia may negatively impact important regional water resources (Menon et al., 2010), contribute significantly to the warming of the Arctic (Allen et al., 2012; Sand et al., 2013), and emissions of volatile organic compounds (VOCs) and nitrogen oxides (NOx) in this region were estimated to influence global warming more significantly than similar emissions from other Northern hemisphere regions (Collins et al., 2013). Thus, these sources contribute significantly to the local-global burden of primary aerosol, greenhouse gases, and reactive trace gases. Crudely estimating their activity and the composition of their emissions can lead to significant errors and uncertainties in regional and global atmospheric models (Dickerson et al., 2002; Venkataraman et al., 2005; Adhikary et al., 2007, 2010; Akagi et al., 2011; Bond et al., 2013; Wiedinmyer et al., 2014).

The Nepal Air Monitoring and Source Testing Experiment (NAMaSTE) was a collaborative involving the International Centre for Integrated Mountain Development (ICIMOD, the in-country lead), MinErgy (a local contractor to ICIMOD), the Institute for Advanced Sustainability

Studies (IASS, fixed site support), and the universities of Drexel, Emory, Iowa (UI), California, Irvine (UCI), Montana (UM), and Virginia (UVA) in the US.

A well-equipped mobile team investigated numerous undersampled emissions sources in and around the Kathmandu Valley and in the rural Terai region in the Indo-Gangetic plains (IGP) of southern Nepal. The sources represented authentic, common practices, but were usually not random and were arranged by the MinErgy and ICIMOD team before the campaign. The source and fixed site measurements commenced on April 11 of 2015 but were cut short by the Gorkha earthquake on April 25. The early termination prevented sampling of on-road mobile sources including heavy duty diesel trucks, which is now planned for phase two. Additional measurements of cooking fires and other sources planned in the Makwanpur District in the foothills south of Kathmandu were also canceled, but many valuable data on similar sources had already been gathered. In this chapter we present a brief summary of the source sampling campaign and the details of the trace gas measurements of fresh emissions obtained by Fourier transform infrared (FTIR) spectroscopy and whole air sampling (WAS). We also present photoacoustic extinctiometer (PAX) data co-collected at 405 and 870 nm to measure the optical properties and estimate the mass of the fresh BC and BrC emissions. Substantial additional source characterization data based on sampling with Teflon and quartz filters and a suite of other real-time aerosol instruments will be presented separately (Jayarathne et al., 2016; Goetz et al., 2016). Several weeks of high quality filter, WAS, aerosol mass spectrometer, and other real-time data from the supersite at Bode will also be presented/discussed separately. Taken together, the NAMaSTE efforts reduce the information gap for these important undersampled sources.

6.2 Source types and site descriptions

Nepal has variable terrain ranging from high mountains to the low elevation plains in the Terai. Our team was based out of the major population center of Kathmandu and we traveled by truck to various locations in and around the Kathmandu Valley while also traveling south to the Terai region. The Terai sits on the southern edge of Nepal in the IGP with intensive agriculture, terrain, and other similarities to the heavily populated region of northern India. The emissions data we present were obtained from many sources including two-wheeled vehicles (motorcycles and scooters), diesel- and gasoline-powered generators, agricultural pumps, garbage fires, cooking fires, crop residue burning, and brick kilns. This section briefly summarizes the significance of each source and how they were sampled in our study.

6.2.1 Motorcycles and scooters

Mobile emissions are extremely important in urban areas as they contribute significantly to degradation of air quality on local to regional scales (Molina and Molina, 2002, 2004; Molina et al., 2007; Dunmore et al., 2015). In the Kathmandu Valley, approximately 80% of registered vehicles are motorcycles or scooters and this is the fastest growing portion of the transport sector in Kathmandu and nationally (MOPIT, 2014). Motorcycles are generally larger with larger engines than scooters and in Nepal both now burn unleaded Euro-3 gasoline. Together, nationally, these two-wheeled vehicles consume about one-third of the gasoline and ~10% of total fuel used for on-road transport (WECS, 2014), with total sales of diesel and gasoline approaching 1 Tg in 2015 (Nepal Oil Corporation Limited, 2015). Vehicle EFs are commonly obtained from bulk exhaust measurements (USEPA, 2015) and the International Vehicle Emissions (IVE) model specifically generates EF for mobile sources in the developing world (Shrestha et al., 2013). However, the detailed source chemistry (e.g. specific air toxics) is poorly

known, especially for the developing world, as most studies focus only on CO, NO_x, $PM_{2.5}$, and a few hydrocarbons or total VOC in developed countries (e.g. Zhang et al., 1993; Pang et al., 2014).

There are a number of approaches to measure vehicular emissions that include in-use sampling while driving as well as more controlled dynamometer studies (Yanowitz et al., 1999; Pelkmans and Debal, 2006). Franco et al. (2013) outline the advantages and drawbacks to these various sampling techniques, though we will not discuss them further here. We were able to measure the emissions exhaust of five motorcycles and one scooter during start-up and idling, which are considered common traffic situations in the Kathmandu Valley. On 13 April 2015, we set up the NAMaSTE emissions measuring equipment next to a motorcycle repair shop and to limit sampling bias, we deliberately tested every motorcycle/scooter that entered the shop for servicing that day. Each motorcycle and scooter was sampled (start-up and idling) pre- and post-servicing (one motorcycle was not sampled post-service). The motorcycle/scooter brand, model, etc. are shown in Table 6.1. The maintenance routine included an oil change, cleaning the air filters and spark plugs, and adjusting the carburetor.

Table 6.1. Details of sampled motorcycles and scooter

Vehicle type	Vehicle Number	Last Servicing (total vehicle mileage)	Years since purchase
Honda Hero CBZ 1	Ba 41 Pa; 8497	1500 km ago (45540 km)	6
Honda Hero CBZ 2	Ba 44 Pa; 3068	1500 km ago (18556 km)	5
Bajaj Pulsar	Ba 48 Pa; 9947	1700 km ago (18352 km)	4
Hero Honda Splendor	Ba 9 Pa; 7341	2500 km ago (35748 km)	15
Bajaj Discover	Ba 22 Pa; 3182	3000 km ago (53775 km)	10
Honda Aviator scooter	Ba 41 Pa; 5913	1600 km ago (17520 km)	3

6.2.2 Generators

Nepal has no significant fossil fuel resources and insufficient hydropower. As a result, load-shedding for many hours per day is common nationally and diesel or gasoline powered generators (a.k.a. gensets) are critical infrastructure for industrial, commercial, institutional, and household use, consuming about 57,000 Mg of fuel per year (World Bank, 2014). Based on fuel use, the emissions from generators could be about six percent of those from the transport sector. A large variety of generators are deployed to meet various size, power, and load capacity needs. In this study we sampled exhaust emissions from one small diesel generator with 5 kVa capacity (Chanqta, CED6500s) and a much larger diesel generator, located on the ICIMOD campus, with 100 kVa capacity running at 1518 RPM, 85% of full load. In addition to the two diesel generators, we sampled the exhaust emissions from one gasoline-fueled generator (Yeeda, Y-113(1133106)) that had a similar capacity (4 kVa) to the smaller diesel generator. Most pollutants from these engines are emitted through the exhaust, though some fraction likely escapes from fuel evaporation.

6.2.3 Agricultural water pumps

The use of diesel-powered agricultural pumps to extract groundwater for irrigation is rapidly rising in rural regions of Nepal and India with few to no operational regulations (Barker and Molle, 2004). The dependence on diesel operated pumps is likely to rise in South Asia as crop production rises with population demands. Although massive groundwater extraction has aided agricultural productivity in the region, the environmental impacts are seldom investigated (Shah et al., 2000). The pumps are estimated to consume ~1.3 Tg/yr of diesel fuel, over the entire IGP. Diesel-powered engine emissions can cause adverse health effects and unfavorably impact air quality, climate, crops, and soils (Lloyd and Cackette, 2001). We sampled the exhaust from two

smaller diesel pumps (Kirloskar, 4.6 kVa and Field Marshall R170a, 5 kVa) in the Terai. We also sampled the exhaust opportunistically from a much larger irrigation pump (Shineray) in suburban Kathmandu. We were unable to confirm fuel type, but suspect it was gasoline based on the emissions chemistry.

6.2.4 Garbage burning

Open burning of garbage is poorly characterized even in the most "developed" countries where it occurs with minimal oversight mostly in rural areas (USEPA, 2006). In developing countries open burning of garbage is much more prevalent, poorly characterized, and much less regulated if at all. In Nepal, as throughout the developing world, open burning of garbage is ubiquitous at a range of scales. Small, meter-scale piles of burning trash are seen along roads and in uncultivated fields. Approximately 10-20 times larger areas of burning trash are also common at landfills, along roadsides and riverbanks, and basically many accessible, uncultivated open spaces; with these areas evidently serving as an informal public resource. Given the large amount of refuse generated and the lack of economically viable alternatives to burning (Pokhrel and Viraraghavan, 2005), garbage burning is estimated to consume about 644,000 Mg of municipal solid waste (MSW) annually in Nepal (Wiedinmyer et al., 2014) and have a major impact on air quality, health, and atmospheric chemistry. The few available previous measurements of garbage burning suggest it is particularly important as a source of BC, hydrogen chloride, particulate chloride, several ozone precursors, and air toxics such as dioxins (Costner, 2005; Christian et al., 2010; Li et al., 2012; Lei et al., 2013; Wiedinmyer et al., 2014; Stockwell et al., 2014, 2015). To our knowledge only one study reports reasonably comprehensive EFs for authentic open burning of garbage in the developing world, namely the landfill fire sampling in Mexico of Christian et al. (2010). Several lab studies have measured the emissions from garbage burning under controlled

conditions in great chemical detail (Yokelson et al., 2013a; Stockwell et al., 2014, 2015), but the relevance of these lab experiments needs further evaluation against a better picture of real-world garbage burning. More real-world data are also needed to evaluate and update the garbage burning global inventory mentioned above (Wiedinmyer et al., 2014).

During NAMaSTE, we were able to contribute a modest but important expansion of the real world garbage-burning sampling. We sampled mixed-garbage burning on 6 occasions and we conducted 3 experiments burning segregated trash since some processing of garbage before combustion is common. The segregated trash experiments isolated plastics and foil-lined bags in separate individual burns. The components in each garbage burn are summarized in Table 6.2. The overall carbon fraction for mixed waste was calculated in Stockwell et al. (2014) by estimating the carbon content of each component in the mixture and the value for overall carbon content calculated there-in is assumed in our mixed garbage EF calculations (0.50). Polyethylene terephthalate (PET) is the most common plastic used in metallized packaging, such as the case for chip and other foil-lined bags, and has a carbon fraction of 0.63 (USEPA, 2010). Most plastic bags are composed of high- and low-polyethylene (HDPE, LDPE) mixed with PET, and thus we estimate a carbon content of 0.745 in this study (USEPA, 2010).

Table 6.2. Garbage composition and sampling details

Sample ID	Contents	Notes	Date	Location
Mixed garbage 1	Many bags full of mixed trash: food waste, paper, plastic bags, cloth, diapers, rubber shoe	A lot of damp material-rekindle with newspaper on occasion; Several flaming and smoldering grabs	14-Apr	ICIMOD campus: 27.64660 °N 85.323063°E
Mixed garbage 2	Mixed waste including cardboard and chip bags	Grass used to ignite	24-Apr	Daunne devi V.D.C. 5 Ganga Basti: 27.50204 °N 83.79593°E
Mixed garbage 3	Roadside garbage burning: cardboard, paper, metal, cans, cloth, newspaper, cigarette packets	-	6-Jun	Jadibuti : 27.675056°N 85.353199°E
Mixed garbage 4	Mixed waste with corn cobs, plastic, leaves	Kathmandu suburb near Manohara River	6-Jun	Purano Sinamangal: 27.686385°N, 85.364453°E
Mixed garbage 5	Household food waste burning; newspaper, egg shells, leafy vegetables, orange peels, foil food packets, cigarette butts, plastic bags, cardboard, paper	-	6-Jun	Mill Road; between Bode and Madhyapur, Thimi: 27.687793°N, 85.388778°E
Mixed garbage 6	Plastic, newspaper, shoe	Large trash fire near Bode ambient site; dominated by flaming combustion, a lot of visible black smoke	6-Jun	Kathmandu: 27.688697°N, 85.395472°E
Mixed Chip bags	Bags with foil lining (chip bags, chocolate wrappers, aluminum foil bags)	Burned quickly, not many grab samples	14-Apr	ICIMOD campus: 27.64660 °N 85.323063°E
Plastics 1	Lots of heavier clear plastic, some plastic cups and food bags; at one point blue re-useable shopping bag thrown in	May have some paper present	14-Apr	ICIMOD campus: 27.64660 °N 85.323063°E
Plastics 2	Primarily burning of plastic bags; blue plastic bags, some cardboard packaging	Southern edge of Bode planning region; flaming combustion	6-Jun	Bode; 27.689209°N, 85.392948°E

6.2.5 Cooking stoves

Most global estimates of domestic biofuel consumption (~3000 Tg/yr) designate domestic biofuel burning as the second largest BB source behind savanna fires (Akagi et al., 2011). In the developing world, it is estimated that the majority of biomass fuel is burned in Asia (~66%; Yevich and Logan, 2003). The solid fuels regularly burned include wood-derived fuels (e.g. hardwood, twigs, sawdust, charcoal) and agricultural residues (e.g. crop waste, livestock dung, etc.) though the fuel choice depends on availability, local customs, and the season. Yevich and Logan (2003) estimate residential wood fuel use for Nepal in 1985 as 9.8 Tg/yr. They do not estimate dung fuel use in Nepal, but the data they provide for Indian states with populations similar to Nepal suggests that about 1-2 Tg/yr of dung is combusted residentially in Nepal.

The cooking fire measurements in this study were conducted in two phases. First measurements were conducted by simulating field cooking in a laboratory to capture emissions from a wide range of stove- and fuel-types. Fuels for the lab tests included wood, dung, mixed wood and dung, biobriquettes, and biogas. Stove types included traditional single-pot mudstove, open 3-stone, bhuse chulo (insulated vertical combustion chamber), rocket stove, chimney stove, and forced draft stove. In the second phase, cooking emissions were sampled from authentic cooking fires in the kitchens of several rural Nepali homes and one restaurant operated out of a personal kitchen. The two kitchens that utilized the traditional 1-pot clay stove were separated from the main dwelling by a mud wall. The ventilation for all cases was by passive draft through the door, open windows, and gaps between the walls and roof. Smoke samples were taken from the upper corner of the kitchen where the inflow and outflow of emissions were somewhat balanced and we were able to grab representative samples of accumulated emissions not needing weighting by the fire-driven flow. Several biofuels are available to the home and restaurant owners including

twigs and larger pieces of hardwood (*Shorea robusta* and *Melia azedarach* [Bakaino]) and dung shaped into logs or cakes sometimes containing minor amounts of straw. Different fuels or a combination of fuels were consumed depending on cooking preference. Our study was designed to bring more comprehensive trace gas and aerosol field sampling to the effort to understand cooking fires. We note that the women tending to the cookstoves were in and out of the kitchens with their children during food preparation so exposure is also a concern. While our concentration data could be used directly for indoor exposure estimates, a better approach for estimating exposure to the air toxics we report is via our ratios to commonly measured species in the available studies more focused on representative exposure.

6.2.6 Crop Residue

Crop residue burning is ubiquitous during the dry season in the Kathmandu Valley and rural Nepal. Globally, burning crop residue post-harvest is widely practiced to enable faster crop rotation; reduce weeds, disease, and pests; and return nutrients to the soil. Alternatives to crop residue burning such as plowing residue into the soil or use as livestock feed have drawbacks including increased risk of wind-erosion of top soil and poor "feed" nutritional quality (Owen and Jayasuriya, 1989). Thus, open burning of crop residue is a prevalent activity in both developing and developed countries and it has important atmospheric impacts, but the emissions are not well characterized (Yevich and Logan, 2003; Streets et al., 2013; Sinha et al., 2014). Data for Indian states with similar population to Nepal suggest that total annual crop residue burning in Nepal is on the order of 6-7 Tg/yr (Yevich and Logan, 2003).

The land-use in southern Nepal is representative of the much larger Indo-Gangetic plains, which are inhabited by nearly a billion people. Crop residue types may impact emissions significantly, thus, mostly in the Terai, we characterized emissions from two regionally important crop types

separately: rice straw and wheat. Additionally, we sampled the emissions from the burning of other crop types important in this region including mustard residue, grass, and a mixture of these residues. The carbon fractions assumed in this study were taken from previous analyses of similar fuels compiled in Table 3.1.

6.2.7 Brick kilns

Brick production is an important industry in South Asia and the number of brick kilns in Nepal and India combined likely exceeds 100,000 (Maithel et al., 2012) with perhaps ~1000 kilns in Nepal that would likely require ~1-2 Tg of fuel per year. However, the industry is neither unambiguously inventoried nor strongly regulated. The previous trace gas and particulate emissions data available on brick kilns are very limited (Christian et al., 2010; Weyant et al., 2014). We were not able to sample a large number of kilns in Nepal, but we were able to greatly expand the number of important trace gas and aerosol species/properties quantified.

During NAMaSTE, we sampled two brick kilns just outside the Kathmandu Valley that employed different common and regionally important technologies. The first kiln sampled was a zig-zag kiln, which is considered relatively advanced due to an airflow system that efficiently transfers heat to multiple brick chambers. We note that many zig-zag kilns in the Kathmandu valley have a chimney upwards of ten meters high to minimize impacts on immediate neighbors. The tall stacks are most easily sampled from a port on the side, but this raises uncertainties due to possible condensation after sampling hot/moist exhaust or losses on stack walls past the sampling point. Therefore we elected to sample the zig-zag emissions from a kiln outside the valley with a shorter chimney and where our inlet could be within several meters of the chimney where emissions had cooled to near ambient temperature. This approach was followed to reliably sample the "real" emissions. The zig-zag chimney emissions were sampled for five hours (9

a.m.-2 p.m.), which captured several firing/feeding cycles lasting about one hour each. By cycles we refer to the periodic addition of a primarily coal/bagasse mix during the day through multiple feeding orifices (a.k.a. stoke holes) above the firing chamber that were moved as the firing progressed. We also occasionally diverted the sampling to capture the emissions from these stoke holes. The smoke emitted from both the chimney and stoke holes mostly appeared white with occasional puffs of brown smoke when coal was added through the stoke holes.

The second kiln was a common batch-type clamp kiln. In clamp kilns green unfired bricks are stacked and brick walls are built up to surround the unfired bricks. Each batch is stacked, fired, cooled and must be unloaded before firing the next batch. There is no chimney to vent emissions as the kiln ventilates freely through the sides and roof. The naturally escaping emissions were sampled at or near ambient temperature about a meter from the roof throughout the day. The clamp kiln smoke always appeared white with no apparent periods of black smoke.

Generally the cheapest type of coal available is used in south Asian kilns. Bricks are typically fired to 700-1100℃ and consume significant amounts of coal and biomass as detailed elsewhere (Maithel et al., 2012). The practice of biomass co-firing to reduce the use of coal is common as it reduces expense, but co-firing in general is also known to reduce fossil-CO_2 emissions and some criteria pollutants such as NO_x and SO_2 (e.g. Al-Naiema et al., 2015). We expect that the emissions change depending on the biomass to coal blending ratios in South Asia and that the blend likely varies considerably between kilns. In the two kilns we measured the primary fuel was coal, however, the clamp kiln was more substantially co-fired with biomass. The coal piles next to the clamp kiln were adjacent to large piles of cut hardwood, thus, the coal was likely co-fired with a substantial amount of hardwood and the emissions data confirms that. We note that we were not on site long enough to measure the emissions from the entire kiln lifetime. Thus, we

cannot probe seasonal variation in brick kiln emissions. However, we did capture 4-5 entire firing cycles from each kiln that should represent the emissions near the end of the dry season production period. Some kiln operators suspect that these emissions may reflect more efficient combustion (and more bricks per kg fuel) than when the kilns are first started up in January under conditions of lower ambient temperature.

6.3 Instrument details

6.3.1 Land-based Fourier transform infrared (LA-FTIR) spectrometer

A rugged, cart-based, mobile FTIR (MIDAC, Inc.) designed to access remote sampling locations (Christian et al., 2007) was used for trace gas measurements. The system can run on battery or generator power. The vibration-isolated optical bench consists of a MIDAC spectrometer with a Stirling cycle cooled mercury-cadmium-telluride (MCT) detector (Ricor, Inc.) interfaced with a closed multipass White cell (Infrared Analysis, Inc.) that is coated with a halocarbon wax (1500 Grade, Halocarbon Products Corp.) to minimize surface losses (Yokelson et al., 2003a). In the grab sampling mode used for the FTIR trace gas data reported in this paper, air samples are drawn into the cell by a downstream pump through several meters of 0.635 cm o.d. corrugated Teflon tubing. The air samples are then trapped in the closed cell by Teflon valves and held for several minutes for signal averaging to increase sensitivity. Once the IR spectra of a grab sample are logged on the system computer a new grab sample can be obtained. This facilitates collecting many grab samples. Cell temperature and pressure are also logged on the system computer (Minco TT176 RTD, MKS Baratron 722A). Spectra were collected at a resolution of 0.50 cm^{-1} covering a frequency range of 600-4200 cm^{-1}. Since the last report of the use of this system (Akagi et al., 2013), several upgrades were made: (1) addition of a retroreflector to the White cell mirrors increased the optical pathlength from 11 m to 17.2 m, lowering previous instrument

detection limits, (2) replacing the Teflon cell coating with halocarbon wax for better measurements of ammonia (NH_3), hydrogen chloride (HCl), hydrogen fluoride (HF), and other species prone to absorption on surfaces, (3) mounting the mirrors to a stable carriage rather than the previous method of gluing them to the cell walls, (4) the above mentioned Stirling cycle detector, which gave the same performance as a liquid-nitrogen-cooled detector without the need for cryogens, (5) the addition of two logged flow meters (APEX, Inc.) and filter holders to enable the system to collect particulate matter on Teflon and quartz filters for subsequent laboratory analyses. The new lower detection limits vary by gas from less than 1 ppb to ~100 ppb and are more than sufficient for near-source ground-based sampling as concentrations are much higher (e.g. ppm range) than in lofted smoke (Burling et al., 2011). Gas-phase species including carbon dioxide (CO_2), carbon monoxide (CO), methane (CH_4), acetylene (C_2H_2), ethylene (C_2H_4), propylene (C_3H_6), formaldehyde (HCHO), formic acid (HCOOH), methanol (CH_3OH), acetic acid (CH_3COOH), furan (C_4H_4O), hydroxyacetone ($C_3H_6O_2$), phenol (C_6H_5OH), 1,3-butadiene (C_4H_6), nitric oxide (NO), nitrogen dioxide (NO_2), nitrous acid (HONO), NH_3, hydrogen cyanide (HCN), HCl, sulfur dioxide (SO_2), and HF were quantified by fitting selected regions of the mid-IR transmission spectra with a synthetic calibration non-linear least-squares method (Griffith, 1996; Yokelson et al., 2007). HF and HCl were the only gases observed to decay during the several minutes of sample storage in the multipass cell. Thus for these species, the results are based on retrievals applied separately to the first ten seconds of data in the cell (Yokelson et al., 2003a). An upper limit 1σ uncertainty for most mixing ratios is ±10%. Post-mission calibrations with NIST-traceable standards indicated that CO, CO_2, and CH_4 had an uncertainty between 1-2%, suggesting an upper limit on the field measurement

uncertainties for CO, CO_2, and CH_4 of 3-5%. The NO_x species have the highest interference from water lines under the humid conditions in Nepal and the uncertainty for NO_x species is ~25%.

In addition to the primary grab sample mode, the FTIR system was also used in a real-time mode to support filter sampling when grab samples were not being obtained. Side by side Teflon and quartz fiber filters preceded by cyclones to reject particles with an aerodynamic diameter > 2.5 microns were followed by logged flow meters. The flow meter output was then combined and directed to the multipass cell where IR spectra are recorded at ~1.1 second time resolution. In real-time/filter mode we did not employ signal averaging of multiple scans and the signal to noise is lower at high time resolution. In addition, there could be sampling losses of sticky species such as NH_3 on the filters. However, the data quality is still excellent for CO_2, CO, and CH_4. This allowed the time-integrated mass of particle species to be compared to the simultaneously sampled time-integrated mass of CO and other gases and provided additional measurements of the emissions for these three gases as described in detail in the filter sampling companion paper (Jayarathne et al., 2016).

6.3.2 Whole air sampling (WAS) in canisters

Whole air samples were collected in evacuated 2 L stainless steel canisters equipped with a bellows valve that were pre-conditioned by pump-and-flush procedures (Simpson et al., 2006). The canisters were filled to ambient pressure directly in plumes (alternately from the FTIR cell for the zig-zag kiln) to enable subsequent measurement and analysis of a large number of gases at UCI (Simpson et al., 2006). Species quantified included CO_2, CO, CH_4 and 93 non-methane organic compounds (NMOCs) by gas chromatography coupled with flame ionization detection, electron capture detection, and quadrupole mass spectrometer detection as discussed in greater detail by Simpson et al. (2011). Peaks of interest in the chromatograms were individually

inspected and manually integrated. The limit of detection for most NMOCs that were sampled was 20 pptv, which was well below the observed levels. Typically ~60 WAS NMOCs were enhanced in the source plumes and we do not report the results for most multiply-halogenated species and the higher alkyl nitrates, which are mostly secondary photochemical products. The species we do not report were not correlated with CO and are generally not emitted directly by combustion (Simpson et al., 2011). Styrene is known to decay in canisters and the styrene data may be lower limits. 96 WAS canisters were sent to Nepal to support the source characterization and ambient monitoring site. Because we anticipated needing canisters for a longer campaign, typically only one emissions sample and one background sample were collected for each source on each day. 48 WAS canisters were filled in all, mostly in April, along with FTIR and other instruments, but some additional source and background measurements were conducted by WAS alone in June after the main campaign. The trace gas measurement techniques used for the reported EFs are indicated in the "method" row near the top of the supplemental and main tables.

6.3.3 Photoacoustic extinctiometers (PAX) at 405 nm and 870 nm

Particle absorption and scattering coefficients (B_{abs}, B_{scat}), single scattering albedo (SSA), and absorption Ångström exponent (AAE) at 405 nm and 870 nm were measured directly at 1 s time resolution using two photoacoustic extinctiometers (PAX, Droplet Measurement Technologies, Inc., CO). This monitored the real-time absorption and scattering resulting from BC and (indirectly) BrC. The two units were mounted with AC/DC power options, a common inlet, desiccator (Silica Gel), and gas scrubber (Purafil) in rugged, shock-mounted, Pelican military-style hard cases. Air samples were drawn in through conductive tubing equipped with 1.0 μm size-cutoff cyclones (URG) at 1 L/min. The continuously sampled air is split between a nephelometer and photoacoustic resonator enabling simultaneous measurements of scattering

and absorption at high time resolution. Once drawn into the acoustic section, modulated laser radiation is passed through the aerosol stream and absorbed by particles in the sample of air. The energy of the absorbed radiation is transferred to the surrounding air as heat and the resulting pressure changes are detected by a sensitive microphone. Scattering coefficients at each wavelength were measured by a wide-angle integrating reciprocal nephelometer, using photodiodes to detect the scattering of the laser light. The estimated uncertainty in absorption and scattering measurements is ~4-11% (Nakayama et al., 2015). Additional details on the PAX instrument can be found elsewhere (Arnott et al., 2006; Nakayama et al., 2015). Due to damage during shipping the PAXs were not available until repaired part-way thru the campaign and PAX data are therefore not available for a few sources.

Calibrations of the two PAXs were performed frequently during the deployment using the manufacturer recommended scattering and absorption calibration procedures utilizing ammonium sulfate particles and a kerosene lamp to generate pure scattering and strongly absorbing aerosols, respectively. The calibrations of scattering and absorption of light were directly compared to measured extinction by applying the Beer-Lambert Law to laser intensity attenuation in the optical cavity (Arnott et al., 2000). As a quality control measure, we frequently compared the measured total light extinction (B_{abs} + B_{scat}) to the independently measured laser attenuation. For nearly all the 1-s data checked, the agreement was within 10% with no statistically significant bias; consistent with (though not proof of) the error estimates in Nakayama et al. (2015).

6.3.4 Other measurements

Two instruments provided CO_2 data that was used in the analysis of the PAX data. An ICIMOD Picarro (G2401) cavity ring-down spectrometer measured CO_2, CO, CH_4, and H_2O in real-time.

A Drexel LI-COR (LI-820) that was factory calibrated immediately before the campaign also measured CO_2 in real time. The sampling inlet of the Picarro and/or LI-COR was co-located with the PAX inlets so that the time-integrated PAX particle data were easily ratioed to time-integrated CO_2 allowing straightforward, accurate synthesis of the PAX data with the mobile FTIR and WAS grab sample measurements as described below. A suite of other instruments (mini-aerosol mass spectrometer; seven wavelength, dual spot aethalometer (model AE33); etc. from Drexel) and the filters employed during the source sampling for subsequent analysis at UI will be described in more detail in companion papers (Jayarathne et al., 2016; Goetz et al., 2016).

6.4 Emission ratio and emission factor determination

The excess mixing ratios above the background level (denoted ΔX for each gas-phase species "X") were calculated for all gas-phase species. The molar emission ratio (ER) for each gaseous species X relative to CO or CO_2 was calculated for the FTIR and WAS species. For the single WAS sample of any source the ER was simply $\Delta X/\Delta CO$ or ΔCO_2. The source-average ER for each FTIR species, typically measured in multiple grab samples, was estimated from the slope of the linear least-square line (with the intercept forced to zero) when plotting ΔX versus ΔCO or ΔCO_2 for all samples of the source (Yokelson et al., 2009; Christian et al., 2010). Forcing the intercept effectively weights the points obtained at higher concentrations that reflect more emissions and have greater signal to noise. Alternate data reduction methods usually have little effect on the results as discussed elsewhere (Yokelson et al., 1999). For a handful of species measured by both FTIR and WAS it is possible to average the ERs from each instrument for a source together as in Yokelson et al., (2009). However, in this study, due to the large number of FTIR samples (~5-30) and small number of WAS samples (typically one) of each source we simply used the FTIR ER for "overlap species" (primarily CH_3OH, C_2H_4, C_2H_2, and CH_4).

From the ERs, emission factors (EFs) were derived in units of grams of species X emitted per kilogram of dry biomass burned by the carbon mass balance method as described in Sect. 2.1. The carbon fraction was either measured directly (ALS Analytics, Tucson, Table 6.3) or assumed based on measurements of similar fuel types (Stockwell et al., 2014; Chapter 4). Our total carbon estimate includes all the gases measured by both FTIR and WAS in grab samples of a source and we include the carbon in elemental and organic carbon (ratioed to CO) measured during filter sampling. Ignoring the carbon emissions not measureable by our suite of instrumentation (typically higher molecular weight oxygenated organic gases) likely inflates the EF estimates by less than ~1-2% (Andreae and Merlet, 2001; Yokelson et al., 2013a; Stockwell et al., 2015).

Table 6.3. Fuel analysis for select fuels

Fuel Type	Carbon (wt%)	Hydrogen (wt%)	Nitrogen (wt%)	Sulfur (wt%)	Chlorine (wt%)	Fluorine (wt%)
Zig-zag kiln coal	72.21	5.72	1.6	1.28	<0.03	<0.03
Clamp kiln coal	66	4.66	1.48	0.68	<0.03	<0.03
Zig-zag kiln brick	0.04	0.22	0.03	n/a	n/a	<0.03
Clamp kiln brick	0.05	0.24	0.03	n/a	n/a	<0.03
RETS laboratory coal	89.46	1.62	0.6	n/a	n/a	n/a
Yak dung (in MT)[a]	37.42	5.45	1.9	0.19	0.05	n/a

[a]Carbon fraction for dung assumed in this work is based on the average of our MT yak dung and the dung value (0.326) in *Keene et al.* (2006)

Biomass fire emissions vary naturally as the mix of combustion processes varies. The relative amount of smoldering and flaming combustion during a fire can be roughly estimated from the modified combustion efficiency (MCE). MCE is defined as the ratio $\Delta CO_2/(\Delta CO_2+\Delta CO)$ and is mathematically equivalent to $(1/(1+\Delta CO/\Delta CO_2)$ (Yokelson et al., 1996; Sect. 2.1). Flaming and smoldering combustion often occur simultaneously during biomass fires, but a very high MCE (~0.99) designates nearly pure flaming (more complete oxidation) while a lower MCE (~0.75-0.84 for biomass fuels) designates pure smoldering. Source-averaged MCE was computed for all

sources using the source average $\Delta CO/\Delta CO_2$ ratio as above. In the context of biomass or other solid fuels, smoldering refers to a mix of solid-fuel pyrolysis and gasification (Yokelson et al., 1997) that does not occur in the liquid fuel sources we sampled (e.g. motorcycles, generators, pumps). However, given the large difference in the heat of formation for CO_2 and CO (283 kJ/mol) and CO being the most abundant carbon-containing emission from incomplete combustion, MCE and $\Delta CO/\Delta CO_2$ were useful qualitative probes of their general operating efficiency.

The time-integrated excess B_{abs} and B_{scat} from the PAXs were used to directly calculate the source average single scattering albedo (SSA, defined in Eqn. 1) at both 870 and 405 nm for each source). The PAX time-integrated excess B_{abs} at 870 and 405 nm were used directly to calculate each source-average AAE (Eqn. 2).

Emissions factors for BC and BrC were calculated from the light absorption measurements made by PAXs at 870 and 405 nm (described in Sect. 6.3.3). Aerosol absorption is a key parameter in climate models, however, inferring absorption from total attenuation of light by particles trapped on a filter, or from the assumed optical properties of a mass measured by thermal/optical processing, incandescence, etc. can sometimes suffer from artifacts (Subramanian et al., 2007). In the PAX, the 870 nm laser is absorbed in-situ by black carbon containing particles only without filter or filter-loading effects that can be difficult to correct. We directly measured aerosol absorption (B_{abs}, Mm^{-1}) and used the literature-recommended mass absorption coefficient (MAC) (4.74 ± 0.63 m^2/g at 870 nm) to calculate the BC concentration ($\mu g/m^3$) (Bond and Bergstrom, 2006). To a good approximation, sp2-hybridized carbon has an AAE of 1.0 ± 0.2 and absorbs light proportional to frequency. Thus, B_{abs} due only to BC at 405 nm would be expected to equal $2.148 \times B_{abs}$ at 870 nm. This assumes any coating effects are similar at both wavelengths

and has other assumptions considered reasonably valid, especially in BB plumes by Lack and Langridge (2013). Following these authors, we assumed that excess absorption at 405 nm, above the projected amount, is associated with BrC absorption and the BrC ($\mu g/m^3$) concentration was calculated using a literature-recommended brown carbon MAC of 0.98 ± 0.45 m^2/g at 404 nm (Lack and Langridge, 2013). The BrC mass calculated this way is considered roughly equivalent to the total organic aerosol (OA) mass, which as a whole weakly absorbs UV light, and not the mass of the actual chromophores. The MAC of bulk OA varies substantially and the BrC mass we calculate with the single average MAC we used is only qualitatively similar to bulk OA mass for "average" aerosol and even less similar to bulk OA for non-average aerosol (Saleh et al., 2014). The BrC mass estimated by PAX in this way was independently sampled and worth reporting, but the filters and mini-AMS provide additional samples of the mass of organic aerosol emissions that have lower per-sample uncertainty for mass. However, the optical properties from the PAX (SSA, AAE, and absorption EFs detailed below) are not impacted by MAC variability or filter artifacts. As mentioned above, the PAXs were run in series or parallel with a CO_2 monitor. The mass ratio of BC and BrC to the simultaneous co-located CO_2, measured by either the Picarro or LI-COR, was multiplied by the FTIR-WAS grab sample EF for CO_2 to determine mass EFs for BC and BrC in g/kg. From the measured ratios of B_{abs} and B_{scat} to CO_2, the EFs for scattering and absorption at 870 and 405 nm (EF B_{abs}, EF B_{scat}) were calculated and reported in units of m^2 emitted per kg of dry fuel burned. The absorption and scattering EFs do not depend on assumptions about the AAE of BC or MAC values. Both the CO_2 and PAX sample were often diluted by using a Dekati Ltd. Axial Diluter (DAD-100), which was factory calibrated to deliver 15.87 SLPM of dilution air at an atmospheric pressure of 1004.6 mbar. Since both instruments samples were diluted by the same amount the dilution factor does not

impact the calculation of PAX/CO_2 ratios. On the other hand, the dilution could have some impact on gas-particle partitioning and the mass of BrC measured. More on the dilution system (and additional aerosol measurements) will be in a forthcoming companion paper (Goetz et al., 2016). Related measurements of elemental and organic carbon on the filters will be discussed by Jayarathne et al., (2016).

6.4.1 Emission factors for sources with mixed fuels

Several of the cooking fires burned a mix of wood and dung, mixed garbage was burned, and the brick kilns co-fired some biomass with the dominant coal fuel. It is not possible to quantify the exact contribution of each fuel to the overall fuel consumption during a specific measurement period or even in total. Thus for the mixed-fuel cooking fires, we simply assumed an equal amount of wood and dung burned and used the average carbon fraction for the two fuels (0.40) (Stockwell et al., 2014; Table 6.3). For mixed garbage we used a rigorous laboratory carbon content determination (0.50, Stockwell et al., 2014, Table 3.2) as opposed to a field determination that relied in part on visual estimates of the amount of components (0.40, Christian et al., 2010). For the zig-zag kiln, we used the measured carbon content of the coal (0.722). For the clamp kiln, which likely had more co-fired biomass, we used a weighted carbon content assuming 10% biomass (at a generic 0.50 carbon content) and 90% coal (measured carbon content 0.660). The weighted average carbon content for the clamp kiln is about 2.5% lower than for the pure coal. The correction is speculative, but in the appropriate direction. The assumed carbon fractions are indicated in each table and the new fuel analyses performed for NAMaSTE for several fuel types are compiled in Table 6.3.

There are a few unavoidable additional uncertainties in assigning EFs to specific fuels for the brick kilns due to the possibility of emissions from the clay during firing. An estimate of the

impact can be made from literature data. Clay typically contains well under one percent organic material and some can be lost during firing though residual C can increase the strength of the fired product and limited permeability makes complete combustion of the C in the clay difficult to achieve (Wattel-Koekkoek et al., 2001; Organic Matter in Clay, 2015). For a generous exploratory estimate, we can assume the green bricks are 1% by mass organic matter that is all C. The brick/coal mass ratio reported by Weyant et al. (2014) is 6-26 and we take 15 as an average. 15 kg of clay at 1% C would have 150 g of C and one kg of coal at 70% C would have 700 g C. Thus, if all of the C in the clay was emitted it would cause about 18% of the total C emissions from the production process as an upper limit. The impact on the EF per kg coal-fuel that we calculated by the CMB method depends on the species-specific ER to CO_2 in the emissions from the clay C. If the ER for a species due to heating clay-C is the same as burning coal-C then there is no effect on the EF computed by the CMB per kg coal even though some of the species is actually coming from the clay. If the ER for "heating" clay-C is much higher or lower than the ER for burning coal-C (e.g. a factor ten), then for some non-CO_2 species, we would calculate increases or decreases in the CMB-calculated EFs relative to what actually is produced from the coal fuel. These are only large if a species is emitted mostly from clay combustion (vide infra).

6.5 Results and Discussion

6.5.1 Overview of aerosol optical properties

As mentioned above, we measured absorption and scattering coefficients as well as single scattering albedo directly at 405 and 870 nm. One wavelength-independent SSA value is often assumed for BB aerosol, but we find, as seen previously, that the SSA varies by wavelength for each source (Liu et al., 2014; McMeeking et al., 2014). The AAE is related to the shape of the

absorption cross-section. The AAE for pure BC is assumed to be ~1 while higher values of AAE indicate relatively more UV absorption and the presence of BrC. Figure 6.1 plots the source-average AAE versus the source-average SSA at 405 nm showing that high AAE is associated with high SSA. In Figure 6.1 we show source-averaged AAEs ranging from ~1-5 and SSA values at 405 nm ranging from 0.37-0.95 for the sources tested in this study. The "high-AAE" sources appearing toward the upper right-hand corner (e.g. dung and open wood cooking, clamp kiln) are associated with significant light absorption that would be overlooked by consideration of BC alone. We note that both PAXs were not operational during the generator and motorcycle sampling days and the PAX 870 was not operational during the irrigation pump sampling and for several garbage burns. We assumed that the pumps emitted only BC (this assumption is supported by the very low SSA) and used the MAC of BC at 405 nm (10.19 m^2/g) to calculate BC for this one source (Bond and Bergstrom, 2006). Both PAXs were operational for only one garbage burn, which had a low AAE near 1. Additional data from the aethalometer and filters, including for tests where one or both PAXs were not operational, will be presented in companion papers (Jayarathne et al., 2016; Goetz et al., 2016).

It is important to consider the differences in optical properties for the aerosol emitted by the various biofuel/stove combinations used in this understudied region with high levels of biofuel use. Dung-fired cooking had a significantly higher AAE (4.63 ± 0.68) than cooking with hardwood (3.01 ± 0.10). The AAE is also generally lower for improved stove types (1.68 ± 0.47) when compared to traditional open cooking (i.e. without an insulated combustion chamber) (Figure 6.1). In general, the optical properties vary significantly by fuel type and the mix of combustion processes. As established in previous studies (e.g. Christian et al., 2003; Liu et al., 2014), BC is emitted by flaming combustion and BrC is emitted primarily during smoldering

combustion and both can contribute strongly to the total overall absorption. Thus, the fuels that burned at a higher average MCE usually produced relatively more BC, which is also reflected in lower AAE and SSA values. These trends are similar to those observed during the third and fourth Fire Lab at Missoula Experiment (FLAME-3, -4) (Lewis et al., 2008; McMeeking et al., 2014; Liu et al., 2014). Additional PAX results will be discussed by fuel type along with the trace gas results in the following sections.

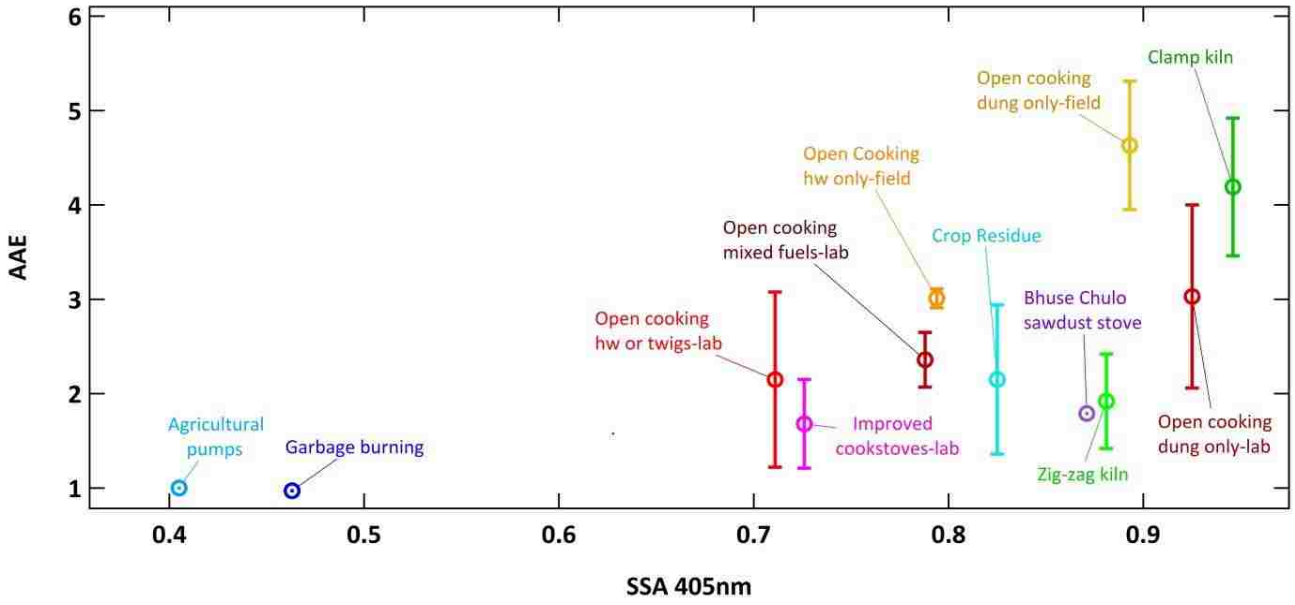

Figure 6.1. The absorption Ångström exponent (AAE) calculated at 405 and 870 nm as a function of single scattering albedo (SSA) at 405 nm for fuel types measured during the NAMaSTE campaign. The error bars represent ±1 standard deviation of AAE measured for different burns (or different samples as is the case for brick kilns). Note: "hw" indicates hardwood fuels.

6.5.2 Motorcycle emissions

The average EFs (g/kg) based on FTIR and WAS for the pre- and post-service fleet are shown in Table 6.4 and bike-specific pre/post results are included in Supplemental Table S6. As a fleet, we found that after servicing MCE, NO_x, and most NMOCs were slightly reduced and CO slightly increased, however, these fleet-average changes are not statistically significant given the high

variability in EF. Interestingly, for individual motorbike-specific comparisons (Table S6), in four out of five bikes, the MCE actually decreased after servicing indicating less efficient (though not necessarily less "clean") combustion, but this result is not statistically significant. To ensure that effects such as background drift did not cause this result we verified that the same results occur when obtaining slopes from plots using absolute (i.e. not background corrected) mixing ratios. A similar lack of reduction in gas-phase pollutants has been reported in the literature following repair and maintenance (Chiang et al., 2008) and has been attributed to the complexity in adjusting carburetors to optimal combustion conditions (Escalambre, 1995). Our high CO emissions did not always correlate with high hydrocarbon emissions. While we do not know the exact cause of this, this effect has been seen in other vehicle studies with a variety of explanations (Beaton et al., 1992; Zhang et al 1995). While the gaseous pollutants were not significantly reduced post-service, the fleet's total particulate emissions did decrease significantly and we refer to Jayarathne et al. (2016) for a detailed comparison.

Table 6.4. Fleet average emission factors (g/kg) and one standard deviation for two-wheeled vehicle measurements

Compound (Formula)	**EF Pre-service fleet** avg (stdev)	**EF Post-service fleet** avg (stdev)
Method	FTIR	FTIR
MCE	0.619	0.601
Carbon Dioxide (CO_2)	1846(690)	1816(562)
Carbon Monoxide (CO)	710(389)	761(327)
Methane (CH_4)	7.60(7.24)	6.74(4.54)
Acetylene (C_2H_2)	11.7(11.1)	7.89(5.83)
Ethylene (C_2H_4)	13.2(3.9)	11.4(4.2)
Propylene (C_3H_6)	3.32(0.75)	2.58(1.03)
Formaldehyde (HCHO)	0.548	0.535
Methanol (CH_3OH)	bdl	bdl
Formic Acid (HCOOH)	9.57E-2(3.57E-2)	5.95E-2(1.84E-2)
Acetic Acid (CH_3COOH)	bdl	bdl
Glycolaldehyde ($C_2H_4O_2$)	bdl	bdl
Furan (C_4H_4O)	bdl	bdl
Hydroxyacetone ($C_3H_6O_2$)	2.10(3.18)	2.41(0.99)
Phenol (C_6H_5OH)	4.84(3.55)	3.02(2.29)
1,3-Butadiene (C_4H_6)	1.30(0.51)	1.19(0.56)
Isoprene (C_5H_8)	bdl	bdl
Ammonia (NH_3)	0.113(0.034)	0.032(0.023)
Hydrogen Cyanide (HCN)	0.841(0.428)	0.678(0.174)
Nitrous Acid (HONO)	bdl	bdl
Sulfur Dioxide (SO_2)	bdl	bdl
Hydrogen Fluoride (HF)	bdl	bdl
Hydrogen chloride (HCl)	bdl	bdl
Nitric Oxide (NO)	2.94(2.39)	1.89(0.81)
Nitrogen Dioxide (NO_2)	bdl	bdl

Note: "bdl" indicates below the detection limit;

C-fraction: 0.85-source is *Kirchstetter et al.* (1999)

CO had the highest emissions of any gas after CO_2 and the FTIR-measured average EFs pre- and post- service over 700 g/kg are about ten times the typical EF for CO observed in BB. The FTIR-measured average MCE for the post service motorcycles was ~0.60, equivalent to a CO/CO_2 molar ER of ~0.66, dramatically highlighting the poor efficiency of the engines. We were

initially surprised by this result, but it is confirmed by WAS in that the one WAS sample of start-up/idling emissions returned a CO/CO_2 ER (0.789) that is within the FTIR-sample range. In fact, even higher CO/CO_2 ERs (3.2 – 4.2) are generated for start-up of motorcycles in the IVE model, which is based on sampling in developing countries (Oanh et al., 2012; Shrestha et al., 2013). Of 11227 vehicles of all types tested by remote sensing during on-road use in Kathmandu in 1993, about 2000 had a CO/CO_2 ER higher than 0.66 (fleet average 0.39, range 0 - 3.8, Zhang et al., 1995).

The next most abundant emissions after CO were: C_2 hydrocarbons (~24 g/kg), "BTEX" (benzene, toluene, ethylbenzene, and xylenes) compounds (~15 g/kg), and then the sum of measured oxygenated volatile organic compounds (OVOCs) and CH_4 each at ~7 g/kg. The OVOC from this source were mostly phenol, hydroxyacetone, and acetone (Table 6.4 and S6). The BTEX and acetone data are from the one motorcycle that was analyzed by WAS pre-service. The WAS provided several overlap species with the FTIR and many additional non-methane hydrocarbons (NMHCs) not measured by FTIR. First we note, in agreement with the FTIR, ethylene and acetylene were the most abundant WAS NMHC species and they accounted for ~38% of the total WAS NMHC emissions. The acetylene to ethylene ratio in this sample was 0.45 which is similar to previous roadside studies of all traffic (Tsai et al., 2006; Ho et al., 2009). Significantly, the WAS sample showed high concentrations of BTEX compounds, some of which are important carcinogens and all of which can lead to significant secondary organic aerosol (SOA) production (Platt et al., 2014). Toluene is a common gasoline additive and is sometimes used as a tracer for gasoline evaporation (Tsai et al., 2006). However, in our motorcycle data, aromatics account for ~31% of the NMHC in the exhaust emissions with toluene being the most abundant aromatic. Platt et al. (2014) measured BTEX emission factors

from about 10-100 g/kg (a range for driving to idling) for two-stroke motor scooter exhaust; also finding that toluene was the most abundant aromatic and with the BTEX accounting for ~40% of VOC. The combustion process in motorcycle engines is generally less efficient than in automobile engines (Platt et al., 2014) and the incomplete combustion can lead to emissions of many NMHC components in the gasoline. For instance, the exhaust emissions of branched C_5-C_6 alkanes, including 2-methylpentane and *i*-pentane (sometimes a tracer for gasoline evaporation (Morikawa et al., 1998; Guo et al., 2004)) were also significant in the motorcycle exhaust. Previous studies also found that the VOC emission profile from motorcycle exhaust was similar to gasoline headspace analysis (Liu et al., 2008). In summary inefficient motorcycle engines produce exhaust containing a suite of NMHCs that overlaps with those produced by fuel evaporation. However, there may be significant variability in headspace and exhaust measurements as observed by Lyu et al. (2015).

The air toxin and common BB tracer HCN was emitted by the motorcycles at about a tenth the ER to CO typically measured for BB. However, because of the very high motorcycle CO emissions, the EF for HCN for motorcycles was actually similar to that for BB. This is of importance for health effects and the use of HCN as a BB tracer in urban areas of developing countries where motorcycles are prevalent (Yokelson et al., 2007; Crounse et al., 2009). A few other emissions stood out in the dataset including high emissions of 1,3-butadiene (~1.3 g/kg). While 1,3-butadiene is not a component of gasoline, it is a known component of vehicle exhaust (e.g. Duffy and Nelson, 1996) and is believed to originate from the combustion of olefins (Perry and Gee, 1995). The EPA has highlighted 1,3-butadiene as having the highest cancer risk of air toxics emitted by US motor vehicles (USEPA, 1993) and exposure in densely populated urban centers can have significant negative health impacts.

One scooter was sampled by FTIR during this campaign and the CO emissions of the smaller scooter engine were only one-fourth to one-half those of the motorcycles (Table S6). The scooter exhaust emissions were also significantly lower for most other species captured by FTIR. The scooter, however, was the only motorbike sampled that produced detectable formaldehyde, a known carcinogen, irritant, and important radical precursor in urban atmospheres (Vaughan et al., 1986; Volkamer et al., 2010).

It is important to note that the average EFs from this study are not intended to represent the entire Kathmandu fleet of vehicles (or even all motorcycle use) as there is significant emissions variability between vehicles depending on running conditions: road conditions, driving patterns, maintenance, emissions control technology (Holmén and Niemeier, 1998; Popp et al., 1999) and engine specifics: model, size, age, power, fuel composition, combustion temperature and pressure, etc. (Zachariadis et al., 2001; Zavala et al., 2006). Larger studies similar to Zhang et al. (1995) are needed to get fleet averages. However, motorcycles and motor scooters have been identified as major contributors to transport sector pollution in Kathmandu (Shrestha et al., 2013) and elsewhere (Oanh et al., 2012; Platt et al., 2014) and we provide chemically detailed real-world EFs for motorcycles under some common operating conditions that were previously unmeasured in Kathmandu.

Because of the diversity in fleet characteristics and how operating conditions are subdivided it is difficult to compare to other studies, but some of the species we measured are explicitly provided in other vehicle emissions estimates (Oanh et al., 2012; Shrestha et al., 2013; Platt et al., 2014). Probably the most direct comparison is with Oanh et al. (2012) who reported EFs (in g/km) specifically for motorcycles for both start-up and running for the Hanoi 2008 average fleet based on the IVE that included some overlap species with our study (NO_x, CH_4, acetaldehyde,

formaldehyde, benzene, and 1, 3-butadiene). Except for 1,3-butadiene our average ratios to CO for these species for start-up and idling are only 3-26% of theirs for start-up or running. Zhang et al. (1995) noted that partially functional catalytic converters convert VOC to CO (rather than CO_2) lowering the VOC/CO ratio and also that these devices were becoming more common in the overall Kathmandu fleet, which points to emission control technology as a source of variability. The motorcycles we tested were all four-stroke and built by some of the world's largest manufacturers in India where catalytic converters are required on two-stroke vehicles, but are not required for four-stroke bikes until 2015. The Indian motorcycle emissions standards are based on an idling test and become increasingly stringent every five years (factor of 14.25 reduction for CO from 1991 to 2010). In response, a variety of emission control measures are incorporated in the motorcycle engines to reduce "engine out" emissions as opposed to "after treatment." Some of these measures are described in detail by Iyer (2012) while others are proprietary. The durability of many of these measures is very low (Ntziachristos et al., 2006, 2009) meaning they deteriorate with age despite minor service. Fuel quality (adulteration) is also noted as a widespread issue for emissions control (Iyer, 2012). In summary, it is quite possible that our VOC/CO ratios are lower than Oanh et al. (2012) mostly because of increased prevalence of emissions control technology (although poorly maintained) in Kathmandu in 2015 compared to Hanoi in 2008.

In general our emission ratios can be used with e.g. CO EFs from other studies to roughly estimate additional chemical details for operating conditions we did not sample. It is also interesting that we observed that the emitted gases did not change significantly after servicing. It is possible that gas-phase pollutants would have decreased post-service under "cruising" conditions, but we were limited to testing start-up and idling emissions. A study in Hong Kong

found that replacing old catalytic converters had a large impact on emissions, but minor servicing did not (Lyu et al., 2015). Thus, major servicing might be required to mitigate gas-phase pollutants in general. Finally, our filter results suggested that the particulate matter (PM) emissions were reduced post-service (Jayarathne et al., 2016). Therefore, it is likely that minor servicing of motorcycles is beneficial if it reduces the PM without making the vast majority of the gases significantly worse. The EFs (in g/kg) here could theoretically be converted to fuel based EFs (g/km) using a conversion factor based on motorcycle fuel economy. However, this is a complex process in practice (Clairotte et al., 2012) and it would probably be more meaningful to combine our ER to CO with fuel-based CO emission factors measured under the appropriate conditions.

6.5.3 Generator emissions

Three generators (two diesel and one gasoline) were sampled about a meter downstream of the exhaust manifold and the EFs are shown in Table 6.5. The larger diesel generator located on the ICIMOD campus is professionally maintained and had a much smaller EF CO (4.10 g/kg) and a higher MCE (0.998) than the smaller (rented) diesel generator (MCE 0.962, EF CO 76.1 g/kg). The smaller rented diesel generator had 18-150 times higher emissions for the five non-CO_2 gases measured from both sources. The one gasoline generator we sampled had much higher CO emissions (> 1000 g/kg) and was much less efficient (MCE 0.437) than both diesel generators. The gasoline-powered motorcycles discussed in Sect. 6.5.2 also had high EF CO (> 700 g/kg) with generally low MCEs.

Not surprisingly, the one diesel generator sampled by FTIR (the small rental) did emit high concentrations of NO_x (~24 g/kg), while NO_x emissions remained below the detection limit for the gasoline-powered generator sampled by FTIR (Vestreng et al., 2009). The gasoline-powered

generator emitted more NMHCs than both diesel generators and likely produces high secondary aerosol that has been observed in gasoline vehicle emission studies (Platt et al., 2013). We measured gasoline generator BTEX emissions that were ~20 times greater than those from the large diesel generator and note that the SOA yields from photooxidation of *m*-xylene, toluene, and benzene are significant (Ng et al., 2007). We were able to measure HCHO emissions by FTIR from the small diesel generator (2.75 g/kg) and the gasoline-generator (0.61 g/kg). Even though the diesel generator ran much cleaner overall (for gas-phase pollutants) it produced significantly more HCHO than the gasoline generator and we recall that HCHO was below the detection limit for gasoline-powered motorcycles we measured. This suggests diesel may tend to produce higher HCHO emissions than gasoline. As mentioned in Sect. 3.2, HCHO is an air toxin and is important in atmospheric chemistry. Overall, OVOCs were not clearly associated with either fuel with the gasoline generator having higher EFs for acetaldehyde, acetone, phenol, and furan, but lower EFs for HCHO and organic acids.

Other evident differences between the generators were potentially based on fuel. The large well-maintained diesel generator emitted more of the heavier NMHCs including heptane, octane, nonane, decane, and methylcyclohexane than the lesser maintained gasoline generator. The gasoline generator had much higher EFs for the smaller-chain NMHCs (C_2H_2, C_2H_4, C_2H_6, C_3H_6, etc.). While the diesel fuel generators we sampled burned cleaner overall in terms of gas-phase pollutants, diesel is normally considered a much dirtier fuel in terms of soot production. The two PAX instruments were not operational for sampling generators, but filters were collected and demonstrated a higher EF PM for the small diesel generator than the gasoline generator as will be highlighted by Jayarathne et al. (2016).

We were able to sample both the smaller diesel generator and the gasoline generator during both start-up and free-running conditions. The diesel generator produced concentrations about twice as high for most measured species during start-up as opposed to free-running conditions, while the gasoline-fueled generator did not show these start-up concentration spikes. Sharp emission spikes peaking during both cold- and hot-startups of diesel engines have been observed previously (Gullet et al., 2006). This is often attributed to periods of incomplete combustion during ignition, and could have significant impacts on air quality as power-cuts are a frequent, intermittent occurrence throughout the valley.

In summary, the well-maintained diesel generator had much lower EFs for overlapping measured gases (except large alkanes, which were a minor overall component), but gasoline could have advantages in terms of NO_x and PM emissions at the cost of increases in most other pollutants unless they could be reduced by better maintenance. Although vehicular emissions are most commonly reported, emissions from gasoline and diesel powered generators can also have large impacts in urban regions subject to significant load-shedding, which is relevant throughout Nepal and especially in the Kathmandu Valley (World Bank, 2014).

Table 6.5. Emission factors (g/kg) for diesel- and gasoline-powered generators

Compound (Formula)	EF Chanqta Diesel Generator	EF ICIMOD Diesel Generator	EF Yeeda Gasoline Generator
Method	FTIR	WAS	FTIR+WAS
Date	12-Apr	8-Jun	12-Apr
MCE	0.962	0.998	0.437
Carbon Dioxide (CO_2)	3024	3180	1293
Carbon Monoxide (CO)	76.1	4.10	1059
Methane (CH_4)	0.532	6.89E-03	11.0
Acetylene (C_2H_2)	0.348	1.59E-02	11.1
Ethylene (C_2H_4)	4.32	2.84E-02	11.0
Propylene (C_3H_6)	0.635	1.79E-02	1.42
Formaldehyde (HCHO)	2.75	nm	0.610
Methanol (CH_3OH)	bdl	bdl	bdl
Formic Acid (HCOOH)	0.417	nm	bdl
Acetic Acid (CH_3COOH)	0.425	nm	bdl
Glycolaldehyde ($C_2H_4O_2$)	bdl	nm	bdl
Furan (C_4H_4O)	bdl	nm	2.59
Hydroxyacetone ($C_3H_6O_2$)	0.294	nm	bdl
Phenol (C_6H_5OH)	bdl	nm	2.94
1,3-Butadiene (C_4H_6)	0.297	bdl	0.549
Isoprene (C_5H_8)	bdl	bdl	bdl
Ammonia (NH_3)	bdl	nm	0.154
Hydrogen Cyanide (HCN)	bdl	nm	bdl
Nitrous Acid (HONO)	1.57	nm	bdl
Sulfur Dioxide (SO_2)	bdl	nm	bdl
Hydrogen Fluoride (HF)	bdl	nm	bdl
Hydrogen chloride (HCl)	bdl	nm	bdl
Nitric Oxide (NO)	16.0	nm	bdl
Nitrogen Dioxide (NO_2)	7.64	nm	bdl
Carbonyl sulfide (OCS)	nm	4.36E-04	1.07E-02
DMS (C_2H_6S)	nm	-	3.18E-04
Chloromethane (CH_3Cl)	nm	1.03E-04	5.71E-04
Bromomethane (CH_3Br)	nm	2.38E-06	-
Methyl iodide (CH_3I)	nm	-	9.47E-06
1,2-Dichloroethene ($C_2H_2Cl_2$)	nm	6.76E-04	9.04E-05
Methyl nitrate (CH_3NO_3)	nm	5.04E-04	1.19E-02
Ethane (C_2H_6)	nm	9.14E-04	0.459
Propane (C_3H_8)	nm	6.09E-04	4.11E-02
i-Butane (C_4H_{10})	nm	1.19E-03	8.26E-02
n-Butane (C_4H_{10})	nm	1.37E-03	7.05E-02
1-Butene (C_4H_8)	nm	7.54E-03	0.148
i-Butene (C_4H_8)	nm	4.35E-03	0.309
trans-2-Butene (C_4H_8)	nm	2.07E-03	9.33E-02
cis-2-Butene (C_4H_8)	nm	1.54E-03	6.47E-02
i-Pentane (C_5H_{12})	nm	6.07E-03	0.545
n-Pentane (C_5H_{12})	nm	3.73E-03	0.154
1-Pentene (C_5H_{10})	nm	5.51E-03	3.09E-02

trans-2-Pentene (C_5H_{10})	nm	1.56E-03	5.54E-02
cis-2-Pentene (C_5H_{10})	nm	6.95E-04	2.92E-02
3-Methyl-1-butene (C_5H_{10})	nm	1.44E-03	2.41E-02
1,2-Propadiene (C_3H_4)	nm	4.10E-04	0.155
Propyne (C_3H_4)	nm	7.23E-04	0.305
1-Butyne (C_4H_6)	nm	8.52E-05	1.33E-02
2-Butyne (C_4H_6)	nm	8.13E-05	9.71E-03
n-Hexane (C_6H_{14})	nm	1.74E-02	6.42E-02
n-Heptane (C_7H_{16})	nm	0.150	5.91E-02
n-Octane (C_8H_{18})	nm	9.13E-02	2.30E-02
n-Nonane (C_9H_{20})	nm	0.100	2.51E-02
n-Decane ($C_{10}H_{22)}$	nm	8.13E-02	-
2,3-Dimethylbutane (C_6H_{14})	nm	1.22E-03	4.06E-02
2-Methylpentane (C_6H_{14})	nm	4.77E-03	0.119
3-Methylpentane (C_6H_{14})	nm	4.02E-03	6.33E-02
2,2,4-Trimethylpentane (C_8H_{18})	nm	6.69E-02	2.97E-02
Cyclopentane (C_5H_{10})	nm	1.82E-03	2.76E-02
Cyclohexane (C_6H_{12})	nm	6.44E-02	8.76E-02
Methylcyclohexane (C_7H_{14})	nm	0.252	4.22E-02
Benzene (C_6H_6)	nm	1.61E-02	1.70
Toluene (C_7H_8)	nm	6.99E-02	2.21
Ethylbenzene (C_8H_{10})	nm	3.26E-02	0.316
m/p-Xylene (C_8H_{10})	nm	0.133	1.41
o-Xylene (C_8H_{10})	nm	4.41E-02	0.414
Styrene (C_8H_8)	nm	1.51E-03	2.17E-02
i-Propylbenzene (C_9H_{12})	nm	5.15E-03	bdl
n-Propylbenzene (C_9H_{12})	nm	7.48E-03	1.06E-02
3-Ethyltoluene (C_9H_{12})	nm	3.33E-02	9.98E-02
4-Ethyltoluene (C_9H_{12})	nm	1.64E-02	3.92E-02
2-Ethyltoluene (C_9H_{12})	nm	1.23E-02	2.82E-02
1,3,5-Trimethylbenzene (C_9H_{12})	nm	2.20E-02	5.89E-02
1,2,4-Trimethylbenzene (C_9H_{12})	nm	4.56E-02	8.87E-02
1,2,3-Trimethylbenzene (C_9H_{12})	nm	1.84E-02	2.57E-02
alpha-Pinene ($C_{10}H_{16}$)	nm	bdl	4.45E-04
beta-Pinene ($C_{10}H_{16}$)	nm	bdl	6.20E-03
Ethanol (C_2H_6O)	nm	-	4.10E-02
Acetaldehyde (C_2H_4O)	nm	6.40E-04	0.252
Acetone (C_3H_6O)	nm	8.62E-02	0.540
Butanal (C_4H_8O)	nm	1.10E-03	5.74E-03
Butanone (C_4H_8O)	nm	-	3.03E-02

Note: "bdl" indicates below the detection limit; "-" indicates concentrations were not greater than background; "nm" indicates not measured

C-fractions: Gasoline (0.85), Diesel (0.87): source is *Kirchstetter et al.* (1999)

6.5.4 Agricultural diesel pump emissions

In this study, two groundwater irrigation diesel pumps were sampled by FTIR and the EFs are reported in Table 6.6. In addition, a surface-water irrigation pump was sampled by WAS

canisters only and showed massively higher CO emissions than the two other pumps in our study indicating it was probably gasoline-powered. The WAS data may be mainly of interest to characterize old or poorly maintained pumps and the EFs are included in Supplemental Table S7.

For the two pumps sampled by FTIR, the grab samples during cold startup differed from the samples during regular continuous operation by a much larger degree than the variability in grab samples for the other sources so we computed EF by two methods. Method one is our standard approach based on the ER plot using all the samples. The startup emissions can be outliers in this approach and get lower weight accordingly. Thus, we also computed ERs from the sum of the individual ERs and used those to generate a second set of EF that weights the startup emissions more. Our standard approach yields the EFs shown in Table 6.6, columns 2 and 4, with an average of those two columns in column 6. We have included columns 3 and 5 with EFs calculated from the sum of excess emissions that emphasizes startup more. The alternate EF calculation reflects the increased emission of hydrocarbon species during ignition. CO also increases substantially while NO_x decreases slightly. We believe the most representative EFs for model input are taken from the standard approach that does not add weight to the start-up conditions, as most pumps are likely operated over longer periods of time. However, all the data are provided should a user prefer a different approach.

Although the 870 nm PAX was not operational on this day, the EFs (m^2/kg) of B_{abs} and B_{scat} for aerosols measured at 405 nm and the SSA are reported in Table 6.6 for the complete sampling cycle. The SSA at 405 nm (0.405 ± 0.137) indicates that the diesel pump emissions were dominated by strongly-absorbing aerosols and if we assume there are no BrC emissions from this source, a reasonable assumption supported by the AE-33 data, the absorption at 405 nm can be

used to get a rough estimate for EF BC. The average EF BC (5.72 ± 0.58 g/kg) is very high compared to typical values closer to 1 g/kg for most sources.

From the average emissions in Table 6.6 we see that the two pumps sampled by FTIR were not as prolific emitters for most pollutants as many other sources sampled in this study. However, the emissions of NO_x and absorbing aerosol were comparatively high. Especially taken together, the emissions from diesel powered generators and agricultural water pumps are likely significant in both urban and rural regions of Kathmandu and should be included in updated emissions inventories.

Table 6.6. Emission factors (g/kg) for agricultural diesel irrigation pumps including EFs weighting only startup emissions.

Compound (Formula)	**EF Ag Pump 1**	**EF Ag Pump 1** emphasize startup	**EF Ag Pump 2**	**EF Ag Pump 2** emphasize startup	**EF Ag pumps** Avg (stdev)
Method	FTIR	FTIR	FTIR	FTIR	-
MCE	0.987	0.974	0.996	0.990	0.992
Carbon Dioxide (CO_2)	3103	3038	3161	3133	3132(41)
Carbon Monoxide (CO)	26.0	51.3	7.36	20.2	16.7(13.2)
Methane (CH_4)	3.80	6.14	1.41	2.85	2.61(1.69)
Acetylene (C_2H_2)	0.413	2.18	0.08	0.748	0.246(0.237)
Ethylene (C_2H_4)	5.37	9.15	1.47	3.04	3.42(2.75)
Propylene (C_3H_6)	1.85	3.26	0.424	0.894	1.14(1.01)
Formaldehyde (HCHO)	0.506	1.23	5.29E-02	0.175	0.280(0.320)
Methanol (CH_3OH)	3.59E-02	0.119	5.77E-03	1.33E-02	2.08E-2(2.13E-2)
Formic Acid (HCOOH)	bdl	bdl	bdl	bdl	bdl
Acetic Acid (CH_3COOH)	bdl	bdl	bdl	bdl	bdl
Glycolaldehyde ($C_2H_4O_2$)	bdl	bdl	bdl	bdl	bdl
Furan (C_4H_4O)	bdl	bdl	bdl	bdl	bdl
Hydroxyacetone ($C_3H_6O_2$)	bdl	bdl	bdl	bdl	bdl
Phenol (C_6H_5OH)	0.449	0.583	0.117	0.258	0.283(0.235)
1,3-Butadiene (C_4H_6)	0.809	1.47	0.194	0.399	0.501(0.435)
Isoprene (C_5H_8)	1.55E-02	7.20E-02	1.93E-02	2.30E-02	1.74E-2(2.69E-3)
Ammonia (NH_3)	9.27E-03	6.42E-02	1.32E-03	1.32E-03	5.29E-3(5.62E-3)
Hydrogen Cyanide (HCN)	0.188	0.458	4.77E-02	0.282	0.118(0.099)
Nitrous Acid (HONO)	0.348	0.307	0.346	0.373	0.347(0.001)
Sulfur Dioxide (SO_2)	bdl	bdl	bdl	bdl	bdl
Hydrogen Fluoride (HF)	bdl	bdl	bdl	bdl	bdl
Hydrogen chloride (HCl)	bdl	bdl	bdl	bdl	bdl
Nitric Oxide (NO)	5.31	5.09	15.9	15.7	10.6(7.5)
Nitrogen Dioxide (NO_2)	2.19	1.86	1.20	1.15	1.69(0.70)

EF Black Carbon (BC)	6.13	-	5.31	-	5.72(0.58)
EF B_{abs} 405 nm (m^2/kg)	62.4	-	54.1	-	58.3(5.9)
EF B_{scat} 405 nm (m^2/kg)	62.9	-	24.0	-	43.4(27.5)
SSA 405 nm	0.502	-	0.307	-	0.405(0.137)

Note: "bdl" indicates below the detection limit; C-fraction: 0.85- source is *Kirchstetter et al.* (1999)

6.5.5 Garbage burning emissions

For an overview of our Nepal garbage burning (GB) data that also allows us to compare to authentic field and lab measured GB, we tabulated (Table 6.7) our study-average Nepal mixed GB EFs along with mixed GB EFs from two lab studies (Yokelson et al., 2013a; Stockwell et al., 2015, Sect. 4.3.8), field measurements of open GB in Mexican landfills (Christian et al., 2010), and a single airborne sample of a Mexican dump fire (Yokelson et al., 2011). Figure 6.2 displays the major emissions from these studies in order of their abundance in the NAMaSTE data. We observe an interesting mix of compounds usually associated with burning biomass (OVOCs) and fossil fuels (NMHC and BTEX) as well as nitrogen and chlorine compounds. Even though the methodology and locales varied considerably, the EFs reported in each study show reasonable agreement for most overlap compounds (Figure 6.2). The average EFs of smoldering compounds for mixed garbage burns in Nepal were generally slightly higher than the other studies and the average MCE was lower (0.923, range in MCE 0.864-0.980). This is consistent with observations by several co-authors that flaming dominated GB is more common in winter months in Nepal when GB also provides heat. The comparison also suggests that the lab results for compounds not measured in the field (e.g. Yokelson et al., 2013a; Stockwell et al., 2015) could be used if scaled with caution. The NAMaSTE-specific EFs for garbage burning are reported for each fire in Table 6.8 along with our study-average for mixed GB EFs and we discuss some emissions next.

Table 6.7. Compiled emission factors (g/kg) for garbage burning from this study and others

Compound (Formula)	**EF Mexican Garbage** Christain et al. [2010] Avg (stdev)	**EF Mixed Garbage** Yokelson et al. [2011]	**EF Lab Garbage** Yokelson et al. [2013a][a]	**EF Lab Garbage** Stockwell et al. [2015] Avg (stdev)[b]	**EF Mixed Garbage** NAMaSTE Avg (stdev)
MCE	0.950(0.026)	0.974	0.967	0.973(0.006)	0.923(0.050)
Particulate Matter (PM2.5)	10(5)	-	10.8	-	-
Black Carbon (BC)	0.646(0.272)	-	-	-	3.30(3.88)
Organic carbon (OC)	5.27(4.89)	-	-	-	-
Carbon Dioxide (CO_2)	1367(65)	1538	1341	1780(32)	1602(142)
Carbon Monoxide (CO)	45.3(22.8)	26.1	28.7	31.3(6.8)	84.7(55.5)
Methane (CH_4)	3.70(4.43)	0.766	0.313	0.795(0.198)	3.97(4.47)
Acetylene (C_2H_2)	0.398(0.275)	bdl	0.435	0.325(0.103)	0.662(0.562)
Ethylene (C_2H_4)	2.19(1.81)	0.322	1.74	0.977(0.048)	3.03(3.29)
Propylene (C_3H_6)	1.26(1.42)	bdl	0.847	0.638(0.046)	1.73(1.34)
Formaldehyde (HCHO)	0.620(0.124)	bdl	0.757	0.915(0.468)	2.33(2.57)
Methanol (CH_3OH)	0.945(1.245)	bdl	0.135	0.167(0.081)	0.783(0.914)
Formic Acid (HCOOH)	0.180(0.121)	bdl	0.175	4.45E-2(3.11E-2)	0.454(0.185)
Acetic Acid (CH_3COOH)	2.42(3.32)	bdl	0.547	bdl	0.872(1.066)
Glycolaldehyde ($C_2H_4O_2$)	nm	nm	nm	0.658(0.817)	2.41(-)
Furan (C_4H_4O)	nm	nm	4.81E-02	0.117(0.048)	0.213(0.192)
Hydroxyacetone ($C_3H_6O_2$)	nm	nm	nm	0.211(0.160)	1.68(1.44)
Phenol (C_6H_5OH)	nm	nm	nm	5.78E-2(1.66E-3)	0.414(0.513)
1,3-Butadiene (C_4H_6)	nm	nm	0.241	0.112(0.007)	0.267(0.329)
Isoprene (C_5H_8)	nm	nm	3.47E-02	0.199(0.043)	0.089(0.064)
Ammonia (NH_3)	1.12(1.21)	0.768	bdl	6.21E-2(-)	0.761(-)
Hydrogen Cyanide (HCN)	bdl	0.473	0.119	5.30E-2(6.34E-2)	0.432(0.169)
Nitrous Acid (HONO)	nm	nm	5.14E-02	0.240(0.124)	0.493(0.100)
Sulfur Dioxide (SO_2)	nm	nm	0.769	0.892(-)	bdl
Hydrogen Fluoride (HF)	nm	nm	nm	bdl	bdl
Hydrogen chloride (HCl)	4.82(4.36)	bdl	10.1	0.797(1.000)	2.32(1.01)
Nitric Oxide (NO)	bdl	bdl	0.421	0.518(0.085)	1.52(0.12)
Nitrogen Dioxide (NO_2)	bdl	6.87	0.695	0.767(0.393)	1.06(0.11)
Carbonyl sulfide (OCS)	nm	nm	nm	nm	7.43E-2(4.60E-2)
DMS (C_2H_6S)	nm	nm	nm	nm	7.39E-3(1.13E-2)
Chloromethane (CH_3Cl)	nm	nm	nm	nm	0.702(0.648)
Bromomethane (CH_3Br)	nm	nm	nm	nm	2.19E-3(2.39E-3)
Methyl iodide (CH_3I)	nm	nm	nm	nm	3.25E-4(1.45E-4)
Dibromomethane (CH_2Br_2)	nm	nm	nm	nm	3.50E-4(4.75E-4)
1,2-Dichloroethene ($C_2H_2Cl_2$)	nm	nm	nm	nm	4.96E-2(1.03E-1)
Methyl nitrate (CH_3NO_3)	nm	nm	nm	nm	5.98E-2(6.84E-2)
Ethane (C_2H_6)	nm	nm	-	nm	1.69(2.09)

Propane (C_3H_8)	nm	nm	nm	nm	0.904(1.169)
i-Butane (C_4H_{10})	nm	nm	1.23E-02	nm	0.122(0.183)
n-Butane (C_4H_{10})	nm	nm	0.103	nm	0.513(0.707)
1-Butene (C_4H_8)	nm	nm	0.310	0.192(0.033)	1.05(1.45)
i-Butene (C_4H_8)	nm	nm	nm	nm	0.625(0.705)
trans-2-Butene (C_4H_8)	nm	nm	2.68E-02	nm	0.172(0.233)
cis-2-Butene (C_4H_8)	nm	nm	2.79E-02	nm	0.144(0.218)
i-Pentane (C_5H_{12})	nm	nm	7.59E-03	nm	0.391(0.639)
n-Pentane (C_5H_{12})	nm	nm	8.72E-02	nm	1.08(1.54)
1-Pentene (C_5H_{10})	nm	nm	3.65E-02	nm	0.731(0.960)
trans-2-Pentene (C_5H_{10})	nm	nm	1.37E-02	nm	0.205(0.260)
cis-2-Pentene (C_5H_{10})	nm	nm	nm	nm	9.29E-2(1.19E-1)
3-Methyl-1-butene (C_5H_{10})	nm	nm	nm	nm	4.12E-2(4.65E-2)
1,2-Propadiene (C_3H_4)	nm	nm	nm	nm	5.47E-2(7.39E-2)
Propyne (C_3H_4)	nm	nm	6.13E-02	nm	8.99E-2(1.14E-1)
1-Butyne (C_4H_6)	nm	nm	-	nm	1.05E-2(1.49E-2)
2-Butyne (C_4H_6)	nm	nm	-	nm	7.34E-3(1.02E-2)
n-Hexane (C_6H_{14})	nm	nm	4.50E-02	nm	0.282(0.309)
n-Heptane (C_7H_{16})	nm	nm	nm	nm	0.231(0.277)
n-Octane (C_8H_{18})	nm	nm	nm	nm	0.147(0.172)
n-Nonane (C_9H_{20})	nm	nm	nm	nm	7.24E-2(6.43E-2)
n-Decane ($C_{10}H_{22)}$	nm	nm	nm	nm	0.126(0.106)
2,3-Dimethylbutane (C_6H_{14})	nm	nm	nm	nm	1.12E-2(1.74E-2)
2-Methylpentane (C_6H_{14})	nm	nm	nm	nm	0.110(0.134)
3-Methylpentane (C_6H_{14})	nm	nm	nm	nm	0.157(0.100)
2,2,4-Trimethylpentane (C_8H_{18})	nm	nm	nm	nm	-(-)
Cyclopentane (C_5H_{10})	nm	nm	2.45E-03	nm	1.46E-2(2.22E-2)
Cyclohexane (C_6H_{12})	nm	nm	nm	nm	9.80E-3(-)
Methylcyclohexane (C_7H_{14})	nm	nm	nm	nm	2.76E-2(4.81E-2)
Benzene (C_6H_6)	nm	nm	0.878	0.328(0.063)	2.61(1.85)
Toluene (C_7H_8)	nm	nm	0.156	0.150(0.048)	0.817(0.960)
Ethylbenzene (C_8H_{10})	nm	nm	7.66E-02	4.29E-2(1.57E-2)	0.498(0.831)
m/p-Xylene (C_8H_{10})	nm	nm	3.27E-02	nm	0.342(0.412)
o-Xylene (C_8H_{10})	nm	nm	2.19E-02	nm	0.223(0.238)
Styrene (C_8H_8)	nm	nm	1.97	0.383(0.144)	0.367(0.274)
i-Propylbenzene (C_9H_{12})	nm	nm	nm	nm	2.12E-2(3.14E-2)
n-Propylbenzene (C_9H_{12})	nm	nm	nm	nm	3.09E-2(2.83E-2)
3-Ethyltoluene (C_9H_{12})	nm	nm	nm	nm	3.55E-2(4.65E-2)
4-Ethyltoluene (C_9H_{12})	nm	nm	nm	nm	1.77E-2(1.52E-2)
2-Ethyltoluene (C_9H_{12})	nm	nm	nm	nm	2.30E-2(2.31E-2)
1,3,5-Trimethylbenzene (C_9H_{12})	nm	nm	nm	1.57E-2(4.74E-3)	3.36E-2(2.52E-2)
1,2,4-Trimethylbenzene (C_9H_{12})	nm	nm	8.31E-03	nm	2.56E-2(2.47E-2)
1,2,3-Trimethylbenzene (C_9H_{12})	nm	nm	nm	nm	1.52E-2(9.49E-3)

alpha-Pinene ($C_{10}H_{16}$)	nm	nm	nm	3.00E-2(1.21E-2)	5.00E-2(5.65E-2)
beta-Pinene ($C_{10}H_{16}$)	nm	nm	1.86E-02	nm	4.15E-2(5.83E-2)
Ethanol (C_2H_6O)	nm	nm	5.91E-02	nm	8.74E-2(5.31E-2)
Acetaldehyde (C_2H_4O)	nm	nm	1.05	0.782(0.463)	2.12(3.20)
Acetone (C_3H_6O)	nm	nm	0.153	0.112(-)	2.30(1.90)
Butanal (C_4H_8O)	nm	nm	4.63E-02	nm	0.259(0.349)
Butanone (C_4H_8O)	nm	nm	3.35E-02	3.75E-2(5.60E-3)	0.212(0.310)

Note: "bdl" indicates below the detection limit; "-" indicates concentrations were not greater than background; "nm" indicates not measured

[a]Additional compounds compiled in *Yokelson et al.*, (2013a)

[b]Additional compounds compiled in *Stockwell et al.*, (2015)

Table 6.8. Emission factors (g/kg) for individual garbage burns sampled during NAMaSTE.

Compound (Formula)	**EF Mixed garbage 1**	**EF Mixed garbage 2**	**EF Mixed garbage 3**	**EF Mixed garbage 4**	**EF Mixed garbage 5**	**EF Mixed garbage 6**	**EF Mixed Chip bags**	**EF Plastics burn 1**	**EF Plastics burn 2**	**EF Mixed garbage** avg (stdev)
Method	FTIR+WAS	FTIR+WAS	WAS	WAS	WAS	WAS	FTIR	FTIR	WAS	-
MCE	0.937	0.980	0.926	0.863	0.864	0.967	0.989	0.962	0.990	0.923(0.050)
Carbon Dioxide (CO_2)	1446	1773	1641	1498	1498	1756	2249	2473	2695	1602(142)
Carbon Monoxide (CO)	61.5	22.8	84	152	151	38.0	15.9	62.2	16.6	84.7(55.5)
Methane (CH_4)	2.22	0.531	4.15	12.5	3.82	0.542	0.279	2.04	0.684	3.97(4.47)
Acetylene (C_2H_2)	1.49	0.261	0.269	0.101	0.674	1.18	0.434	2.23	0.298	0.662(0.562)
Ethylene (C_2H_4)	9.33	0.768	2.05	1.72	3.725	0.578	1.85	9.36	0.477	3.03(3.29)
Propylene (C_3H_6)	1.98	0.426	1.940	1.999	3.884	0.167	0.520	3.53	0.150	1.73(1.34)
Formaldehyde (HCHO)	4.15	0.507	nm	nm	nm	nm	0.475	5.23	nm	2.33(2.57)
Methanol (CH_3OH)	1.23	0.146	0.271	2.429	0.590	3.38E-02	3.43E-02	0.98	bdl	0.783(0.914)
Formic Acid (HCOOH)	0.585	0.323	nm	nm	nm	nm	0.126	5.30	nm	0.454(0.185)
Acetic Acid (CH_3COOH)	1.63	0.118	nm	nm	nm	nm	4.42E-02	2.22	nm	0.872(1.066)
Glycolaldehyde ($C_2H_4O_2$)	2.41	bdl	nm	nm	nm	nm	2.44E-02	4.56	nm	2.41(-)
Furan (C_4H_4O)	0.349	7.77E-02	nm	nm	nm	nm	bdl	0.234	nm	0.213(0.192)
Hydroxyacetone ($C_3H_6O_2$)	2.70	0.664	nm	nm	nm	nm	bdl	2.59	nm	1.68(1.44)
Phenol (C_6H_5OH)	0.776	5.09E-02	nm	nm	nm	nm	0.127	1.42	nm	0.414(0.513)
1,3-Butadiene (C_4H_6)	0.930	0.127	0.205	0.177	0.116	4.86E-02	0.192	1.07	3.41E-04	0.267(0.329)
Isoprene (C_5H_8)	0.145	bdl	1.84E-02	0.103	bdl	6.80E-04	9.59E-02	0.226	bdl	6.67E-2(6.86E-2)
Ammonia (NH_3)	bdl	0.761	nm	nm	nm	nm	bdl	5.66E-02	nm	0.761(-)
Hydrogen Cyanide (HCN)	0.551	0.312	nm	nm	nm	nm	0.374	0.955	nm	0.432(0.169)
Nitrous Acid (HONO)	0.564	0.422	nm	nm	nm	nm	0.164	2.50	nm	0.493(0.100)
Sulfur Dioxide (SO_2)	bdl	bdl	nm	nm	nm	nm	bdl	bdl	nm	bdl
Hydrogen Fluoride (HF)	bdl	bdl	nm	nm	nm	nm	bdl	bdl	nm	bdl
Hydrogen chloride (HCl)	3.03	1.61	nm	nm	nm	nm	bdl	77.9	nm	2.32(1.01)
Nitric Oxide (NO)	1.43	1.61	nm	nm	nm	nm	2.02	2.36	nm	1.52(0.12)
Nitrogen Dioxide (NO_2)	1.14	0.983	nm	nm	nm	nm	1.20	1.69	nm	1.06(0.11)
Carbonyl sulfide (OCS)	0.133	2.71E-02	8.62E-02	8.03E-02	0.106	1.33E-02	nm	nm	2.03E-02	7.43E-2(4.60E-2)
DMS (C_2H_6S)	-	1.27E-03	1.89E-03	2.70E-02	6.74E-03	4.71E-05	nm	nm	1.19E-02	7.39E-3(1.13E-2)
Chloromethane (CH_3Cl)	0.895	5.05E-02	0.343	1.59	1.26	6.55E-02	nm	nm	5.72E-02	0.702(0.648)
Bromomethane (CH_3Br)	6.71E-03	5.47E-04	2.93E-03	1.16E-03	1.41E-03	3.96E-04	nm	nm	5.53E-05	2.19E-3(2.39E-3)
Methyl iodide (CH_3I)	3.26E-04	-	4.41E-04	4.81E-04	2.55E-04	1.21E-04	nm	nm	1.54E-05	3.25E-4(1.45E-4)
1,2-Dichloroethene ($C_2H_2Cl_2$)	0.260	1.44E-02	4.75E-03	2.70E-03	1.02E-02	4.92E-03	nm	nm	5.94E-04	4.96E-2(1.03E-1)
Methyl nitrate (CH_3NO_3)	0.185	6.45E-02	2.21E-02	1.02E-02	7.61E-02	8.44E-04	nm	nm	7.99E-02	5.98E-2(6.84E-2)
Ethane (C_2H_6)	5.64	6.09E-02	0.830	2.11	1.42	7.19E-02	nm	nm	3.04E-02	1.69(2.09)
Propane (C_3H_8)	3.15	2.52E-02	0.388	0.913	0.920	3.01E-02	nm	nm	1.68E-02	0.904(1.169)
i-Butane (C_4H_{10})	0.445	1.25E-03	3.81E-02	5.79E-02	6.52E-02	-	nm	nm	0.002	0.122(0.183)
n-Butane (C_4H_{10})	1.87	1.41E-02	0.190	0.341	0.650	1.19E-02	nm	nm	1.86E-02	0.513(0.707)
1-Butene (C_4H_8)	3.89	8.36E-02	0.569	0.502	1.23	5.51E-02	nm	nm	6.45E-02	1.05(1.45)
i-Butene (C_4H_8)	1.93	5.80E-02	0.508	0.400	0.829	2.62E-02	nm	nm	7.90E-03	0.625(0.705)
trans-2-Butene (C_4H_8)	0.630	7.09E-03	9.55E-02	0.135	0.160	6.89E-03	nm	nm	1.28E-02	0.172(0.233)

cis-2-Butene (C_4H_8)	0.580	6.04E-03	7.27E-02	9.72E-02	0.102	4.91E-03	nm	nm	9.46E-03	0.144(0.218)
i-Pentane (C_5H_{12})	1.13	-	2.00E-02	-	2.43E-02	-	nm	nm	3.00E-02	0.391(0.639)
n-Pentane (C_5H_{12})	4.09	3.90E-02	0.435	0.698	1.21	1.69E-02	nm	nm	1.85E-02	1.08(1.54)
1-Pentene (C_5H_{10})	2.53	4.19E-02	0.341	0.374	1.07	2.86E-02	nm	nm	3.75E-02	0.731(0.960)
trans-2-Pentene (C_5H_{10})	0.700	1.67E-02	0.108	0.126	0.270	6.63E-03	nm	nm	9.65E-03	0.205(0.260)
cis-2-Pentene (C_5H_{10})	0.320	7.43E-03	5.14E-02	5.73E-02	0.118	2.83E-03	nm	nm	4.29E-03	9.29E-2(1.19E-1)
3-Methyl-1-butene (C_5H_{10})	0.129	3.80E-03	3.99E-02	2.63E-02	4.66E-02	1.98E-03	nm	nm	2.79E-03	4.12E-2(4.65E-2)
1,2-Propadiene (C_3H_4)	0.198	1.74E-02	2.84E-02	3.92E-03	6.76E-02	1.25E-02	nm	nm	5.38E-03	5.47E-2(7.39E-2)
Propyne (C_3H_4)	0.315	3.27E-02	5.41E-02	1.18E-02	9.60E-02	2.92E-02	nm	nm	1.10E-02	8.99E-2(1.14E-1)
1-Butyne (C_4H_6)	3.61E-02	2.08E-03	-	1.84E-03	1.12E-02	1.17E-03	nm	nm	8.69E-04	1.05E-2(1.49E-2)
2-Butyne (C_4H_6)	2.46E-02	1.07E-03	-	1.47E-03	8.79E-03	7.65E-04	nm	nm	4.00E-04	7.34E-3(1.02E-2)
n-Hexane (C_6H_{14})	0.761	-	0.101	0.126	0.417	5.05E-03	nm	nm	1.54E-02	0.282(0.309)
n-Heptane (C_7H_{16})	0.707	9.86E-03	9.61E-02	0.154	0.413	5.41E-03	nm	nm	5.10E-03	0.231(0.277)
n-Octane (C_8H_{18})	0.411	1.24E-02	6.53E-02	0.078	0.313	1.36E-03	nm	nm	1.24E-02	0.147(0.172)
n-Nonane (C_9H_{20})	0.134	3.81E-03	5.94E-02	0.076	0.158	3.68E-03	nm	nm	2.77E-02	7.24E-2(6.43E-2)
n-Decane ($C_{10}H_{22)}$	0.266	1.00E-02	7.99E-02	0.153	0.224	2.36E-02	nm	nm	bdl	0.126(0.106)
2,3-Dimethylbutane (C_6H_{14})	3.73E-02	-	3.11E-03	8.79E-04	3.62E-03	-	nm	nm	2.70E-03	1.12E-2(1.74E-2)
2-Methylpentane (C_6H_{14})	0.342	3.36E-03	4.32E-02	6.59E-02	9.48E-02	-	nm	nm	4.35E-03	0.110(0.134)
3-Methylpentane (C_6H_{14})	8.60E-02	-	0.228	bdl	bdl	bdl	nm	nm	1.64E-03	0.157(0.100)
2,2,4-Trimethylpentane (C_8H_{18})	bdl	bdl	bdl	bdl	bdl	bdl	nm	nm	bdl	bdl
Cyclopentane (C_5H_{10})	5.84E-02	1.63E-04	1.00E-02	4.35E-03	1.41E-02	3.05E-04	nm	nm	7.39E-04	1.46E-2(2.22E-2)
Cyclohexane (C_6H_{12})	bdl	9.80E-03	bdl	bdl	bdl	bdl	nm	nm	2.85E-03	9.80E-3(-)
Methylcyclohexane (C_7H_{14})	0.100	1.71E-03	3.61E-03	-	5.23E-03	bdl	nm	nm	-	2.76E-2(4.81E-2)
Benzene (C_6H_6)	5.66	0.389	2.74	1.59	3.60	1.68	nm	nm	0.285	2.61(1.85)
Toluene (C_7H_8)	2.68	5.74E-02	0.574	0.645	0.802	0.139	nm	nm	3.23E-02	0.817(0.960)
Ethylbenzene (C_8H_{10})	2.18	2.11E-02	0.232	0.239	0.289	2.75E-02	nm	nm	1.61E-02	0.498(0.831)
m/p-Xylene (C_8H_{10})	1.14	3.42E-02	0.279	0.329	0.228	3.55E-02	nm	nm	1.41E-02	0.342(0.412)
o-Xylene (C_8H_{10})	0.657	1.78E-02	0.153	0.195	0.296	1.92E-02	nm	nm	7.75E-03	0.223(0.238)
Styrene (C_8H_8)	0.347	3.33E-03	0.493	0.811	0.349	0.199	nm	nm	2.00E-03	0.367(0.274)
i-Propylbenzene (C_9H_{12})	6.80E-02	bdl	-	9.97E-03	5.58E-03	1.20E-03	nm	nm	1.19E-03	2.12E-2(3.14E-2)
n-Propylbenzene (C_9H_{12})	7.19E-02	3.29E-03	2.45E-02	2.43E-02	5.79E-02	3.73E-03	nm	nm	2.35E-03	3.09E-2(2.83E-2)
3-Ethyltoluene (C_9H_{12})	0.128	4.97E-03	2.95E-02	2.67E-02	2.18E-02	2.50E-03	nm	nm	1.84E-03	3.55E-2(4.65E-2)
4-Ethyltoluene (C_9H_{12})	4.28E-02	2.59E-03	2.03E-02	2.26E-02	1.69E-02	1.22E-03	nm	nm	9.27E-04	1.77E-2(1.52E-2)
2-Ethyltoluene (C_9H_{12})	6.49E-02	2.45E-03	1.79E-02	2.06E-02	2.95E-02	2.72E-03	nm	nm	1.65E-03	2.30E-2(2.31E-2)
1,3,5-Trimethylbenzene (C_9H_{12})	6.33E-02	3.78E-03	3.73E-02	4.34E-02	5.17E-02	2.40E-03	nm	nm	9.73E-04	3.36E-2(2.52E-2)
1,2,4-Trimethylbenzene (C_9H_{12})	7.24E-02	5.70E-03	2.49E-02	2.34E-02	2.29E-02	4.25E-03	nm	nm	1.67E-03	2.56E-2(2.47E-2)
1,2,3-Trimethylbenzene (C_9H_{12})	2.15E-02	2.53E-03	2.21E-02	2.49E-02	1.55E-02	4.76E-03	nm	nm	1.44E-03	1.52E-2(9.49E-3)
alpha-Pinene ($C_{10}H_{16}$)	1.66E-02	bdl	0.135	2.40E-02	2.48E-02	bdl	nm	nm	7.81E-03	5.00E-2(5.65E-2)
beta-Pinene ($C_{10}H_{16}$)	bdl	bdl	-	bdl	8.27E-02	3.10E-04	nm	nm	-	4.15E-2(5.83E-2)
Ethanol (C_2H_6O)	-	6.01E-02	0.103	0.147	0.117	1.06E-02	nm	nm	-	8.74E-2(5.31E-2)
Acetaldehyde (C_2H_4O)	8.39	0.271	1.167	2.51	0.276	0.108	nm	nm	0.143	2.12(3.20)
Acetone (C_3H_6O)	5.38	1.01	1.04	2.42	3.57	0.380	nm	nm	0.950	2.30(1.90)
Butanal (C_4H_8O)	0.907	4.22E-02	7.68E-02	0.102	0.415	1.40E-02	nm	nm	6.21E-02	0.259(0.349)
Butanone (C_4H_8O)	0.755	5.37E-02	1.94E-03	0.419	1.89E-02	2.54E-02	nm	nm	0.472	0.212(0.310)
EF Black Carbon (BC)	0.561	6.04	nm	nm	nm	nm	1.58	1.69	nm	3.30(3.88)

EF Brown Carbon (BrC)	-	-	nm	nm	nm	nm	-	-	nm	-
EF B_{abs} 405 (m^2/kg)	5.72	60.2	nm	nm	nm	nm	16.1	17.3	nm	-
EF B_{scat} 405 (m^2/kg)	197	52	nm	nm	nm	nm	26.6	70.0	nm	-
EF B_{abs} 870 (m^2/kg)	nm	28.6	nm	nm	nm	nm	nm	nm	nm	-
EF B_{scat} 870 (m^2/kg)	nm	14.1	nm	nm	nm	nm	nm	nm	nm	-
SSA 405 nm	0.972	0.463	nm	nm	nm	nm	0.623	0.802	nm	-
SSA 870 nm	-	0.329	nm	nm	nm	nm	-	-	nm	-
AAE	-	0.971	nm	nm	nm	nm	-	-	nm	-

Note: "bdl" indicates below the detection limit; "-" indicates concentrations were not greater than background; "nm" indicates not measured; See Table 6.2 for garbage compositions
C-fractions: mixed garbage (0.50)-source is *Stockwell et al.* (2014); plastics (0.74) & chip bags (0.63)- source is *USEPA*, 2010 (see Sect. 2.1.4 for details)

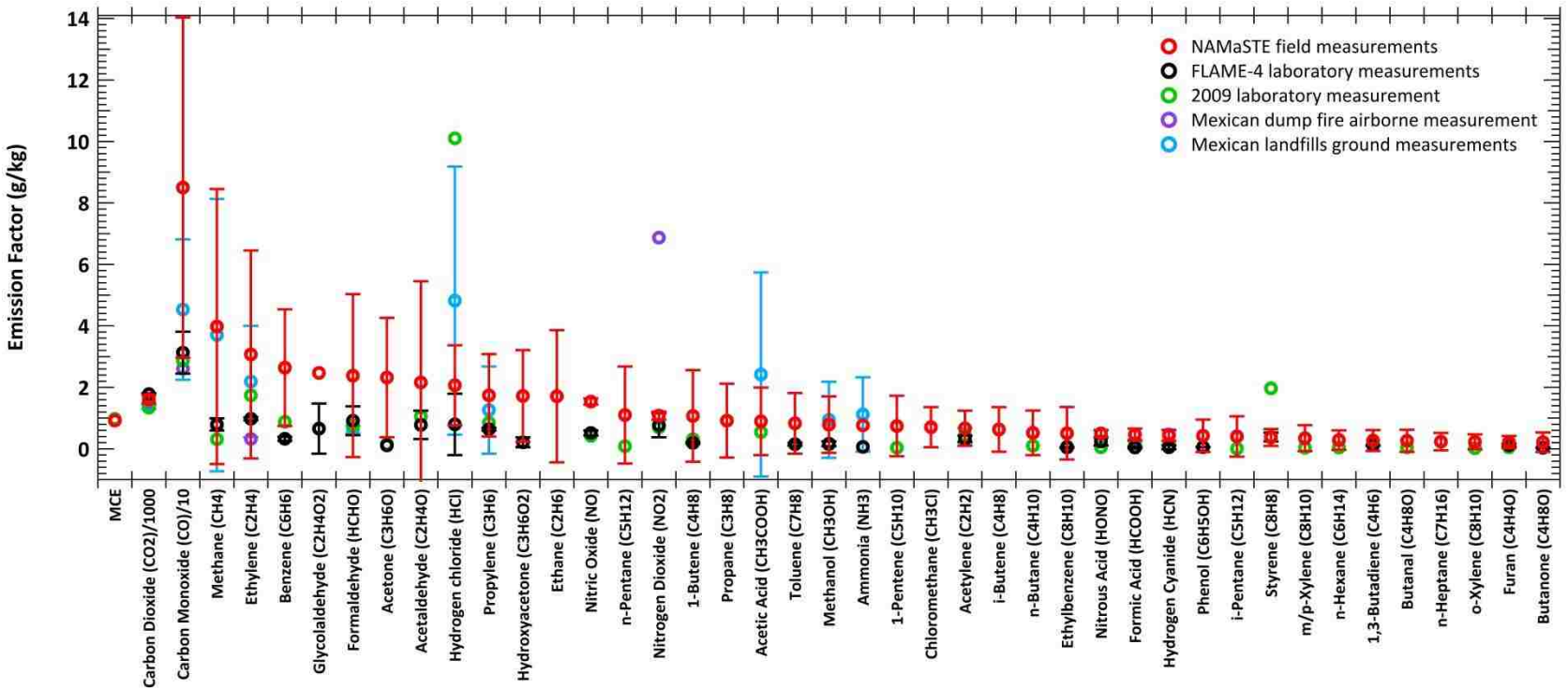

Figure 6.2. Garbage burning emission factors (g/kg) compiled for laboratory measurements (Yokelson et al., 2013a; Stockwell et al., 2015) (green, black), field measurements of open burning in Mexican landfills (Christian et al., 2010) (blue), a single airborne measurement from a Mexican dump fire (Yokelson et al., 2011) (purple) and our current study of mixed garbage (red). Error bars indicate one standard deviation of the EF for each study where available.

The laboratory mixed garbage-burning experiments during FLAME-4 were the first to yield a glycolaldehyde EF (0.658 g/kg) for trash burning. Our 14 April fire burning "mostly plastics" in Nepal produced a very high glycolaldehyde EF (4.56 g/kg). In both cases, the actual glycolaldehyde source is probably paper products, since glycolaldehyde is a product of cellulose pyrolysis (Richards et al., 1987). Glycolaldehyde in our first Nepal segregated plastics burn likely resulted from newspaper used as kindling for ignition. This burn also had high EFs for a few other OVOCs, especially formic and acetic acid and formaldehyde (5.30, 2.22, and 5.23 g/kg). The high EFs in this study indicate that garbage burning may be an important source of these aldehydes and acids. Co-firing paper with plastics is also the likely reason our 14 April "mostly plastics" simulation burned at a significantly lower MCE than the pure plastic shopping bags that were burned during the FLAME-4 campaign. Most garbage is a more complex mixture than just paper and plastic so our average EFs for garbage burning in Nepal in Table 6.8 are based on only the results from sampling mixed garbage burns.

NMHCs were major emissions with ethylene and acetylene always important for both the mixed garbage and the mostly plastic burns. Interestingly, benzene (a carcinogen) was just below ethylene as the most abundant NMHC in mixed garbage burning emissions overall (Figure 6.2). Estimates of waste burning by country for all countries are presented in Wiedinmyer et al. (2014). For Nepal, the estimated amount of waste burned is 644 Gg per year. Based on our average benzene EF for garbage burning (2.61 ± 1.85 g/kg), we estimate that trash-burning in Nepal produces ~ 1.68 Gg benzene (range 0.490 – 2.87 Gg) annually. The central estimate of Wiedinmyer et al. (2014) is 0.580 Gg/yr of benzene emitted from Nepali garbage burning; at the lower end of our range, but only 34% of our mean.

As observed in Figure 6.2, EF HCl varies significantly between experiments and within the same study. Yokelson et al. (2013a) reported a lab-measured EF HCl of 10.1 g/kg, whereas Stockwell et al. (2014) reported their highest lab-measured EF HCl at 1.52 g/kg. These values are close to the upper and lower end of EF HCl for authentic Mexican landfill fires (1.65-9.8 g/kg) (Christian et al., 2010). HCl fell below the detection limit in some FTIR grab samples collected during NAMaSTE, indicating that GB emissions can differ depending on which components are burning during a particular grab sample. Our 14 April burn with fuels that were mostly plastics had extremely high EF HCl (77.9 g/kg), suggesting that many of the bags burned were made from polyvinyl chloride (PVC). Our average EF for HCl for mixed GB was 2.32 ± 1.01 well within the range for Mexican GB. The other major halogenated emission detected from mixed GB was chloromethane (by WAS) at an EF up to 1.59 g/kg (average 0.702 ± 0.648 g/kg).

HCN is considered useful as a BB tracer (Li et al. 2000), but was emitted by the mixed garbage and mostly plastic burns with an EF HCN that is similar to BB. We did not collect data in Nepal for acetonitrile, which is also used as a BB tracer, but the high CH_3CN/HCN ratios in Stockwell et al. (2015) for laboratory garbage burning suggests a similar issue may occur. This should be factored into any source apportionment based on using these compounds as tracers in regions where the emission sources include BB and either or both of garbage burning and motorcycles (e.g. Sect. 3.2).

Carbonyl sulfide (OCS) is emitted by natural (oceans, volcanoes, etc.), BB, and anthropogenic (automobiles, fossil fuel combustion) sources (Kettle et al., 2002). Two of our mixed garbage burns had high EF OCS (> 0.1 g/kg) and these are the first measurements reporting an EF OCS for GB. Burns 1 and 5 (Table 6.8) both had high OCS and both had a higher percentage of food waste. Because OCS is relatively inert in the troposphere, it freely transports into the stratosphere

where it photodissociates and oxidizes and can ultimately condense into particles. The other S-species we could measure remained low (DMS) or below detection (SO_2).

The global garbage burning inventory of Wiedinmyer et al. (2014) had to rely on the EF BC (actually a filter-based EC measurement) from just one study (0.65 g/kg, Christian et al., 2010). Both PAXs were operational during one mixed garbage burn and we measured an EF BC of 6.04 g/kg (with an AAE ~1) almost ten times larger than the previously measured EF for BC suggesting a strongly BC-dominated aerosol. In addition, we can estimate an upper limit for EF BC for some of the other trash fires by assuming all 405 nm absorption is due to BC while the 870 PAX was not operational. This provides our 405-estimated values in Table 6.8 and they range from ~0.561-1.69 g/kg. Thus, our EF of 6.04 g/kg is likely a high end value from a flaming dominated garbage fire (MCE 0.980) while our lower values come from fires with more smoldering (MCE ~0.96) that are probably more common. Overall our PAX data suggests an upward revision for the literature-average garbage burning EF BC to something above 1 g/kg. However, with only one robust PAX-based EF BC determination, we will rely on the detailed EC/OC particulate analysis from NAMaSTE to better characterize this source in Jayarathne et al. (2016).

6.5.6 Cooking fire emissions

There were two main goals of our cooking fire measurements. One was to increase the amount of chemically- and optically-detailed trace gas and aerosol information that has been quantified in the field to allow more comprehensive assessments of the atmospheric and health impacts. The second was to obtain this type of detailed information for cooking fires that represent the most common global practice (open hardwood-fuel cooking fires); a major undersampled regional

cooking practice (dung-fueled cooking fires); and, in exploratory fashion, a diverse range of stove/fuel combinations being considered as mitigation strategies.

First, we illustrate the range of cooking technologies that we sampled and support some basic observations by plotting the MCE of all the stove/fuel combinations that we tested in decreasing order in Figure 6.3. Several things stand out. Firstly, the biogas, the bhuse chulo sawdust, and biobriquette-fueled stoves had the highest MCE in our (limited) testing out of the wide range of possibilities and generally had smaller gas-phase EFs. The two measurements for biogas varied substantially and the differences could be a gas leak through the supply line and/or lingering BB emissions present in the laboratory room, thus we favor the field values. Biogas has proven to be a viable alternative to traditional wood sources especially in rural Nepal where agriculture and animal husbandry are the main sources of income (Katuwal and Bohara, 2009), however, biogas stoves remain unaffordable for poorer households. The higher MCEs in our emissions survey study suggest more extensive testing of biogas or the bhuse chulo could be warranted. The complete individual emissions for all stoves/fuels measured during NAMaSTE are included in Supplement Table S8. Another apparent feature of Figure 6.3 is the sharp drop off in MCE for the tests on the right side of the figure, which were mostly field measurements as opposed to the generally higher MCE in lab measurements. This suggests that "lower" MCE near 0.92 for wood and 0.90 for dung are apparently representative of real world use. More field tests were planned but were not completed due to the earthquake. However, lower stove MCE in the field compared to lab testing has been reported previously (Bertschi et al., 2003a; Roden et al., 2008; Stockwell et al., 2014) and the literature average MCE for field use is close to 0.92 (Akagi et al., 2011). Thus, we are fairly confident in adjusting the lab data for open cooking to reflect lower

efficiency to use the lab tests to augment the field data. The straightforward adjustment procedure is described next.

As in Stockwell et al. (2014, 2015) we obtained field representative values from the lab data by multiplying the lab ER-to-CH_4 (measured by FTIR or WAS) for smoldering compounds and the lab ER-to-CO_2 (measured by FTIR or WAS) for flaming compounds by the field EF for CH_4 and CO_2, respectively. Our full original NAMaSTE data are in Table S8 and the adjusted laboratory data for gases for traditional open hardwood and dung cooking-fires were averaged together with our authentic field values to estimate our NAMaSTE-average EF for open wood and dung cooking-fires. Those estimates along with values from a few other studies that reported a reasonably large number of EFs for cooking fires burning wood and dung are shown in Table 6.9 and form the basis for much of the ensuing discussion.

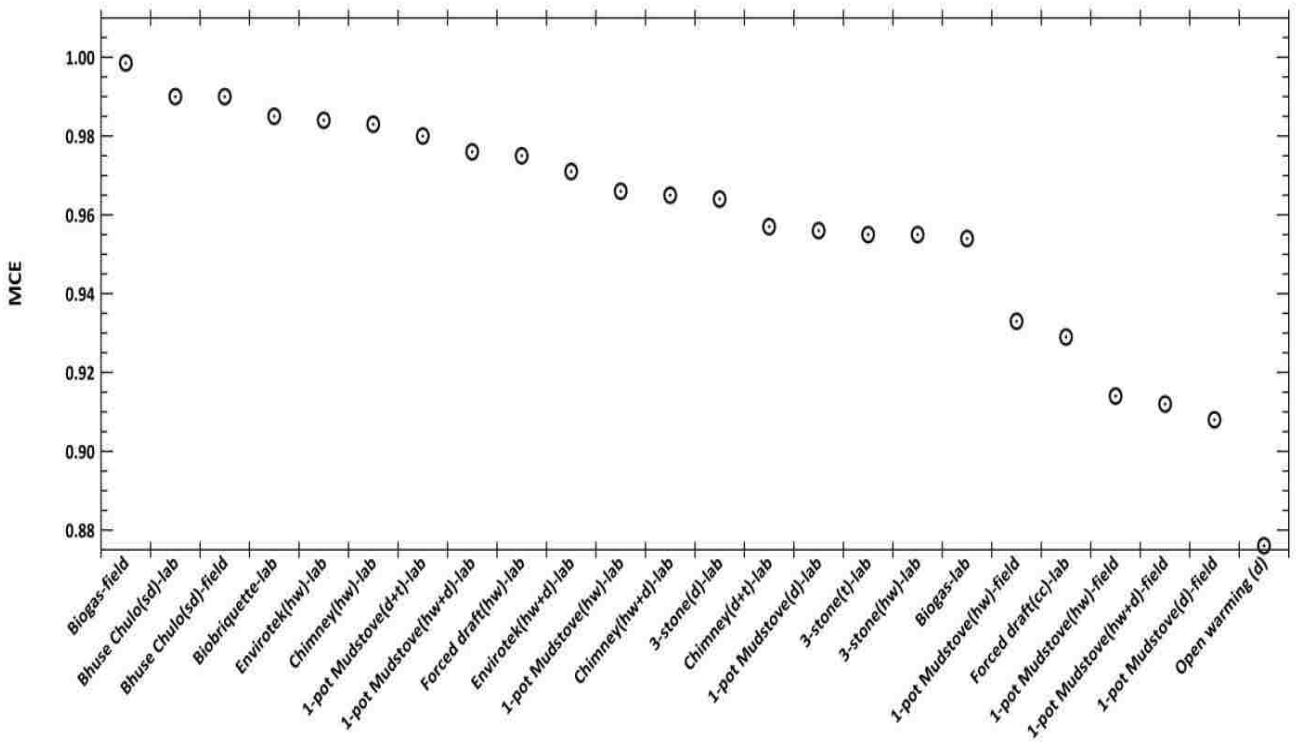

Figure 6.3. The modified combustion efficiency (MCE) shown in descending order for each cookstove/fuel combination measured in this study. The stove-type is listed followed by the main fuel constituents and an indication whether the source was a lab or field measurement. Note: "hw" indicates hardwood fuels; "d" indicates dung; "cc" indicates charcoal; "t" indicates twigs; and "sd" indicates sawdust.

Table 6.9. Compiled emission factors (g/kg) and one standard deviation for open traditional cooking fires using dung and wood fuels. The NAMaSTE values include field measurements and adjusted laboratory measurements.

Compound (Formula)	**EF Hardwood cooking EF** NAMaSTE avg (stdev)[a]	**EF Dung cooking** NAMaSTE avg (stdev)	**EF wood open cooking** Akagi et al. [2011] avg (stdev)	**EF wood open cooking** Stockwell et al. [2015] avg (stdev)[b]	**EF Dung burning** Akagi et al. [2011] avg (stdev)
MCE	0.923	0.898	0.927	0.927	0.839
PM	-	-	6.73(1.61)	-	22.9
Carbon Dioxide (CO_2)	1462(16)	1129(80)	1548(125)	1548(125)	859(15)
Carbon Monoxide (CO)	77.2(13.5)	80.9(13.8)	77.4(26.2)	77.4 (26)	105(10)
Methane (CH_4)	5.16(1.39)	6.65(0.46)	4.86(2.73)	4.86(0.20)	11.0(3.3)
Acetylene (C_2H_2)	0.764(0.363)	0.593(0.443)	0.970(0.503)	0.602(0.361)	nm
Ethylene (C_2H_4)	2.70(1.17)	4.23(1.39)	1.53(0.66)	2.21(1.40)	1.12(0.23)
Propylene (C_3H_6)	0.576(0.195)	1.47(0.58)	0.565(0.338)	0.317(0.145)	1.89(0.42)
Formaldehyde (HCHO)	1.94(0.75)	2.42(1.40)	2.08(0.86)	1.70(0.74)	nm
Methanol (CH_3OH)	1.92(0.61)	2.38(0.90)	2.26(1.27)	2.05(1.63)	4.14(0.88)
Formic Acid (HCOOH)	0.179(0.071)	0.341(0.308)	0.220(0.168)	0.620(0.533)	0.460(0.308)
Acetic Acid (CH_3COOH)	3.14(1.11)	7.32(6.59)	4.97(3.32)	8.90(9.27)	11.7(5.1)
Glycolaldehyde ($C_2H_4O_2$)	0.238(0.155)	0.499(0.260)	1.42(-)	0.455(0.149)	nm
Furan (C_4H_4O)	0.241(0.024)	0.534(0.209)	0.400(-)	0.228(0.162)	0.950(0.220)
Hydroxyacetone ($C_3H_6O_2$)	1.26(0.09)	3.19(2.24)	nm	0.480(0.367)	9.60(2.38)
Phenol (C_6H_5OH)	0.496(0.159)	1.008(0.348)	3.32(-)	0.264(0.085)	2.16(0.36)
1,3-Butadiene (C_4H_6)	0.204(0.144)	0.409(0.306)	nm	3.37E-2(9.67E-3)	nm
Isoprene (C_5H_8)	4.16E-2(2.23E-2)	0.325(0.443)	nm	0.145(0.077)	nm
Ammonia (NH_3)	0.259(0.253)	3.00(1.33)	0.865(0.404)	7.88E-2(6.90E-2)	4.75(1.00)
Hydrogen Cyanide (HCN)	0.557(0.247)	2.01(1.25)	nm	0.221(0.005)	0.530(0.300)
Nitrous Acid (HONO)	0.452(0.068)	0.276(0.101)	nm	0.291(0.169)	nm
Sulfur Dioxide (SO_2)	bdl	bdl	nm	0.499	6.00E-2(-)
Hydrogen Fluoride (HF)	bdl	bdl	nm	bdl	nm
Hydrogen chloride (HCl)	7.51E-2(7.99E-2)	3.76E-2(3.59E-2)	nm	bdl	nm
Nitric Oxide (NO)	1.62(1.30)	2.22(1.02)	1.72(0.75)	0.319(0.089)	0.500
Nitrogen Dioxide (NO_2)	0.577(0.348)	0.898(0.444)	0.490(0.330)	1.11(0.28)	nm
Carbonyl sulfide (OCS)	1.87E-2(1.15E-2)	0.148(0.123)	nm	nm	nm
DMS (C_2H_6S)	0.255(0.359)	2.37E-2(7.67E-4)	nm	nm	nm
Chloromethane (CH_3Cl)	2.36E-2(1.62E-2)	1.60(1.53)	nm	nm	nm
Bromomethane (CH_3Br)	5.61E-4(3.01E-4)	5.34E-3(3.02E-3)	nm	nm	nm
Methyl iodide (CH_3I)	1.23E-4(1.11E-4)	4.39E-4(1.78E-4)	nm	nm	nm
1,2-Dichloroethene ($C_2H_2Cl_2$)	1.24E-4(3.00E-5)	4.97E-3(-)	nm	nm	nm
Methyl nitrate (CH_3NO_3)	6.96E-3(5.73E-3)	1.46E-2(1.94E-2)	nm	nm	nm
Ethane (C_2H_6)	0.160(0.122)	1.075(0.300)	1.50(0.50)	nm	nm
Propane (C_3H_8)	0.202(0.140)	0.457(0.137)	nm	nm	nm
i-Butane (C_4H_{10})	0.406(0.478)	0.215(0.126)	nm	nm	nm
n-Butane (C_4H_{10})	1.11(1.48)	0.29(0.09)	nm	nm	nm
1-Butene (C_4H_8)	0.726(0.904)	0.399(0.331)	nm	0.245(0.148)	nm
i-Butene (C_4H_8)	0.846(1.113)	0.281(0.091)	nm	nm	nm
trans-2-Butene (C_4H_8)	6.78E-2(5.98E-2)	0.151(0.010)	nm	nm	nm
cis-2-Butene (C_4H_8)	5.51E-2(4.76E-2)	0.102(0.016)	nm	nm	nm
i-Pentane (C_5H_{12})	8.58E-2(1.58E-2)	0.811(0.387)	nm	nm	nm
n-Pentane (C_5H_{12})	2.18E-2(1.73E-2)	0.190(0.254)	nm	nm	nm
1-Pentene (C_5H_{10})	1.43E-2(9.36E-3)	0.168(0.086)	nm	nm	nm
trans-2-Pentene (C_5H_{10})	1.05E-2(8.30E-3)	0.115(0.035)	nm	nm	nm
cis-2-Pentene (C_5H_{10})	8.69E-3(-)	5.14E-2(7.55E-3)	nm	nm	nm
3-Methyl-1-butene (C_5H_{10})	7.43E-3(5.79E-3)	5.58E-2(3.50E-2)	nm	nm	nm
1,2-Propadiene (C_3H_4)	2.33E-2(1.07E-2)	7.15E-2(6.76E-2)	nm	nm	nm
Propyne (C_3H_4)	6.39E-2(3.07E-2)	0.172(0.156)	nm	nm	nm
1-Butyne (C_4H_6)	1.28E-2(4.73E-3)	2.29E-2(1.38E-2)	nm	nm	nm
2-Butyne (C_4H_6)	1.02E-2(6.56E-3)	1.86E-2(9.11E-3)	nm	nm	nm
n-Hexane (C_6H_{14})	1.85E-2(-)	0.291(0.248)	nm	nm	nm

n-Heptane (C_7H_{16})	1.01E-2(1.35E-2)	0.114(0.069)	nm	nm	nm
n-Octane (C_8H_{18})	1.75E-2(-)	4.77E-2(9.85E-3)	nm	nm	nm
n-Nonane (C_9H_{20})	4.87E-2(6.40E-2)	4.68E-2(2.55E-2)	nm	nm	nm
n-Decane ($C_{10}H_{22}$)	6.90E-2(9.61E-2)	4.71E-2(4.03E-2)	nm	nm	nm
2,3-Dimethylbutane (C_6H_{14})	1.57E-2(1.16E-2)	0.112(0.105)	nm	nm	nm
2-Methylpentane (C_6H_{14})	9.93E-3(1.29E-2)	0.231(0.192)	nm	nm	nm
3-Methylpentane (C_6H_{14})	6.79E-3(6.63E-3)	0.155(0.137)	nm	nm	nm
2,2,4-Trimethylpentane (C_8H_{18})	-(-)	0.100(0.080)	nm	nm	nm
Cyclopentane (C_5H_{10})	4.06E-3(-)	0.146(0.178)	nm	nm	nm
Cyclohexane (C_6H_{12})	1.16E-2(-)	0.224(0.255)	nm	nm	nm
Methylcyclohexane (C_7H_{14})	1.62E-2(-)	4.76E-2(3.96E-2)	nm	nm	nm
Benzene (C_6H_6)	1.05(0.19)	1.96(0.45)	nm	2.58(2.68)	nm
Toluene (C_7H_8)	0.241(0.160)	1.26(0.05)	nm	0.290(0.311)	nm
Ethylbenzene (C_8H_{10})	4.19E-2(4.25E-2)	0.366(0.085)	nm	nm	nm
m/p-Xylene (C_8H_{10})	9.57E-2(7.99E-2)	0.601(0.294)	nm	0.265(0.380)	nm
o-Xylene (C_8H_{10})	3.93E-2(4.31E-2)	0.228(0.083)	nm	nm	nm
Styrene (C_8H_8)	8.71E-2(6.69E-2)	0.255(0.091)	nm	0.234(0.306)	nm
i-Propylbenzene (C_9H_{12})	1.70E-2(1.67E-2)	1.87E-2(1.40E-2)	nm	nm	nm
n-Propylbenzene (C_9H_{12})	1.78E-2(1.58E-2)	3.10E-2(1.45E-2)	nm	nm	nm
3-Ethyltoluene (C_9H_{12})	2.62E-2(5.41E-3)	5.61E-2(2.38E-2)	nm	nm	nm
4-Ethyltoluene (C_9H_{12})	2.07E-2(1.19E-2)	3.57E-2(1.74E-2)	nm	nm	nm
2-Ethyltoluene (C_9H_{12})	2.10E-2(1.16E-2)	3.39E-2(1.34E-2)	nm	nm	nm
1,3,5-Trimethylbenzene (C_9H_{12})	2.14E-2(-)	1.79E-2(8.32E-3)	nm	7.01E-2(9.27E-2)	nm
1,2,4-Trimethylbenzene (C_9H_{12})	1.74E-2(2.35E-2)	3.91E-2(1.65E-2)	nm	nm	nm
1,2,3-Trimethylbenzene (C_9H_{12})	2.16E-2(-)	2.34E-2(4.30E-3)	nm	nm	nm
alpha-Pinene ($C_{10}H_{16}$)	2.02E-2(2.33E-2)	0.348(0.487)[c]	nm	0.197(0.257)	nm
beta-Pinene ($C_{10}H_{16}$)	4.67E-2(-)	0.471(-)[c]	nm	nm	nm
Ethanol (C_2H_6O)	0.128(0.017)	0.563(0.589)	nm	nm	nm
Acetaldehyde (C_2H_4O)	0.541(0.362)	1.88(1.63)	nm	0.792(0.439)	nm
Acetone (C_3H_6O)	0.524(0.256)	1.63(0.38)	nm	nm	nm
Butanal (C_4H_8O)	8.28E-3(6.27E-3)	5.40E-2(2.19E-2)	nm	nm	nm
Butanone (C_4H_8O)	0.232(0.286)	0.262(0.109)	nm	8.04E-2(4.98E-2)	nm
EF Black Carbon (BC)	0.221(0.127)	4.15E-2(3.18E-2)	0.833(0.453)	nm	nm
EF Brown Carbon (BrC)	8.59(5.62)	5.54(1.66)	nm	nm	nm
EF B_{abs} 405 (m^2/kg)	10.6(6.8)	5.85(1.95)	nm	nm	nm
EF B_{scat} 405 (m^2/kg)	40.4(23.8)	49.5(5.8)	nm	nm	nm
EF B_{abs} 870 (m^2/kg)	1.04(0.60)	0.197(0.151)	nm	nm	nm
EF B_{scat} 870 (m^2/kg)	1.51(0.52)	0.922(0.324)	nm	nm	nm
EF B_{abs} 405 just BrC (m^2/kg)	8.40(5.48)	5.43(1.62)	nm	nm	nm
EF B_{abs} 405 just BC (m^2/kg)	2.24(1.28)	0.423(0.324)	nm	nm	nm
SSA 405 nm	0.605(0.061)	0.811(0.164)	nm	nm	nm
SSA 870 nm	0.794(0.009)	0.893(0.043)	nm	nm	nm
AAE	3.01(0.10)	4.63(0.68)	nm	nm	nm

Note: "bdl" indicates below the detection limit; "-" indicates concentrations were not greater than background; "nm" indicates not measured
[a] NAMaSTE gas-phase data include adjusted laboratory and unadjusted field values. Aerosol values include field measurements only
[b]This includes laboratory adjusted values (see *Stockwell* et al., (2014,2015)); additional gas-phase compounds are reported therein
[c]High monoterpene values likely due to wood kindling

We focus next on dung cooking-fires, which are prevalent in South Asia. To our knowledge, there are very few studies that report any EFs for dung burning (Akagi et al., 2011) and this work significantly expands the gas-phase emissions data. The NAMaSTE-derived dung cooking-fire average in Table 6.9 includes 4 traditional dung cooking-fires (1-pot mud stoves and 3-stone)

and an open fire intended to represent an authentic open warming fire outside a rural home. The open warming fire had a lower MCE (0.876) than our two field dung cooking-fires (0.910 ± 0.003) that was slightly closer to the low MCE (0.839) average value reported in Akagi et al. (2011) based on open pasture burning of dung in Brazil (Christian et al., 2007) and laboratory burns of Indian dung (Keene et al., 2006).

As shown for dung-fuel cooking-fires in Table 6.9, our EFs for CH_4 (6.65 ±0.46 g/kg) are lower than the literature average reported in Akagi et al. (2011) (11 g/kg), although both are within the range (3-18 g/kg) reported by Smith et al. (2000) for simulated rural cooking in India. OVOCs were major emissions and we provide the first EFs for many OVOCs (e.g. formaldehyde, acetone, glycolaldehyde, acetaldehyde, etc.). Acetic acid and hydroxyacetone were the most abundant OVOCs, though the Nepal EFs (7.32 and 3.19 g/kg) are lower than the Brazil EFs (14.3 and 9.6 g/kg) reported by Christian et al. (2007) at a lower MCE. This work considerably expands our knowledge of NMHCs from this source and reports a much higher EF for C_2H_4 (4.23 g/kg) and also many previously unobserved NMHCs at high levels. In particular, our new NMHC data include high emissions for BTEX compounds, especially benzene and toluene (1.96, 1.26 g/kg). Other notable compounds with high emissions that were previously unobserved include chloromethane (1.60 g/kg) and carbonyl sulfide (0.148 g/kg). This is consistent with the elevated Cl and S content in the dung sample from MT (0.19 % S, 0.05 % Cl; Table 6.3). Chloromethane is the main form of organic chlorine in the atmosphere (Lobert et al., 1999) and is discussed more below.

As expected, the high N-content of dung (1.9% Table 6.3) led to high emissions for N-containing gases including NH_3 (3 g/kg), NO_x (~3 g/kg), and HCN (~2 g/kg). Our NO_x EF is higher than previously reported and this is an EPA regulated criteria pollutant that is an important precursor

to ozone, acid rain, and nitrate aerosols. The high NH_3 (3.00 ±1.33 g/kg) and acetic acid (7.32 ± 6.59 g/kg) emissions we observed, also previously observed in Brazil dung-fire emissions, might lead to ammonium acetate in secondary aerosol. Laboratory measurements during FLAME-4 were the first to report HCN from wood cooking fires (Stockwell et al., 2014; Sect. 4.3.4), though the ERs to CO were about 5 times lower than what is typically observed for other BB fuels. The NAMaSTE real-world wood cooking fires had higher HCN EFs (0.557 ± 0.247 g/kg) than in the lab (0.221 g/kg); however, our HCN to CO ratio for dung burning is 3.5 times higher than for wood. Despite the lower ER for wood, its dominance as a fuel mean both should be considered an important source of HCN in the atmosphere. The cooking source continues during the monsoon, when open burning is reduced, and likely contributes to the large HCN anomaly observed by satellite in the anticyclone over the Asian monsoon (Park et al., 2008; Randel et al., 2010; Glatthor et al., 2015). The NAMaSTE $\Delta HCN/\Delta CO$ ratios should be considered when using HCN in any source apportionment of pollution sources in areas subject to BB and dung cooking along with the motorcycles and garbage burning mentioned above.

Yevich and Logan (2003) estimated annual Asian use of dung as a biofuel in 1985 at 123 (±50%) Tg, with India accounting for 93 Tg. The NAMaSTE field measurements of dung burning were conducted in the Terai region that makes up the southern part of Nepal and likely represents similar cooking conditions as those in northern India. Fernandes et al. (2007) estimated that only 75 Tg/yr of dung is burned globally while Yevich and Logan (2003) estimated a slightly higher global value (136 Tg). If we take the average of these two studies as an estimate of dung biofuel use (106 Tg), then we estimate from our EFs that 0.78 Tg acetic acid, 0.21 Tg HCN, and 0.17 Tg CH_3Cl are emitted from dung burning each year. This accounts for ~33, 51, and over 100% of the previously estimated total biofuel burning emissions for these species in the late 1990s

(Andreae and Merlet, 2001). Our estimate of HCN emitted solely from burning dung accounts for ~4-8% of HCN thought to be emitted by total BB annually in earlier work (Li et al., 2000). Our estimate of CH_3Cl emitted by dung burning alone is ~18% of the total global CH_3Cl emitted by BB in the inventory of Lobert et al. (1999). They also cited a high Cl content of dung (4360 mg/kg) and concluded BB was the largest source of CH_3Cl in the atmosphere. The contribution of dung burning to acetic acid, HCN, CH_3Cl, and other species should be included in updated inventories of global BB and biofuel emissions.

We report the first BrC emissions data from dung burning (to our knowledge) in Table 6.9 based on our NAMaSTE field-measured values only. Our EF BrC of 5.54 ± 1.66 g/kg is qualitative, but substantial and our more rigorously measured AAE (4.63±0.68) is higher than our NAMaSTE value for wood cooking (3.01 ± 0.10). Expressed in terms of light absorption, BrC accounted for ~93% of aerosol absorption at 405 nm for dung burning and 79% for wood burning. In addition, for dung burning the BC absorption EF at 870 nm was only 3.5% of the "BrC-only" absorption EF at 405 nm. Even for wood burning, the BC absorption EF at 870 nm was just 12% of the BrC absorption EF at 405 nm. From these values we see that dung cooking fires are an important BrC source in South Asia and that BrC from cooking fires in general is of great importance for understanding their climate impacts. Our EF BC (0.04 g/kg) for dung is lower than the suggested EF reported in Venkataraman et al. (2005) (0.12g/kg) for lab-burned cattle dung, though it is within the low end of the range estimated by Xiao et al. (2015) (0.03-0.3 g/kg) for dung cooking-fires. The sum of our BC and BrC emissions (~5.5 g/kg) is significantly lower than total carbon (EC+OC, 22 g/kg) reported for lab measurements of dung cooking-fires in Keene et al. (2006), but the methods used are difficult to compare. Both studies highlight the need for more measurements of this source. The SSA for dung cooking-fires is statistically higher at both

wavelengths than for wood cooking, but both sources produced fresh smoke with SSA < 0.9 indicating it would (initially) warm the atmosphere and cool the surface, impacting climate (Praveen et al., 2012). Our values of EF B_{abs}, EF B_{scat}, AAE, and SSA at 405 and 870 nm shown in Table 6.9 for dung and wood burning are independent of MAC estimates and can be used in models directly to estimate the optical properties, forcing, etc.

Open cooking fires using hardwood fuel are the most common cooking technology globally. Our NAMaSTE measurements significantly increase the number of gases that have been measured in hardwood open cooking-fire emissions in the field. We report a few new OVOCs with high EF such as acetone (0.524 g/kg) and many new EFs for NMHCs (Table 6.9). The NAMaSTE results include lower emissions of total BTEX compounds from wood cooking fires (~1.5 g/kg) than dung cooking fires (~5.5 g/kg) but confirm the high EF for these species previously reported in lab studies (~3.2 g/kg, Stockwell et al., 2015). DMS emissions have not been reported previously for open cooking, and the EF is relatively high (0.255 g/kg) for a BB source (Simpson et al., 2011). Rather than walk the reader through all the data in Table 6.9 we reiterate the main result, which is that models can now use much improved speciation of the trace gases emitted by cooking fires. This can be seen by comparing columns 2 and 4 (the literature average) in Table 6.9. The agreement is good for most species previously measured in the field. For example, the NAMaSTE-average MCE (0.923) is very close to the Akagi et al. (2011) field average MCE (0.927). In addition, NAMaSTE provides data in column 2 for about 70 gases not previously measured in field work to our knowledge. The data will be used to update the tables in Akagi et al., (2011) creating a new literature average.

The numerous trace gas EFs we measured for open-hardwood cooking-fires in Nepal also present an important validation opportunity for cooking-fire trace gas measurements made on

simulated cooking fires in a lab study that featured many advanced instruments mostly never deployed on field cooking-fires. In FLAME-4, the lab cooking-fire EF for trace gases were adjusted to the field average MCE (0.927) and reported in Table S4. In Table 6.8 we show the overlap species between NAMaSTE and FLAME-4. There are a few noticeable deviations between the lab and NAMaSTE EF for NMOC. The lab/field EF ratios are shown in parentheses for acetic acid (2.8), hydroxyacetone (0.38), BTEX (2), and HCN (0.40). However, comparing columns 2 and 5 shows agreement within one standard deviation of the mean for more than 70% of the ~26 overlap species. Fuel S and N content differences may explain the EF differences for SO_2 and NO_x. In general the agreement suggests the FLAME-4 trace gas EF are useful, especially for the > 100 species that study measured that were not measured in the field (Stockwell et al., 2015; Hatch et al., 2015; Chapter 5).

As noted earlier, aerosol emissions from wood cooking-fires are a major global issue. Our EF BC (0.221±0.127 g/kg) for hardwood cooking fires is significantly lower than the Akagi et al. (2011) literature average (0.833 ±0.025 g/kg) based on EC measurements, but was within the range reported in Christian et al. (2010) (0.205-0.674 g/kg). Our BC and BrC combine to ~9 g/kg which is ~40 % larger than the typical value for $PM_{2.5}$ from biofuel sources (~7 g/kg, Akagi et al., 2011). To our knowledge we report the first field-measured EF B_{abs} and EF B_{scat} for wood cooking-fires at 405 and 870 nm (Table 6.9), which can be used in models without MAC assumptions. We also provide rare measurements of SSA and AAE for fresh cooking fire aerosol in Table 6.9 and S8. Our AAE for hardwood cooking-fires (3.01) is higher than Praveen et al. (2012) measured in hardwood cooking-fire smoke (2.2) in the IGP in northern India. More work is required to examine how methodological differences, aging, and sample size vs real regional variability affect measurements of regional averages. Our hardwood cooking SSAs (0.794, 870

nm; 0.605, 405 nm) indicate an absorbing fresh aerosol, but SSA has been seen to increase rapidly with aging in BB plumes (Abel et al., 2003; Yokelson et al., 2009; Akagi et al., 2012). In summary, our PAX data from Nepal increases the total amount of sampling and approaches used to estimate regional average cooking-fire aerosol properties. Incorporating our data would nudge the regional average for hardwood cooking-fires towards higher BrC/BC ratios and we show that dung cooking-fires are also an important BrC source. Additional NAMaSTE aerosol data will be reported in companion papers (Jayarathne et al., 2016; Goetz et al., 2016).

Health impacts of indoor cooking-fire emissions are a major global concern (Davidson et al., 1986; Fullerton et al., 2008, etc.). We did not target exposure assessment in NAMaSTE, but our data can be used in a piggy-back approach with studies focused on longer-term exposure to a key indoor air pollutant to estimate exposure to other air toxic gases not measured in those exposure studies following Akagi et al. (2014). We give one example. Based on our measurements it is possible to extrapolate concentrations of trace species not measured in previous studies. For example, assuming similar emission profiles, we can scale indoor CO measured by Davidson et al. (1986) to estimate indoor benzene concentrations and exposures. In their study indoor concentrations of CO were 21 ppm, which would equate to 183 ppb benzene using the ER (benzene / CO) from our study for dung cooking. The same approach can be extended to any of the gases we measured for any of the stove and fuel types. Overall, we were able to survey a very large variety of cooking technologies, practices, and fuel options representative of a diverse region and identify candidate technologies for further testing and possible wider use. The large amount of new gas and aerosol data from NAMaSTE as a whole should improve model representation and help to better understand the local and regional climate, chemistry, and health impacts of domestic and industrial biofuel use.

6.5.7 Crop residue fire emissions

We present the first detailed measurements of trace gas chemistry and aerosol properties for burning authentic Nepali crop residues and we also significantly expand the field emissions characterization for global agricultural residue fires. The EFs for each fire are compiled in Table 6.10. We examine the representativeness of our trace gas grab sampling, justify a small adjustment to the trace gas data, and then discuss the implications of the trace gas and aerosol results.

A detailed suite of EF for several crop residues commonly burned in the US and globally that is based on continuous lab measurements over the course of whole fires is reported in Stockwell et al. (2014, 2015). A few fuels they measured overlap with our Nepal study, including wheat and rice straw. The average MCE (0.954) for our Nepal grab samples burning wheat varieties is very close to the lab measured wheat straw burning MCE (0.956), though other crop types do not compare as well. When we compare our Nepal-average MCE for all our crop residue fire grab samples (0.952) to earlier field measurements we find that the MCEs reported in Mexico (0.925) by Yokelson et al. (2011) and in the US (0.930) by Liu et al. (2016) are significantly lower. In addition, the previous field studies obtained more grab samples of a larger number of fires and sampled from the air, which is unlikely to return too low an MCE. The MCE that we obtained from the real-time FTIR CO and CO_2 measurements that supported filter collection was also lower (e.g. ~0.933) and closer to the above-mentioned field MCE values. Thus, we believe our Nepal-average MCE based on grab samples is likely biased upwards. Thus, to make our Nepal EFs more representative of the likely Nepal (and regional) average, we have adjusted to the average airborne-measured field MCE (0.925) observed for crop residue burning in another developing country (Mexico) according to procedures originally established in Stockwell et al.

(2014) and also described in Sect. 3.6 above. These adjusted EFs for selected compounds are included in Table 6.11 along with values from selected other previous studies. Additional compounds measured in this study (both original and adjusted) are included in Supplemental Table 6.10.

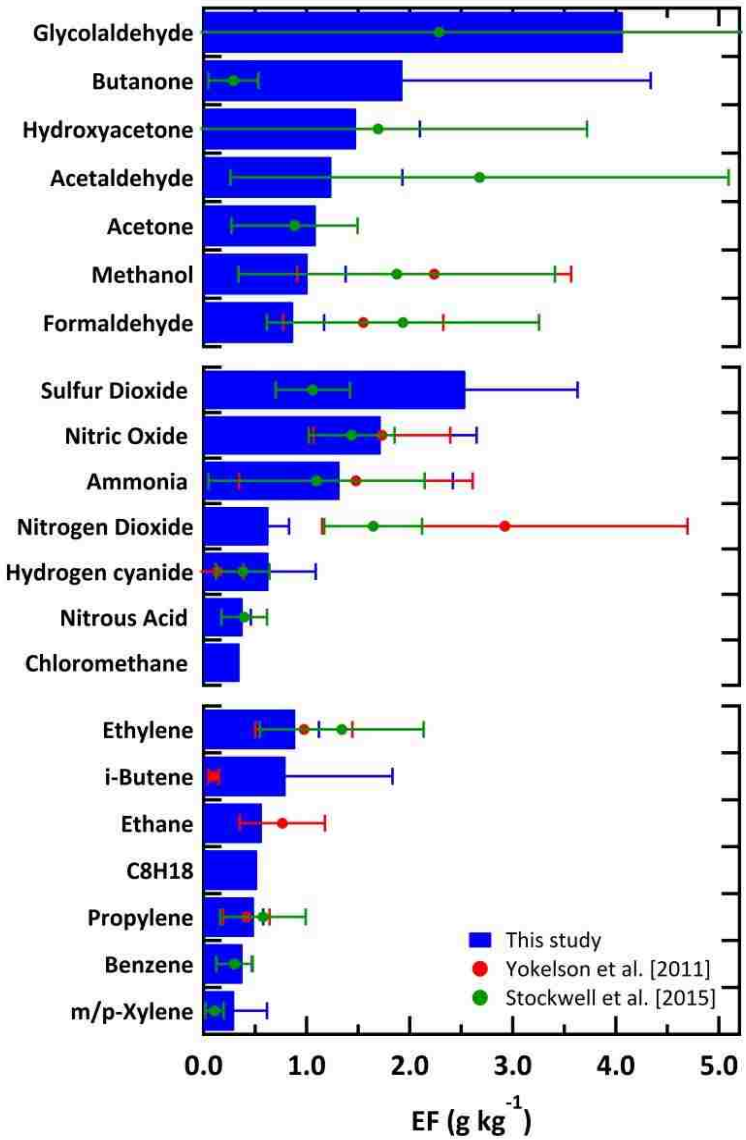

Figure 6.4. The emission factors (g/kg) and ± one standard deviation for the most abundant OVOCs, NMHCs, and S-/N- containing compounds emitted from crop residue burns. The crop residue fires from other studies (Yokelson et al., 2011; Stockwell et al., 2015) are shown in red and green.

Table 6.10. Emission factors (g/kg) and one standard deviation for crop residue (CR) fires

Compound (Formula)	**EF CR Fire 1**-mixed (rice, wheat, mustard, lentil, grass)	**EF CR Fire 2**-rice residue	**EF CR Fire 3**-wheat residue	**EF CR Fire 4**-mustard residue	**EF CR Fire 5**-grass	**EF** Wheat stubble burn	**EF** leafy greens used as insect repellent	**EF (g/kg) CR Avg (stdev)**
Method	FTIR+WAS	FTIR	FTIR	FTIR	FTIR	FTIR+WAS	FTIR+WAS	-
Date Measured	24-Apr	24-Apr	24-Apr	24-Apr	24-Apr	24-Apr	24-Apr	-
C-content (%)	0.43	0.42	0.42	0.42	0.46	0.42	0.50	-
MCE	0.957	0.968	0.949	0.920	0.961	0.956	0.817	0.952(0.017)
Carbon Dioxide (CO_2)	1480	1474	1445	1395	1601	1427	1280.567	1470(71)
Carbon Monoxide (CO)	42.4	31.4	49.4	77.0	41.7	41.9	183	47.3(15.6)
Methane (CH_4)	1.76	1.21	1.94	2.95	1.99	1.60	16.8	1.91(0.58)
Acetylene (C_2H_2)	0.225	0.187	0.124	0.302	0.287	0.239	2.02	0.227(0.066)
Ethylene (C_2H_4)	0.809	0.741	0.428	1.00	0.676	0.865	6.89	0.753(0.195)
Propylene (C_3H_6)	0.377	0.319	0.387	0.512	0.312	0.362	3.50	0.378(0.072)
Formaldehyde (HCHO)	0.650	0.947	0.472	0.957	0.813	1.34	4.66	0.863(0.297)
Methanol (CH_3OH)	0.436	0.699	0.529	1.13	1.05	1.06	13.30	0.819(0.303)
Formic Acid (HCOOH)	0.101	0.170	0.109	0.114	0.224	0.295	1.37	0.169(0.078)
Acetic Acid (CH_3COOH)	0.553	0.831	0.364	0.804	2.03	3.06	24.41	1.27(1.05)
Glycolaldehyde ($C_2H_4O_2$)	0.103	0.772	2.66	bdl	0.520	0.902	6.02	0.991(0.981)
Furan (C_4H_4O)	0.219	6.88E-02	0.117	9.53E-02	9.84E-02	0.140	0.878	0.123(0.053)
Hydroxyacetone ($C_3H_6O_2$)	0.700	1.74	0.581	1.87	1.41	1.21	19.87	1.25(0.53)
Phenol (C_6H_5OH)	0.528	9.54E-02	0.288	0.297	0.202	0.316	1.80	0.288(0.144)
1,3-Butadiene (C_4H_6)	0.147	0.157	0.209	0.326	0.141	0.157	1.27	0.189(0.071)
Isoprene (C_5H_8)	6.77E-02	3.85E-02	1.21E-02	1.98E-02	1.14E-02	bdl	0.41	2.99E-2(2.38E-2)
Ammonia (NH_3)	0.356	0.157	0.683	1.46	0.278	0.472	2.20	0.567(0.472)
Hydrogen Cyanide (HCN)	0.141	0.189	0.123	0.732	0.328	0.628	3.40	0.357(0.262)
Nitrous Acid (HONO)	0.439	0.281	0.290	0.440	0.432	0.496	0.99	0.396(0.089)
Sulfur Dioxide (SO_2)	bdl	2.83	1.50	4.19	2.17	bdl	bdl	2.67(1.15)
Hydrogen Fluoride (HF)	bdl	bdl	bdl	bdl	bdl	bdl	bdl	bdl
Hydrogen chloride (HCl)	bdl	bdl	bdl	bdl	bdl	2.65E-02	bdl	2.65E-2(bdl)
Nitric Oxide (NO)	1.49	0.52	2.99	1.70	2.94	1.25	3.22E+00	1.81(0.97)
Nitrogen Dioxide (NO_2)	0.716	0.462	0.471	0.507	0.874	0.944	0.687	0.662(0.213)
Carbonyl sulfide (OCS)	1.69E-02	nm	nm	nm	nm	5.06E-02	0.20	3.38E-2(2.38E-2)
DMS (C_2H_6S)	5.19E-04	nm	nm	nm	nm	7.85E-03	1.05E-02	4.18E-3(5.18E-3)
Chloromethane (CH_3Cl)	0.221	nm	nm	nm	nm	-	1.70E+00	0.221(-)
Bromomethane (CH_3Br)	2.05E-04	nm	nm	nm	nm	-	1.92E-03	2.05E-4(-)
Methyl iodide (CH_3I)	2.77E-05	nm	nm	nm	nm	-	-	2.77E-5(-)
1,2-Dichloroethene ($C_2H_2Cl_2$)	1.01E-04	nm	nm	nm	nm	-	5.14E-04	1.01E-4(-)
Methyl nitrate (CH_3NO_3)	1.63E-02	nm	nm	nm	nm	0.189	1.11E-01	0.103(0.122)
Ethane (C_2H_6)	0.358	nm	nm	nm	nm	-	-	0.358(-)
Propane (C_3H_8)	0.118	nm	nm	nm	nm	-	8.38E-01	0.118(-)

i-Butane (C_4H_{10})	8.46E-03	nm	nm	nm	nm	4.89E-02	5.63E-02	2.87E-2(2.86E-2)
n-Butane (C_4H_{10})	3.10E-02	nm	nm	nm	nm	-	1.90E-01	3.10E-2(0.00E0)
1-Butene (C_4H_8)	7.82E-02	nm	nm	nm	nm	8.50E-02	4.45E-01	8.16E-2(4.86E-3)
i-Butene (C_4H_8)	4.41E-02	nm	nm	nm	nm	1.048	3.61E-01	0.546(0.710)
trans-2-Butene (C_4H_8)	3.16E-02	nm	nm	nm	nm	9.45E-02	0.153	6.30E-2(4.45E-2)
cis-2-Butene (C_4H_8)	2.23E-02	nm	nm	nm	nm	0.116	1.14E-01	6.90E-2(6.61E-2)
i-Pentane (C_5H_{12})	5.57E-03	nm	nm	nm	nm	8.35E-02	-	4.45E-2(5.51E-2)
n-Pentane (C_5H_{12})	1.44E-02	nm	nm	nm	nm	9.57E-02	4.87E-02	5.50E-2(5.75E-2)
1-Pentene (C_5H_{10})	2.44E-02	nm	nm	nm	nm	8.41E-02	1.20E-01	5.43E-2(4.22E-2)
trans-2-Pentene (C_5H_{10})	1.81E-02	nm	nm	nm	nm	0.164	6.35E-02	9.10E-2(1.03E-1)
cis-2-Pentene (C_5H_{10})	8.78E-03	nm	nm	nm	nm	7.23E-02	0.028	4.06E-2(4.49E-2)
3-Methyl-1-butene (C_5H_{10})	1.09E-02	nm	nm	nm	nm	4.43E-02	6.52E-02	2.76E-2(2.36E-2)
1,2-Propadiene (C_3H_4)	7.67E-03	nm	nm	nm	nm	bdl	3.57E-02	7.67E-3(-)
Propyne (C_3H_4)	2.29E-02	nm	nm	nm	nm	bdl	9.98E-02	2.29E-2(-)
1-Butyne (C_4H_6)	3.49E-03	nm	nm	nm	nm	bdl	9.91E-03	3.49E-3(-)
2-Butyne (C_4H_6)	2.22E-03	nm	nm	nm	nm	bdl	1.90E-02	2.22E-3(-)
n-Hexane (C_6H_{14})	9.66E-03	nm	nm	nm	nm	-	9.14E-03	9.66E-3(-)
n-Heptane (C_7H_{16})	4.69E-03	nm	nm	nm	nm	1.08E-01	5.80E-03	5.61E-2(7.28E-2)
n-Octane (C_8H_{18})	bdl	nm	nm	nm	nm	8.18E-02	bdl	8.18E-2(-)
n-Nonane (C_9H_{20})	bdl	nm	nm	nm	nm	bdl	bdl	bdl(bdl)
n-Decane ($C_{10}H_{22)}$	3.40E-03	nm	nm	nm	nm	0.165	2.47E-02	8.41E-2(1.14E-1)
2,3-Dimethylbutane (C_6H_{14})	2.41E-04	nm	nm	nm	nm	-	-	2.41E-4(-)
2-Methylpentane (C_6H_{14})	1.39E-03	nm	nm	nm	nm	-	-	1.39E-3(-)
3-Methylpentane (C_6H_{14})	bdl	nm	nm	nm	nm	-	-	-(-)
2,2,4-Trimethylpentane (C_8H_{18})	bdl	nm	nm	nm	nm	0.298	4.29E-02	0.298(-)
Cyclopentane (C_5H_{10})	8.96E-04	nm	nm	nm	nm	4.43E-03	-	2.66E-3(2.50E-3)
Cyclohexane (C_6H_{12})	bdl	nm	nm	nm	nm	-	6.08E-03	-(-)
Methylcyclohexane (C_7H_{14})	bdl	nm	nm	nm	nm	3.31E-02	bdl	3.31E-2(-)
Benzene (C_6H_6)	0.304	nm	nm	nm	nm	0.215	6.93E-01	0.259(0.062)
Toluene (C_7H_8)	0.173	nm	nm	nm	nm	0.134	0.846	0.154(0.028)
Ethylbenzene (C_8H_{10})	4.08E-02	nm	nm	nm	nm	4.47E-02	0.188	4.27E-2(2.77E-3)
m/p-Xylene (C_8H_{10})	4.87E-02	nm	nm	nm	nm	0.358	4.09E-01	0.203(0.218)
o-Xylene (C_8H_{10})	2.92E-02	nm	nm	nm	nm	8.94E-02	0.113	5.93E-2(4.26E-2)
Styrene (C_8H_8)	1.25E-02	nm	nm	nm	nm	bdl	3.31E-02	1.25E-2(-)
i-Propylbenzene (C_9H_{12})	1.41E-03	nm	nm	nm	nm	bdl	bdl	1.41E-3(-)
n-Propylbenzene (C_9H_{12})	4.04E-03	nm	nm	nm	nm	bdl	1.85E-02	4.04E-3(-)
3-Ethyltoluene (C_9H_{12})	5.32E-03	nm	nm	nm	nm	0.124	3.13E-02	6.46E-2(8.39E-2)
4-Ethyltoluene (C_9H_{12})	3.48E-03	nm	nm	nm	nm	7.08E-02	0.017	3.72E-2(4.76E-2)
2-Ethyltoluene (C_9H_{12})	3.35E-03	nm	nm	nm	nm	7.59E-02	1.45E-02	3.96E-2(5.13E-2)
1,3,5-Trimethylbenzene (C_9H_{12})	2.55E-03	nm	nm	nm	nm	8.50E-02	1.24E-02	4.38E-2(5.83E-2)
1,2,4-Trimethylbenzene (C_9H_{12})	4.15E-03	nm	nm	nm	nm	0.340	3.76E-02	0.172(0.237)
1,2,3-Trimethylbenzene (C_9H_{12})	2.87E-03	nm	nm	nm	nm	0.291	0.020	0.147(0.203)
alpha-Pinene ($C_{10}H_{16}$)	1.36E-03	nm	nm	nm	nm	bdl	0.049	1.36E-3(-)
beta-Pinene ($C_{10}H_{16}$)	bdl	nm	nm	nm	nm	bdl	bdl	bdl
Ethanol (C_2H_6O)	2.09E-02	nm	nm	nm	nm	interference[c]	1.00	2.09E-2(-)

Acetaldehyde (C_2H_4O)	0.514	nm	nm	nm	nm	1.18	3.85	0.848(0.472)
Acetone (C_3H_6O)	0.688	nm	nm	nm	nm	interference[c]	7.90	0.688(-)
Butanal (C_4H_8O)	1.52E-02	nm	nm	nm	nm	0.334	0.131	0.174(0.225)
Butanone (C_4H_8O)	0.154	nm	nm	nm	nm	2.49	0.838	1.32(1.65)
BC	0.794	0.330	0.636	1.66	0.737	nm	nm	0.831(0.497)
BrC	8.87	20.4	3.71	14.1	7.56	nm	nm	10.9(6.5)
EF Babs 405 (m^2/kg)	16.8	23.3	10.1	30.8	14.9	nm	nm	19.2(8.0)
EF Bscat 405 (m2/kg)	88.5	238	22.5	142	90.9	nm	nm	116(80)
EF Babs 870 (m2/kg)	3.76	1.56	3.02	7.87	3.49	nm	nm	3.94(2.36)
EF Bscat 870 (m2/kg)	19.2	79.9	4.14	42.3	19.8	nm	nm	33.1(29.5)
EF Babs 405 just BrC (m2/kg)	8.69	20.0	3.64	13.8	7.41	nm	nm	10.7(6.3)
EF Babs 405 just BC (m2/kg)	8.08	3.36	6.48	16.9	7.50	nm	nm	8.47(5.06)
SSA 870	0.836	0.981	0.579	0.843	0.850	nm	nm	0.818(0.146)
SSA 405	0.841	0.911	0.690	0.822	0.859	nm	nm	0.825(0.082)
AAE	1.96	3.53	1.58	1.78	1.90	nm	nm	2.15(0.79)

Note: "bdl" indicates below the detection limit; "-" indicates concentrations were not greater than background; "nm" indicates not measured

[a]NAMaSTE EF values are adjusted to lower MCE (0.925); The EF of smoldering NMOCs adjusted based on their ratio to CH_4 and the flaming compounds adjusted based on their ratio to CO_2; Particle-phase values remain unadjusted

[b] HCl values were based on the first few retrievals

[c] Solvents were being used nearby and interfered with ethanol and acetone signals

Table 6.11. Summary of emission factors (g/kg) and one standard deviation for crop residue burns from this study and others.

Compound (Formula)	**EF Crop Residue** Yokelson et al. [2011] avg (stdev)[a]	**EF Crop Residue (food fuels)** Stockwell et al. [2015] avg (stdev)	**EF Crop Residue** NAMaSTE avg (stdev)[b,c]
MCE	0.925	0.925	0.925
Carbon Dioxide (CO_2)	1398(55)	1353(80)	1401(68)
Carbon Monoxide (CO)	71.9(28.4)	68.7(25.2)	72.3(23.9)
Methane (CH_4)	4.21(3.53)	3.49(2.19)	2.79(0.85)
Acetylene (C_2H_2)	0.193(0.059)	0.331(0.277)	0.216(0.063)
Ethylene (C_2H_4)	0.974(0.470)	1.34(0.80)	0.890(0.230)
Propylene (C_3H_6)	0.417(0.224)	0.576(0.415)	0.492(0.094)
Formaldehyde (HCHO)	1.55(0.78)	1.93(1.32)	0.865(0.298)
Methanol (CH_3OH)	2.24(1.33)	1.87(1.53)	1.01(0.37)
Formic Acid (HCOOH)	0.840(0.571)	0.633(0.846)	0.119(0.055)
Acetic Acid (CH_3COOH)	3.80(2.35)	3.88(3.64)	0.871(0.719)
Glycolaldehyde ($C_2H_4O_2$)	-	2.29(3.04)	4.07(4.03)
Furan (C_4H_4O)	-	0.355(0.445)	0.116(0.049)
Hydroxyacetone ($C_3H_6O_2$)	-	1.69(2.03)	1.48(0.62)
Phenol (C_6H_5OH)	-	0.494(0.480)	0.341(0.170)
1,3-Butadiene (C_4H_6)	0.127(0.060)	3.63E-3(4.51E-3)	0.180(0.068)
Isoprene (C_5H_8)	-	0.220(0.170)	1.97E-2(1.57E-2)
Ammonia (NH_3)	1.48(1.13)	1.10(1.05)	1.32(1.10)
Hydrogen Cyanide (HCN)	0.134(0.252)	0.381(0.259)	0.630(0.463)
Nitrous Acid (HONO)	-	0.395(0.221)	0.377(0.084)
Sulfur Dioxide (SO_2)	-	1.06(0.36)	2.54(1.09)
Hydrogen Fluoride (HF)	-	-	bdl
Hydrogen chloride (HCl)	-	0.472(0.320)	2.65E-2(-)
Nitric Oxide (NO)	1.73(0.66)	1.44(0.42)	1.72(0.93)
Nitrogen Dioxide (NO_2)	2.92(1.77)	1.65(0.47)	0.630(0.203)
Ethane (C2H6)	0.764(0.414)	-	0.566(-)
Propane (C3H8)	0.237(0.126)	-	0.186(-)
1-Butene (C_4H_8)	0.113(0.050)	0.134(0.100)	0.119(0.007)
Benzene (C6H6)	-	0.301(0.177)	0.379(0.091)
Toluene (C7H8)	-	0.296(0.228)	0.224(0.041)
Ethylbenzene (C8H10)	-	-	6.24E-2(4.05E-3)
m/p-Xylene (C_8H_{10})	-	0.107(0.088)	0.297(0.319)
PM	5.26(1.98)	-	-
EF Black Carbon (BC)	-	-	0.831(0.497)
EF Brown Carbon (BrC)	-	-	10.9(6.5)
EF B_{abs} 405 (m^2/kg)	-	-	19.2(8.0)
EF B_{scat} 405 (m^2/kg)	-	-	116(80)
EF B_{abs} 870 (m^2/kg)	-	-	3.94(2.36)
EF B_{scat} 870 (m^2/kg)	-	-	33.1(29.5)
EF B_{abs} 405 just BrC (m^2/kg)	-	-	10.7(6.3)
EF B_{abs} 405 just BC (m^2/kg)	-	-	8.47(5.06)
SSA 405 nm	-	-	0.818(0.146)
SSA 870 nm	-	-	0.825(0.082)
AAE	-	-	2.15(0.79)

[a]*Yokelson* et al. (2011) data are adjusted to a lower carbon fraction (0.42)
[b]NAMaSTE gas-phase EF values are adjusted to MCE 0.925
[c]Additional gas-phase compounds are inTable 6.10

Figure 6.4 shows the top OVOCs, NMHCs, and S- or N-containing compounds emitted and shows good agreement with literature values for overlap species. As noted in Stockwell et al. (2014), glycolaldehyde (the simplest "sugar-like" molecule) is a major emission from crop residue fires and Figure 6.4 shows that glycolaldehyde is the dominant NMOC by mass from the NAMaSTE crop residue fires. When we compare to other fuel-types, the EFs of glycolaldehyde from our study, smoldering Indonesian rice straw (Christian et al., 2003), and an assortment of US crop residue fuels (Stockwell et al., 2014; Sect. 4.3.5) are significantly higher than from other BB sources (Burling et al., 2011; Johnson et al., 2013; Akagi et al., 2013). Glycolaldehyde was below the detection limit for one NAMaSTE crop-type (mustard residue), suggesting emissions variability by fuel-type and/or fuel-properties. Our average glycolaldehyde EF (4.07 g/kg ± 4.03) is similar to typical EFs for total PM from BB and glycolaldehyde has also been shown to be an efficient aqueous phase SOA precursor (Ortiz-Montalvo et al., 2012). Other oxygenated species emitted in large amounts by the crop residues burned in NAMaSTE include butanone (methyl ethyl ketone) (1.93 ± 2.41 g/kg) and hydroxyacetone (1.48 ± 0.62 g/kg). The Nepal data are higher or similar to previous data for many OVOC, but noticeably lower for methanol, formaldehyde, and organic acids. As expected the emissions of OVOCs were greater than NMHCs, though there are also large emissions of C_2 NMHCs and BTEX compounds.

Figure 6.4 shows several major S- and N-containing compounds including significant SO_2 emissions (2.54 g/kg). While the SO_2 emissions are large compared to most BB types, the emissions from other S-containing compounds (OCS, DMS) are limited. SO_2 is an important precursor of sulfate aerosols and was also a significant emission from grasses and crop residue in Stockwell et al. (2014). This update is important to include in emissions inventories as many global and regional estimates rely on the much smaller value (0.4 g/kg) reported by Andreae and

Merlet (2001) (Streets et al., 2003). Yokelson et al. (2011) noted high emissions of NO_x from crop residue fires sampled near the beginning of the Mexican dry season when plant N content may be higher. Our Nepal NO_x (~2.5 g/kg) emissions for this fire type were measured in April, 6 months after the dry season started in October and may reflect lower fuel N content. The higher NO_x emissions (4.65 g/kg) in Mexico may have also reflected higher wind speed as an important mechanism, but one that requires airborne sampling to probe.

Unlike US crop residue fires (Stockwell et al., 2014), HCl remained below the detection limit in nearly every crop residue burn. As a landlocked country these crops are not as influenced by chlorine-rich maritime air. Additionally, in comparison to US crops, most rural agriculture in Nepal may be less augmented by chemical pesticides. There are, however, detectable emissions of CH_3Cl, which have not been measured previously in the field for crop residue burning. This new information for CH_3Cl should be considered when assessing global emissions of reactive chlorine (Lobert et al., 1999).

The absorption and scattering coefficients at 405 and 870 nm were measured for 5 of the 6 crop residue fires. The fire-average SSA at 870 nm and AAE for these crop residue fires span a wide range. SSA (870) ranges from 0.579-0.981 (average 0.82 for both 870 and 405 nm) and AAE ranges from ~1.58-3.53 (average near 2). The AAE as a function of SSA colored by MCE is shown in Figure 6.5 for all the real-time 1 s data collected during crop residue fires. The AAE increases sharply at high SSA, while the MCE distinctly decreases at increasing SSA. These observations support previous interpretations that BrC is produced primarily by smoldering combustion at lower MCEs for most BB fuel-types (Liu et al., 2014; McMeeking et al., 2014). Similar trends were observed for all other fuel-types except for the zig-zag brick kiln, which will be discussed in the next section. The BC and OC literature average for crop residue fires reported

by Akagi et al. (2011) were based on only two fires. Our average EF BC (0.831 ± 0.497 g/kg) from 5 crop residue fires is similar to the literature value (0.75 g/kg), while we report the EF for BrC for the first time (10.9 ± 6.5 g/kg), which is considerably larger than the global average OC reported in Akagi et al., (2011), but in good agreement with the NAMaSTE, simultaneously-measured filter organic mass (~10 g/kg) (Jayarathne et al., 2016). More importantly from an absorption standpoint, we report EFs for B_{abs} and B_{scat} at both wavelengths for this fuel-type in column 4 of Table 6.11.

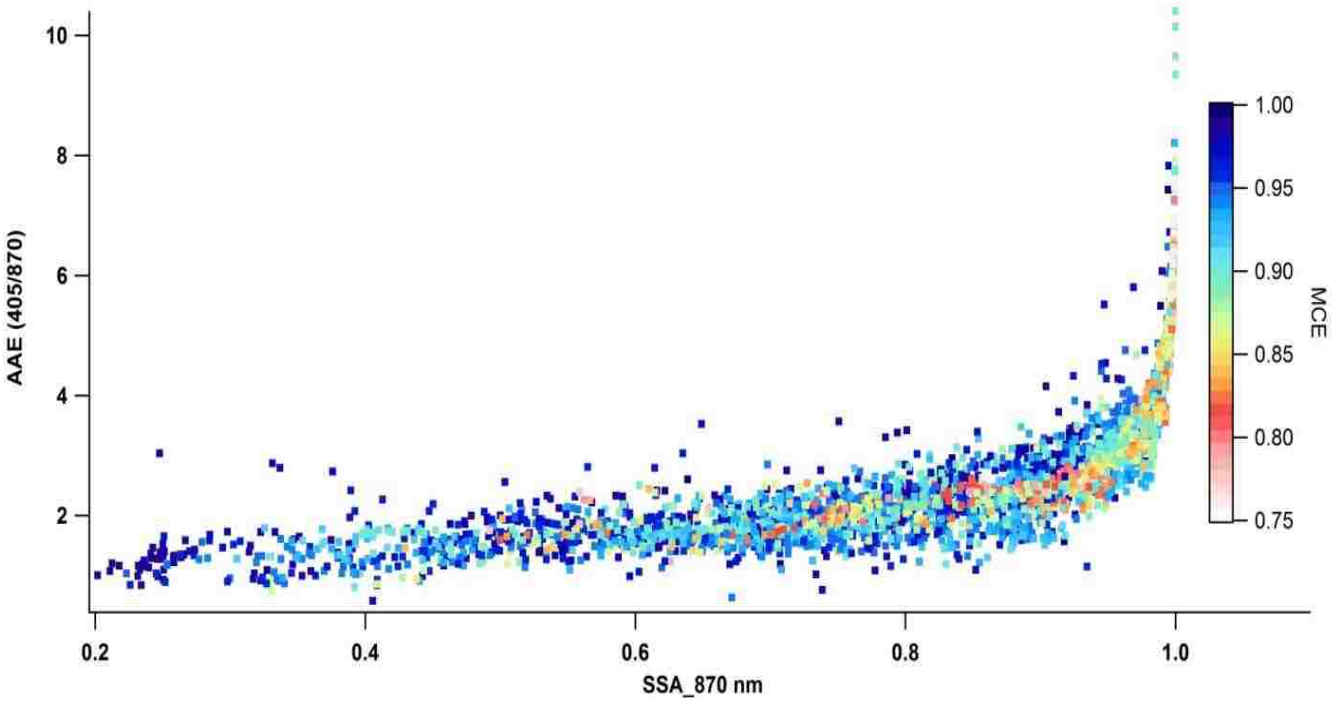

Figure 6.5. The AAE calculated at 405 and 870 nm versus SSA at 870 nm for all crop residue burn samples measured every second during emissions collection. Each data point is colored by MCE. The AAE increases sharply at high SSA, while the MCE distinctly decreases at increasing SSA. BC emissions are associated mostly with high MCE flaming and BrC emissions are associated mostly with low MCE smoldering. Most source-types demonstrated a similar trend.

6.5.8 Brick kiln emissions

Very little is known about the chemical composition of brick kiln emissions. There are very few studies and most of what is reported focuses on a few key pollutants including CO, PM, and BC

(Weyant et al., 2014). A previous study measured a larger suite of emissions from authentic brick kilns in Mexico (Christian et al., 2010), however, the fuel burned in those kilns was primarily biomass and the NMOC emissions were somewhat comparable to those from biomass burns. Coal is the main fuel used in brick kilns globally and to our knowledge NAMaSTE produced the first quantitative emissions data for numerous atmospherically-significant species from authentic coal-fired brick kilns in a region heavily influenced by this source. The individual EFs for both brick kilns sampled in this study are reported in Table 6.12. There are large differences between the two kilns types that stand out in Table 6.12 despite our lack of opportunity to measure inherent kiln variability. We will first discuss the kiln emissions individually and then follow with a detailed kiln comparison.

Table 6.12. Emission factors (g/kg) for a single clamp kiln, zig-zag kiln, and stoke holes on the zig-zag kiln.

Compound (Formula)	EF clamp kiln	EF zig - zag kiln	EF coal stoke holes at zig-zag kiln
Method	FTIR+WAS	FTIR+WAS	FTIR
MCE	0.950	0.994	0.861
Carbon Dioxide (CO_2)	2102	2620	2234
Carbon Monoxide (CO)	70.9	10.1	230
Methane (CH_4)	19.5	8.73E-02	4.59
Acetylene (C_2H_2)	5.58E-02	1.65E-02	1.87E-02
Ethylene (C_2H_4)	1.27	4.32E-02	0.445
Propylene (C_3H_6)	1.49	6.58E-02	0.808
Formaldehyde (HCHO)	8.21E-02	bdl	bdl
Methanol (CH_3OH)	1.77	0.112	0.437
Formic Acid (HCOOH)	0.241	5.84E-02	0.180
Acetic Acid (CH_3COOH)	0.430	0.471	11.3
Glycolaldehyde ($C_2H_4O_2$)	bdl	bdl	bdl
Furan (C_4H_4O)	0.383	bdl	bdl
Hydroxyacetone ($C_3H_6O_2$)	1.81	bdl	1.61
Phenol (C_6H_5OH)	0.429	1.54E-02	bdl
1,3-Butadiene (C_4H_6)	0.103	1.51E-02	bdl
Isoprene (C_5H_8)	8.66E-02	2.46E-02	1.47
Ammonia (NH_3)	0.317	bdl	bdl
Hydrogen Cyanide (HCN)	1.39	0.446	2.28
Nitrous Acid (HONO)	0.320	4.45E-02	1.33
Sulfur Dioxide (SO_2)	13.0	12.7	28.5
Hydrogen Fluoride (HF)	bdl	0.629	0.888
Hydrogen chloride (HCl)	bdl	1.24	1.86
Nitric Oxide (NO)	bdl	1.28	10.4
Nitrogen Dioxide (NO_2)	0.297	8.21E-02	1.36
Carbonyl sulfide (OCS)	-	3.42E-03	nm
DMS (C_2H_6S)	-	3.68E-05	nm
Chloromethane (CH_3Cl)	-	2.22E-02	nm
Bromomethane (CH_3Br)	2.62E-03	2.59E-03	nm
Methyl iodide (CH_3I)	bdl	2.01E-03	nm
1,2-Dichloroethene ($C_2H_2Cl_2$)	-	4.45E-05	nm
Methyl nitrate (CH_3NO_3)	2.36E-05	2.92E-03	nm
Ethane (C_2H_6)	5.37	2.06E-03	nm
Propane (C_3H_8)	3.00	1.97E-03	nm
i-Butane (C_4H_{10})	0.342	1.60E-03	nm
n-Butane (C_4H_{10})	1.16	1.92E-03	nm
1-Butene (C_4H_8)	0.347	1.68E-03	nm
i-Butene (C_4H_8)	0.428	1.47E-03	nm
trans-2-Butene (C_4H_8)	0.346	1.44E-03	nm
cis-2-Butene (C_4H_8)	0.214	9.65E-04	nm
i-Pentane (C_5H_{12})	0.349	3.70E-02	nm
n-Pentane (C_5H_{12})	0.811	3.26E-02	nm
1-Pentene (C_5H_{10})	0.233	1.60E-03	nm
trans-2-Pentene (C_5H_{10})	0.249	2.64E-03	nm
cis-2-Pentene (C_5H_{10})	0.093	9.01E-04	nm
3-Methyl-1-butene (C_5H_{10})	5.72E-02	3.32E-04	nm
1,2-Propadiene (C_3H_4)	4.97E-04	2.15E-05	nm
Propyne (C_3H_4)	1.80E-03	bdl	nm
1-Butyne (C_4H_6)	bdl	bdl	nm
2-Butyne (C_4H_6)	bdl	bdl	nm
n-Hexane (C_6H_{14})	0.670	2.16E-02	nm
n-Heptane (C_7H_{16})	0.617	3.04E-03	nm
n-Octane (C_8H_{18})	0.549	1.58E-03	nm

n-Nonane (C_9H_{20})	0.434	2.42E-03	nm
n-Decane ($C_{10}H_{22}$)	0.428	2.02E-03	nm
2,3-Dimethylbutane (C_6H_{14})	0.127	3.59E-03	nm
2-Methylpentane (C_6H_{14})	0.398	4.84E-03	nm
3-Methylpentane (C_6H_{14})	0.312	1.17E-02	nm
2,2,4-Trimethylpentane (C_8H_{18})	bdl	8.02E-04	nm
Cyclopentane (C_5H_{10})	0.134	8.53E-04	nm
Cyclohexane (C_6H_{12})	5.55E-02	2.98E-03	nm
Methylcyclohexane (C_7H_{14})	5.84E-02	bdl	nm
Benzene (C_6H_6)	1.68	8.25E-03	nm
Toluene (C_7H_8)	1.05	2.80E-02	nm
Ethylbenzene (C_8H_{10})	0.279	1.35E-02	nm
m/p-Xylene (C_8H_{10})	1.06	5.74E-02	nm
o-Xylene (C_8H_{10})	0.377	2.18E-02	nm
Styrene (C_8H_8)	2.62E-03	4.56E-03	nm
i-Propylbenzene (C_9H_{12})	2.84E-02	4.07E-04	nm
n-Propylbenzene (C_9H_{12})	3.82E-02	1.82E-03	nm
3-Ethyltoluene (C_9H_{12})	0.091	6.93E-03	nm
4-Ethyltoluene (C_9H_{12})	3.55E-02	3.69E-03	nm
2-Ethyltoluene (C_9H_{12})	2.76E-02	2.30E-03	nm
1,3,5-Trimethylbenzene (C_9H_{12})	5.88E-02	4.30E-03	nm
1,2,4-Trimethylbenzene (C_9H_{12})	8.46E-02	5.59E-03	nm
1,2,3-Trimethylbenzene (C_9H_{12})	2.76E-02	2.03E-03	nm
alpha-Pinene ($C_{10}H_{16}$)	bdl	1.49E-03	nm
beta-Pinene ($C_{10}H_{16}$)	bdl	1.31E-03	nm
Ethanol (C_2H_6O)	-	4.84E-03	nm
Acetaldehyde (C_2H_4O)	4.13E-02	6.94E-02	nm
Acetone (C_3H_6O)	-	1.46E-01	nm
Butanal (C_4H_8O)	bdl	2.19E-03	nm
Butanone (C_4H_8O)	-	2.29E-03	nm
EF Black Carbon (BC)	1.72E-2(7.50E-3)	0.112(0.063)	nm
EF Brown Carbon (BrC)	1.74(0.34)	0.913(0.278)	nm
EF B_{abs} 405 (m^2/kg)	1.86(0.24)	2.03(0.70)	nm
EF B_{scat} 405 (m^2/kg)	32.8(2.1)	21.2(12.8)	nm
EF B_{abs} 870 (m^2/kg)	8.16E-2(3.56E-2)	0.530(0.300)	nm
EF B_{scat} 870 (m^2/kg)	0.670(0.129)	1.75(0.25)	nm
EF B_{abs} 405 just BrC (m^2/kg)	1.70(0.33)	0.895(0.273)	nm
EF B_{abs} 405 just BC (m^2/kg)	0.155(0.102)	1.14(0.64)	nm
SSA 405 nm	0.946(0.007)	0.881(0.098)	nm
SSA 870 nm	0.895(0.029)	0.779(0.103)	nm
AAE	4.19(0.73)	1.92(0.50)	nm

Note: "bdl" indicates below the detection limit; "-" indicates concentrations were not greater than background; "nm" indicates not measured; C-fractions: zigzag kiln (0.722), clamp kiln (0.644) (see Sect. 2.4)

6.5.8.1 Zig-zag emissions

The zig-zag kiln emissions had a very high average MCE (0.994) and the EFs for most smoldering compounds (e.g. most NMOC) were much reduced. Not surprisingly, the EFs for flaming compounds including HCl, HF, NO_x, and SO_2 were high. High emissions of NO_x and S-containing gases are important as ozone and aerosol precursors and because they can enhance deposition and O_3 impacts on nearby crops and negatively impact crop yield. The latter issue is

especially relevant since brick kilns are commonly seasonal and located on land leased from farmers, where the depletion of the soil to collect clay for bricks is already another agricultural productivity issue.

The zig-zag kiln was the only source in our NAMaSTE study that emitted detectable quantities of HF. It has been suspected that brick kilns are an important source of atmospheric fluorides since fluorine is typically present in raw brick materials (USEPA, 1997). We found HF was a major emission from the zig-zag brick kiln with an average EF of 0.629 g/kg and a peak concentration of ~13 ppm. HF is a phytotoxic air pollutant and agricultural areas with visible foliar damage in Pakistan were suspected to be impacted by HF emissions from nearby brick kilns (Ahmad et al., 2012). While HF is rapidly transformed to particulate fluoride, much previous work confirms adverse effects of HF or particulate fluoride from various sources on crops (Haidouti, 1993; Ahmad et al., 2012). Since many brick kilns are present in agricultural regions, this first confirmation of high HF emissions is an important finding and should also be included in assessments of kiln impacts on agriculture. HF emissions from brick kilns likely vary considerably depending on the F-content of the clay (and possibly the coal) being fired (as discussed further below). HF is also very reactive, but perhaps particle fluoride could serve as a regional indicator for brick kilns with more work.

Because of the large number of FTIR grab samples over the sampling day, which lasted approximately 5 hours, we can construct a rough time series of the kiln emissions with resolution averaging about 12 minutes. To emphasize chemistry, normalize for fuel consumption rates, and account for somewhat arbitrary grab sample dilution, in Figure 6.6 we plot selected ERs to CO_2. The ERs of HCl and HF to CO_2 rise first and track together over time. The ERs of NO and SO_2 rise next and their observed peak is about 2 hours after the halogens. This is consistent with the

halogens being driven from clay at 500-600 ºC (USEPA, 1997). The halogen peaks are then followed by a peak in the NO_x and SO_2 emissions likely from the coal fuel.

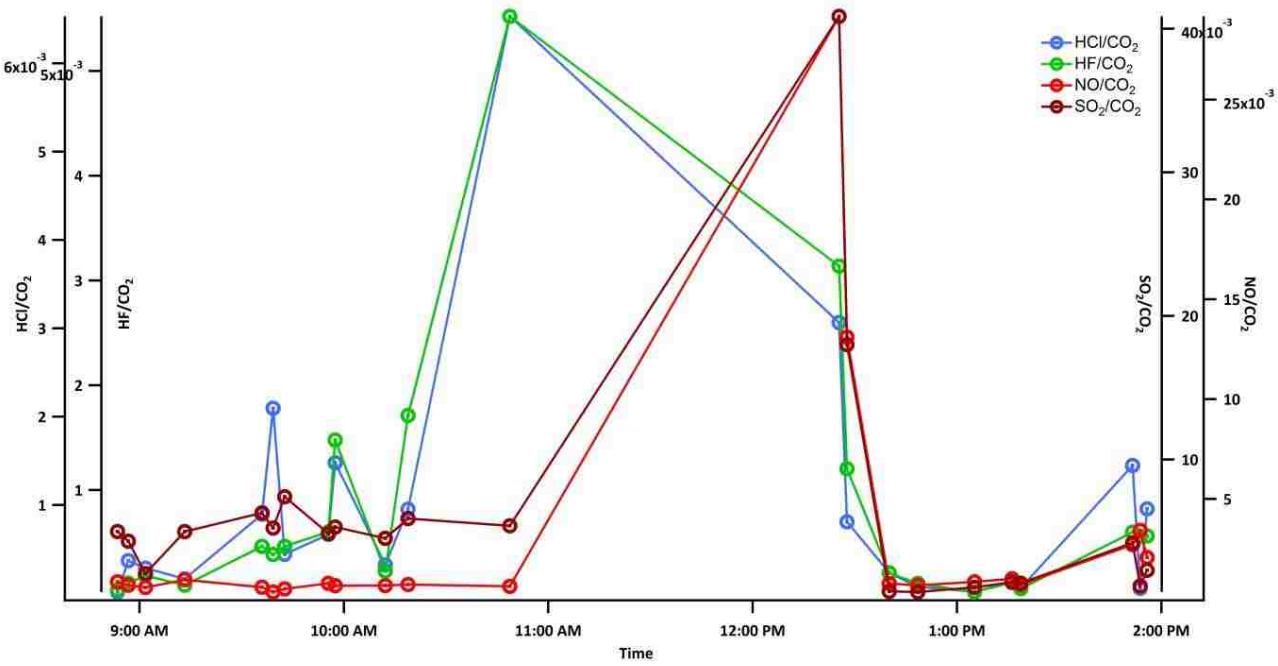

Figure 6.6. Emission ratios (to CO_2) for HF, HCl, SO_2, and NO over time for the zig-zag kiln.

As noted in Sect. 2.1.7, in hopes of obtaining representative emissions from this particular brick kiln, we sampled the smoke coming out of the top of the chimney stack, but we also sampled the lesser amount of emissions escaping the coal-feeder stoke holes located on the "roof" of the kiln. Table 6.12 also includes the EFs specific to the emissions from the stoke holes. The MCE is significantly reduced (0.861), consequently the EFs of smoldering compounds are much higher with e.g. high EF CO (230 g/kg). Oddly, the stoke hole smoke also had higher EFs for HF, HCl, NO_x, and SO_2; compounds normally emitted during flaming combustion. This is probably because the stoke holes are much closer to the combustion zone and many internally generated species are scavenged in the kiln and stack walls before being emitted from the stack. Some kilns have internal water reservoirs below the stack to scavenge the smoke as rudimentary emissions

control. However, these stoke hole emissions do not need to be weighted much if at all in an assessment of overall emissions as the vents are normally closed.

Table 6.12 includes the EFs for BC and BrC, and the EFs for scattering and absorption at 405 and 870 nm calculated from all the real-time PAX (and co-located CO_2) data above background for separate plumes throughout the sampling day, that we then averaged together. The SSA at 870 nm (0.779 ± 0.103) indicates that BC contributes to the absorption in the fresh emissions while the AAE (1.92 ± 0.50) implies that the emissions are not pure BC. The PAX data suggest that a little under half the absorption at 405 nm is due to BrC. Weyant et al. (2014) reported a range of EFs for EC for South Asian brick kilns (0.01-3.7 g/kg) and our EF BC (0.112 g/kg) falls within the range they report. We note that for all the other sources sampled in NAMaSTE and in the BB literature, high values of SSA and AAE are mostly associated with a low MCE (smoldering) and low SSA/AAE is associated with high MCE (flaming). This is illustrated for crop residues in Figure 6.5. For the zig-zag kiln this pattern is less pronounced. In the zig-zag kiln, the highest MCE values are not clustered at the lowest SSA/AAE (Figure 6.7). Nearly all the real time data from the zig-zag kilns was at high MCE (>0.95), but accompanied by some evidence for BrC emissions. Given the plethora of possible UV-absorbing compounds in OA, characterizing the variety of primary and secondary "BrC types" with different absorption intensities, abundances, and lifetimes is an important area for future research (Saleh et al., 2014).

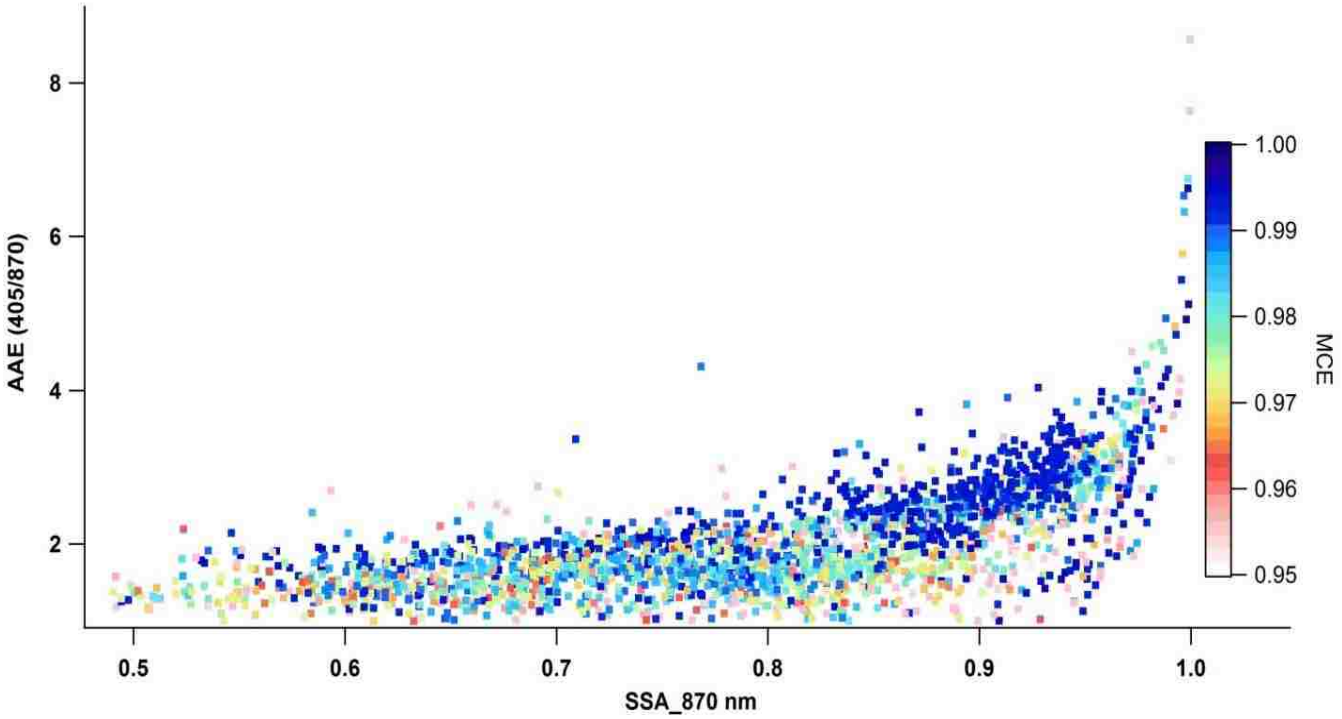

Figure 6.7. The AAE calculated at 405 and 870 nm versus SSA at 870 nm for the zig-zag kiln measured every second during emissions collection. Each data point is colored by MCE. This deviates from the typical trend in that the highest MCEs are not clustered at the lowest SSA/AAEs. Some BrC is emitted at a variety of "higher" MCEs.

6.5.8.2 Clamp kiln emissions

The clamp kiln emissions had a lower average MCE (0.950) than the zig-zag kiln (though still reflecting primarily efficient combustion), which is not surprising since we estimate the fuel had a larger component of biomass. Consequently the EFs for most products of incomplete combustion are ~5-3000 times higher than those from the zig-zag kiln and also higher than values reported for a clamp kiln in Mexico that burned mostly sawdust at an average MCE of 0.968 (Christian et al., 2010). Even though the MCE was lower, the clamp kiln EF SO_2 (13.0 g/kg) was almost the same as the zig-zag kiln. This is most likely rationalized at least in part by the higher sulfate emission factors for the zig-zag kiln (Jayarathne et al., 2016). For all grab samples of the clamp kiln, the NO remained below the detection limit while NO_2 only had

detectable quantities for three grab samples near the end of the day. HCl and HF probably remained below the detection limit because of lower halogen content in the clay (vide infra and Table 6.3).

If we convert and sum the NO_2, NO, and HONO emissions to "NO_x as NO" this quantity is more than 3.5 times higher from the zig-zag kiln. The coal from both kilns had similar N content so the difference in NO_x emissions is most likely traced to the higher MCE in the zig-zag kiln. However, we cannot completely rule out a different contribution of "thermal NO_x" between the kilns. Co-firing coal with biomass is a common practice in power plants as it has been shown to decrease combustion zone temperature and thermally-dependent NO_x formation, thereby reducing several criteria pollutants including NO_x (USEPA, 2007; Al-Naiema et al., 2015). Thus, the lower NO_x EFs from the clamp kiln could be partly due to co-firing with more biomass.

The differences in NMOC emissions for the two kiln types were dramatic. We simply list some common pollutants/precursors of concern and include the approximate EF_{CK}/EF_{ZZ} ratio in parentheses after each: CO (7), CH_4 (223), ethane (2604), ethylene (30), benzene (203), methanol (16), phenol (28). In addition, many species were emitted at high levels from the clamp kiln but were below the detection limit from the zig-zag kiln including: formaldehyde, furan, hydroxyacetone, and ammonia. The main emissions overall from the clamp kiln in order of mass were: CO_2, CO, CH_4, SO_2, ethane, propane, hydroxyacetone, BrC, methanol, and benzene. Methane is an important short-lived climate pollutant and the CH_4 EF for the clamp kiln (19.5 g/kg) is among the highest seen for any combustion source. The other alkanes were also extremely enhanced all the way through *n*-decane which had an EF of 0.428 g/kg. These enormous EFs for alkanes are not typical for BB and might reflect burning coal inefficiently. Another possible explanation is that used motor oil is reportedly sometimes disposed of as fuel in

brick kilns or added to the fuel to impart color to bricks (USEPA, 1997; Christian et al., 2010). The enhancement observed for the alkanes throughout the C_1-C_{10} size range that we could measure suggests that even larger alkanes are also enhanced. Large alkanes have recently attracted attention as important SOA precursors (Presto et al., 2010). In our clamp kiln data the sum of the EFs for NMOCs we measured that are known to have high yields for SOA (BTEX plus phenol) is ~5 g/kg, which is already much larger than the initial EF OA as crudely approximated from the EF BrC (~2.0 ± 0.4 g/kg).

The EF BC (0.02 g/kg) for the clamp kiln was much lower than for the zig-zag kiln and the co-collected filter data are consistent with this result. Weyant et al. (2014) also noted similar "low" EFs for EC for several brick kilns measured in that study. The EF BrC was greater for the clamp kiln than the zig-zag kiln, which is consistent with the filter OC and an expected result given a more significant biomass contribution to overall fuel. The AAE and SSA were slightly greater for the clamp kiln than the zig-zag kiln (Table 6.12).

We had only one sample of the coal from each kiln and the elemental analysis is shown in Table 6.3. The likely higher fuel variability for the non-C trace substances limits us to a few general comments. The measured emissions of the sulfur species from both kilns (including stoke holes) accounted for about 60-111% of the nominal S in the coal, which is a good match given experimental uncertainty. The measured emissions of N-containing species from both kilns were significantly lower than the nominal coal N. Much of the missing N was likely emitted as N_2, especially at high MCE (Kuhlbusch et al., 1991; Burling et al., 2010). Finally, the zig-zag kiln emissions had significantly higher halogen content than the 0.3 g/kg upper limit for the zig-zag coal. This is consistent with our speculation above that much of the halogen emissions come from the clay and that this is a source of kiln to kiln variability.

This is by no means an exhaustive evaluation of South Asian brick kiln emissions. However, because there are so few studies detailing the chemical composition of brick kiln emissions, this is a valuable addition to the current body of measurements. In terms of comparative pollution between the two technologies, there are some trade-offs. The clamp kiln we sampled produced far more of BrC and a large suite of NMOC pollutants and precursors typically associated with inefficient combustion of biomass (e.g. HCHO and benzene) or (likely) inefficient combustion of motor oil or coal (e.g. alkanes). The zig-zag kiln we sampled produced significantly more BC, NO_x, HCl, and HF; where the latter two could be larger because of the clay and not the kiln design. For SO_2 the kilns were not significantly different. Ultimately, since the zig-zag kiln is thought to produce significantly more bricks per unit fuel use than the clamp kiln (e.g. Weyant et al., 2014), this ratio should be further investigated for scaling emissions (on a per brick basis). The zig-zag kiln is very likely preferred from the standpoint of pollutants emitted per brick produced, which is a major factor in selecting mitigation strategies. More measurement and modeling studies will clearly be needed to fully assess the impact of brick kiln emissions and subsequent atmospheric chemistry in the region.

6.6 Conclusions

We investigated the trace gas and aerosol emissions from a large suite of major undersampled sources around Kathmandu and the Indo-Gangetic plain of southern Nepal. Our source characterization included motorcycles, kilns, wood and dung cooking-fires, crop-residue burning, diesel and gasoline generators, agricultural pumps, and open garbage burning. We report the emission factors (grams of compound emitted per kilogram of dry fuel burned) for ~80 important trace gases measured by FTIR and WAS, including important NMHCs up to C_{10} and many oxygenated organic compounds. We also measured aerosol mass and optical properties

using two PAX systems at 405 and 870 nm. We report important aerosol optical properties that include emission factors (in m^2/kg) for scattering and absorption at 405 and 870 nm, single scattering albedo, and absorption Ångström exponent. From the direct measurements of absorption we estimated black and brown carbon emission factors (in g/kg).

Although we were not able to sample the transport sector extensively due to the Gorkha earthquake, we were able to measure several motorbikes pre- and post-service. The minor maintenance led to minimal if any reduction of gaseous pollutants consistent with the idea that more major servicing is needed to reduce gas-phase pollutants. Motorcycles were in general among the least efficient sources sampled and the CO EF was on the order of ~700 g/kg, about ten times that of a typical biomass fire. For most fossil fuel sources, including generators and agricultural pumps, diesel burned more efficiently than gasoline, but produced more NO_x, HCHO, and aerosol.

Numerous trace gas emissions (many for the first time in the field) were quantified for open cooking fires and several improved cooking stoves with several fuel variations. Authentic open dung cooking-fires emitted high levels of BrC (5.54 ± 1.66 g/kg), NH_3 (3.00 ± 1.33 g/kg), organic acids (7.66 ± 6.90 g/kg), and HCN (2.01 ± 1.25 g/kg), where the latter could contribute to space-based observations of high levels of HCN in the lower stratosphere above the Asian Monsoon. HCN and some alkynes > C_2 (previously linked to BB) were also observed from several non-BB sources. BTEX compounds were major emissions of both dung (~4.5 g/kg) and wood (~1.5 g/kg) cooking-fires and a simple method to estimate indoor exposure to the many important air toxics we measured in the emissions is described. Our PAX data suggest relatively more absorption by BrC as opposed to BC from cooking fires than may be currently recognized;

especially for dung burning. Biogas, as expected, emerged as the most efficient and least polluting cooking technology out of approximately a dozen types subjected to limited testing.

The first global garbage burning inventory relied on measurements from very few studies and information for many compounds is often limited to laboratory simulations (Wiedinmyer et al., 2014). Our authentic Nepali garbage burning data shift the global average observed for this source to lower MCE and significantly more BC and BTEX emissions than in previous measurements while supporting previous measurements of high HCl. Crop residue burning produced EFs in good agreement with literature values with relatively high emissions of oxygenated organic compounds (~12 g/kg) and SO_2 (2.54 ± 1.09 g/kg). We observed an EF for BrC of ~11 g/kg or about 4 times higher than the previous organic carbon literature average, which was based on less data. Our EF BrC is qualitative, but in agreement with our absorption data and SSA in showing that BrC absorption is important for this major global BB type.

There are very few studies detailing the chemical emissions from brick kilns. While we were only able to sample two brick kilns in this study, we present a significant expansion in chemical speciation data. The two brick kilns sampled had different designs and utilized different clay, coal, and amounts of biomass for co-firing with the main coal fuel. Consequently the two kilns produced very different emissions. A zig-zag kiln burning primarily coal at high efficiency produced larger amounts of BC, NO_x, HF, and HCl, (the halogen compounds most likely from the clay) while the clamp kiln (with relatively more biomass fuel) produced dramatically more organic gases, organic aerosol (BrC), and aerosol precursors including large alkanes. Both kilns were significant SO_2 sources with their emission factors averaging ~13 g/kg.

Overall, we report the first, or rare, optically- and chemically-detailed emissions data for many undersampled BB sources and other undersampled sources in developing countries. Companion papers will report results from other co-deployed techniques such as filter sampling and mini-AMS, a source apportionment for a fixed supersite, and model interpretation as guidance for mitigation strategies. Future measurements and modeling are also needed to better understand the evolution of the emissions we report here.

References

Abel, S. J., Haywood, J. M., Highwood, E. J., Li, J., and Buseck, P. R.: Evolution of biomass burning aerosol properties from an agricultural fire in southern Africa, Geophys. Res. Lett., 30 (15), 1783, doi: 10.1029/2003GL017342, 2003.

Adhikary, B., Carmichael, G. R., Tang, Y., Leung, L. R., Qian, Y., Schauer, J. J., Stone, E. A., Ramanathan, V., and Ramana, M. V.: Characterization of the seasonal cycle of south Asian aerosols: A regional-scale modeling analysis, J. Geophys. Res., 112, D22S22, doi:10.1029/2006JD008143, 2007.

Adhikary, B., Carmichael, G. R., Kulkarni, S., Wei, C., Tang, Y., D'Allura, A., Mena-Carrasco, M., Streets, D. G., Zhang, Q., Pierce, R. B., Al-Saadi, J. A., Emmons, L. K., Pfister, G. G., Avery, M. A., Barrick, J. D., Blake, D. R., Brune, W. H., Cohen, R. C., Dibb, J. E., Fried, A., Heikes, B. G., Huey, L. G., O'Sullivan, D. W., Sachse, G. W., Shetter, R. E., Singh, H. B., Campos, T. L., Cantrell, C. A., Flocke, F. M., Dunlea, E. J., Jimenez, J. L., Weinheimer, A. J., Crounse, J. D., Wennberg, P. O., Schauer, J. J., Stone, E. A., Jaffe, D. A., and Reidmiller, D. R.: A regional scale modeling analysis of aerosol and trace gas distributions over the eastern Pacific during the INTEX-B field campaign, Atmos. Chem. Phys., 10, 2091-2115, doi:10.5194/acp-10-2091-2010, 2010.

Ahmad, M. N., van den Berg, L. J. L., Shah, H. U., Masood, T., Büker, P., Emberson, L., and Ashmore, M.: Hydrogen fluoride damage to vegetation from peri-urban brick kilns in Asia: A growing but unrecognised problem?, Environ. Pollut., 162, 319-324, doi:10.1016/j.envpol.2011.11.017, 2012.

Akagi, S. K., Yokelson, R. J., Wiedinmyer, C., Alvarado, M. J., Reid, J. S., Karl, T., Crounse, J. D., and Wennberg, P. O.: Emission factors for open and domestic biomass burning for use in atmospheric models, Atmos. Chem. Phys., 11, 4039–4072, doi:10.5194/acp-11-4039-2011, 2011.

Akagi, S. K., Craven, J. S., Taylor, J.W., McMeeking, G. R., Yokelson, R. J., Burling, I. R., Urbanski, S. P., Wold, C. E., Seinfeld, J. H., Coe, H., Alvarado, M. J., and Weise, D. R.: Evolution of trace gases and particles emitted by a chaparral fire in California, Atmos. Chem. Phys., 12, 1397–1421, doi:10.5194/acp-12-1397- 2012, 2012.

Akagi, S. K., Yokelson, R. J., Burling, I. R., Meinardi, S., Simpson, I., Blake, D. R., McMeeking, G. R., Sullivan, A., Lee, T., Kreidenweis, S., Urbanski, S., Reardon, J., Griffith, D. W. T., Johnson, T. J., Weise, D. R.: Measurements of reactive trace gases and variable O_3 formation rates in some South Carolina biomass burning plumes, Atmos. Chem. Phys., 13, 1141-1165, doi:10.5194/acp-13-1141-2013, 2013.

Akagi, S. K., Burling, I. R., Mendoza, A., Johnson, T. J., Cameron, M., Griffith, D. W. T., Paton-Walsh, C., Weise, D. R., Reardon, J., Yokelson, R. J.: Field measurements of trace gases emitted by prescribed fires in southeastern US pine forests using an open-path FTIR system, Atmos. Chem. Phys., 14, 199-215, doi:10.5194/acp-14-199-2014, 2014.

Allen, R. J., Sherwood, S. C., Norris, J. R., and Zender, C. S.: Recent Northern Hemisphere tropical expansion primarily driven by black carbon and tropospheric ozone, Nature, 485, 350-354, doi:10.1038/nature11097, 2012.

Al-Naiema, I., Estillore, A. D., Mudunkotuwa, I. A., Grassian, V. H., and Stone, E. A.: Impacts of co-firing biomass on emissions of particulate matter to the atmosphere, Fuel, 162, 111-120, doi:10.1016/j.fuel.2015.08.054, 2015.

Alvarado, M. J. and Prinn, R. G.: Formation of ozone and growth of aerosols in young smoke plumes from biomass burning: 1. Lagrangian parcel studies, J. Geophys. Res., 114, D09306, doi:10.1029/2008JD011144, 2009.

Alvarado, M. J., Wang, C., and Prinn, R. G.: Formation of ozone and growth of aerosols in young smoke plumes from biomass burning: 2.Three-dimensional Eulerian studies, J. Geophys. Res., 114, D09307, doi:10.1029/2008JD011186, 2009.

Alvarado, M. J., Logan, J. A., Mao, J., Apel, E., Riemer, D., Blake, D., Cohen, R. C., Min, K.-E., Perring, A. E., Browne, E. C., Wooldridge, P. J., Diskin, G. S., Sachse, G. W., Fuelberg, H., Sessions,W. R., Harrigan, D. L., Huey, G., Liao, J., Case-Hanks, A., Jimenez, J. L., Cubison, M. J., Vay, S. A., Weinheimer, A. J., Knapp, D. J., Montzka, D. D., Flocke, F. M., Pollack, I. B., Wennberg, P. O., Kurten, A., Crounse, J., St. Clair, J. M., Wisthaler, A., Mikoviny, T., Yantosca, R. M., Carouge, C. C., and Le Sager, P.: Nitrogen oxides and PAN in plumes from boreal fires during ARCTAS-B and their impact on ozone: an integrated analysis of aircraft and satellite observations, Atmos. Chem. Phys., 10, 9739–9760, doi:10.5194/acp-10-9739-2010, 2010.

Alvarado, M. J., Yokelson, R. J., Akagi, S. A., Burling, I. R., Fischer, E., McMeeking, G. R., Travis, K., Craven, J. S., Seinfeld, J. H., Taylor, J. W., Coe, H., Urbanski, S. P., Wold, C. E., and Weise, D. R.: Lagrangian photochemical modeling of ozone formation and aerosol evolution in biomass burning plumes: toward a sub-grid scale parameterization, 12th Annual CMAS Conference, Chapel Hill, NC, 28-30 October, 2013.

Alvarado, M. J., Lonsdale, C. R., Yokelson, R. J., Akagi, S. K., Coe, H., Craven, J. S., Fischer, E. V., McMeeking, G. R., Seinfeld, J. H., Soni, T., Taylor, J. W., Weise, D. R., and Wold, C. E.: Investigating the links between ozone and organic aerosol chemistry in a biomass burning plume from a prescribed fire in California chaparral, Atmos. Chem. Phys., 15, 6667-6688, doi:10.5194/acp-15-6667-2015, 2015.

Andreae, M. O. and Gelencsér, A.: Black carbon or brown carbon? The nature of light-absorbing carbonaceous aerosols, Atmos. Chem. Phys., 6, 3131-3148, doi:10.5194/acp-6-3131-2006, 2006.

Andreae, M. O. and Merlet, P.: Emission of trace gases and aerosols from biomass burning, Global Biogeochem. Cy., 15(4), 955–966, doi:10.1029/2000GB001382, 2001.

Andreae, M. O. and Ramanathan, V.: Climate's dark forcings, Science, 340, 280-281, doi:10.1126/science.1235731, 2013.

Andreae, M. O., Artaxo, P., Fischer, H., Freitas, S. R., Grégoire, J. –M., Hansel, A., Hoor, P., Kormann, R., Krejci, R., Lange, L., Lelieveld, J., Lindinger, W., Longo, K., Peters, W., de Reus, M., Scheeren, B., Silvia Dias, M. A. F.,

Ström, J., van Velthoven, P. F. J., and Williams, J.: Transport of biomass burning smoke to the upper troposphere by deep convection in the equatorial region, Geophys. Res. Lett., 28, 951-954, doi: 10.1029/2000GL012391, 2001.

Arnott, W. P., Moosmüller, H., and Walker, J. W.: Nitrogen dioxide and kerosene-flame soot calibration of photoacoustic instruments for measurement of light absorption by aerosols, Rev. Sci. Instrum. 71, 4545–4552, 2000.

Arnott, W. P., Walker, J. W., Moosmüller, H., Elleman, R. A., Jonsson, H. H., Buzorius, G., Conant, W. C., Flagan, R. C., and Seinfeld, R. H.: Photoacoustic insight for aerosol light absorption aloft from meteorological aircraft and comparison with particle soot absorption photometer measurements: DOE Southern Great Plains climate research facility and the coastal stratocumulus imposed perturbation experiments, J. Geophys. Res., 111(D5), 1–16, doi:10.1029/2005JD005964, 2006.

Arola, A., Schuster, G., Myhre, G., Kazadzis, S., Dey, S., and Tripathi, S. N.: Inferring absorbing organic carbon content from AERONET data, Atmos. Chem. Phys., 11, 215–225, doi:10.5194/acp-11-215-2011, 2011.

Atkinson, R., Aschmann, S. M., and Arey, J.: Reactions of OH and NO_3 radicals with phenol, cresols, and 2-nitrophenol at 296 ± 2K, Environ. Sci. Technol., 26, 1397-1403, doi: 10.1021/es00031a018, 1992.

Aurell, J., Gullet, B. K., and Yamamoto, D.: Emissions from open burning of simulated military waste from forward operating bases, Environ. Sci. Technol., 46, 11004-11012, DOI: 10.1021/es303131k, 2012.

Azeez, A. M., Meier, D., and Odermatt, J.: Temperature dependence of fast pyrolysis volatile products from European and African biomasses, J. Anal. Appl. Pyrolysis, 90, 81-92, doi:10.1016/j.jaap.2010.11.005, 2011.

Ballhorn, U., Siegert, F., Mason, M., and Limin, S.: Derivation of burn scar depths and estimation of carbon emissions with LIDAR in Indonesian peatlands, PNAS, 106(50), 21213–21218, 2009.

Barker, R., and Molle, F.: Evolution of Irrigation in South and Southeast Asia, Comprehensive Assessment of Water Management in Agriculture Research Report No. 5, International Water management Institute, Colombo, Sri Lanka, 2004.

Barnes, I., Solignac, G., Mellouki, A., and Becker, K. H.: Aspects of the atmospheric chemistry of amides, ChemPhysChem., 11, 3844-3857, doi: 10.1002/cphc.201000374, 2010.

Bateman, A. P., Nizkorodov, S. A., Laskin, J., and Laskin, A.: High-resolution electrospray ionization mass spectrometry analysis of water-soluble organic aerosols collected with a particle into liquid sampler, Anal. Chem., 82, 8010-8016, doi:10.1021/ac1014386, 2010.

Beaton, S. P., Bishop, G. A., and Stedman, D. H.: Emissions characteristics of Mexico City vehicles, J. Air Waste Manag. Assoc., 42, 1424-1429, doi: 10.1080/10473289.1992.10467088, 1992.

Becker, S., Halsall, C. J., Tych, W., Kallenborn, R., Schlabach, M., and Manø, S.: Changing sources and environmental factors reduce the rates of decline of organochlorine pesticides in the Arctic atmosphere, Atmos. Chem. Phys., 12, 4033-4044, doi:10.5194/acp-12-4033-2012, 2012.

Berndt, T., Böge, O., and Rolle, W.: Products of the gas-phase reactions of NO_3 radicals with furan and tetramethylfuran, Environ. Sci. Technol., 31, 1157-1162, 1997.

Bertschi, I. T., Yokelson, R. J., Ward, D. E., Christian, T. J., and Hao, W. M.: Trace gas emissions from the production and use of domestic biofuels in Zambia measured by open-path Fourier transform infrared spectroscopy, J. Geophys. Res., 108(D13), 8469, doi:10.1029/2002JD002158 , 2003a.

Bertschi, I. T., Yokelson, R. J., Ward, D. E., Babbitt, R. E., Susott, R. A., Goode, J. G., and Hao, W. M.: Trace gas and particle emissions from fires in large diameter and belowground biomass fuels, J. Geophys. Res., 108(D13), 8472, doi:10.1029/2002JD002100, 2003b.

Bierbach, A., Barnes, I., Becker, K. H., and Wiesen, E.: Atmospheric chemistry of unsaturated carbonyls: butenedial, 4-oxo-2-pentenal, 3-hexene-2,5-dione, maleic anhydride, 3H-furan-2-one, and 5-methyl-3H-furan-2-one, Environ. Sci. Technol., 28, 715-729, doi: 10.1021/es00053a028, 1994.

Bierbach, A., Barnes, I., and Becker, K. H.: Product and kinetic study of the OH-initiated gas-phase oxidation of furan, 2-methylfuran, and furanaldehydes at 300K, Atmos. Environ., 29, 2651-2660, doi: 10.1016/1352-2310(95)00096-H, 1995.

Biswell, H.: Prescribed Burning in California Wildlands Vegetation Management, University of California Press, Berkeley, CA, USA, 255 pp., 1999.

Bocchini, P., Galletti, G. C., Camarero, S., and Martinez, A. T.: Absolute quantitation of lignin pyrolysis products using an internal standard, J. Chromatogr. A, 773, 227-232, doi: 10.1016/S0021-9673(97)00114-3, 1997.

Bond, T. C., Streets, D. G., Yarber, K. F., Nelson, S. M., Woo, J.-H., and Klimont, Z.: A technology-based global inventory of black and organic carbon emissions from combustion, J. Geophys. Res., 109, D14203, doi:10.1029/2003JD003697, 2004.

Bond, T. C., and Bergstrom, R.: Light absorption by carbonaceous particles: An investigative review, Aerosol Sci. Technol., 40, 27–67, doi:10.1080/02786820500421521, 2006.

Bond, T. C., Doherty, S. J., Fahey, D.W., Forster, P. M., Berntsen, T., DeAngelo, B. J., Flanner, M. G.,Ghan, S., Kärcher, B., Koch, D., Kinne, S., Kondo, Y., Quinn, P. K., Sarofim, M. C., Schultz, M. G., Schulz, M., Venkataraman, C., Zhang, H., Zhang, S., Bellouin, N., Guttikunda, S. K., Hopke, P. K., Jacobson, M. Z., Kaiser, J. W. , Klimont, Z., Lohmann, U., Schwarz, J. P., Shindell, D., Storelvmo, T., Warren, S. G., and

Zender, C. S.: Bounding the role of black carbon in the climate system: A scientific assessment, J. Geophys. Res., 118, 5380-5552, doi:10.1002/jgrd.50171, 2013.

Bryden, M., Still, D., Scott, P., Hoffa, G., Ogle, D., Bailis, R., and Goyer, K.: Design Principles for Wood Burning Cookstoves, U.S. Environmental Protection Agency, Office of Air and Radiation, Washington DC, 2005.

Burling, I. R., Yokelson, R. J., Griffith, D. W. T., Johnson, T. J., Veres, P., Roberts, J. M., Warneke, C., Urbanski, S. P., Reardon, J., Weise, D. R., Hao, W. M., and de Gouw, J.: Laboratory measurements of trace gas emissions from biomass burning of fuel types from the southeastern and southwestern United States, Atmos. Chem. Phys., 10, 11115–11130, doi:10.5194/acp-10-11115-2010, 2010.

Burling, I. R., Yokelson, R. J., Akagi, S. K., Urbanski, S. P., Wold, C. E., Griffith, D. W. T., Johnson, T. J., Reardon, J., and Weise, D. R.: Airborne and ground-based measurements of the trace gases and particles emitted by prescribed fires in the United States, Atmos. Chem. Phys., 11, 12197–12216, doi:10.5194/acp-11-12197-2011, 2011.

Cabañas, B., Villanueva, F., Martin, P., Baeza, M. T., Salgado, S., and Jiménez, E.: Study of reaction processes of furan and some furan derivatives initiated by Cl atoms, Atmos. Environ., 39, 1935-1944, doi: 10.1016/j.atmosenv.2004.12.013, 2005.

Capes, G., Murphy, J. G., Reeves, C. E., McQuaid, J. B., Hamilton, J. F., Hopkins, J. R., Crosier, J., Williams, P. I., and Coe, H.: Secondary organic aerosol from biogenic VOCs over West Africa during AMMA, Atmos. Chem. Phys., 9, 3841-3850, doi:10.5194/acp-9-3841-2009, 2009.

Chacon-Madrid, H. J. and Donahue, N. M.: Fragmentation vs. functionalization: chemical aging and organic aerosol formation, Atmos. Chem. Phys., 11, 10553-10563, doi:10.5194/acp-11-10553-2011, 2011.

Chan, M. N., Kautzman, K. E., Chhabra, P. S., Surratt, J. D., Chan, M. N., Crounse, J. D., Kurten, A., Wennberg, P. O., Flagan, R. C., and Seinfeld, J. H.: Secondary organic aerosol formation from photooxidation of naphthalene and alkylnapthalenes: implications for oxidation of intermediate volatility organic compounds (IVOCs), Atmos. Chem. Phys., 9, 3049-3060, doi:10.5194/acp-9-3049-2009, 2009.

Chang, D. and Song, Y.: Estimates of biomass burning emissions in tropical Asia based on satellite-derived data, Atmos. Chem. Phys., 10, 2335-2351, doi:10.5194/acp-10-2335-2010, 2010.

Chen, Y., and Bond, T. C.: Light absorption by organic carbon from wood combustion, Atmos. Chem. Phys., 10, 1773–1787, doi:10.5194/acp-10-1773-2010, 2010.

Chen, P., Kang, S., Li, C., Rupakheti, M., Yan, F., Li, Q., Ji, Z., Zhang, Q., Luo, W., and Sillanpää, M.: Characteristics and sources of polycyclic aromatic hydrocarbons in atmospheric aerosols in the Kathmandu Valley, Nepal, Sci. Total Environ., 538, 86-92, doi:10.1016/j.scitotenv.2015.08.006, 2015.

Chhabra, P. S., Flagan, R. C., and Seinfeld, J. H.: Elemental analysis of chamber organic aerosol using an aerodyne high-resolution aerosol mass spectrometer, Atmos. Chem. Phys., 10, 4111–4131, doi:10.5194/acp-10-4111-2010, 2010.

Chhabra, P. S., Ng, N. L., Canagaratna, M. R., Corrigan, A. L., Russell, L. M., Worsnop, D. R., Flagan, R. C., and Seinfeld, J. H.: Elemental composition and oxidation of chamber organic aerosol, Atmos. Chem. Phys., 11, 8827-8845, doi:10.5194/acp-11-8827-2011, 2011.

Chiang, H., Tsai, J., Yao, Y., and Ho, W.: Deterioration of gasoline vehicle emissions and effectiveness of tune-up for high-polluted vehicles, Transpn. Res. –D, 13, 47-53, doi:10.1016/j.trd.2007.07.004, 2008.

Christian, T., Kleiss, B., Yokelson, R. J., Holzinger, R., Crutzen, P. J., Hao, W. M., Saharjo, B. H., and Ward, D. E.: Comprehensive laboratory measurements of biomass-burning emissions: 1. Emissions from Indonesian, African, and other fuels, J. Geophys. Res., 108, 4719, doi:10.1029/2003JD003704, 2003.

Christian, T. J., Kleiss, B., Yokelson, R. J., Holzinger, R., Crutzen, P. J., Hao, W. M., Shirai, T., and Blake, D. R.: Comprehensive laboratory measurements of biomass-burning emissions: 2. First intercomparison of open path FTIR, PTR-MS, GC-MS/FID/ECD, J. Geophys. Res., 109, D02311, doi:10.1029/2003JD003874, 2004.

Christian, T. J., Yokelson, R. J., Carvalho Jr., J. A., Griffith, D. W. T., Alvarado, E. C., Santos, J. C., Neto, T. G. S., Veras, C. A. G., and Hao, W. M.: The tropical forest and fire emissions experiment: Trace gases emitted by smoldering logs and dung on deforestation and pasture fires in Brazil, J. Geophys. Res., 112, D18308, doi:10.1029/2006JD008147, 2007.

Christian, T. J., Yokelson, R. J., Cárdenas, B., Molina, L. T., Engling, G., and Hsu, S.-C.: Trace gas and particle emissions from domestic and industrial biofuel use and garbage burning in central Mexico, Atmos. Chem. Phys., 10, 565–584, doi:10.5194/acp-10-565-2010, 2010.

Chung, C. E., Lee, K., and Müller, D.: Effect of internal mixture on black carbon radiative forcing, Tellus B, 64, 1–13, doi:10.3402/tellusb.v64i0.10925, 2012.

Clairotte, M., Adam, T. W., Chirico, R., Giechaskiel, B., Manfredi, U., Elsasser, M., Sklorz, M., DeCarlo, P. F., Heringa, M. F., Zimmermann, R., Martini, G., Krasenbrink, A., Vicet, A., Tournié, E., Prevot, A. S. H. and Astorga, C.: Online characterization of regulated and unregulated gaseous and particulate exhaust emissions from two-stroke mopeds: A chemometric approach, 717, 28–38, doi: 10.1016/j.aca.2011.12.029, 2012.

Clarke, A. D., Noone, K. J., Heintzenberg, J., Warren, S. G., and. Covert, D. S: Aerosol light absorption measurement techniques: Analysis and intercomparisons, Atmos. Environ., 21, 1455-1465, doi:10.1016/0004-6981(67)90093-5, 1987.

Coeur-Tourneur, C., Cassez, A., and Wenger, J. C.: Rate coefficients for the gas-phase reaction of hydroxyl radicals with 2-methoxyphenol (guaiacol) and related compounds, J. Phys. Chem., 114, 11645-11650, doi: 10.1021/jp1071023, 2010.

Collins, W. J., Fry, M. M., Yu, H., Fuglestvedt, J. S., Shindell, D. T., and West, J. J.: Global and regional temperature-change potentials for near-term climate forcers, Atmos. Chem. Phys., 13, 2471-2485, doi:10.5194/acp-13-2471-2013, 2013.

Costner, P.: Estimating Releases and Prioritizing Sources in the Context of the Stockholm Convention: Dioxin Emission Factors for Forest Fires, Grassland and Moor Fires, Open Burning of Agricultural Residues, Open Burning of Domestic Waste, Landfill and Dump Fires, The International POPs Elimination Project, Mexico, 40, 2005.

Crounse, J. D., DeCarlo, P. F., Blake, D. R., Emmons, L. K., Campos, T. L., Apel, E. C., Clarke, A. D., Weinheimer, A. J., McCabe, D. C., Yokelson, R. J., Jimenez, J. L., and Wennberg, P. O.: Biomass burning and urban air pollution over the Central Mexican Plateau, Atmos. Chem. Phys., 9, 4929–4944, doi:10.5194/acp-9-4929-2009, 2009.

Crutzen, P. J. and Andreae, M. O.: Biomass burning in the tropics: Impact on atmospheric chemistry and biogeochemical cycles, Science, 250, 1669–1678, doi:10.1126/science.250.4988.1669, 1990.

Cubison, M. J., Ortega, A. M., Hayes, P. L., Farmer, D. K., Day, D., Lechner, M. J., Brune, W. H., Apel, E., Diskin, G. S., Fisher, J. A., Fuelberg, H. E., Hecobian, A., Knapp, D. J., Mikoviny, T., Riemer, D., Sachse, G. W., Sessions, W., Weber, R. J., Weinheimer, A. J., Wisthaler, A., and Jimenez, J. L.: Effects of aging on organic aerosol from open biomass burning smoke in aircraft and laboratory studies, Atmos. Chem. Phys., 11, 12049-12064, doi:10.5194/acp-11-12049-2011, 2011.

Davidson, C. I., Lin, S., Osborn, J. F., Pandey, M. R., Rasmussen, R. A. and Khalil, M. A. K.: Indoor and outdoor air pollution in the Himalayas, Environ. Sci. Technol., 20, 561-567, doi: 10.1021/es00148a003, 1986.

DeCarlo, P. F., Ulbrich, I. M., Crounse, J., de Foy, B., Dunlea, E. J., Aiken, A. C., Knapp, D., Weinheimer, A. J., Campos, T., Wennberg, P. O., and Jimenez, J. L.: Investigation of the sources and processing of organic aerosol over the Central Mexican Plateau from aircraft measurements during MILAGRO, Atmos. Chem. Phys., 10, 5257-5280, doi:10.5194/acp-10-5257-2010, 2010.

de Gouw, J. A., C. Warneke, D. D. Parrish, J. S. Holloway, M. Trainer, and F. C. Fehsenfeld, Emission sources and ocean uptake of acetonitrile (CH_3CN) in the atmosphere, J. Geophys. Res., 108(D11), 4329, doi:10.1029/2002JD002897, 2003.

Desyaterik, Y., Sun, Y., Shen, X., Lee, T., Wang, X., Wang, T., and Collet Jr., J. L.: Speciation of "brown" carbon in cloud water impacted by agricultural biomass burning in eastern China, J. Geophys. Res. Atmos., 118, 7389-7399, doi:10.1002/jgrd.50561, 2013.

Dickerson, R. R., Andreae, M. O., Campos, T., Mayol-Bracero, O. L., Neususess C., and Streets, D. G.: Analysis of black carbon and carbon monoxide observed over the Indian Ocean: Implications for emissions and photochemistry, J. Geophys. Res., 107, D19, 8017, doi:10.1029/2001JD000501, 2002.

Dong, J., and DeBusk, S. M.: GC-MS analysis of hydrogen sulfide, carbonyl sulfide, methanethiol, carbon disulfide, methyl thicyanate and methyl disulfide in mainstream vapor phase cigarette smoke, Chromatographia, 71, 259-265, doi: 10.1365/s10337-009-1434-z, 2010.

Duffy, B. L. and Nelson, P. F.: Non-methane exhaust composition in the Sydney harbor tunnel: A focus on benzene and 1,3-butadiene, Atmos. Environ., 30, 15, 2759-2768, doi:10.1016/1352-2310(95)00372-X, 1996.

Dunmore, R. E., Hopkins, J. R., Lidster, R. T., Lee, J. D., Evans, M. J., Rickard, A. R., Lewis, A. C., and Hamilton, J. F.: Diesel-related hydrocarbons can dominate gas phase reactive carbon in megacities, Atmos. Chem. Phys., 15, 9983-9996, doi:10.5194/acp-15-9983-2015, 2015.

Eckhardt, S., Breivik, K., Manø, S., Stohl, A.: Record high peaks in PCB concentrations in the Arctic atmosphere due to long-range transport of biomass burning emissions, Atmos. Chem. Phys., 7, 4527-4536, doi:10.5194/acp-7-4527-2007, 2007.

Escalambre, R: A Technican's Guide to Advanced Automotive Emissions Systems. Delmar, Publishers, Albany, 242, 1995.

Feng, Y., Ramanathan, V., and Kotamarthi, V. R.: Brown carbon: a significant atmospheric absorber of solar radiation?, Atmos. Chem. Phys. Discuss., 13, 2795-2833, doi:10.5194/acpd-13-2795-2013, 2013.

Ferek, R. J., Reid, J. S., Hobbs, P. V., Blake, D. R., and Liousse, C.: Emission factors of hydrocarbons, halocarbons, trace gases, and particles from biomass burning in Brazil, J. Geophys. Res., 103(D24), 32107–32118, doi:10.1029/98JD00692, 1998.

Fernandes, S. M., Trautmann, N. M., Streets, D. G., Roden, C. A., and Bond, T. C.: Global biofuel use, 1850–2000, Global Biogeochem. Cy., 21, GB2019, doi:10.1029/2006GB002836, 2007.

Fisseha, R., Dommen, J., Sax, M., Paulsen, D., Kalberer, M., Maurer, R., Hofler, F., Weingartner, E., and Baltensperger, U.: Identification of organic acids in secondary organic aerosol and the corresponding gas phase from chamber experiments, Anal. Chem., 76, 6535–6540, doi:10.1021/Ac048975f, 2004.

Forster, P., Ramaswamy, V., Artaxo, P., Berntsen, T., Betts, R., Fahey, D. W., Haywood, J., Lean, J., Lowe, D. C., Myhre, G., Nganga, J., Prinn, R., Raga, G., Schulz, M., and Van Dorland, R.: Radiative Forcing of Climate Change,

in Climate Change 2007: The Physical Science Basis. Contribution of Working Group I to the Fourth Assessment Report of the Intergovernmental Panel on Climate Change, edited by S. Solomon, D. Qin, M. Manning, Z. Chen, M. Marquis, K. B. Averyt, M. Tignor, and H. L. Miller, pp. 129–234, Cambridge Univ. Press, Cambridge, United Kingdom and New York, NY, USA, 2007.

Franco, V., Kousoulidou, M., Muntean, M., Ntziachristos, L., Hausberger, S., and Dilara, P.: Road vehicle emission factors development: A review, Atmos. Environ., 70, 84-97, doi:10.1016/j.atmosenv.2013.01.006, 2013.

Friedli, H. R., E. Atlas, V. R. Stroud, L. Giovanni, T. Campos, and Radke, L. F.: Volatile organic trace gases emitted from North American wildfires, Global Biogeochem. Cy., 15(2), 435-452, doi: 10.1029/2000GB001328, 2001.

Fullerton, D. G., Bruce, N., and Gordon, S. B.: Indoor air pollution from biomass fuel smoke is a major health concern in the developing world, Trans. R. Soc. Trop. Med. Hyg., 102, 843-851, doi:10.1016/j.trstmh.2008.05.028, 2008.

Ge, X., Wexler, A. S., and Clegg, S. L.: Amospheric amines-Part I. A review, Atmos. Environ., 45, 524-546, doi:10.1016/j.atmosenv.2010.10.012, 2011.

Geron, C., and Hays, M.: Air emissions from organic soil burning on the coastal plain of North Carolina, Atmos. Environ., 64, 192-199, doi: 10.1016/j.atmosenv.2012.09.065, 2013.

Glatthor, N., Höpfner, M., Stiller, G. P., von Clarmann, T., Funke, B., Lossow, S., Eckert, E., Grabowski, U., Kellmann, S., Linden, A., A. Walker, K., and Wiegele, A.: Seasonal and interannual variations in HCN amounts in the upper troposphere and lower stratosphere observed by MIPAS, Atmos. Chem. Phys., 15, 563-582, doi:10.5194/acp-15-563-2015, 2015.

Goetz et al.: Speciated aerosol emission factors and mass spectral characterization of South Asian combustion sources, in preparation, 2016.

Gomez Alvarez, E. G., Borras, E., Viidanoja, J., and Hjorth, J.: Unsaturated dicarbonyl products from the OH-initiated photo-oxidation of furan, 2-methylfuran and 3-methylfuran, Atmos. Environ, 43, 1603-1612, doi:10.1016/j.atmosenv.2008.12.019, 2009.

Goode, J. G., Yokelson, R. J., Susott, R. A., and Ward, D. E.: Trace gas emissions from laboratory biomass fires measured by Fourier transform infrared spectroscopy: Fires in grass and surface fuels, J. Geophys. Res., 104, 21237 – 21 245, doi:10.1029/1999JD900360, 1999.

Govender, N., Trollope, W. S. W, and van Wilgen, B. W.: The effect of fire season, fire frequency, rainfall and management on fire intensities in savanna vegetation in South Africa, J. Appl. Ecol., 43, 748–758, doi: 10.1111/j.1365-2664.2006.01184.x, 2006.

Gras, J. L., Jensen, J. B., Okada, K., Ikegami, M., Zaizen, Y., and Makino, Y.: Some optical properties of smoke aerosol in Indonesia and tropical Australia, Geophys. Res. Lettr. 26, 1393-1396, doi: 10.1029/1999GL900275, 1999.

Graus, M., Muller, M., and Hansel, A.: High Resolution PTR-TOF: Quantification and formula confirmation of VOC in real time, J. Am. Soc. Mass. Spectr., 21/6, 1037–1044, doi:10.1016/j.jasms.2010.02.006, 2010.

Greenberg, J. P., Friedli, H., Guenther, A. B., Hanson, D., Harley, P., and Karl, T.: Volatile organic emissions from the distillation and pyrolysis of vegetation, Atmos. Chem. Phys., 6, 81–91, doi:10.5194/acp-6-81-2006, 2006.

Grell, G., Freitas, S. R., Stuefer, M., and Fast, J.: Inclusion of biomass burning in WRF-Chem: impact of wildfires on weather forecasts, Atmos. Chem. Phys., 11, 5289-5303, doi:10.5194/acp-11-5289-2011, 2011.

Grieshop, A. P., Logue, J. M., Donahue, N. M., and Robinson, A. L.: Laboratory investigation of photochemical oxidation of organic aerosol from wood fires 1: measurement and simulation of organic aerosol evolution, Atmos. Chem. Phys., 9, 1263–1277, doi:10.5194/acp-9-1263-2009, 2009.

Griffith, D. W. T., Mankin, W. G., Coffey, M. T., Ward, D. E., and Riebau, A.: FTIR remote sensing of biomass burning emissions of CO_2, CO, CH_4, CH_2O, NO, NO_2, NH_3, and N_2O, in: Global Biomass Burning: Atmospheric, Climatic, and Biospheric Implications, edited by: Levine, J. S., MIT Press, Cambridge, 230–239, 1991.

Griffith, D. W. T.: Synthetic calibration and quantitative analysis of gas phase infrared spectra, Appl. Spectrosc., 50, 59–70, 1996.

Gullett, B. K., Touati, A., Oudejans, L., and Ryan, S. P.: Real-time emission characterization of organic air toxic pollutants during steady state and transient operation of a medium duty diesel engine, Atmos. Environ., 40, 4037-4047, doi:10.1016/j.atmosenv.2006.03.031, 2006.

Guo, H., Wang, T., Blake, D. R., Simpson, I. J., Kwok, Y. H., and Li, Y. S.: Regional and local contributions to ambient nonmethane volatile organic compounds at a polluted rural/coastal site in Pearl River Delta, China, Atmos. Environ., 40, 2345–2359, doi:10.1016/j.atmosenv.2005.12.011, 2006.

Haidouti, C., Chronopoulou, A., Chronopoulos, J.: Effects of fluoride emissions from industry on the fluoride concentration of soils and vegetation, Biochem. Syst. Ecol., 21, 195-208, doi:10.1016/0305-1978(93)90037-R, 1993.

Hardy, C. C., Conard, S. G., Regelbrugge, J. C., and Teesdale, D. R.: Smoke emissions from prescribed burning of southern California chaparral, Res. Pap. PNW-RP-486, US Department of Agriculture, Forest Service, Pacific Northwest Research Station, Portland, OR, 1996.

Harrison, M. A. J.; Barra, S.; Borghesi, D.; Vione, D.; Arsene, C.; and Olariu, R. L.: Nitrated phenols in the atmosphere: A review, Atmos. Environ., 39, 231–248, doi: 10.1016/j.atmosenv.2004.09.044, 2005.

Hatch, L. E., Luo, W., Pankow, J. F., Yokelson, R. J., Stockwell, C. E., and Barsanti, K. C.: Identification and Quantification of gaseous organic compounds emitted from biomass burning using two-dimensional gas chromatography-time-of-flight mass spectrometry, Atmos. Chem. Phys., 15, 1865-1899, doi: 10.5194/acp-15-1865-2015, 2015.

Hawthorne, S. B., Krieger, M. S., Miller, D. J., and Mathiason, M. B.: Collection and quantitation of methoxylated phenol tracers for atmospheric-pollution from residential wood stoves, Environ. Sci. Technol., 23, 470-475, doi: 10.1021/es00181a013, 1989.

Hawthorne, S. B., Miller, D. J., Langenfeld, J. J., and Krieger, M. S.: PM-10 High-volume collection and quantitation of semivolatile and nonvolatile phenols, methoxylated phenols, alkanes, and polycyclic aromatic-hydrocarbons from winter urban air and their relationship to wood smoke emissions, Environ. Sci.Technol., 26, 2251–2262, doi:10.1021/es00035a026, 1992.

Hecobian, A., Zhang, X., Zheng, M., Frank, N., Edgerton, E. S., and Weber, R. J.: Water-Soluble Organic Aerosol material and the light-absorption characteristics of aqueous extracts measured over the Southeastern United States, Atmos. Chem. Phys., 10, 5965–5977, doi:10.5194/acp-10-5965-2010, 2010.

Heigenmoser, A., Liebner, F., Windeisen, E., and Richter, K.: Investigation of thermally treated beech (Fagus sylvatica) and spruce (Picea abies) by means of multifunctional analytical pyrolysis-GC/MS, J. Anal. Appl. Pyrolysis, 100, 117-126, doi: 10.1016/j.jaap.2012.12.005, 2013.

Hennigan, C. J., Miracolo, M. A., Engelhart, G. J., May, A. A., Presto, A. A., Lee, T., Sullivan, A. P., McMeeking, G. R., Coe, H., Wold, C.E., Hao, W. M., Gilman, J. B., Kuster, W. C., de Gouw, J., Schichtel, B. A., Collett Jr., J. L., Kreidenweis, S. M., and Robinson, A. L.: Chemical and physical transformations of organic aerosol from the photo-oxidation of open biomass burning emissions in an environmental chamber, Atmos. Chem. Phys., 11, 7669-7686, doi:10.5194/acp-11-7669-201, 2011.

Henze, D. K., Seinfeld, J. H., Ng, N. L., Kroll, J. H., Fu, T.-M., Jacob, D. J., and Heald, C. L.: Global modeling of secondary organic aerosol formation from aromatic hydrocarbons: high- vs. low-yield pathways, Atmos. Chem. Phys., 8, 2405-2420, doi:10.5194/acp-8-2405-2008, 2008.

Hildebrandt, L., Donahue, N. M., and Pandis, S. N.: High formation of secondary organic aerosol from the photo-oxidation of toluene, Atmos. Chem. Phys., 9, 2973–2986, doi:10.5194/acp-9-2973-2009, 2009.

Hinkel, M., Reischl, A., Schramm, K.-W., Trautner, F., Reissinger, M., Hutzinger, O.: Concentration levels of nitrated phenols in conifer needles, Chemosphere, 18, 2433–2439, 1989.

Ho, K. F., Lee, S. C., Ho, W. K., Blake, D. R., Cheng, Y., Li, Y. S., Ho, S. S. H., Fung, K., Louie, P. K. K., and Park, D.: Vehicular emission of volatile organic compounds (VOCs) from a tunnel study in Hong Kong, Atmos. Chem. Phys., 9, 7491-7504, doi:10.5194/acp-9-7491-2009, 2009.

Hobbs, P. V., and Radke, L. F., Cloud condensation nuclei from a simulated forest fire, Science, 163, 279-280, 1969.

Hobbs, P. V., Sinha, P., Yokelson, R. J., Christian, T. J., Blake, D. R., Gao, S., Kirchstetter, W., Novakov, T., and Pilewskie, P.: Evolution of gases and particles from a savanna fire in South Africa, J. Geophys. Res., 108 (D13), 8485, doi: 10.1029/2002JD002352, 2003.

Holmén, B. A., and Niemeier, D. A.: Characterizing the effects of driver variability on real-world vehicle emissions, Transpn. Res. –D, 3, 117-128, doi:10.1016/S1361-9209(97)00032-1, 1998.

Holzinger, R., Warneke, C., Hansel, A., Jordan, A., Lindinger, W., Scharffe, D. H., Schade, G., and Crutzen, P. J.: Biomass burning as a source of formaldehyde, acetaldehyde, methanol, acetone, acetonitrile, and hydrogen cyanide, Geophys. Res. Lett., 26, 1161–1164, doi: 10.1029/1999GL900156, 1999.

Iinuma, Y. Böge, O., Gräfe, R., and Herrmann, H.: Methyl-nitrocatechols: Atmospheric tracer compounds for biomass burning secondary organic aerosols, Environ. Sci. Technol., 44, 8453-8459, doi: 10.1021/es102938a, 2010.

Im, Y., Jang, M., Beardsley, R. L.: Simulation of aromatic SOA formation using the lumping model integrated with explicit gas-phase kinetic mechanisms and aerosol-phase reactions, Atmos. Chem. Phys., 14,4013-4027, doi:10.5194/acp-14-4013-2014, 2014.

Ingemarsson, A., Nilsson, U., Nilsson, M., Pederson, J. R., and Olsson, J. O.: Slow pyrolysis of spruce and pine samples studied with GC/MS and GC/FTIR/FID, Chemosphere, 36 (14), 2879-2889, doi: 10.1016/S0045-6535(97)10245-4, 1998.

IPCC, 2006: 2006 IPCC Guidelines for National Greenhouse Gas Inventories, prepared by the National Greenhouse Gas Inventories Programme, edited by: Eggleston, H. S., Buendia, L.,Miwa, K., Ngara, T., and Tanabe, K., Institute for Global Environmental Strategies (IGES), Hayama, Japan, 2006.

Iyer N. V.: A Technical Assessment of Emissions and Fuel Consumption Reduction Potential from Two and Three Wheelers in India, available at: http://www.theicct.org/sites/default/files/publications/Iyer_two-three-wheelers_India_August2012.pdf, The International Council on Clean Transportation, Washington, D. C., 2012.

Jayarathne, T., Stockwell, C. E., Christian, T. J., Bhave, P. V., Praveen, P. S., Panday, A. K., Adhikari, S., Maharjan, R., Goetz, J. D., DeCarlo, P. F., Saikawa, E., Yokelson, R. J., and Stone E. A.: Nepal Ambient Monitoring and Source Testing Experiment (NAMaSTE): Emissions of particulate matter from wood and dung cooking fires, brick kilns, generators, trash and crop residue burning, in preparation, 2016.

Jetter, J., Zhao, Y., Smith, K. R., Khan, B., Yelverton, T., DeCarlo, P., and Hays, M. D.: Pollutant emissions and energy efficiency under controlled conditions for household biomass cookstoves and implications for metrics useful in setting international test standards, Environ. Sci. Technol., 46, 10827-10834, doi:10.1021/es301693f , 2012.

Jiang, G., Nowakowski, D. J., and Bridgwater, A. V.: Effect of the temperature on the composition of lignin pyrolysis products, Energy Fuels, 24, 4470-4475, doi:10.1021/ef100363c, 2010.

Johnson, T. J., Disselkamp, R. S., Su, Y.-F., Fellows, R. J., Alexander, M. L., and Driver, C. J.: Gas-Phase Hydrolysis of SOCl2 at 297 and 309 K: Implications for Its Atmospheric Fate, J. Phys. Chem. A, 107, 6183–6190, doi:10.1021/jp022090v, 2003.

Johnson, T. J., Masiello, T., and Sharpe, S. W.: The quantitative infrared and NIR spectrum of CH2I2 vapor: vibrational assignments and potential for atmospheric monitoring, Atmos. Chem. Phys., 6, 2581–2591, doi:10.5194/acp-6-2581-2006, 2006.

Johnson, M., Edwards, R., Frenk, C. A., and Masera, O.: Infield greenhouse gas emissions from cookstoves in rural Mexican households, Atmos. Environ. 42, 1206–1222, 2008.

Johnson, T. J., Profeta, L. T. M., Sams, R. L., Griffith, D.W. T., and Yokelson, R. L.: An infrared spectral database for detection of gases emitted by biomass burning, Vib. Spectrosc., 53, 97–102, doi:10.1016/j.vibspec.2010.02.010, 2010.

Johnson, T. J., Sams, R. L., Profeta, L. T. M., Akagi, S. K., Burling, I. R., Williams, S. D., and Yokelson, R. J.: Quantitative IR spectrum and vibrational assignments for glycolaldehyde: Application to measurements in biomass burning plumes, J. Phys. Chem. A, 117, 4096-4107, doi:10.1021/jp311945p, 2013.

Jordan, T. B., and Seen, A. J.: Effect of airflow setting on the organic composition of woodheater emissions, Environ. Sci. Technol., 39, 3601-3610, doi: 10.1021/es0487628, 2005.

Jordan, A., Haidacher, S., Hanel, G., Hartungen, E., M¨ark, L., Seehauser, H., Schottkowsky, R., Sulzer, P., and Märk, T. D.: A high resolution and high sensitivity proton-transfer-reaction time-of-flight mass spectrometer (PTR-TOF-MS), Int. J. Mass Spectrom., 286, 122–128, doi: 10.1016/j.ijms.2009.07.005, 2009.

Karl, T. G., Christian, T. J., Yokelson, R. J., Artaxo, P., Hao, W. M., and Guenther, A.: The Tropical Forest and Fire Emissions Experiment: method evaluation of volatile organic compound emissions measured by PTR-MS, FTIR, and GC from tropical biomass burning, Atmos. Chem. Phys., 7, 5883–5897, doi:10.5194/acp-7-5883-2007, 2007.

Katuwal, H. and Bohara, A. K.: Biogas: A promising renewable technology and its impact on rural households in Nepal, J. Renewable Sustainable Energy, 13, 2668-2674, doi:10.1016/j.rser.2009.05.002, 2009.

Keene, W. C., M. A. K. Khalil, D. J. Erickson III, A. McCulloch, T. E. Graedel, J. M. Lobert, M. L. Aucott, S. L. Gong, D. B. Harper, G. Kleiman, P. Midgley, R. M. Moore, C. Seuzaret, W. T. Sturges, C. M. Benkovitz, V. Koropalov, L. A. Barrie, and Y. F. Li, Composite global emissions of reactive chlorine from anthropogenic and natural sources: Reactive Chlorine Emissions Inventory, J. Geophys. Res., 104, 8429 – 8440, 1999.

Keene, W. C., Lobert, J. M., Crutzen, P. J., Maben, J. R., Scharffe, D. H., and Landmann, T.: Emissions of major gaseous and particulate species during experimental burns of southern African biomass, J. Geophys. Res., 111, D04301, doi:10.1029/2005JD006319, 2006.

Kerminen, V. M., Lihavainen, H., Komppula, M., Viisanen, Y., and Kulmala, M.: Direct observational evidence linking atmospheric aerosol formation and cloud droplet activation, Geophys. Res. Lett., 32, L14803, doi:10.1029/2005gl023130, 2005.

Kessel, S., Auld, J., Crowley, J., Horowitz, A., Sander, R., Tucceri, M., Veres P., and Williams, J.: Measurement of carbon suboxide (C3O2) with PTR-TOF-MS – Atmospheric Sources and Sinks, 6th International Conference on proton transfer reaction mass spectrometry and its applications, University of Innsbruck, February 3-8, 190-191, 2013.

Kettle, A. J., Kuhn, U., von Hobe, M., Kesselmeier, J., and Andreae, M. O.: Global budget of atmospheric carbonyl sulfide: Temporal and spatial variations of the dominant sources and sinks, J. Geophys. Res., 107(D22), 4658, doi:10.1029/2002JD002187, 2002.

Kirchstetter, T. W., Harley, R. A., Kreisberg, N. M., Stolzenburg, M. R., and Hering, S. V.: On-road measurement of fine particle and nitrogen oxide emission from light- and heavy-duty motor vehicles, Atmos. Environ., 33, 2955-2968, doi: 10.1016/S1352-2310(99)00089-8, 1999.

Kirchstetter, T. W., Novakov, T., and Hobbs, P. V.: Evidence that the spectral dependence of light absorption by aerosols is affected by organic carbon, J. Geophys. Res., 109, D21208, doi:10.1029/2004JD004999, 2004.

Kirkby, J., Curtius, J., Almeida, J., Dunne, E., Duplissy, J., Ehrhart, S., Franchin, A., Gagné, S., Ickes, L., Kürten, A., Kupc, A., Metzger, A., Riccobono, F., Rondo, L., Schobesberger, S., Tsagkogeorgas, G., Wimmer, D., Amorim, A., Bianchi, F., Breitenlechner, M., David, A., Dommen, J., Downard, A., Ehn, M., Flagan, R. C., Haider, S., Hansel, A., Hauser, D., Jud, W., Junninen, H., Kreissl, F., Kvashin, A., Laaksonen, A., Lehtipalo, K., Lima, J., Lovejoy, E. R., Makhmutov, V., Mathot, S., Mikkilä, J., Minginette, P., Mogo S., Nieminen, T., Onnela, A., Pereira, P., Petäjä, T., Schnitzhofer, R., J. H. Seinfeld, Sipilä, M., Stozhkov, Y., Stratmann, F., Tomé, A., Vanhanen, J., Viisanen, Y., Vrtala, A., Wagner, P. E., Walther, H., Weingartner, E., Wex, H., Winkler, P. M., Carslaw, K. S., Worsnop, D. R., Baltensperger, U., and Kulmala, M.: Role of sulphuric acid, ammonia and galactic cosmic rays in atmospheric aerosol nucleation, Nature, 476, 429–433, 2011.

Kitanovski, Z., Grgić, I., Yasmeen, F., Claeys, M., and Čusak, A.: Development of a liquid chromatographic method based on ultraviolet-visible and electrospray ionization mass spectrometric detection for the identification of nitrocatechols and related tracers in biomass burning atmospheric organic aerosol, Rapid Commun. Mass Sp., 26, 793–804, doi: 10.1002/rcm.6170, 2012.

Knapp, E. E., Estes, B. L., and Skinner, C.N.: Ecological effects of prescribe fire season: a literature review and synthesis for managers, Gen. Tech. Rep., PSW-GTR-224, Department of Agriculture, Forest service, Alabany, CA, 2009.

Komazaki, Y., Hashimoto, S., Inoue, T., and Tanaka, S.: Direct collection of HNO_3 and HCl by a diffusion scrubber without inlet tubes, Atmos. Environ., 36, 1241–1246, doi:10.1016/S1352-2310(01)00571-4, 2002.

Kudo, S., Tanimoto, H., Inomata, S., Saito, S., Pan, X., Kanaya, Y., Taketani, F., Wang, Z., Chen, H., Dong, H., Zhang, M., and Yamaji, K.: Emissions of nonmethane volatile organic compounds from open crop residue burning in the Yangtze River Delta region, China, J. Geophys. Res. Atmos., 119, 7684-7698, doi: 10.1002/2013JD021044, 2014.

Kuhlbusch, T. A., Lobert, J. M., Crutzen, P. J., and Warneck, P.: Molecular nitrogen emissions from denitrification during biomass burning, Nature, 351, 135–137, doi:10.1038/351135a0, 1991.

Laaksonen, A., Hamed, A., Joutsensaari, J., Hiltunen, L., Cavalli F., Junkermann, W., Asmi, A., Fuzzi, S., and Facchini, M. C.: Cloud condensation nucleus production from nucleation events at a highly polluted region, Geophys. Res. Lett., 32, L06812, doi:10.1029/2004gl022092, 2005.

Lack, D. A. and Cappa, C. D.: Impact of brown and clear carbon on light absorption enhancement, single scatter albedo and absorption wavelength dependence of black carbon, Atmos. Chem. Phys., 10, 4207-4220, doi:10.5194/acp-10-4207-2010, 2010.

Lack, D. A. and Corbett, J. J.: Black carbon from ships: a review of the effects of ship speed, fuel quality and exhaust gas scrubbing, Atmos. Chem. Phys., 12, 3985-4000, doi:10.5194/acp-12-3985-2012, 2012.

Lack, D. A. and Langridge, J. M.: On the attribution of black and brown carbon light absorption using the Ångström exponent, Atmos. Chem. Phys., 13, 10535-10543, doi:10.5194/acp-13-10535-2013, 2013.

Lara, L. L., Artaxo, P., Martinelli, L. A., Camargo, P. B., Victoria, R. L., and Ferraz, E. S. B.: Properties of aerosols from sugarcane burning emissions in Southeastern Brazil, Atmos. Environ., 39, 4627–4637, doi:10.1016/j.atmosenv.2005.04.026, 2005.

Lauraguais, A., Coeur-Tourneur, C., Cassez, A., Deboudt, K., Fourmentin, M., and Choël, M.: Atmospheric reactivity of hydroxyl radicals with guaiacol (2-methoxyphenol), a biomass burning emitted compound: Secondary organic aerosol formation and gas-phase oxidation products, Atmos. Environ., 86, 155–163, doi: 10.1016/j.atmosenv.2013.11.074, 2014.

Lehmann, C. M. B. and Gay, D. A.: Monitoring long-term trends of acidic wet deposition in US precipitation: Results from the National Atmospheric Deposition Program, Power Plant Chem., 13, 386–393, 2011.

Lei, W., Li, G., and Molina, L. T.: Modeling the impacts of biomass burning on air quality in and around Mexico City, Atmos. Chem. Phys., 13, 2299-2319, doi:10.5194/acp-13-2299-2013, 2013.

Lemieux, P. M.: Evaluation of Emissions from the Open Burning of Household Waste in Barrels, EPA/600/SR-97/134, United States Environmental Protection Agency, Office of Research and Development, Washington DC, 1998.

Lemieux, P.M., Lutes, C.C., Abbott, J.A., and Aldous, K.M.: Emissions of Polychlorinated Dibenzo-p-dioxins and Polychlorinated Dibenzofurans from the Open Burning of Household Waste in Barrels, Environ.Sci. Technol., 34 (3), 377-384, doi:10.1021/es990465t, 2000.

Lemieux, P. M., Gullett, B.K., Lutes, C.C., Winterrowd, C. K., Winters, D. L.: Variables affecting emissions of PCDD/Fs from uncontrolled combustion of household waste in barrels, J. Air Waste Manage. Assoc., 53, 523-531, doi: 10.1080/10473289.2003.10466192, 2003.

Levin, E. J. T., McMeeking, G. R., Carrico, C. M., Mack, L. E., Kreidenweis, S. M., Wold, C. E., Moosmüller, H., Arnott, W. P., Hao, W. M., Collett Jr., J. L., and Malm, W. C.: Biomass burning smoke aerosol properties measured during Fire Laboratory at Missoula Experiments (FLAME), J. Geophys. Res., 115, D18210, doi:10.1029/2009JD013601, 2010.

Levin, E. J. T., McMeeking, G. R., DeMott, P. J., McCluskey, C. S., Stockwell, C. E., Yokelson, R. J., and Kreidenweis, S. M.: A new method to determine the number concentrations of refractory black carbon ice nucleating particles, Aerosol Sci. Technol., 48, 1264-1275, doi:10.1080/02786826.2014.977843, 2014.

Levoni, C., Cervino, M., Guzzi, R., and Torricella, F.: Atmospheric aerosol optical properties: a database of radiative characteristics for different components and classes, App. Opt., 36 (30), 8031-8041, 1997.

Lewis, K., Arnott, W. P., Moosmüller, H., and Wold, C. E.: Strong spectral variation of biomass smoke light absorption and single scattering albedo observed with a novel dual-wavelength photoacoustic instrument, J. Geophys. Res., 113, D16203, doi:10.1029/2007jd009699, 2008.

Li, G., Lei, W., Bei, N., and Molina, L. T.: Contribution of garbage burning to chloride and $PM_{2.5}$ in Mexico City, Atmos. Chem. Phys., 12, 8751-8761, doi :10.5194/acp-12-8751-2012, 2012.

Li, J., Posfai, M., Hobbs, P. V and Buseck, P. R.: Individual aerosol particles from biomass burning in southern Africa: 2. Compositions and aging of inorganic particles, J. Geophys. Res., 108, 8484, doi:10.1029/2002JD002310, 2003.

Li, Q., Jacob, D. J., Bey, I., Yantosca, R. M., Zhao, Y., Kondo, Y., and Notholt, J.: Atmospheric hydrogen cyanide (HCN): biomass burning source, ocean sink?, Geophys. Res. Lett., 27(3), 357–360, 2000.

Li, Q., Steele, P. H., Yu, F., Mitchell, B., and Hassan, E.-B., M.: Pyrolytic spray increases levoglucosan production during fast pyrolysis, J. Anal. Appl. Pyrolysis, 100, 33-40, doi: 10.1016/j.jaap.2012.11.013, 2013.

Lin, P., Engling, G., and Yu, J. Z.: Humic-like substances in fresh emissions of rice straw burning and in ambient aerosols in the Pearl River Delta Region, China, Atmos. Chem. Phys., 10, 6487-6500, doi:10.5194/acp-10-6487-2010, 2010.

Liu, S., Aiken, A. C., Arata, C., Manvendra, K. D., Stockwell, C. E., Yokelson, R. J., Stone, E. A., Jayarathne, T., Robinson, A. L., DeMott, P. J., and Kreidenweis, S. M.: Aerosol single scattering albedo dependence on biomass combustion efficiency: Laboratory and field studies, Geophys. Res. Lett., 41, 742-748, doi:10.1002/2013GL058392, 2014.

Liu, X., Huey, G., Yokelson, R. J., Zhang, Y., Anderson, B. E., Beyersdorf, A., Campuzano-Jost, P., St. Clair, J. M., Crounse, J. D., Diskin, G. S., Jimenez, J. L., King, L., Mikoviny, T., Peischl, J., Perring, A., Pollack, I. B., Ryerson, T. B., Sachse, G., Schwarz, J., Tanner, D. J., Thornhill, L., Wang, Y., Weber, R.J., Wennberg, P. O., and Wisthaler, A.: Agricultural Fires in the Southeastern U.S. during SEAC4RS: Emissions of Trace Gases and Particles and Evolution of Ozone, Reactive Nitrogen, and Organic Aerosol, in preparation, 2016.

Liu, Y., Shao, M., Fu, L., Lu, S., Zeng, L., and Tang, D.: Source profiles of volatile organic compounds (VOCs) measured in China: Part I, Atmos. Environ, 42, 6247-6260, doi:10.1016/j.atmosenv.2008.01.070, 2008.

Liu, Y., Shi, Q., Zhang, Y., He, Y., Chung, K. H., Zhao, S., and Xu, C.: Characterization of red pine pyrolysis bio-oil by gas chromatography−mass spectrometry and negative-ion electrospray ionization fourier transform ion cyclotron resonance mass spectrometry, Energy Fuels, 26, 4532-4539, doi: 10.1021/ef300501t, 2012.

Lloyd, A. C., and Cackette, T. A.: Diesel engines: Environmental impact and control, J. Air Waste Manag. Assoc., 51, 809-847, doi: 10.1080/10473289.2001.10464315, 2001.

Lobert, J. M., Scharffe, D. H., Hao, W. M., Kuhlbusch, T. A., Seuwen, R., Warneck, P., and Crutzen, P. J.: Experimental evaluation of biomass burning emissions: Nitrogen and carbon containing compounds, in: Global Biomass Burning: Atmospheric, Climatic, and Biospheric Implications, Levine, J. S., MIT Press, Cambridge, 289–304, 1991.

Lobert, J. M., Keene, W. C., Logan, J. A., and Yevich, R.: Global chlorine emissions from biomass burning: Reactive Chlorine Emissions Inventory, J. Geophys. Res., 104, 8373–8389, doi:10.1029/1998jd100077, 1999.

L'Orange, C., Volckens, J., and DeFoort, M.: Influences of stove type and cooking pot temperature on particulate matter emissions from biomass cook stoves, Energy Sustainable Dev., 16, 448-455, doi: 10.1016/j.esd.2012.08.008, 2012a.

L'Orange, C., DeFoort, M., and Willson, B.: Influence of testing parameters on biomass stove performance and development of an improved testing protocol, Energy Sustainable Dev., 16, 3-12, doi:10.1016/j.esd.2011.10.008, 2012b.

Lüthi, Z. L., Škerlak, B., Kim, S.-W., Lauer, A., Mues, A., Rupakheti, M., and Kang, S.: Atmospheric brown clouds reach the Tibetan Plateau by crossing the Himalayas, Atmos. Chem. Phys., 15, 6007–6021, doi:10.5194/acp-15-6007-2015, 2015.

Lyu, X. P., Guo, H., Simpson, I. J., Meinardi, S., Louie, P. K. K., Ling, Z. H., Wang, Y., Liu, M., Luk, C. W. Y., Wang, N., and Blake, D. R.: Effectiveness of replacing catalytic converters in LPG-fueled vehicles in Hong Kong, Atmos. Chem. Phys. Discuss., 15, 35939-35990, doi:10.5194/acpd-15-35939-2015, 2015.

Ma, Y. and Hays, M. D.: Thermal extraction-two-dimensional gas chromatography-mass spectrometry with heart-cutting for nitrogen heterocyclics in biomass burning aerosols, J. Chromatogr. A, 1200, 228-234, doi: 10.1016/j.chroma.2008.05.078, 2008.

MacCarty, N., Ogle, D., Still, D., Bond, T., and Roden, C.: A laboratory comparison of the global warming impact of five major types of biomass cooking stoves, Energy Sustainable Dev., 12, 5−14, 2008.

Maithel, S., Lalchandani, D., Malhotra, G., Bhanware, P., Uma, R., Ragavan, S., Athalye, V., Bindiya, K. R, Reddy, S., Bond, T., Weyant, C., Baum, E., Thoa, V. T. K., Phuong, N. T., and Thanh, T. K.: Brick Kilns Performance Assessment, 164 pp, Greentech, New Delhi, 2012.

Marlier, M. E., DeFries, R. S., Voulgarakis, A., Kinney, P. L., Randerson, J. T., Shindell, D. T., Chen, Y., and Faluvegi, G.: El Niño and health risks from landscape fire emissions in southeast Asia, Nature Climate Change, 3, 131-136, doi:10.1038/nclimate1658, 2013.

Martínez, J. D., Puy, N., Murillo, R., Garciá, T., Navarro, M. V., and Mastral, A. M.: Waste tyre pyrolysis- A review, Renewable Sustainable Energy Rev., 23, 179-213, doi:10.1016/j.rser.2013.02.038, 2013.

Mason, S. A., Trentmann, J., Winterrath, T., Yokelson, R. J., Christian, T. J., Carlson, L. J., Warner, T. R., Wolfe, L. C., and Andreae, M. O.: Intercomparison of two box models of the chemical evolution in biomass-burning smoke plumes, J. Atmos. Chem., 55, 273-297, doi: 10.1007/s10874-006-9039-5, 2006.

Mastral, A. M., Murillo, R., Callen, M. S., Garcia, T., and Snape, C. E.: Influence of process variables on oils from tire pyrolysis and hydropyrolysis in a swept fixed bed reactor, Energy & Fuels, 14(4), 739-744, doi:10.1021/ef990183e, 2000.

May, A. A., Lee, T., McMeeking, G. R., Akagi, S., Sullivan, A. P., Urbanski, S., Yokelson, R. J., and Kreidenweis, S. M.: Observations and analysis of organic aerosol evolution in some prescribed fire smoke plumes, Atmos. Chem. Phys., 15, 6323-6335, doi:10.5194/acp-15-6323-2015, 2015.

McCarty,J. L., Justice, C. O., and Korontzi, S.: Agricultural burning in Southeastern United States detected by MODIS, Remote Sen. Environ., 108, 151-162, doi:10.1016/j.rse.2006.03.020, 2007.

McCarty, J. L., Korontzi, S., Justice, C. O., and Loboda, T.: The spatial and temporal distribution of crop residue burning in the contiguous United States, Sci. Total Environ., 407, 5701-5712, doi: 10.1016/j.scitotenv.2009.07.009, 2009.

McCulloch, A., Aucott, M. L., Benkovitz, C. M., Graede, T. E., Kleiman, G., Midgley, P. M., and Li, Y. F.: Global emissions of hydrogen chloride and chloromethane from coal combustion, incineration and industrial activities: Reactive Chlorine Emissions Inventory, J. Geophys. Res., 104(D7), 8391–8403, 1999.

McKenzie, L.M., Ward, D. E., Hao, W. M.: Chlorine and bromine in the biomass of tropical and temperate ecosystems, Biomass Burning and Global Change, vol. 1, Remote Sensing, Modeling and Inventory Development, and Biomass Burning in Africa., J. S. Levine, 241-248, MIT Press, Cambridge, Massachusetts, 241-248, 1996.

McMeeking, G. R., Kreidenweis, S. M., Baker, S., Carrico, C. M., Chow, J. C., Collet Jr., J. L., Hao, W. M., Holden, A. S., Kirchstetter, T. W., Malm, W. C., Moosmüller, H., Sullivan, A. P., and Wold, C. E.: Emissions of trace gases and aerosols during the open combustion of biomass in the laboratory, J. Geophys. Res., 114, D19210, doi:10.1029/2009JD011836, 2009.

McMeeking, G. R., Fortner, E., Onasch T. B., Taylor, J.W., Flynn, M., Coe, H., and Kreidenweis, S. M.: Impacts of nonrefractory material on light absorption by aerosols emitted from biomass burning, J. Geophys. Res. Atmos., 119, 12272-12286, doi:10.1002/2014JD021750, 2014.

Meinardi, S., Simpson, I. J., Blake, N. J., Blake, D. R., and Rowland, F. S.: Dimethyl disulfide (DMDS) and dimethyl sulfide (DMS) emissions from biomass burning in Australia, Geophys. Res. Lett., 30(9), 1454, doi:10.1029/2003GL016967, 2003.

Melvin, M. A.: 2012 national prescribed fire use survey report, Technical Report 01-12, Coalition of Prescribed Fire Councils, Inc., 1–19, 2012.

Menon, S., Koch, D., Beig, G., Sahu, S., Fasullo, J., and Orlikowski, D.: Black carbon aerosols and the third polar ice cap, Atmos. Chem. Phys., 10, 4559-4571, doi:10.5194/acp-10-4559-2010, 2010.

Mohr, C., Lopez-Hilfiker, F. D., Zotter, P., Prévôt, A. S. H ., Xu, L., Ng, N. L., Herndon, S. C., Williams, L. R., Franklin, J. P., Zahniser, M. S., Worsnop, D. R., Knighton, W. B., Aiken, A. C., Gorkowski, K. J., Dubey, M. K.,

Allan, J. D., and Thornton, J. A.: Contribution of nitrated phenols to wood burning brown carbon light absorption in Detling, United Kingdom during winter time, Environ. Sci. Technol., 47, 6316–6324, doi:10.1021/es400683v, 2013.

Molina, L. T. and Molina, M. J. (Eds.): Air Quality in the Mexico Megacity: An Integrated Assessment, Kluwer Academic Publishers, Dordrecht, The Netherlands, 2002.

Molina, M. J. and Molina, L. T., Megacities and Atmospheric Pollution, J. Air Waste Manage. Assoc., 54, 6, 644–680, 2004.

Molina, L. T., Kolb, C. E., de Foy, B., Lamb, B. K., Brune, W. H., Jimenez, J. L., Ramos-Villegas, R., Sarmiento, J., Paramo-Figueroa, V. H., Cardenas, B., Gutierrez-Avedoy, V., and Molina, M. J.: Air quality in North America's most populous city – overview of the MCMA-2003 campaign, Atmos. Chem. Phys., 7, 2447-2473, doi:10.5194/acp-7-2447-2007, 2007.

Moosmüller, H., Chakrabarty, R. K., and Arnott, W. P.: Aerosol Light Absorption and its Measurement: A Review, J. Quant. Spectrosc. Ra., 110, 844–878, 2009.

MOPIT: Details of Registration of Transport Fiscal Year 2046/47-2070/74, Ministry of Physical Infrastructure and Transport, Government of Nepal, Kathmandu, 2014.

Morikawa, T., Wakamatsu, S., Tanaka, M., Uno, I., Kamiura, T., and Maeda, T.: C2-C5 Hydrocarbon concentrations in central Osaka, Atmos. Environ., 32, 2007-2016, doi: 10.1016/S1352-2310(97)00509-8, 1998.

Müller, M., Graus, M., Ruuskanen, T. M., Schnitzhofer, R., Bamberger, I., Kaser, L., Titzmann, T., Hörtnagl, L., Wohlfahrt, G., and Hansel, A.: First eddy covariance flux measurements by PTR-TOF, Atmos. Meas. Tech., 3, 387-395, doi:10.5194/amt-3-387-2010, 2010.

Müller, M., George, C., and D'Anna, B.: Enhanced spectral analysis of C-TOF aerosol mass spectrometer data: iterative residual analysis and cumulative peak fitting, Int. J. Mass Spectrom., 306, 1–8, doi:10.1016/j.ijms.2011.04.007, 2011.

Müller, M., Mikoviny, T., Jud, W., D'Anna, B., and Wisthaler, A.: A new software tool for the analysis of high resolution PTR-TOF mass spectra, Chemometr. Intell. Lab., 127, 158–165, doi:10.1016/j.chemolab.2013.06.011, 2013.

Na, K., Song, C., and Cocker III, D. R.: Formation of secondary organic aerosol from the reaction of styrene with ozone in the presence and absence of ammonia and water, Atmos. Environ., 40, 1889-1900, doi: 10.1016/j.atmosenv.2005.10.063, 2006.

Nakayama, T. Suzuki, H., Kagamitani, S., and Ikeda, Y.: Characterization of a three wavelength Photoacoustic Soot Spectrometer (PASS-3) and a Photoacoustic Extinctiometer (PAX), J. Meteorol. Soc. Japan, 93(2), 285–308, doi:10.2151/jmsj.2015-016, 2015.

Natangelo, M., Mangiapan, S., Bagnati, R., Benfenati, E., and Fanelli, R.: Increased concentrations of nitrophenols in leaves from a damaged forestal site, Chemosphere, 38, 1495–1503, doi: 10.1016/S0045-6535(98)00370-1, 1999.

Nepal Oil Corporation Limited: http://www.nepaloil.com.np/import-and-sales-22.html, last access: 8 January, 2015.

Ng, N. L., Kroll, J. H., Chan, A. W. H., Chhabra, P. S., Flagan, R. C., and Seinfeld, J. H.: Secondary organic aerosol formation from m-xylene, toluene, and benzene, Atmos. Chem. Phys., 7, 3909–3922, doi:10.5194/acp-7-3909-2007, 2007.

Novakov, T. and Penner, J. E.: Large contribution of organic aerosols to cloud-condensation-nuclei concentrations, Nature, 365, 823–826, 1993.

Ntziachristos, L., Mamakos, A., Samaras, Z., Xanthopoulos, A., and Iakovou, E.: Emission control options for power two wheelers in Europe, Atmos. Environ., 40, 4547-4561, doi: 10.1016/j.atmosenv.2006.04.003, 2006.

Ntziachristos, L., Geivanidis, S., Samaras, Z., Xanthopoulos, A., Steven, H., and Bugsel, B.: Study on possible new measures concerning motorcycle emissions, Revised Version, Report No: 08.RE.0019.V4, European Commission, Brussels, 2009. Available at: http://righttoride.eu/regulationdocuments/report_measures_motorcycle_emissions_en.pdf

Nyman, J. A. and Chabreck, R. H.: Fire in coastal marshes: history and recent concerns, Fire in the wetlands: a management perspective, in: Tall Timbers Fire Ecology Conference 19th Proceedings, Tallahassee, FL, 134–141, 1995

Oanh, N. T. K., Bich, T. L., Tipayarom, D., Manadhar, B. R., Prapat, P., Simpson, C. D., and Liu, L.-J. S.: Characterization of particulate matter emission from open burning of rice straw, Atmos. Environ., 45, 493–502, 2011.

Oanh, N. T. K., Phuong, M. T. T., and Permadi, D. A.: Analysis of motorcycle fleet in Hanoi for estimation of air pollution emission and climate mitigation co-benefit of technology implementation, Atmos. Environ., 59, 438-448, doi:10.1016/j.atmosenv.2012.04.057, 2012.

OCIA: Organisation Internationale des Constructeurs d'Automobiles http://www.oica.net/category/production-statistics/, last access: 31 October 2013, 2013.

Olariu, R. I., Klotz, B., Barnes, I., Becker, K. H., and Mocanu, R.: FT-IR study of the ring-retaining products from the reaction of OH radicals with phenol, o-, m-, and p-cresol, Atmos. Environ., 36, 3685–3697, doi: 10.1016/S1352-2310(02)00202-9, 2002.

Organic Matter in Clays: Detailed Overview: available at: https://digitalfire.com/4sight/education/organic_matter_in_clays_detailed_overview_325.html, last access: 11 January, 2015.

Ortiz-Montalvo, D. L., Lim, Y. B., Perri, M .J., Seitzinger, S. P., Turpin, B. J.: Volatility and Yield of Glycolaldehyde SOA formed through Aqueous Photochemistry and Droplet Evaporation, Aerosol Sci. Technol., 46, 1002−1014, doi:10.1080/02786826.2012.686676, 2012.

Ortega, J., Turnipseed, A., Guenther, A. B., Karl, T. G., Day, D. A., Gochis, D., Huffman, J. A., Prenni, A. J., Levin, E. J. T., Kreidenweis, S. M., DeMott, P. J., Tobo, Y., Patton, E. G., Hodzic, A., Cui, Y. Y., Harley, P. C., Hornbrook, R. S., Apel, E. C., Monson, R. K., Eller, A. S. D., Greenberg, J. P., Barth, M. C., Campuzano-Jost, P., Palm, B. B., Jimenez, J. L., Aiken, A. C., Dubey, M. K., Geron, C., Offenberg, J., Ryan, M. G., Fornwalt, P. J., Pryor, S. C., Keutsch, F. N., DiGangi, J. P., Chan, A. W. H., Goldstein, A. H., Wolfe, G. M., Kim, S., Kaser, L., Schnitzhofer, R., Hansel, A., Cantrell, C. A., Mauldin, R. L., and Smith, J. N.: Overview of the Manitou Experimental Forest Observatory: site description and selected science results from 2008 to 2013, Atmos. Chem. Phys., 14, 6345-6367, doi:10.5194/acp-14-6345-2014, 2014.

Owen, E. and Jayasuriya, M. C. N.: Use of crop residues as animal feed in developing countries, Research and Development in Agriculture, 6, 129-138, 1989.

Page, S. E., Siegert, F., Rieley, J. O., Boehm, H. D. V., Jaya, A., and Limin, S.: The amount of carbon released from peat and forest fires in Indonesia during 1997, Nature, 420, 61–65, doi:10.1038/nature01131, 2002.

Pang, Y., Fuentes, M., and Rieger, P.: Trends in the emissions of volatile organic compounds (VOCs) from light-duty gasoline vehicles tested on chassis dynamometers in Southern California, Atmos. Environ., 83, 127-135, doi:10.1016/j.atmosenv.2013.11.002, 2014.

Park, R. J., Jacob, D. J., and Logan, J. A.: Fire and biofuel contributions to annual mean aerosol concentrations in the United States, Atmos. Environ., 41, 7389–7400, 2007.

Park, M., Randel, W. J., Emmons, L. K., Bernath, P. F., Walker, K. A., and Boone, C. D.: Chemical isolation in the Asian monsoon anticyclone observed in Atmospheric Chemistry Experiment (ACE-FTS) data, Atmos. Chem. Phys., 8, 757–764, doi:10.5194/acp-8-757-2008, 2008.

Parker, L. and Blodgett, J.: Greenhouse Gas Emissions: Perspectives on the Top 20 Emitters and Developed versus Developing Nations, Congressional Research Service (CRS) Report for Congress, RL32721, Washington DC, 2008.

Pehlken, A. and Essadiqi, E.: Scrap tire recycling in Canada CANMET-MCL, Report for Natural Resources Canada, Ottawa, Canada, MTL 2005-08(CF), 2005.

Pelkmans, L. and Debal, P.: Comparison of on-road emissions with emissions measured on chassis dynamometer test cycles, Transpn. Res. –D, 11, 233-241,doi: 10.1016/j.trd.2006.04.001, 2006.

Perry, R. and Gee, I. L.: Vehicle emissions in relation to fuel composition, Sci. Total Environ., 169, 149-156, doi:10.1016/0048-9697(95)04643-F, 1995.

Petters, M. D., M. T. Parsons, A. J. Prenni, P. J. DeMott, S. M. Kreidenweis, C. M. Carrico, A. P. Sullivan, G. R. McMeeking, E. Levin, C. E. Wold, J. L. Collett, Jr., and H. Moosmüller: Ice nuclei emissions from biomass burning, J. Geophys. Res., 114, D07209, doi: 10.1029/2008JD011532, 2009.

Pfister, G. G., Emmons, L. K., Hess, P. G., Honrath, R., Lamarque, J. –F., Val Martin, M., Owen, R. C., Avery, M. A., Browell, E. V., Holloway, J. S., Nedelec, P., Purvis, R., Ryerson, T. B., Sachse, G. W., and Schlager, H.: Ozone production from the 2004 North American boreal fires, J. Geophys. Res., 111 (D24), doi: 10.1029/2006JD007695, 2006.

Pfister, G. G., Wiedinmyer, C., and Emmons, L. K.: Impacts of the fall 2007 California wildfires on surface ozone: Integrating local observation with global model simulations, Geophys. Res. Lett., 35, L19814, doi:10.1029/2008GL034747, 2008.

Phousongphouang, P. T. and Arey, J.: Rate constants for the gas- phase reactions of a series of alkylnaphthalenes with the OH radical, Environ. Sci. Technol., 36, 1947–1952, doi: 10.1021/es011434c, 2002.

Pittman, C. U., Jr.: Mohan, D., Eseyin, A., Li, Q., Ingram, L., Hassan, E.-B., M., Mitchell, B., Guo, H., and Steele, P. H.: Characterization of bio-oils produced from fast pyrolysis of corn stalks in an auger reactor, Energy Fuels, 26, 3816-3825, doi: 10.1021/ef3003922, 2012.

Platt, S. M., El Haddad, I., Zardini, A. A., Clairotte, M., Astorga, C., Wolf, R., Slowik, J. G., Temime-Roussel, B., Marchand, N., Ježek, I., Drinovec, L., Močnik, G., Möhler, O., Richter, R., Barmet, P., Bianchi, F., Baltensperger, U., and Prévôt, A. S. H.: Secondary organic aerosol formation from gasoline vehicle emissions in a new mobile environmental reaction chamber, Atmos. Chem. Phys., 13, 9141-9158, doi:10.5194/acp-13-9141-2013, 2013.

Platt, S. M., Haddad, I. E., Pieber, R. –J., Zardini, A. A., Clairotte, M., Suarez-Bertoa, R., Barmet, P., Pfaffenberger, L., Wolf, R., Slowik, J. G., Fuller, S. J., Kalberer, M., Chirico, R., Dommen, J., Astorga, C., Zimmermann, R., Marchand, N., Hellebust, S., Temime-Roussel, B., Baltensperger, U., and Prévôt, A. S. H.: Two-stroke scooters are a dominant source of air pollution in many cities, Nat. Commun., 5, 379, doi: 10.1038/ncomms4749, 2014.

Pokhrel, D., and Viraraghavan, T.: Municipal solid waste management in Nepal: practices and challenges, Waste Manag., 25, 555-562, doi:10.1016/j.wasman.2005.01.020, 2005.

Popp, P. J., Bishop, G. A., and Stedman, D. H.: Development of a high-speed ultraviolet spectrometer for remote sensing of mobil source nitric oxide emissions, J. Air and Waste Manage. Assoc., 49, 1463-1468, doi:10.1080/10473289.1999.10463978, 1999.

Pratt, K. A., Murphy, S. M., Subramanian, R., DeMott, P. J., Kok, G. L., Campos, T., Rogers, D. C., Prenni, A. J., Heymsfield, A. J., Seinfeld, J. H. and Prather, K. A.: Flight-based chemical characterization of biomass burning aerosols within two prescribed burn smoke plumes, Atmos. Chem. Phys., 11(24), 12549–12565, doi:10.5194/acp-11-12549-2011, 2011.

Praveen, P. S., Ahmed, T., Kar, A., Rehman, I. H., and Ramanathan, V.: Link between local scale BC emissions in the Indo-Gangetic Plains and large scale atmospheric solar absorption, Atmos. Chem. Phys., 12, 1173-1187, doi:10.5194/acp-12-1173-2012, 2012.

Presto, A. A., Miracolo, M. A., Donahue, N. M., and Robinson, A. L.: Secondary organic aerosol formation from high NO_x photo-oxidation of low volatility precursors: n-Alkanes, Environ. Sci. Technol., 44(6), 2029-2034, doi:10.1021/es903712r, 2010.

Putero, D., Cristofanelli, P., Marinoni, A., Adhikary, B., Duchi, R., Shrestha, S. D., Verza, G. P., Landi, T. C., Calzolari, F., Busetto, M., Agrillo, G., Biancofiore, F., Di Carlo, P., Panday, A. K., Rupakheti, M., and Bonasoni, P.: Seasonal variation of ozone and black carbon observed at Paknajol, an urban site in the Kathmandu Valley, Nepal, Atmos. Chem. Phys. Discuss., 15, 22527-22566, doi:10.5194/acpd-15-22527-2015, 2015.

Radke, L. F., Hegg, D. A., Hobbs, P. V., Nance, J. D., Lyons, J. H., Laursen, K. K., Weiss, R. E., Riggan, P. J. and Ward, D. E.: Particulate and trace gas emissions from large biomass fires in North America, in Global Biomass Burning: Atmospheric, Climatic, and Biospheric Implications, Levine, J. S., MIT Press, Cambridge, MA, USA, 209–224, 1991.

Ramanathan, V. and Carmichael, G.: Global and regional climate changes due to black carbon, Nature Geoscience, 1, 221-227, doi:10.1038/ngeo156, 2008.

Randel, W. J., Park, M., Emmons, L., Kinnison, D., Bernath, P., Walker, K. A., Boone, C., and Pumphrey, H.: Asian monsoon transport of pollution to the stratosphere, Science, 328 (5978), 611-613, doi: 10.1126/science.1182274, 2010.

Randerson, J. T., van der Werf, G. R., Collatz, G. J., Giglio, L., Still, C. J., Kasibhatla, P., Miller, J. B., White, J. W. C., De-Fries, R. S., and Kasischke, E. S.: Fire emissions from C3 and C4 vegetation and their influence on interannual variability of atmospheric CO2 and d13CO2, Global Biogeochem. Cy., 19, GB2019, doi:10.1029/2004GB002366, 2005.

Randerson, J. T., Chen, Y., van der Werf, G. R., Rogers, B. M., and Morton, D. C.: Global burned area and biomass burning emissions from small fires, J. Geophys. Res., 117, G04012, doi:10.1029/2012JG002128, 2012.

Rappold, A. G., Stone, S. L., Cascio, W. E., Neas, L. M., Kilaru, V. J., Carraway, M. S., Szykman, J. J., Ising, A., Cleve, W. E., Meredith, J. T., Vaughan-Batten, H., Deyneka, L., and Devlin. R. B.: Peat bog wildfire smoke exposure in rural North Carolina is associated with cardiopulmonary emergency department visits assessed through syndromic surveillance, Environ. Health Perspect., 119, 1415–1420, 2011.

Rehbein, P. J. G., Jeong, C.-H., J., McGuire, M . L., Yao, X., Corbin, J. C., and Evans, G. J.: Cloud and fog processing enhanced gas-to-particle partitioning of trimethylamine, Environ. Sci. Technol., 45, 4346-4352, doi: 10.1021/es1042113, 2011.

Reid, J. S., Hobbs, P. V., Ferek, R. J., Martins, J. V., Blake, D. R., Dunlap, M. R., and Liousse, C.: Physical, chemical, and radiative characteristics of the smoke dominated regional hazes over Brazil, J. Geophys. Res., 103, 32059–32080, doi:10.1029/98JD00458, 1998.

Reid, J. S., Koppmann, R., Eck, T. F., and Eleuterio, D. P.: A review of biomass burning emissions part II: intensive physical properties of biomass burning particles, Atmos. Chem. Phys., 5, 799-825, doi:10.5194/acp-5-799-2005, 2005a.

Reid, J. S., Eck, T. F., Christopher, S. A., Koppmann, R., Dubovik, O., Eleuterio, D. P., Holben, B. N., Reid, E. A., and Zhang, J.: A review of biomass burning emissions part III: intensive optical properties of biomass burning particles, Atmos. Chem. Phys., 5, 827-849, doi:10.5194/acp-5-827-2005, 2005b.

Reid, J. S., Hyer, E. J., Johnson, R., Holben, B. N., Yokelson, R. J., Zhang, J., Campbell, J. R., Christopher, S. A., Di Girolamo , L., Giglio, L., Holz, R. E., Kearney, C., Miettinen, J., Reid, E. A., Turk, F. J., Wang, J., Xian, P., Zhao, G., Balasubramanian, R., Chew, B. N., Janai, S., Lagrosas, N., Lestari, P., Lin, N.-H., Mahmud, M.. Nguyen, A. X., Norris, B., Oahn, N. T.K., Oo, M., Salinas, S. V., Welton, E. J., Liew, S. C.: Observing and understanding the Southeast Asian aerosol system by remote sensing: An initial review and analysis for the Seven Southeast Asian Studies (7SEAS) program, Atmos. Res., 122, 403-468, doi:10.1016/j.atmosres.2012.06.005, 2013.

Richards, G. N.: Glycolaldehyde from pyrolysis of cellulose, J. Anal. Appl. Pyrolysis, 10, 251-255, doi:10.1016/0165-2370(87)80006-2, 1987.

Rippen, G., Zietz, E., Frank, R., Knacker, T., Klöpffer, W.: Do airborne nitrophenols contribute to forest decline? Environ.Technol. Lett., 8, 475–482, doi: 10.1080/09593338709384508, 1987.

RMA: U.S. Scrap tire management summary, Rubber Manufacturers Association, Washington DC, available at: http://www.rma.org/download/scrap-tires/market-reports/US_STMarkets2009.pdf (last access: April 9, 2014), 2011.

Roden, C. A., Bond, T. C., Conway, S., Pinel, A. B. O., MacCarty, N., and Still, D. Laboratory and field investigations of particulate and carbon monoxide emissions from traditional and improved cookstoves, Atmos. Environ., 43, 1170−1181, doi:10.1016/j.atmosenv.2008.05.041, 2008.

Rosenfeld, D.: TRMM observed first direct evidence of smoke from forest fires inhibiting rainfall, Geophys. Res. Lett., 26 (20), 3105-3108, doi: 10.1029/1999GL006066, 1999.

Rohr, A. C., and Wyzga, R. E.: Attributing health effects to individual particulate matter constituents, Atmos. Environ., 62, 130-152, 2012.

Roth, C.: Micro-Gasification: Cooking with Gas from Biomass, Deutsche Gesellschaft fur Internationalle Zusammenarbeit (GIZ) GmbH, Eschborn, Germany, 2011.

Rothman, L. S., Gordon, I. E., Barbe, A., Benner, D. C., Bernath, P. F., Birk, M., Boudon, V., Brown, L. R., Campargue, A., Champion, J. P., Chance, K., Coudert, L. H., Dana, V., Devi, V. M., Fally, S., Flaud, J. M., Gamache, R. R., Goldman, A., Jacquemart, D., Kleiner, I., Lacome, N., Lafferty, W. J., Mandin, J. Y., Massie, S. T., Mikhailenko, S. N., Miller, C. E., Moazzen-Ahmadi, N., Naumenko, O. V., Nikitin, A. V., Orphal, J., Perevalov, V. I., Perrin, A., Predoi-Cross, A., Rinsland, C. P., Rotger, M., Simeckov´a, M., Smith, M. A. H., Sung, K., Tashkun, S. A., Tennyson, J., Toth, R. A., Vandaele, A. C., and Vander Auwera, J.: The HITRAN 2008 molecular spectroscopic database, J. Quant. Spectrosc. Ra., 110, 533–572, doi:10.1016/j.jqsrt.2009.02.013, 2009.

Ryerson, T.B., Andrews, A. E., Angevine, W. M., Bates, T. S., Brock, C. A., Cairns, B., Cohen, R. C., Cooper, O. R., de Gouw, J. A., Fehsenfeld, F. S., Ferrare, R. A., Fischer, M. L., Flagan, R. C., Goldstein, A. H., Hair, J. W., Hardesty, R. M., Hostetler, C. A., Jimenez, J. L., Langford, A. O., McCauley, E., McKeen, S. A., Molina, L. T., Nenes, A., Oltmans, S. J., Parrish, D. D., Pederson, J. R., Pierce, R. B., Prather, K., Quinn, P. K., Seinfeld, J. H., Senff, C. J., Sorooshian, A., Stutz, J., Surratt, J. D., Trainer, M., Volkamer, R., Williams, E. J., and Wofsy, S. C.: The 2010 California Research at the Nexus of Air Quality and Climate Change (CalNex) field study, J. Geophys. Res. Atmos., 118, 5830-5866, doi:10.1002/jgrd.50331, 2013.

Saleh, R., Robinson, E. S., Tkacik, D. S., Ahern, A. T., Liu, S., Aiken, A. C., Sullivan, R. C., Presto, A. A., Dubey, M. K., Yokelson, R. J., Donahue, N. M., and Robinson, A. L.: Brownness of organics in aerosols from biomass burning linked to their black carbon content, Nat. Geosci., 7, 647-650, doi: 10.1038/NGEO2220, 2014.

Sand, M., Berntsen, T. K., Kay, J. E., Lamarque, J. F., Seland, Ø., and Kirkevåg, A.: The Arctic response to remote and local forcing of black carbon, Atmos. Chem. Phys., 13, 211-224, doi:10.5194/acp-13-211-2013, 2013.

Sarkar, C., Sinha, V., Kumar, V., Rupakheti, M., Panday, A., Mahata, K. S., Rupakheti, D., Kathayat, B., and Lawrence, M. G.: Overview of VOC emissions and chemistry from PTR-TOF-MS measurements during the SusKat-ABC campaign: high acetaldehyde, isoprene and isocyanic acid in wintertime air of the Kathmandu Valley, Atmos. Chem. Phys. Discuss., 15, 25021-25087, doi:10.5194/acpd-15-25021-2015, 2015

Schade, G. W., and Crutzen, P. J.: Emission of aliphatic amines from animal husbandry and their reactions: Potential source of N_2O and HCN, J. Atmos. Chem., 22, 319-346, doi: 10.1007/BF00696641, 1995.

Schiller, C.L., Locquiao, S., Johnson, T.J., Harris, G.W.: Atmospheric measurements of HONO by tunable diode laser absorption spectroscopy, Journal of Atmospheric Chemistry, 40, 275–293, 2001.

Schimel, D., Alves, D., Enting, I., Heimann, M., Joos, F., Raynaud, D., Wigley, T., Prather, M., Derwent, R., Ehhalt, D., Fraser, P., Sanhueza, E., Zhou, X., Jonas, P., Charlson, R., Rodhe, H., Sadasivan, S., Shine, K. P., Fouquart, Y., Ramaswamy, V., Solomon, S., Srinivasan, J., Albritton, D., Isaksen, I., Lal, M., Wuebbles, D.: Radiative forcing of climate change: Climate Change 1995: The Science of Climate Change, Houghton J. T., Meira Filho L. G., Callander B. A., Harris N., Kattenberg, A., Maskell, K.**,** Cambridge Univ. Press, Cambridge, 1996.

Shafizadeh, F.: Introduction to pyrolysis of biomass, J. Anal. Appl. Pyrolysis, 3, 283-305, doi: 10.1016/0165-2370(82)80017-X, 1982.

Shah, T., Molden, D., Sakthivadivel, R., and Seckler, D.: The Global Groundwater Situation: Overview and Opportunities and Challenges, International Water Management Institute, Colombo, Sri Lanka, 2000.

Sharpe, S. W., Johnson, T. J., Sams, R. L., Chu, P. M., Rhoderick, G. C., and Johnson, P. A.: Gas-phase databases for quantitative infrared spectroscopy, Appl. Spectrosc., 58, 1452–1461, 2004.

Shea, R. W., Shea, B. W., Kauffman, J. B, Ward, D. E., Haskins, C. I., and Scholes M. C.: Fuel biomass and combustion factors associated with fires in savanna ecosystems of South Africa and Zambia, J. Geophys. Res., 101, 23,551–23,568, doi:10.1029/95JD02047, 1996.

Shon, Z., and Kim, K.: Photochemical oxidation of reduced sulfur compounds in an urban location based on short time monitoring data, Chemosphere, 63,1859-1869, doi: 10.1016/j.chemosphere.2005.10.021, 2006.

Shrestha, S. R., Oanh, N. T. K., Zu, Q., Rupakheti, M., and Lawrence, M. G.: Analysis of the vehicle fleet in the Kathmandu Valley for estimation of environment and climate co-benefits of technology intrusions, Atmos. Environ., 81, 579-590, doi:10.1016/j.atmosenv.2013.09.050, 2013.

Simmleit, N., and Schulten, H.-S.: Thermal degradation products of spruce needles, Chemosphere, 18, 1855-1869, doi: 10.1016/0045-6535(89)90469-4, 1989.

Simoneit, B. R. T., Rogge, W. F., Mazurek, M. A., Standley, L. J., Hildemann, L. M., Cass, G. R.: Lignin pyrolysis products, lignans, and resin acids as specific tracers of plant classes in emissions from biomass combustion, Environ. Sci. Technol., 27, 2533–2541, doi: 10.1021/es00048a034, 1993.

Simoneit, B. R. T., Kobayashi, M., Mochida, M., Kawamura, K., and Huebert, B. J.: Aerosol particles collected on aircraft flights over the northwestern Pacific region during the ACE-Asia campaign: Composition and major sources of the organic compounds, J. Geophys. Res., 109, D19S09, doi:10.1029/2004JD004565, 2004a.

Simoneit, B. R. T., Kobayashi, M., Mochida, M., Kawamura, K., Lee, M., Lim, H.-J., Turpin, B. J., and Komazaki, Y.: Composition and major sources of organic compounds of aerosol particulate matter sampled during the ACE-Asia campaign, J. Geophys. Res., 109, D19S10, doi:10.1029/2004JD004598, 2004b.

Simpson, I. J., Rowland, F. S., Meinardi, S., and Blake, D. R.: Influence of biomass burning during recent fluctuations in the slow growth of global tropospheric methane, Geophys. Res. Lett., 33, L22808, doi:10.1029/2006GL027330, 2006.

Simpson, I. J., Akagi, S. K., Barletta, B., Blake, N. J., Choi, Y., Diskin, G. S., Fried, A., Fuelberg, H. E., Meinardi, S., Rowland, F. S., Vay, S. A., Weinheimer, A. J., Wennberg, P. O., Wiebring, P., Wisthaler, A., Yang, M., Yokelson, R. J., and Blake, D. R.: Boreal forest fire emissions in fresh Canadian smoke plumes: C1-C10 volatile organic compounds (VOCs), CO_2, CO, NO_2, NO, HCN and CH_3CN, Atmos. Chem. Phys., 11, 6445-6463, doi:10.5194/acp-11-6445-2011, 2011.

Sinha, P., Hobbs, P. V., Yokelson, R. J., Bertschi, I. T., Blake, D. R., Simpson, I. J., Gao, S., Kirchstetter, T. W., and Novakov, T.: Emissions of trace gases and particles from savanna fires in southern Africa, J. Geophys. Res., 108, 8487, doi:10.1029/2002JD002325, 2003.

Sinha, V., Kumar, V., and Sarkar, C.: Chemical composition of pre-monsoon air in the Indo-Gangetic Plain measured using a new air quality facility and PTR-MS: high surface ozone and strong influence of biomass burning, Atmos. Chem. Phys., 14, 5921-5941, doi:10.5194/acp-14-5921-2014, 2014.

Sjöström, E. Wood chemistry: fundamentals and applications, Second edition, Academic Press, San Diego, USA, 1993.

Smith, J. N., Dunn, M. J., VanReken, T. M., Iida, K., Stolzenburg, M. R., McMurry, P. H., and Huey, L. G.: Chemical composition of atmospheric nanoparticles formed from nucleation in Tecamac, Mexico: Evidence for an important role for organic species in nanoparticle growth, Geophys. Res. Lett., 35, L04808, doi:10.1029/2007gl032523, 2008.

Smith, K., Uma, R., Kishore, V. V. N., Lata, K., Joshi, V., Zhang, J., Rasmussen, R. A., and Khalil, M. A. K.: Greenhouse gases from small-scale combustion devices in developing countries: Household stoves in India, Rep. EPA-600/R-00-052, U.S. Environ. Prot. Agency, Research Triangle Park, N. C., 2000.

Smith, K. R., Frumkin, H., Balakrishnan, K., Butler, C. D., Chafe, Z. A., Fairlie, I., Kinney, P., Kjellstrom, T., Mauzerall, D. L., McKone, T. E., McMichael, A. J., and Schneider, M.: Energy and human health, Annu. Rev. Public Health, 34, 1–25, 2013.

Smith, K. R., Frumkin, H., Balakrishnan, K., Butler, C. D., Chafe, Z. A., Fairlie, I., Kinney, P., Kjellstrom, T., Mauzerall, D. L., McKone, T. E., McMichael, A. J., and Schneider, M.: Energy and human health, Annu. Rev. Public Health, 34, 1–25, doi: 10.1146/annurev-publhealth-031912-114404, 2013.

Smith, S. J., Pitcher, H., and Wigley, T. M. L.: Global and regional anthropogenic sulfur dioxide emissions, Global and Planetary Change, 29, 99-119, 2001.

Smith, S.J., van Aardenne, J., Klimont, Z., Andres, R. J., Volke, A., and Delgado Arias, S.: Anthropogenic sulfur dioxide emissions: 1850-2005, Atmos. Chem. Phys., 11, 1101-1116, doi:10.5194/acp-11-1101-2011, 2011.

Song, C., Na, K., Warren, B., Malloy, Q., and Cocker, D. R.: Impact of propene on secondary organic aerosol formation from m-xylene, Environ. Sci. Technol., 41, 6990–6995, doi: 10.1021/es062279a, 2007.

Sotiropoulou, R. E. P., Tagaris, E., Pilinis, C., Anttila, T., and Kulmala, M.: Modeling new particle formation during air pollution episodes: Impacts on aerosol and cloud condensation nuclei, Aerosol Sci. Tech., 40, 557–572, doi: 10.1080/02786820600714346, 2006.

St. Clair, J. M., Spencer, K. M., Beaver, M. R., Crounse, J. D., Paulot, F., and Wennberg, P. O.: Quantification of hydroxyacetone and glycolaldehyde using chemical ionization mass spectrometry, Atmos. Chem. Phys., 14, 4251-4262, doi:10.5194/acp-14-4251-2014, 2014.

Streets, D. G., Yarber, K. F., Woo, J. H., and Carmichael, G. R.: Biomass burning in Asia: annual and seasonal estimates and atmospheric emissions, Global Biogeochem. Cy., 17(4), 1099, doi:10.1029/2003GB002040, 2003.

Stockwell, C. E., Yokelson, R. J., Kreidenweis, S. M., Robinson, A. L., DeMott, P. J., Sullivan, R. C., Reardon, J., Ryan, K. C., Griffith, D. W. T., and Stevens, L.: Trace gas emissions from combustion of peat, crop residue, domestic biofuels, grasses, and other fuels: configuration and Fourier transform infrared (FTIR) component of the fourth Fire Lab at Missoula Experiment (FLAME-4), Atmos. Chem. Phys., 14, 9727-9754, doi:10.5194/acp-14-9727-2014, 2014.

Stockwell, C. E., Veres, P. R., Williams, J., and Yokelson, R. J.: Characterization of biomass burning emissions from cooking fires, peat, crop residue, and other fuels with high-resolution proton-transfer-reaction time-of-flight mass spectrometry, Atmos. Chem. Phys., 15, 845-865, doi: 10.5194/acp-15-845-2015, 2015.

Streets, D. G., Yarber, K. F., Woo, J. H., and Carmichael, G. R.: Biomass burning in Asia: annual and seasonal estimates and atmospheric emissions, Global Biogeochem. Cy., 17, 1099, doi:10.1029/2003GB002040, 2003.

Strollo, C. M., and Ziemann, P. J.: Products and mechanism of secondary organic aerosol formation from the reaction of 3-methylfuran with OH radicals in the presence of NO_x, Atmos. Environ., 77, 534-543, doi: 10.1016/j.atmosenv.2013.05.033, 2013.

Subramanian, R., Roden, C. A., Boparai, P., and Bond, T. C.: Yellow beads and missing particles: Trouble ahead for filter-based absorption measurements, Aerosol Sci. Technol., 41, 630-637, doi:10.1080/02786820701344589, 2007.

Thompson, A. M.: The oxidizing capacity of the Earth's atmosphere: Probable past and future changes, Science, 256(5060), 1157-1165, doi: 10.1126/science.256.5060.1157, 1992.

Tkacik, D., Robinson, E., Ahern, A., Saleh, R., Veres, P., Stockwell, C., Simpson, I., Meinardi, S., Blake, D., Presto, A., Sullivan, R., Donahue, N., and Robinson, A.: A dual chamber enhancement method to quantify aerosol formation: biomass burning secondary organic aerosol, in preparation, 2016.

Toda, K., Obata, T., Obokin, V. A., Potemkin, V. L., Hirota, K., Takeuchi, M., Arita, S., Khodzher, T. V., and Grachev, M. A.: Atmospheric methanethiol emitted from a pulp and paper plant on the shore of Lake Baikal, Atmos. Environ., 44, 2427-2433, doi: 10.1016/j.atmosenv.2010.03.037, 2010.

Toon, O. B., and Ackerman, T. P.: Algorithms for the calculation of scattering by stratified spheres, Appl. Opt., 20, 3657-3660, doi: 10.1364/AO.20.003657, 1981.

Trentmann, J., Andreae, M. O., and Graf, H.-.F: Chemical processes in a young biomass-burning plume, J. Geophys. Res., 108, 4705, doi: 10.1029/2003JD003732, 2003.

Trentmann, J., Yokelson, R. J., Hobbs, P. V., Winterrath, T., Christian, T. J., Andreae, M. O., and Mason, S. A.: An analysis of the chemical processes in the smoke plume from a savanna fire, J. Geophys. Res., 110, D12301, doi:10.1029/2004JD005628, 2005.

Tsai, W. Y., Chan, L. Y., Blake, D. R., and Chu, K. W.: Vehicular fuel composition and atmospheric emissions in South China: Hong Kong, Macau, Guangzhou, and Zhuhai, Atmos. Chem. Phys., 6, 3281-3288, doi:10.5194/acp-6-3281-2006, 2006.

Turetsky, M. R., Kane, E. S., Harden, J. W., Ottmar, R. D., Manies, K. L., Hoy E., and Kasischke, E. S.: Recent acceleration of biomass burning and carbon losses in Alaskan forests and peatlands, Nature Geoscience, 4, 27–31, doi:10.1038/ngeo1027, 2011.

UNFPA: State of the world population 2012, E.12.III.H., Information and External Relations Division of UNFPA, United Nations Population Fund, New York, 2012.

USEPA: Motor vehicle-related air toxics study, available at: http://www3.epa.gov/otaq/regs/toxics/airtox1a.pdf (last access: 11 November 2015), United States Environmental Protection Agency, 1993.

USEPA: Air Emissions from Scrap Tire Combustion, EPA-600/R-97-115, Office of Research and Development, Washington DC, 1997.

USEPA: Compilation of air pollutant emission factors (AP-42), Section 11.3: Brick and structural clay product manufacturing, Midwest Research Institute for the Office of Air Quality Planning and Standards, U.S. Environmental Protection Agency, 1997.

USEPA: An inventory of sources and environmental releases of dioxin-like compounds in the United States for the years 1987, 1995, and 2000, EPA/600/P-03/002F, National Center for Environmental Assessment, Office of Research and Development, Washington, DC, 677 pp., 2006.

USEPA: Environmental and sustainable technology evaluation: Biomass co-firing in industrial boilers – Minnesota Power's Rapids Energy Center, United States Environmental Protection Agency, EPA/600/R-08/057, 2007.

USEPA: Plastics, available at: http: http://www3.epa.gov/climatechange/wycd/waste/downloads/plastics-chapter10-28-10.pdf (last access: 11 November 2015), United States Environmental Protection Agency, 2010.

USEPA: Inventory of U.S. Greenhouse Gas Emissions and Sinks: 1990-2011, EPA 430-R-13-001, Office of Atmospheric Programs, Washington DC, 2013.

USEPA: The Compilation of Air Pollutant Emission Factors, Volume I: Stationary Point and Area Sources, available at: http://www3.epa.gov/ttnchie1/ap42/, United States Environmental Protection Agency, 2015.

Vakkari, V., Kerminen, V.-M., Beukes, J. P., Tiitta, P., van Zyl, P. G., Josipovic, M., Venter, A. D., Jaars, K., Worsnop, D. R., Kulmala, M., and Laakso,L.: Rapid changes in biomass burning aerosols by atmospheric oxidation, Geophys. Res. Lett., 41, 2644-2651, doi:10.1002/2014GL059396, 2014.

van der A, R. J., Eskes, H. J., Boersma, K. F., van Noije, T. P. C., Van Roozendael, M., De Smedt, I., Peters, D. H. M. U., and Meijer, E.W.: Trends, seasonal variability and dominant NO_x source derived from a ten year record of NO_2 measured from space, J. Geophys. Res., 113, D04302, doi:10.1029/2007JD009021, 2008.

van der Werf, G. R., Randerson, J. T., Giglio, L., Collatz, G. J., Mu, M., Kasibhatla, P. S., Morton, D. C., DeFries, R. S., Jin, Y., and van Leeuwen, T. T.: Global fire emissions and the contribution of deforestation, savanna, forest, agricultural, and peat fires (19972009), Atmos. Chem. Phys., 10, 11707–11735, doi:10.5194/acp-10-11707-2010, 2010.

Vaughan, T. L., Strader, C., Davis, S., and Daling, J. R.: Formaldehyde and cancers of the pharynx, sinus and nasal cavity: II. Residential exposures, Int. J. Cancer, 38, 685-688, doi: 10.1002/ijc.2910380511, 1986.

Venkataraman, C., Habib, G., Eiguren-Fernandez, A., Miguel A. H., and Friedlander S. K.: Residential Biofuels in South Asia: Carbonaceous Aerosol Emissions and Climate Impacts, Science, 307, 1454-1456, doi:10.1126/science.1104359, 2005.

Veres, P., Roberts, J. M., Burling, I. R., Warneke, C., de Gouw, J., and Yokelson, R. J.: Measurements of gas-phase inorganic and organic acids from biomass fires by negative-ion proton-transfer chemical-ionization mass spectrometry, J. Geophys. Res., 115, D23302, doi:10.1029/2010JD014033, 2010.

Vestreng, V., Ntziachristos, L., Semb, A., Reis, S., Isaksen, I. S. A., and Tarrasón, L.: Evolution of NOx emissions in Europe with focus on road transport control measures, Atmos. Chem. Phys., 9, 1503-1520, doi:10.5194/acp-9-1503-2009, 2009.

Villanueva, F., Barnes, I., Monedero, E., Salgado, S., Gómez, M.V., Martin, P.: Primary product distribution from the Cl-atom initiated atmospheric degradation of furan: Environmental implications. Atmos. Environ., 41, 8796–8810, doi: 10.1016/j.atmosenv.2007.07.053, 2007.

Volkamer, R., Sheehy, P., Molina, L. T., and Molina, M. J.: Oxidative capacity of the Mexico City atmosphere – Part 1: A radical source perspective, Atmos. Chem. Phys., 10, 6969-6991, doi:10.5194/acp-10-6969-2010, 2010.

Wade, D. D. and Lunsford, J. D.: A guide for prescribed fire in southern forests, USDA Forest Service Southern Region, Atlanta, GA, USA, 56 pp., 1989.

Wagner, V., Jenkin, M.E., Saunders, S.M., Stanton, J., Wirtz, K., Pilling, M.J.: Modelling of the photooxidation of toluene: conceptual ideas for validating detailed mechanisms, Atmos. Chem. Phys., 3, 89–106, doi:10.5194/acp-3-89-2003, 2003.

Ward, D. E. and Radke, L. F.: Emissions measurements from vegetation fires: A Comparative evaluation of methods and results, in: Fire in the Environment: The Ecological, Atmospheric and Climatic Importance of Vegetation Fires, edited by: Crutzen, P. J. and Goldammer, J. G., John Wiley, New York, 53–76, 1993.

Warneke, C., Roberts, J. M., Veres, P., Gilman, J., Kuster, W. C., Burling, I., Yokelson, R. J., de Gouw, J. A.: VOC identification and inter-comparison from laboratory biomass burning using PTR-MS and PIT-MS, Int. J. Mass Spectrom. Ion Proc., 303, 6-14, doi: 10.1016/j.ijms.2010.12.002, 2011.

Washenfelder, R. A., Flores, J. M., Brock, C. A., Brown, S. S., and Rudich, Y.: Broadband measurements of aerosol extinction in the ultraviolet spectral region, Atmos. Meas. Tech., 6, 861-877, doi:10.5194/amt-6-861-2013, 2013.

Wattel-Koekkoek, E. J. W., van Genuchten, P. P. L., Buurman, P., and van Lagen, B.: Amount and composition of clay-associated soil organic matter in a range of kaolinitic and smectitic soils, 99, 27-49, doi:10.1016/S0016-7061(00)00062-8, 2001.

Webster, C. R., May, R. D., Trimble, C. A., Chave, R. G., and Kendall, J.: Aircraft (ER-2) laser infrared absorption spectrometer (ALIAS) for in-situ stratospheric measurements of HCI, N2O, CH4, NO2, and HNO3, Appl. Opt., 33, 454–472, doi:10.1364/AO.33.000454, 1994.

WECS: Energy consumption situation in Nepal (Year 2011/12), Water and Energy Commission Secretariat, Government of Nepal, Kathmandu, 2014.

Weyant, C., Athalye, V., Ragavan, S., Rajarathnam, U., Lalchandani, D., Maithel, S., Baum, E., and Bond, T. C.: Emissions from South Asian Brick Production, Environ. Sci. Technol., 48, 6477–6483, doi: 10.1021/es500186g, 2014.

WHO: Global Health Risks: Mortality and Burden of Disease Attributable to Selected Major Risks, Department of Health Statistics and Informatics in the Information, Evidence and Research Cluster of the World Health Organization, Geneva, Switzerland, 2009.

Wiedinmyer, C., Akagi, S. K., Yokelson, R. J., Emmons, L. K., Al-Saadi, J.A., Orlando, J. J., and Soja, A.J.: The Fire INventory from NCAR (FINN): a high resolution global model to estimate the emissions from open burning, Geosci. Model Dev., 4, 625-641, doi:10.5194/gmd-4-625-2011, 2011.

Wiedinmyer, C., Yokelson, R. J., and Gullett, B. K.: Global emissions of trace gases, particulate matter, and hazardous air pollutants from open burning of domestic waste, Environ. Sci. Technol., 48, 9523–9530, doi:10.1021/es502250z, 2014.

Williams, C. J., and Yakvitt, J. B.: Botanical composition of peat and degree of peat decomposition in three temperate peatlands, Ecoscience, 10, 85-95, 2003.

Woodall, B. D., Yamamoto, D. P., Gullett, B. K., and Touati, A.: Emissions from small-scale burns of simulated deployed U.S. military waste, Environ. Sci. Technol., 46, 10997-11003, doi: 10.1021/es3021556, 2012.

Wooster, M. J., Freeborn, P. H., Archibald, S., Oppenheimer, C., Roberts, G. J., Smith, T. E. L., Govender, N., Burton, M., and Palumbo, I.: Field determination of biomass burning emission ratios and factors via open-path FTIR spectroscopy and fire radiative power assessment: headfire, backfire and residual smouldering combustion in African savannahs. Atmos. Chem. Phys., 11, 11591–11615, doi:10.5194/acp-11-11591-2011, 2011.

Worden, J., Wecht, K., Frankenberg, C., Alvarado, M., Bowman, K., Kort, E., Kulawik, S., Lee, M., Payne, V., and Worden, H.: CH_4 and CO distributions over tropical fires during October 2006 as observed by the Aura TES satellite instrument and modeled by GEOS-Chem, Atmos. Chem. Phys., 13(7), 3679–3692, doi:10.5194/acp-13-3679-2013, 2013.

World Bank: Diesel Power Generation: Inventories and black carbon emissions in Kathmandu Valley, Nepal, International Bank for Reconstruction and Development, Washington DC, 2014.

Xiao, Q., Saikawa, E., Yokelson, R. J., Chen, P., Li, C., and Kang, S.: Indoor air pollution from burning yak dung as a household fuel in Tibet, 102, 406-412, doi:10.1016/j.atmosenv.2014.11.060, 2015.

Yanowitz, J., Graboski, M.S., Ryan, L.B.A., Alleman, T., and McCormick, R.: Chassis dynamometer study of emissions from 21 in-use heavy-duty diesel vehicles, Environ. Sci. Technol., 33, 209-216, doi:10.1021/es980458p, 1999.

Yee, L. D., Kautzman, K. E., Loza, C. L., Schilling, K. A., Coggen, M. M., Chhabra, P. S., Chan, M. N., Chan, A. W. H., Hersey, S. P., Crounse, J. D., Wennberg, P. O., Flagan, R. C., and Seinfeld, J. H.: Secondary organic aerosol formation from biomass burning intermediates: phenol and methoxyphenols, Atmos. Chem. Phys., 13, 8019-8043, doi:10.5194/acp-13-8019-2013, 2013.

Yevich, R. and Logan, J. A.: An assessment of biofuel use and burning of agricultural waste in the developing world, Global Biogeochem. Cy., 17(4), 1095, doi:10.1029/2002GB001952, 2003.

Yokelson, R. J., Griffith, D. W. T., and Ward, D. E.: Open path Fourier transform infrared studies of large-scale laboratory biomass fires, J. Geophys. Res., 101, 21067–21080, doi:10.1029/96JD01800, 1996.

Yokelson, R. J.,Ward, D. E., Susott, R. A., Reardon, J., and Griffith, D. W. T.: Emissions from smoldering combustion of biomass measured by open-path Fourier transform infrared spectroscopy, J. Geophys. Res., 102(D15), 18865–18877, 1997.

Yokelson, R. J., Goode, J. G., Ward, D. E., Susott, R. A., Babbitt, R. E., Wade, D. D., Bertschi, I., Griffith, D. W. T., and Hao, W. M.: Emissions of formaldehyde, acetic acid, methanol, and other trace gases from biomass fires in North Carolina measured by airborne Fourier transform infrared spectroscopy, J. Geophys. Res., 104, 30109–30125, doi:10.1029/1999jd900817, 1999.

Yokelson, R. J., Bertschi, I. T., Christian, T. J., Hobbs, P. V., Ward, D. E., and Hao,W. M.: Trace gas measurements in nascent, aged, and cloud-processed smoke from African savanna fires 30 by airborne Fourier transform infrared spectroscopy, AFTIR, with coincident measurements of aerosol optical depth, J. Geophys. Res., 108, 8478, doi:10.1029/2002JD002322, 2003a.

Yokelson, R. J., Christian, T. J., Bertschi, I. T., and Hao, W. M.: Evaluation of adsorption effects on measurements of ammonia, acetic acid, and methanol, J. Geophys. Res., 108, 4649, doi:10.1029/2003JD003549, 2003b.

Yokelson, R. J., Karl, T., Artaxo, P., Blake, D. R., Christian, T. J., Griffith, D. W. T., Guenther, A., and Hao, W. M.: The Tropical Forest and Fire Emissions Experiment: overview and airborne fire emission factor measurements, Atmos. Chem. Phys., 7, 5175–5196, doi:10.5194/acp-7-5175-2007, 2007.

Yokelson, R. J., Christian, T. J., Karl, T. G., and Guenther, A.: The tropical forest and fire emissions experiment: laboratory fire measurements and synthesis of campaign data, Atmos. Chem. Phys., 8, 3509–3527, doi:10.5194/acp-8-3509-2008, 2008.

Yokelson, R. J., Crounse, J. D., DeCarlo, P. F., Karl, T., Urbanski, S., Atlas, E., Campos, T., Shinozuka, Y., Kapustin, V., Clarke, A. D., Weinheimer, A., Knapp, D. J., Montzka, D. D., Holloway, J., Weibring, P., Flocke, F., Zheng, W., Toohey, D., Wennberg, P. O., Wiedinmyer, C., Mauldin, L., Fried, A., Richter, D., Walega, J., Jimenez, J. L., Adachi, K., Buseck, P. R., Hall, S. R., and Shetter, R.: Emissions from biomass burning in the Yucatan, Atmos. Chem. Phys., 9, 5785–5812, doi:10.5194/acp-9-5785-2009, 2009.

Yokelson, R. J., Burling, I. R., Urbanski, S. P., Atlas, E. L., Adachi, K., Buseck, P. R., Wiedinmyer, C., Akagi, S. K., Toohey, D. W., and Wold, C. E.: Trace gas and particle emissions from open biomass burning in Mexico, Atmos. Chem. Phys. 11, 6787-6808, doi:10.5194/acpd-11-6787-2011, 2011.

Yokelson, R. J., Burling, I. R., Gilman, J. B., Warneke, C., Stockwell, C. E., de Gouw, J., Akagi, S. K., Urbanski, S. P., Veres, P., Roberts, J. M., Kuster, W. C., Reardon, J., Griffith, D. W. T., Johnson, T. J., Hosseini, S., Miller, J.W., Cocker III, D. R., Jung, H., and Weise, D. R.: Coupling field and laboratory measurements to estimate the emission factors of identified and unidentified trace gases for prescribed fires, Atmos. Chem. Phys., 13, 89–116, doi:10.5194/acp-13-89-2013, 2013a.

Yokelson, R. J., Andreae, M. O., and Akagi, S. M.: Pitfalls with the use of enhancement ratios or normalized excess mixing ratios measured in plumes to characterize pollution sources and aging, Atmos. Meas. Tech., 6, 2155-2158, doi:10.5194/amt-6-2155-2013, 2013b.

Yu, F. and Luo, G.: Modeling of gaseous methylamines in the global atmosphere: impacts of oxidation and aerosol uptake, Atmos. Chem. Phys., 14, 12455–12464, doi:10.5194/acp-14-12455-2014, 2014.

Zachariadis, T., Ntziachristos, L., and Samaras, Z.: The effect of age and technological change on motor vehicle emissions, Transp. Res. Part D, 6, 221-227, doi: 10.1016/S1361-9209(00)00025-0, 2001.

Zavala, M., Herndon, S. C., Slott, R. S., Dunlea, E. J., Marr, L. C., Shorter, J. H., Zahniser, M., Knighton, W. B., Rogers, T. M., Kolb, C. E., Molina, L. T., and Molina, M. J.: Characterization of on-road vehicle emissions in the Mexico City Metropolitan Area using a mobile laboratory in chase and fleet average measurement modes during the MCMA-2003 field campaign, Atmos. Chem. Phys., 6, 5129-5142, doi:10.5194/acp-6-5129-2006, 2006.

Zhang, J., Smith, K. R., Ma, Y., Ye, S., Qi, W., Liu, P., Khalil, M. A. K., Rasmussen, R. A., and Thorneloe, S.A.: Greenhouse Gases and other airborne pollutants from household stoves in China: a database for emission factors, Atmos. Environ., 34, 4537–49, 2000.

Zhang, X., Lin, Y. –H., Surratt, J. D., Zotter, P., and Weber, R. J.: Sources, composition and absorption Ångström exponent of light-absorbing organic components in aerosol extracts from the Los Angeles Basin, Environ. Sci. Technol., 47, 3685–3693, doi:10.1021/ES305047B, 2013.

Zhang, Y., Stedman, D. H., Guenther, P. L., Beaton, S. P. and Peterson, J. E.: On-road hydrocarbon remote sensing in the Denver area, Environ. Sci. Technol., 27, 1885-1891, doi: 10.1021/es00046a018, 1993.

Zhang, Y., Stedman, D. H., Bishop, G. A., Guenther, P. L., and Beaton, S. P.: Worldwide on-road vehicle exhaust emissions study by remote sensing, Environ. Sci. Technol., 29, 2286-2294, doi: 10.1021/es00009a020, 1995.

Ziemann, P. J., and Atkinson, R.: Kinetics, products, and mechanisms of secondary organic aerosol formation, Chem. Soc. Rev., 41, 6582-6605, doi: 10.1039/c2cs35122f, 2012.

APPENDIX Supplementary Tables

Table S1. Fuel-type average emission factors (g/kg) calculated by OP-FTIR

Fuel type avg (stack burns, room burns)	African grass (19,1)	Alfalfa Organic CO (3)	Black Spruce AK(5,7)	Chamise CA (7,1)	Giant Cutgrass SC (5,3)	Hay Organic CO(6,2)	Juniper (2)	Manzanita CA (3,1)	Millet Ghana (2)
MCE	0.978(0.005)	0.918(0.008)	0.951(0.012)	0.929(0.020)	0.948(0.013)	0.949(0.007)	0.962(0.002)	0.943(0.013)	0.938(0.010)
Carbon Dioxide (CO_2)	1570(13)	1382(28)	1737(28)	1687(50)	1549(23)	1418(18)	1780(7)	1706(29)	1491(14)
Carbon Monoxide (CO)	22.7(4.7)	78.2(7.6)	57.0(13.5)	81.5(22.2)	53.7(13.1)	48.7(6.3)	45.0(1.8)	66.1(15.0)	62.5(10.3)
Methane (CH_4)	0.411(0.229)	5.38(2.07)	2.42(0.76)	3.13(1.46)	1.51(0.62)	2.73(1.13)	1.27(0.71)	2.04(0.38)	1.64(0.50)
Water (H_2O)	7.04E-2(1.67E-2)	2.15E-2(1.58E-2)	8.46E-2(4.18E-2)	5.73E-2(7.81E-2)	5.02E-2(2.14E-2)	3.36E-2(4.76E-2)	8.16E-2(1.07E-2)	8.71E-2(1.05E-1)	6.62E-2(2.66E-2)
Acetylene (C_2H_2)	6.75E-2(3.01E-2)	0.631(0.206)	0.751(0.284)	1.05(0.69)	0.438(0.270)	0.367(0.144)	0.220(0.029)	0.783(0.389)	0.184(0.048)
Ethylene (C_2H_4)	0.216(0.129)	2.18(0.05)	2.27(0.82)	2.38(1.53)	0.698(0.279)	1.26(0.28)	0.688(0.211)	1.77(0.71)	0.450(0.012)
Propylene (C_3H_6)	8.31E-2(2.73E-2)	1.27(0.38)	0.599(0.179)	0.535(0.308)	0.149(0.091)	0.602(0.268)	0.270(0.172)	0.410(0.184)	-
Methanol (CH_3OH)	0.152(0.129)	3.54(2.96)	0.972(0.301)	0.935(0.406)	0.214(0.235)	1.41(0.95)	0.379(0.223)	0.812(0.096)	0.356(0.183)
Formaldehyde (HCHO)	0.410(0.270)	1.24(0.43)	1.35(0.45)	1.63(0.90)	0.421(0.220)	0.999(0.557)	0.412(0.142)	1.13(0.38)	0.429(0.054)
Furan (C_4H_4O)	8.84E-2(2.55E-2)	0.263(0.138)	0.164(0.045)	0.176(0.099)	0.106(0.027)	0.201(0.103)	9.16E-02	0.115(0.001)	-
Nitrous Acid (HONO)	0.167(0.035)	0.468(0.302)	0.518(0.152)	0.664(0.236)	0.219(0.036)	0.285(0.057)	0.263(0.014)	0.954(0.321)	-
Nitric Oxide (NO)	1.46(0.33)	2.62(0.46)	1.97(0.32)	2.08(0.49)	2.23(0.69)	2.18(0.53)	3.45(0.00)	1.54(0.23)	0.890(0.043)
Nitrogen Dioxide (NO_2)	0.997(0.174)	1.34(0.37)	2.06(0.33)	0.905(0.415)	1.12(0.32)	1.07(0.28)	1.22(0.04)	0.924(0.744)	0.823(0.593)
Hydrogen Cyanide (HCN)	0.116(0.035)	1.06(0.43)	0.226(0.068)	0.329(0.209)	0.461(0.159)	0.484(0.105)	0.114(0.024)	0.185(0.050)	-
Acetic Acid (CH_3COOH)	0.699(0.472)	5.69(7.07)	1.58(0.84)	1.67(0.71)	0.611(0.532)	1.82(1.18)	0.348(0.150)	1.33(0.47)	0.646(0.247)
Formic Acid (HCOOH)	6.50E-2(4.27E-2)	0.144(0.170)	0.309(0.164)	0.174(0.077)	7.25E-2(5.71E-2)	0.122(0.098)	3.60E-2(7.41E-3)	0.255(0.024)	5.94E-2(2.09E-2)
Glycolaldehyde ($C_2H_4O_2$)	0.183(0.201)	6.43E-02	0.369(0.204)	0.139(0.059)	0.229(0.217)	0.616(0.484)	-	-	-
Hydrogen Chloride (HCl)	0.265(0.061)	5.87E-2(1.97E-2)	4.95E-2(3.01E-2)	2.87E-02	0.455(0.236)	0.297(0.115)	0.125(0.043)	9.23E-03	8.28E-2(5.73E-2)
Ammonia (NH_3)	9.02E-2(8.36E-2)	6.63(2.47)	0.358(0.076)	1.07(0.33)	0.782(0.279)	2.17(0.49)	1.05(0.44)	0.989(0.103)	0.184(0.057)
Sulfur dioxide (SO_2)	0.973(0.284)	1.20(0.65)	1.01(0.13)	0.555(0.243)	2.35(0.53)	1.83(0.48)	1.23(0.05)	-	-

note: parenthesis indicate one standard deviation

Table S1. continued

Fuel type	Peat Canadian (2)	Peat IN (2,1)	NC Peat (2,1)	Plastic bag (1)	Ponderosa pine (11,4)	Rice Straw (7,4)	Sawgrass SC (12,1)	Sugar Cane LA(2,1)	Tires (2)	Trash (2)
MCE	0.805(0.009)	0.816(0.065)	0.726(0.067)	0.994	0.917(0.032)	0.941(0.023)	0.959(0.004)	0.926(0.010)	0.963(0.003)	0.973(0.006)
CO_2	1274(19)	1637(204)	1066(287)	3127	1672(80)	1407(67)	1605(9)	1365(31)	2882(14)	1793(28)
CO	197(9)	233(72)	276(139)	11.7	95.9(35.5)	55.8(21.6)	43.6(4.1)	69.6(8.9)	70.6(6.4)	31.5(6.9)
CH_4	6.25(2.17)	12.8(6.6)	10.9(5.3)	0.305	4.90(2.55)	2.68(1.69)	0.914(0.450)	3.02(0.58)	1.43(0.05)	0.801(0.201)
H_2O	2.36E-2(5.71E-2)	4.32E-2(1.45E-1)	-	0.191	3.54E-2(3.67E-1)	2.26E-2(1.53E-1)	6.03E-2(2.02E-2)	5.73E-2(2.36E-2)	0.442(0.211)	9.22E-2(7.16E-3)
C_2H_2	0.101(0.003)	0.178(0.046)	0.162(0.079)	0.548	1.07(0.41)	0.207(0.081)	0.193(0.048)	0.729(0.245)	1.13(0.27)	0.328(0.105)
C_2H_4	0.815(0.293)	1.39(0.62)	1.27(0.77)	1.13	3.99(1.98)	0.990(0.420)	0.426(0.170)	2.03(0.37)	1.23(0.19)	0.984(0.050)
C_3H_6	0.498	1.49(0.63)	1.17(0.63)	0.511	1.22(0.48)	0.418(0.276)	0.141(0.109)	0.658(0.167)	-	0.643(0.047)
CH_3OH	0.751(0.351)	3.24(1.39)	2.83(2.87)		2.86(1.90)	0.966(1.062)	0.173(0.100)	1.77(0.68)	-	0.169(0.081)
HCHO	1.43(0.37)	1.25(0.79)	1.41(1.16)	0.224	3.07(1.52)	0.947(0.582)	0.366(0.133)	3.14(1.33)	-	0.922(0.473)
C_4H_4O	0.879(0.036)	0.890(0.267)	1.78(1.84)	-	0.284(0.147)	0.104(0.035)	8.26E-2(2.88E-2)	0.235(0.028)	2.18E-02	8.38E-02
HONO	0.179	0.103	0.483(0.499)		0.799(0.202)	0.286(0.117)	0.185(0.055)	0.554(0.174)	1.51	0.242(0.125)
NO	-	1.85(0.56)	0.511(0.121)	0.644	1.59(0.39)	1.77(0.34)	2.02(0.20)	1.18(0.19)	3.44(0.06)	0.522(0.084)
NO_2	-	2.36(0.03)	2.31(1.46)	1.7	2.02(0.86)	1.46(0.40)	0.949(0.188)	1.30(0.44)	2.54	0.772(0.394)
HCN	1.77(0.55)	3.30(0.79)	4.45(3.02)	-	0.593(0.318)	0.324(0.145)	0.258(0.042)	0.435(0.108)	0.361	5.34E-2(6.39E-2)
CH_3COOH	1.86(1.35)	7.65(3.65)	8.46(8.46)	-	4.86(3.71)	1.99(2.11)	0.502(0.330)	6.41(2.72)	1.25	-
HCOOH	0.400(0.059)	0.552(0.048)	0.441(0.339)	5.14E-02	0.834(0.518)	0.318(0.432)	4.88E-2(2.94E-2)	1.18(0.66)	7.42E-02	4.47E-2(3.13E-2)
$C_2H_4O_2$	-	-	-	-	0.784(0.702)	1.33(1.43)	0.142(0.056)	5.07(2.61)	-	0.664(0.825)
HCl	-	-	7.68E-03	-	5.21E-2(2.44E-2)	0.438(0.298)	1.72(0.34)	0.105(0.039)	-	0.803(1.009)
NH_3	2.21(0.24)	1.39(0.97)	1.87(0.37)	-	1.56(0.68)	0.979(0.705)	0.151(0.076)	1.211(0.012)	-	6.25E-02
SO_2	-	-	-	-	0.980(0.258)	1.29(0.34)	1.83(0.09)	0.871	26.2(2.2)	0.897

note: parenthesis indicate one standard deviation

Table S1. continued

Fuel type	Wheat Straw Conv (4,1)	Wheat Straw Organic (6,2)	Wiregrass (7,2)	Cook Douglas Fir 3stone	Cook Douglas Fir Chips Envirofit Rocket G3300	Cook Douglas Fir Chips Phlips Gasifier	Cook Millet Ezy Stove	Cook Okote 3stone	Cook Okote Envirofit Rocket G3300	Cook Red Oak 3Stone	Cook Red Oak Envirofit Rocket G3300	Cook Red Oak in Ezy Stove
MCE	0.959(0.003)	0.957(0.012)	0.969(0.004)	0.963	0.974	0.984	0.950	0.968	0.966	0.972	0.985	0.985
CO_2	1450(61)	1505(24)	1654(7)	1640	1662	1682	1503	1589	1586	1628	1661	1656
CO	39.7(3.5)	43.5(12.0)	34.0(4.0)	39.8	28.1	17.3	49.9	33.5	35.8	30.2	15.9	16.3
CH_4	1.46(0.44)	1.73(0.67)	0.611(0.171)	1.27	0.897	0.374	2.64	1.37	1.32	1.29	0.231	0.412
H_2O	3.85E-2(3.94E-2)	9.15E-2(9.38E-2)	6.95E-2(1.37E-2)	9.92E-02	0.146	0.230	8.94E-02	0.140	0.139	0.150	0.137	0.190
C_2H_2	0.175(0.070)	0.134(0.028)	0.100(0.022)	0.412	5.54E-02	0.158	0.419	1.07	1.26	0.411	5.18E-02	0.235
C_2H_4	0.604(0.138)	0.561(0.091)	0.283(0.047)	0.387	0.111	0.156	0.838	1.03	0.828	0.370	6.28E-02	0.205
C_3H_6	0.213(0.092)	0.220(0.070)	7.18E-2(2.97E-2)	-	-	5.99E-03	-	0.113	-	5.77E-02	-	1.19E-02
CH_3OH	0.520(0.221)	1.15(0.55)	0.181(0.101)	0.702	0.558	8.72E-02	0.773	5.66E-02	6.60E-02	0.897	0.428	0.810
HCHO	0.779(0.340)	1.13(0.27)	0.343(0.076)	0.628	0.508	0.207	0.815	0.239	0.252	0.504	0.206	0.403
C_4H_4O	9.43E-2(3.92E-2)	0.184(0.087)	5.02E-2(1.89E-2)	8.67E-02	-	-	-	-	-	8.66E-02	-	1.60E-02
HONO	0.179(0.043)	0.195(0.029)	0.213(0.037)	0.183	-	-	-	0.508	0.661	0.221	-	-
NO	1.26(0.16)	1.23(0.16)	1.88(0.12)	0.339	0.476	0.607	1.03	0.238	0.287	0.423	0.651	0.565
NO_2	1.08(0.19)	1.45(0.58)	0.653(0.233)	1.04	1.14	1.66	-	0.942	-	1.49	0.980	1.57
HCN	0.104(0.014)	0.134(0.043)	9.55E-2(1.22E-2)	-	-	-	-	6.06E-02	4.30E-02	5.86E-02	-	-
CH_3COOH	0.658(0.286)	2.52(1.51)	0.365(0.120)	0.632	0.721	7.60E-02	1.98	-	-	4.16	1.74	2.99
HCOOH	6.24E-2(2.14E-2)	0.198(0.069)	4.85E-2(1.83E-2)	0.143	0.167	5.01E-02	0.128	3.74E-02	3.84E-02	0.321	0.150	0.244
$C_2H_4O_2$	0.432(0.000)	0.257(0.160)	0.183(0.065)	9.42E-02	0.183	0.261	-	-	-	0.151	-	0.108
HCl	0.474(0.523)	0.730(0.119)	6.62E-2(3.21E-2)	-	-	-	-	-	-	-	-	-
NH_3	0.208(0.140)	0.235(0.207)	0.153(0.096)	1.94E-02	2.06E-02	1.12E-02	0.226	-	7.09E-04	2.31E-02	2.20E-02	1.85E-02
SO_2	0.739(0.148)	1.13(0.36)	1.00(0.09)	-	-	-	-	0.523	-	-	-	-

note: parenthesis indicate one standard deviation

Table S2. Fuel type emission ratios to CO (mol/mol) calculated by OP-FTIR

Fuel type avg (stack burns, room burns)	African grass (19,1)	Alfalfa Organic CO (3)	Black Spruce AK (5,7)	Chamise CA (7,1)	Giant Cutgrass SC (5,3)	Hay Organic CO (6,2)	Juniper (2)
MCE	0.978(0.005)	0.918(0.008)	0.951(0.012)	0.929(0.020)	0.948(0.013)	0.949(0.007)	0.962(0.002)
Carbon Dioxide (CO_2)	45.9(10.0)	11.3(1.3)	20.5(5.4)	14.3(4.6)	19.2(4.3)	18.8(2.6)	25.2(1.1)
Carbon Monoxide (CO)	1	1	1	1	1	1	1
Methane (CH_4)	2.95E-2(1.19E-2)	1.19E-1(4.12E-2)	7.37E-2(1.36E-2)	6.48E-2(1.59E-2)	4.90E-2(1.40E-2)	9.58E-2(2.77E-2)	4.89E-2(2.56E-2)
Water (H_2O)	4.97E-3(1.31E-3)	4.20E-4(2.98E-4)	2.44E-3(1.47E-3)	1.13E-3(1.38E-3)	1.58E-3(7.63E-4)	1.18E-3(1.48E-3)	2.83E-3(4.82E-4)
Acetylene (C_2H_2)	3.10E-3(9.19E-4)	8.75E-3(2.93E-3)	1.40E-2(3.76E-3)	1.27E-2(5.69E-3)	8.33E-3(3.43E-3)	8.27E-3(3.29E-3)	5.29E-3(8.93E-4)
Ethylene (C_2H_4)	8.87E-3(3.89E-3)	2.81E-2(3.41E-3)	3.92E-2(8.91E-3)	2.67E-2(1.16E-2)	1.30E-2(4.06E-3)	2.57E-2(3.68E-3)	1.52E-2(4.09E-3)
Propylene (C_3H_6)	2.04E-3(5.25E-4)	1.08E-2(3.06E-3)	6.97E-3(1.28E-3)	4.14E-3(1.68E-3)	2.03E-3(1.53E-3)	8.01E-3(2.49E-3)	3.96E-3(2.40E-3)
Methanol (CH_3OH)	5.20E-3(3.68E-3)	3.93E-2(3.17E-2)	1.52E-2(4.49E-3)	1.00E-2(3.45E-3)	3.99E-3(4.80E-3)	2.43E-2(1.36E-2)	7.30E-3(4.05E-3)
Formaldehyde (HCHO)	1.56E-2(7.64E-3)	1.52E-2(6.99E-3)	2.23E-2(6.44E-3)	1.74E-2(6.04E-3)	8.06E-3(5.33E-3)	1.92E-2(9.72E-3)	8.50E-3(2.62E-3)
Furan (C_4H_4O)	1.45E-3(3.44E-4)	1.32E-3(7.36E-4)	1.21E-3(3.46E-4)	9.08E-4(4.48E-4)	8.51E-4(3.01E-4)	1.65E-3(7.01E-4)	8.17E-04
Nitrous Acid (HONO)	4.45E-3(8.62E-4)	3.42E-3(2.30E-3)	5.54E-3(1.70E-3)	4.81E-3(9.71E-4)	2.55E-3(7.77E-4)	3.50E-3(5.99E-4)	3.49E-3(3.24E-4)
Nitric Oxide (NO)	6.14E-2(1.31E-2)	3.18E-2(8.94E-3)	3.45E-2(1.11E-2)	2.67E-2(1.24E-2)	4.19E-2(1.96E-2)	4.29E-2(1.42E-2)	7.16E-2(2.75E-3)
Nitrogen Dioxide (NO_2)	2.71E-2(4.26E-3)	1.07E-2(4.14E-3)	2.32E-2(6.87E-3)	6.85E-3(2.81E-3)	1.36E-2(5.67E-3)	1.39E-2(5.13E-3)	1.66E-2(1.21E-3)
Hydrogen Cyanide (HCN)	4.71E-3(1.25E-3)	1.39E-2(5.13E-3)	4.16E-3(1.07E-3)	3.85E-3(1.55E-3)	8.87E-3(1.97E-3)	1.03E-2(2.01E-3)	2.62E-3(4.58E-4)
Acetic Acid (CH_3COOH)	1.27E-2(6.82E-3)	3.32E-2(4.09E-2)	1.45E-2(6.07E-3)	9.09E-3(3.32E-3)	6.41E-3(5.64E-3)	1.74E-2(9.54E-3)	3.59E-3(1.42E-3)
Formic Acid (HCOOH)	1.66E-3(7.95E-4)	1.08E-3(1.29E-3)	3.73E-3(1.56E-3)	1.21E-3(4.16E-4)	9.97E-4(8.00E-4)	1.49E-3(9.93E-4)	4.86E-4(8.13E-5)
Glycolaldehyde ($C_2H_4O_2$)	2.80E-3(3.07E-3)	3.73E-4(0.00E0)	3.36E-3(1.53E-3)	6.02E-4(2.25E-4)	2.42E-3(2.25E-3)	5.55E-3(3.92E-3)	-
Hydrogen Chloride (HCl)	9.47E-3(3.45E-3)	5.50E-4(2.03E-4)	7.59E-4(4.09E-4)	2.16E-04	7.60E-3(3.74E-3)	4.77E-3(1.60E-3)	2.13E-3(6.51E-4)
Ammonia (NH_3)	5.87E-3(4.38E-3)	1.39E-1(4.82E-2)	1.22E-2(2.97E-3)	2.08E-2(4.80E-3)	2.88E-2(1.12E-2)	7.52E-2(9.75E-3)	3.81E-2(1.48E-2)
Sulfur dioxide (SO_2)	1.92E-2(5.49E-3)	6.42E-3(3.66E-3)	9.84E-3(1.59E-3)	3.61E-3(2.64E-3)	2.29E-2(6.20E-3)	1.73E-2(5.19E-3)	1.20E-2(9.20E-4)

note: parenthesis indicate one standard deviation

Table S2. Continued

Fuel type	Manzanita CA (3,1)	Millet Ghana (2)	Peat Canadian (2)	Peat IN (2,1)	NC Peat (2,1)	Plastic bags	Ponderosa pine (11,4)	Rice Straw (7,4)
MCE	0.943(0.013)	0.938(0.010)	0.805(0.009)	0.816(0.065)	0.726(0.067)	0.994159	0.917(0.032)	0.941(0.023)
CO_2	17.2(4.5)	15.4(2.7)	4.12(0.24)	4.88(1.94)	2.83(1.09)	170	12.3(3.9)	17.5(4.6)
CO	1	1	1	1	1	1	1	1
CH_4	5.44E-2(3.14E-3)	4.78E-2(2.20E-2)	5.52E-2(1.69E-2)	9.18E-2(2.64E-2)	7.06E-2(8.11E-3)	4.57E-02	8.65E-2(1.62E-2)	8.06E-2(1.72E-2)
H_2O	2.00E-3(2.25E-3)	1.61E-3(3.96E-4)	1.97E-4(4.60E-4)	5.23E-4(1.15E-3)	1.67E-3(5.19E-3)	2.55E-02	1.60E-3(4.34E-3)	1.42E-3(2.46E-3)
C_2H_2	1.21E-2(4.23E-3)	3.15E-3(3.00E-4)	5.55E-4(6.01E-6)	8.34E-4(7.17E-5)	6.74E-4(1.85E-4)	5.05E-02	1.21E-2(3.10E-3)	4.31E-3(2.08E-3)
C_2H_4	2.59E-2(7.20E-3)	7.31E-3(1.40E-3)	4.11E-3(1.31E-3)	5.87E-3(2.08E-3)	4.69E-3(1.36E-3)	9.64E-02	4.07E-2(8.14E-3)	1.77E-2(3.52E-3)
C_3H_6	4.28E-3(1.57E-3)	-	1.64E-03	4.16E-3(8.72E-4)	2.94E-3(7.87E-4)	2.91E-02	8.42E-3(1.54E-3)	4.71E-3(1.13E-3)
CH_3OH	1.11E-2(3.82E-3)	5.26E-3(3.42E-3)	3.38E-3(1.71E-3)	1.37E-2(9.71E-3)	9.49E-3(6.58E-3)	-	2.44E-2(8.24E-3)	1.31E-2(6.56E-3)
HCHO	1.57E-2(3.24E-3)	6.56E-3(1.89E-3)	6.74E-3(1.48E-3)	4.98E-3(2.36E-3)	4.79E-3(2.40E-3)	1.79E-02	2.92E-2(7.01E-3)	1.54E-2(5.20E-3)
C_4H_4O	7.92E-4(2.90E-4)	-	1.84E-3(1.55E-4)	1.68E-3(7.76E-4)	2.53E-3(1.80E-3)	-	1.25E-3(2.00E-4)	8.59E-4(2.49E-4)
HONO	8.54E-3(2.41E-3)	-	5.25E-04	2.69E-04	1.04E-3(5.10E-4)	-	5.48E-3(1.64E-3)	3.07E-3(5.96E-4)
NO	2.31E-2(8.41E-3)	1.35E-2(2.87E-3)	-	8.75E-3(6.05E-4)	2.51E-3(1.34E-3)	5.14E-02	1.87E-2(7.95E-3)	3.22E-2(9.83E-3)
NO_2	8.79E-3(6.52E-3)	8.61E-3(7.20E-3)	-	7.58E-3(1.86E-3)	9.93E-3(1.10E-2)	8.75E-02	1.39E-2(5.29E-3)	1.67E-2(4.24E-3)
HCN	3.06E-3(2.89E-4)	0.00E0(0.00E0)	9.39E-3(3.29E-3)	1.55E-2(5.45E-3)	1.67E-2(5.87E-3)	-	6.24E-3(1.56E-3)	5.95E-3(1.07E-3)
CH_3COOH	8.61E-3(2.54E-3)	5.04E-3(2.68E-3)	4.47E-3(3.40E-3)	1.85E-2(1.52E-2)	1.11E-2(1.11E-2)	-	2.21E-2(9.15E-3)	1.32E-2(9.08E-3)
HCOOH	2.17E-3(2.32E-4)	6.04E-4(3.04E-4)	1.23E-3(1.28E-4)	1.61E-3(8.20E-4)	7.54E-4(5.80E-4)	2.68E-03	5.09E-3(1.67E-3)	2.54E-3(2.06E-3)
$C_2H_4O_2$	-	-	-	-	-	-	3.92E-3(3.10E-3)	8.47E-3(5.00E-3)
HCl	1.18E-04	1.09E-3(8.84E-4)	-	-	1.66E-05	-	4.66E-4(1.54E-4)	5.95E-3(4.48E-3)
NH_3	2.31E-2(5.58E-3)	5.04E-3(2.34E-3)	1.86E-2(2.78E-3)	9.15E-3(2.83E-3)	8.64E-3(1.72E-3)	-	2.73E-2(9.64E-3)	2.51E-2(6.68E-3)
SO_2	-	-	-	-	-	-	5.22E-3(1.31E-3)	1.07E-2(4.07E-3)

Table S2. Continued

Fuel type	Sawgrass SC (12,1)	Sugar Cane LA (2,1)	Tires (2)	Trash (2)	Wheat Straw Conv (4,1)	Wheat Straw Organic (6,2)	Wiregrass (7,2)
MCE	0.959(0.004)	0.926(0.010)	0.963(0.003)	0.973(0.006)	0.959(0.003)	0.957(0.012)	0.969(0.004)
CO_2	23.6(2.2)	12.6(1.8)	26.1(2.5)	37.2(8.7)	23.4(1.8)	23.5(6.1)	31.4(3.6)
CO	1	1	1	1	1	1	1
CH_4	3.61E-2(1.40E-2)	7.57E-2(6.48E-3)	3.55E-2(1.95E-3)	4.43E-2(1.42E-3)	6.34E-2(1.52E-2)	6.79E-2(1.01E-2)	3.12E-2(7.55E-3)
H_2O	2.20E-3(8.72E-4)	1.25E-3(3.59E-4)	9.98E-3(5.55E-3)	4.70E-3(1.39E-3)	1.54E-3(1.53E-3)	3.32E-3(3.12E-3)	3.22E-3(7.71E-4)
C_2H_2	4.76E-3(1.05E-3)	1.11E-2(2.40E-3)	1.72E-2(2.52E-3)	1.11E-2(1.14E-3)	4.72E-3(1.60E-3)	3.65E-3(1.53E-3)	3.23E-3(8.97E-4)
C_2H_4	9.65E-3(3.07E-3)	2.91E-2(1.92E-3)	1.73E-2(1.09E-3)	3.18E-2(5.40E-3)	1.51E-2(2.21E-3)	1.33E-2(2.23E-3)	8.36E-3(1.23E-3)
C_3H_6	2.08E-3(1.49E-3)	6.24E-3(7.57E-4)	-	1.38E-2(2.04E-3)	3.53E-3(1.41E-3)	3.10E-3(6.55E-4)	1.34E-3(4.49E-4)
CH_3OH	3.45E-3(1.79E-3)	2.18E-2(5.52E-3)	-	4.54E-3(1.26E-3)	1.12E-2(4.36E-3)	2.22E-2(6.13E-3)	4.72E-3(2.81E-3)
HCHO	7.81E-3(2.49E-3)	4.11E-2(1.27E-2)	-	2.64E-2(8.20E-3)	1.80E-2(6.98E-3)	2.53E-2(6.57E-3)	9.55E-3(2.54E-3)
C_4H_4O	7.85E-4(2.78E-4)	1.39E-3(9.86E-5)	1.19E-04	1.30E-03	9.43E-4(3.88E-4)	1.55E-3(6.31E-4)	6.23E-4(2.56E-4)
HONO	2.56E-3(8.41E-4)	4.68E-3(9.92E-4)	1.19E-02	4.42E-3(1.39E-3)	2.70E-3(6.76E-4)	2.74E-3(8.17E-4)	3.82E-3(9.73E-4)
NO	4.37E-2(6.28E-3)	1.61E-2(4.46E-3)	4.56E-2(4.89E-3)	1.61E-2(6.04E-3)	2.99E-2(6.05E-3)	2.84E-2(8.96E-3)	5.25E-2(7.78E-3)
NO_2	1.35E-2(3.59E-3)	1.13E-2(3.15E-3)	2.05E-02	1.62E-2(1.12E-2)	1.66E-2(1.49E-3)	2.09E-2(7.33E-3)	1.21E-2(5.22E-3)
HCN	6.15E-3(8.82E-4)	6.42E-3(7.63E-4)	4.98E-03	1.56E-3(1.76E-3)	2.72E-3(2.39E-4)	3.14E-3(1.15E-3)	3.07E-3(5.71E-4)
CH_3COOH	5.21E-3(2.96E-3)	4.02E-2(1.23E-2)	7.76E-03	-	7.71E-3(3.14E-3)	2.52E-2(9.22E-3)	5.05E-3(1.99E-3)
HCOOH	6.74E-4(3.99E-4)	9.52E-3(4.27E-3)	6.01E-04	9.54E-4(8.14E-4)	9.50E-4(2.70E-4)	2.78E-3(7.15E-4)	8.95E-4(4.00E-4)
$C_2H_4O_2$	1.33E-3(3.48E-4)	3.16E-2(1.26E-2)	-	8.70E-3(1.03E-2)	4.91E-03	2.82E-3(2.33E-3)	2.45E-3(6.94E-4)
HCl	3.05E-2(7.31E-3)	1.08E-3(2.71E-4)	-	1.73E-2(2.08E-2)	8.67E-3(9.53E-3)	1.33E-2(3.10E-3)	1.48E-3(7.32E-4)
NH_3	5.63E-3(2.76E-3)	2.75E-2(3.21E-3)	-	3.87E-03	8.99E-3(6.22E-3)	7.50E-3(5.36E-3)	7.12E-3(4.08E-3)
SO_2	1.83E-2(1.85E-3)	5.73E-03	1.62E-1(1.12E-3)	1.48E-02	8.26E-3(1.68E-3)	9.06E-3(3.10E-3)	1.30E-2(2.21E-3)

Table S2. Continued

Fuel type	Cook Douglas Fir 3stone	Cook Douglas Fir Chips Envirofit Rocket G3300	Cook Douglas Fir Chips Phlips Gasifier	Cook Millet Ezy Stove	Cook Okote 3stone	Cook Okote Envirofit Rocket G3300	Cook Red Oak 3Stone	Cook Red Oak Envirofit Rocket G3300	Cook Red Oak in EzyStove
MCE	0.963	0.974	0.984	0.950	0.968	0.966	0.972	0.985	0.985
CO_2	26.2	37.7	61.7	19.2	30.2	28.2	34.3	66.5	64.8
CO	1	1	1	1	1	1	1	1	1
CH_4	5.56E-02	5.59E-02	3.78E-02	9.25E-02	7.17E-02	6.46E-02	7.50E-02	2.54E-02	4.43E-02
H_2O	3.87E-03	8.08E-03	2.06E-02	2.79E-03	6.49E-03	6.02E-03	7.73E-03	1.34E-02	1.81E-02
C_2H_2	1.11E-02	2.13E-03	9.80E-03	9.03E-03	3.43E-02	3.78E-02	1.47E-02	3.51E-03	1.55E-02
C_2H_4	9.72E-03	3.96E-03	9.00E-03	1.68E-02	3.09E-02	2.31E-02	1.22E-02	3.95E-03	1.26E-02
C_3H_6	-	-	2.30E-04	-	2.25E-03	-	1.27E-03	-	4.86E-04
CH_3OH	1.54E-02	1.74E-02	4.40E-03	1.36E-02	1.48E-03	1.61E-03	2.60E-02	2.35E-02	4.36E-02
HCHO	1.47E-02	1.69E-02	1.11E-02	1.52E-02	6.64E-03	6.57E-03	1.56E-02	1.21E-02	2.31E-02
C_4H_4O	8.96E-04	-	-	-	-	-	1.18E-03	-	4.05E-04
HONO	2.74E-03	-	-	-	9.04E-03	1.10E-02	4.37E-03	-	-
NO	7.93E-03	1.58E-02	3.27E-02	1.92E-02	6.63E-03	7.48E-03	1.31E-02	3.82E-02	3.24E-02
NO_2	1.59E-02	2.47E-02	5.82E-02	-	1.71E-02	-	3.00E-02	3.75E-02	5.88E-02
HCN	-	-	-	-	1.88E-03	1.25E-03	2.01E-03	-	-
CH_3COOH	7.40E-03	1.20E-02	2.05E-03	1.85E-02	-	-	6.44E-02	5.10E-02	8.56E-02
HCOOH	2.18E-03	3.62E-03	1.76E-03	1.56E-03	6.78E-04	6.53E-04	6.47E-03	5.74E-03	9.11E-03
$C_2H_4O_2$	1.10E-03	3.04E-03	7.02E-03	-	-	-	2.33E-03	-	3.09E-03
HCl	-	-	-	-	-	-	-	-	-
NH_3	8.02E-04	1.21E-03	1.07E-03	7.45E-03	-	3.26E-05	1.26E-03	2.28E-03	1.87E-03
SO_2	-	-	-	-	6.83E-03	-	-	-	-

Table S3. Emission factors (g /kg) for all fuels including species from PTR-TOF-MS extended analysis

Fuel type (number of fires)	African grass (18) EF	Alfalfa Organic (3) EF	Black Spruce (4) EF	Chamise (6) EF	Giant Cutgrass (5) EF	Hay Organic (6) EF	Juniper (2) EF
MCE	0.978(0.005)	0.918(0.008)	0.959(0.008)	0.925(0.020)	0.956(0.003)	0.950(0.006)	0.962(0.002)
OP-FTIR species							
CO_2	1565(14)	1352(35)	1724(35)	1656(60)	1553(9)	1395(31)	1772(11)
CO	22.6(4.8)	76.5(7.3)	46.5(8.7)	84.6(22.0)	45.0(3.6)	46.2(5.1)	44.7(1.7)
CH_4	0.407(0.236)	5.25(1.99)	1.89(0.66)	3.37(1.49)	1.33(0.30)	2.34(0.57)	1.26(0.70)
NH_3	9.03E-2(8.53E-2)	6.47(2.36)	0.322(0.040)	1.01(0.33)	0.776(0.275)	2.13(0.45)	1.04(0.44)
C_2H_2	6.39E-2(2.63E-2)	0.617(0.204)	0.734(0.284)	1.19(0.69)	0.317(0.147)	0.409(0.125)	0.219(0.029)
HCN	0.124(0.030)	1.03(0.41)	0.236(0.074)	0.363(0.220)	0.389(0.093)	0.481(0.108)	0.113(0.024)
C_2H_4	0.207(0.125)	2.14(0.06)	2.06(0.78)	2.64(1.56)	0.625(0.139)	1.22(0.29)	0.685(0.208)
HCHO	0.427(0.275)	1.21(0.43)	1.51(0.53)	1.76(0.92)	0.504(0.237)	1.00(0.60)	0.410(0.141)
NO	1.45(0.32)	2.56(0.46)	1.88(0.19)	1.93(0.51)	2.41(0.79)	2.23(0.57)	3.43(0.00)
CH_3OH	0.157(0.132)	3.45(2.86)	0.942(0.347)	0.993(0.425)	0.288(0.274)	1.02(0.63)	0.377(0.221)
HCl	0.259(0.059)	0.057(0.019)	5.20E-2(3.29E-2)	2.83E-2(0.00E0)	0.452(0.235)	0.291(0.111)	0.125(0.043)
C_3H_6	8.60E-2(2.58E-2)	1.24(0.36)	0.545(0.219)	0.584(0.307)	0.176(0.103)	0.498(0.142)	0.269(0.171)
HCOOH	6.50E-2(4.34E-2)	0.140(0.165)	0.329(0.170)	0.169(0.082)	7.19E-2(5.64E-2)	0.118(0.093)	0.036(0.007)
NO_2	0.986(0.179)	1.31(0.37)	2.36(0.37)	0.908(0.420)	1.15(0.37)	1.04(0.31)	1.22(0.04)
HONO	0.172(0.033)	0.455(0.292)	0.526(0.044)	0.693(0.243)	0.224(0.038)	0.269(0.059)	0.262(0.015)
CH_3COOH	0.724(0.470)	5.54(6.86)	1.63(0.91)	1.68(0.75)	0.606(0.524)	1.77(1.12)	0.346(0.148)
$C_2H_4O_2$	0.181(0.199)	6.24E-02	0.383(0.222)	0.136(0.058)	0.226(0.214)	0.597(0.462)	-
SO_2	0.954(0.284)	1.17(0.62)	0.929(0.013)	0.550(0.243)	2.33(0.53)	1.80(0.48)	1.22(0.05)
C_4H_4O	5.94E-2(4.21E-2)	0.217(0.116)	0.122(0.043)	0.180(0.112)	0.108(0.029)	0.156(0.076)	5.67E-2(4.86E-2)
PTR-TOF-MS species							
Formula	**African grass (3) EF**	**Alfalfa Organic CO (2) EF**	**Black Spruce AK(1) EF**	**Chamise CA (1) EF**	**Giant Cutgrass SC (2) EF**	**Hay Organic CO (1) EF**	**Juniper (1) EF**
C_3H_4	-	-	-	3.34E-1(5.42E-2)	-	0.283(0.015)	-
C_2H_3N	1.91E-2(1.73E-2)	0.671(0.110)	5.06E-2(1.74E-2)	8.65E-2(3.26E-2)	0.194(0.096)	0.363(0.152)	7.56E-2(4.28E-2)
C_2H_2O	0.238(0.240)	1.12(0.76)	0.716(0.414)	0.790(0.447)	0.297(0.271)	1.04(0.69)	0.158(0.082)
C_2H_4O	0.304(0.289)	3.10(1.71)	0.968(0.405)	1.04(0.50)	0.491(0.350)	1.78(1.01)	0.314(0.197)
C_4H_2	2.95E-4(2.49E-4)	3.59E-3(1.03E-3)	3.51E-3(2.16E-3)	3.66E-3(2.18E-3)	1.46E-3(5.12E-4)	2.30E-3(1.28E-3)	1.26E-3(2.39E-4)
C_4H_4	6.46E-3(6.34E-3)	4.01E-2(2.82E-3)	4.13E-2(2.26E-2)	4.38E-2(1.99E-2)	1.60E-2(6.48E-3)	3.00E-2(1.99E-2)	1.14E-2(1.97E-3)
C_3H_2O	9.53E-3(8.78E-3)	2.33E-2(4.18E-3)	3.50E-2(1.85E-2)	2.23E-2(1.09E-2)	-	2.31E-2(2.26E-2)	-
C_4H_6	1.87E-2(1.68E-2)	0.200(0.026)	0.181(0.099)	0.186(0.082)	6.42E-2(3.65E-2)	0.155(0.081)	8.63E-2(4.48E-2)
C3H4O	0.114(0.106)	0.433(0.040)	0.404(0.206)	0.457(0.228)	0.197(0.139)	0.497(0.380)	0.140(0.071)
C_4H_8	1.76E-2(1.37E-2)	0.230(0.030)	0.125(0.078)	0.150(0.090)	4.22E-2(2.16E-2)	0.162(0.068)	7.68E-2(2.85E-2)
C_3H_6O	8.64E-2(7.12E-2)	0.827(0.111)	0.717(0.784)	0.298(0.175)	0.197(0.141)	0.584(0.412)	0.153(0.118)
C_2H_6S	3.06E-3(2.15E-3)	-	-	1.36E-2(8.43E-3)	-	-	-
C_5H_6	7.19E-3(6.21E-3)	8.76E-2(9.31E-3)	0.108(0.057)	0.096(0.042)	2.97E-2(1.30E-2)	0.071(0.040)	3.25E-2(1.23E-2)
C_3O_2	3.49E-4(1.32E-4)	1.10E-3(1.73E-4)	-	-	-	-	-

C_5H_8	2.43E-2(1.75E-2)	0.430(0.026)	0.440(0.246)	0.466(0.210)	0.134(0.105)	0.452(0.256)	0.196(0.102)
C_4H_6O	7.18E-2(6.92E-2)	0.299(0.034)	0.230(0.121)	0.230(0.117)	0.113(0.083)	0.356(0.263)	8.38E-2(4.80E-2)
$C_3H_4O_2$	8.49E-2(7.88E-2)	0.115(0.023)	0.223(0.138)	0.143(0.075)	7.13E-2(6.93E-2)	0.196(0.169)	4.41E-2(1.72E-2)
C_4H_8O	1.76E-2(1.62E-2)	0.287(0.064)	6.34E-2(4.22E-2)	7.11E-2(2.94E-2)	5.65E-2(4.68E-2)	0.173(0.111)	3.11E-2(2.65E-2)
$C_3H_6O_2$	8.42E-2(1.01E-1)	0.880(0.592)	0.293(0.199)	0.191(0.073)	0.188(0.217)	0.843(0.636)	7.73E-2(5.13E-2)
C_6H_6	3.87E-2(2.65E-2)	0.526(0.259)	0.595(0.250)	0.809(0.423)	0.280(0.172)	0.408(0.235)	0.271(0.018)
C_5H_4O	2.50E-2(2.51E-2)	0.129(0.027)	8.49E-2(4.45E-2)	0.101(0.029)	5.74E-2(5.30E-2)	0.163(0.146)	3.55E-2(2.30E-2)
C_5H_6O	5.20E-2(5.00E-2)	0.292(0.084)	0.150(0.092)	0.133(0.059)	7.67E-2(7.07E-2)	0.282(0.193)	5.71E-2(4.27E-2)
C_6H_{10}	3.94E-3(3.22E-3)	6.19E-2(6.66E-3)	4.23E-2(2.65E-2)	3.08E-2(1.24E-2)	1.00E-2(6.62E-3)	3.60E-2(1.95E-2)	2.34E-2(1.49E-2)
$C_4H_4O_2$	0.104(0.104)	0.179(0.088)	0.214(0.131)	0.195(0.065)	8.64E-2(9.08E-2)	0.297(0.263)	4.35E-2(2.43E-2)
C_5H_8O	1.93E-2(1.84E-2)	0.150(0.036)	7.89E-2(4.35E-2)	7.56E-2(2.28E-2)	3.71E-2(2.94E-2)	0.130(0.084)	3.08E-2(2.07E-2)
$C_4H_6O_2$	8.09E-2(8.00E-2)	0.462(0.197)	0.197(0.121)	0.225(0.071)	0.147(0.157)	0.516(0.395)	6.01E-2(4.01E-2)
$C_4H_8O_2$	1.30E-2(1.34E-2)	9.79E-2(5.67E-2)	2.98E-2(2.21E-2)	3.79E-2(8.06E-3)	2.73E-2(3.23E-2)	9.14E-2(7.24E-2)	1.12E-2(8.34E-3)
C_7H_6	3.00E-3(2.60E-3)	4.29E-2(9.28E-3)	3.77E-2(1.69E-2)	3.08E-2(1.10E-2)	9.30E-3(4.46E-3)	2.75E-2(1.81E-2)	1.20E-2(6.65E-3)
C_7H_8	2.52E-2(2.04E-2)	0.455(0.064)	2.35(1.18)	0.382(0.187)	0.118(0.072)	0.41(0.23)	0.286(0.096)
C_6H_6O	3.68E-2(3.27E-2)	0.387(0.083)	0.195(0.106)	0.310(0.145)	0.144(0.061)	0.315(0.171)	8.07E-2(4.64E-2)
$C_5H_4O_2$	0.200(0.193)	0.238(0.062)	0.307(0.189)	0.281(0.074)	0.156(0.146)	0.542(0.437)	7.76E-2(4.36E-2)
$C_5H_6O_2$	0.103(0.109)	0.232(0.139)	0.205(0.138)	0.206(0.073)	9.17E-2(1.03E-1)	0.352(0.285)	4.79E-2(2.93E-2)
$C_5H_8O_2$	2.40E-2(2.46E-2)	0.101(0.051)	6.45E-2(4.29E-2)	6.75E-2(1.67E-2)	3.16E-2(3.50E-2)	0.117(0.094)	1.99E-2(1.67E-2)
C_8H_6	-	-	-	6.23E-2(5.95E-3)	-	7.37E-2(8.95E-3)	-
C_8H_8	4.32E-3(3.45E-3)	0.104(0.019)	7.32E-2(3.47E-2)	9.22E-2(4.70E-2)	3.51E-2(1.67E-2)	6.56E-2(3.02E-2)	3.53E-2(9.42E-3)
C_7H_6O	7.03E-3(5.60E-3)	8.55E-2(2.99E-2)	6.59E-2(2.71E-2)	8.99E-2(4.33E-2)	3.93E-2(1.44E-2)	5.79E-2(3.44E-2)	2.91E-2(9.39E-3)
C_8H_{10}	6.90E-3(5.41E-3)	0.146(0.024)	0.188(0.087)	0.113(0.053)	4.04E-2(2.54E-2)	0.107(0.047)	6.45E-2(3.65E-2)
$C_6H_4O_2$	2.33E-3(1.16E-3)	-	-	0.389(0.179)	-	4.09E-2(1.45E-2)	-
$C_6H_6O_2$	5.65E-2(5.65E-2)	0.186(0.115)	0.160(0.106)	0.358(0.216)	5.47E-2(5.03E-2)	0.323(0.247)	4.13E-2(3.21E-2)
$C_7H_{10}O$	1.36E-2(1.17E-2)	0.192(0.082)	5.23E-2(3.04E-2)	3.18E-2(7.75E-3)	2.71E-2(2.67E-2)	0.120(0.082)	2.24E-2(1.72E-2)
$C_5H_4O_3$	2.62E-2(2.53E-2)	3.09E-2(1.62E-2)	7.26E-2(4.88E-2)	5.45E-2(2.23E-2)	1.85E-2(1.04E-2)	0.128(0.145)	8.66E-3(2.33E-3)
$C_6H_8O_2$	2.94E-2(3.58E-2)	0.240(0.164)	9.75E-2(6.91E-2)	9.13E-2(2.48E-2)	4.85E-2(5.85E-2)	0.245(0.191)	3.06E-2(2.33E-2)
$C_5H_6O_3$	6.77E-2(1.02E-1)	4.22E-2(3.10E-2)	0.106(0.074)	0.100(0.035)	3.81E-2(3.99E-2)	0.124(0.112)	1.64E-2(7.69E-3)
C_9H_8	2.44E-2(1.67E-2)	4.26E-2(1.65E-2)	-	-	-	-	-
C_8H_6O	4.09E-3(3.50E-3)	4.13E-2(4.36E-3)	2.49E-2(1.22E-2)	3.33E-2(1.52E-2)	1.77E-2(5.66E-3)	2.68E-2(1.65E-2)	9.44E-3(3.63E-3)
C_9H_{10}	2.20E-3(1.74E-3)	4.38E-2(5.17E-3)	4.83E-2(2.45E-2)	4.27E-2(1.88E-2)	1.26E-2(8.20E-3)	3.08E-2(1.59E-2)	2.01E-2(8.97E-3)
C_8H_8O	3.26E-2(3.15E-2)	0.117(0.020)	0.109(0.059)	0.127(0.070)	9.91E-2(8.27E-2)	0.136(0.098)	2.99E-2(1.85E-2)
C_9H_{12}	5.87E-3(5.04E-3)	7.90E-2(9.46E-3)	0.112(0.058)	0.041(0.010)	1.98E-2(1.42E-2)	5.40E-2(3.11E-2)	3.44E-2(2.27E-2)
$C_7H_6O_2$	9.51E-3(8.17E-3)	5.76E-2(2.41E-2)	4.92E-2(2.14E-2)	5.92E-2(3.44E-2)	2.40E-2(1.24E-2)	3.81E-2(1.88E-2)	1.28E-2(4.71E-3)
$C_8H_{10}O$	1.69E-2(1.61E-2)	0.178(0.066)	5.93E-2(3.51E-2)	4.73E-2(6.64E-3)	4.35E-2(3.79E-2)	0.128(0.070)	2.89E-2(2.31E-2)
$C_7H_8O_2$	2.94E-2(3.34E-2)	0.207(0.136)	0.126(0.082)	0.088(0.026)	5.78E-2(7.22E-2)	0.202(0.174)	3.35E-2(3.06E-2)
$C_6H_6O_3$	3.59E-2(4.25E-2)	5.85E-2(5.11E-2)	0.134(0.102)	0.069(0.031)	1.73E-2(1.55E-2)	0.108(0.098)	1.97E-2(1.24E-2)
$C_{10}H_8$	2.70E-2(3.00E-2)	0.158	0.138(0.069)	0.135(0.056)	5.06E-2(2.99E-2)	7.95E-2(4.92E-2)	4.30E-2(3.39E-3)
$C_{10}H_{10}$	4.69E-3(5.28E-3)	-	2.77E-2(1.84E-2)	2.41E-2(1.39E-2)	1.08E-2(4.80E-3)	2.79E-2(8.97E-3)	-
$C_{10}H_{16}$	4.50E-3(3.53E-3)	0.123(0.021)	9.81E-2(4.30E-2)	7.45E-2(3.87E-2)	3.11E-2(1.51E-2)	6.94E-2(2.87E-2)	3.91E-2(1.78E-2)
$C_{11}H_{10}$	-	-	-	5.22E-2(1.76E-2)	-	4.00E-2(3.78E-3)	-

Species Formula	African grass (3) EF	Alfalfa Organic CO (2) EF	Black Spruce AK(1) EF	Chamise CA (1) EF	Giant Cutgrass SC (2) EF	Hay Organic CO (1) EF	Juniper (1) EF
C_2H_7N	1.51E-2(6.98E-3)	0.137(0.023)	7.52E-03	1.81E-02	1.09E-02	0.200	7.27E-03
CH_4S	2.60E-3(2.50E-3)	0.141(0.047)	1.29E-02	2.70E-03	1.53E-2(1.09E-2)	0.127	1.92E-03
C_2H_5NO	-	-	-	-	-	-	-
C_3H_9N	8.02E-3(6.19E-3)	3.84E-2(5.07E-3)	4.81E-03	2.24E-03	2.19E-2(2.01E-2)	0.312	4.93E-04
C_5H_4	2.35E-3(1.37E-3)	1.01E-2(5.15E-3)	7.45E-03	3.61E-03	4.93E-3(4.50E-3)	1.45E-02	1.07E-03
C_5H_{10}	6.10E-3(3.28E-3)	7.40E-2(1.83E-2)	3.99E-02	1.94E-02	2.93E-2(2.87E-3)	4.60E-02	1.32E-02
C_6H_{12}	3.12E-3(1.61E-3)	4.26E-2(0.00E0)	1.76E-02	-	1.31E-2(3.00E-3)	2.61E-02	-
$C_5H_{10}O$	-	-	-	-	-	-	-
C_4H_9NO	1.43E-2(6.04E-3)	8.99E-2(2.60E-2)	-	1.06E-02	1.93E-02	0.106	4.86E-03
$C_3H_4O_3$	3.25E-3(9.42E-4)	4.30E-3(2.39E-3)	6.68E-03	1.28E-03	6.52E-3(6.92E-3)	7.07E-03	2.05E-04
$C_4H_{11}NO$	3.65E-3(2.33E-3)	-	-	-	-	-	-
C_6H_4O	2.52E-3(1.61E-3)	2.19E-02	2.79E-03	-	5.30E-3(1.63E-3)	-	-
C_7H_{10}	1.57E-2(5.67E-3)	0.196(0.047)	0.283	3.77E-02	6.48E-2(2.26E-3)	0.231	4.89E-02
C_6H_8O	4.17E-2(1.20E-2)	0.337(0.115)	9.54E-02	2.98E-02	0.109(0.079)	0.411	1.99E-02
C_7H_{12}	6.66E-3(4.28E-3)	9.09E-2(3.17E-2)	3.95E-02	9.51E-03	2.56E-2(1.04E-3)	5.56E-02	7.44E-03
$C_6H_{10}O$	-	-	2.41E-02	-	3.50E-02	-	-
$C_4H_4O_3$	1.55E-2(5.67E-3)	1.02E-2(4.12E-3)	2.01E-02	4.51E-03	1.77E-2(2.15E-2)	1.86E-02	1.58E-03
$C_4H_6O_3$	3.59E-2(1.15E-2)	0.105(0.061)	6.25E-02	2.26E-02	0.109(0.110)	0.238	1.01E-02
$C_5H_{10}O_2$	4.43E-3(2.45E-3)	5.71E-2(1.87E-2)	1.68E-02	9.93E-03	2.37E-02	5.87E-02	6.85E-03
C_7H_5N	-	-	2.31E-02	-	3.62E-02	-	-
C_7H_8O	3.65E-2(5.72E-3)	0.339(0.077)	0.123	4.03E-02	0.125(0.038)	0.328	3.40E-02
C_8H_{12}	-	-	0.139	-	3.45E-02	-	-
C_8H_{14}	3.33E-3(2.10E-3)	4.76E-2(1.90E-2)	1.52E-02	5.28E-03	8.80E-3(4.89E-3)	2.44E-02	6.33E-03
$C_6H_{10}O_2$	-	6.16E-02	-	9.64E-03	-	-	4.70E-03
$C_5H_8O_3$	4.30E-2(1.66E-2)	0.231(0.131)	6.84E-02	3.47E-02	0.162(0.174)	0.538	2.04E-02
$C_6H_{12}O_2$	-	-	1.57E-02	-	1.30E-02	-	-
C_9H_{14}	5.10E-3(1.70E-3)	7.75E-2(2.81E-2)	0.102	8.43E-03	2.06E-2(4.07E-3)	7.53E-02	1.37E-02
$C_6H_4O_3$	3.12E-2(9.21E-3)	1.91E-2(2.46E-2)	3.65E-02	5.08E-03	3.34E-2(3.34E-2)	0.147	3.69E-03
$C_7H_{10}O_2$	1.45E-2(0.00E0)	0.165(0.086)	3.43E-02	7.58E-03	4.58E-2(5.10E-2)	0.202	5.16E-03
C_9H_8O	7.80E-3(1.52E-3)	-	-	-	-	-	-
$C_8H_6O_2$	3.82E-3(1.27E-3)	1.73E-2(5.72E-3)	1.25E-02	5.01E-03	1.74E-02	3.03E-02	2.49E-03
$C_9H_{10}O$	8.26E-3(3.84E-3)	5.77E-2(1.53E-2)	3.05E-02	6.56E-03	3.56E-2(2.05E-3)	6.69E-02	9.29E-03
$C_{10}H_{14}$	2.06E-3(7.17E-6)	5.92E-2(0.00E0)	0.108	-	1.68E-02	7.14E-02	-
$C_8H_8O_2$	1.37E-2(2.91E-3)	4.78E-2(3.64E-2)	5.28E-02	4.89E-03	4.57E-2(4.60E-2)	0.109	8.36E-03
$C_9H_{12}O$	6.87E-3(0.00E0)	9.98E-02	-	1.36E-02	1.08E-02	-	8.31E-03
$C_7H_6O_3$	9.76E-3(3.40E-3)	2.93E-2(2.40E-2)	2.95E-02	4.27E-03	1.94E-2(2.32E-2)	6.08E-02	3.42E-03
$C_8H_{10}O_2$	2.65E-2(8.16E-3)	0.165(0.075)	5.74E-02	1.09E-02	5.56E-2(5.81E-2)	0.189	8.16E-03
$C_7H_8O_3$	1.17E-2(4.16E-3)	4.25E-2(3.54E-2)	1.48E-02	5.49E-03	2.27E-2(2.13E-2)	5.38E-02	3.37E-03
$C_8H_{12}O_2$	-	8.25E-2(4.10E-2)	1.31E-02	4.15E-03	2.27E-02	6.94E-02	2.16E-03

$C_{10}H_8O$	5.58E-2(1.93E-2)	4.50E-2(1.80E-2)	5.42E-02	9.63E-03	5.29E-2(4.14E-2)	7.39E-02	7.45E-03
$C_{11}H_{13}$	-	6.09E-2(1.53E-2)	3.59E-02	1.02E-02	1.86E-02	5.43E-02	8.96E-03
$C_{10}H_{10}O$	1.02E-2(2.49E-3)	7.83E-2(1.72E-2)	3.35E-02	1.31E-02	4.24E-02	8.39E-02	9.95E-03
$C_{11}H_{14}$	-	-	-	-	-	-	-
$C_9H_8O_2$	1.23E-2(3.19E-3)	4.44E-02	2.41E-02	-	3.19E-2(1.54E-2)	5.46E-02	-
$C_{10}H_{12}O$	-	-	-	-	-	-	-
$C_{11}H_{16}$	-	0.132	6.32E-02	-	2.53E-02	0.121	-
$C_9H_{10}O_2$	3.29E-2(9.95E-3)	0.194(0.111)	8.68E-02	1.26E-02	0.116(0.124)	0.352	1.14E-02
$C_{11}H_{18}$	-	-	4.35E-02	-	1.56E-02	-	-
$C_8H_{10}O_3$	1.29E-2(5.71E-3)	8.71E-2(1.57E-2)	2.04E-02	2.59E-02	7.04E-02	9.82E-02	8.78E-03
$C_{10}H_{12}O_2$	-	-	-	-	-	-	-

Table S3. Continued

Fuel type (number of fires)	Manzanita (2) EF	Millet Ghana (2) EF	Peat Canadian (2) EF	Peat IN (2)EF	NC Peat (2) EF	Ponderosa pine (8) EF	Rice Straw (7) EF
MCE	0.932(0.002)	0.938(0.010)	0.805(0.009)	0.808(0.090)	0.687(0.007)	0.913(0.029)	0.938(0.028)
OP-FTIR species							
CO_2	1656(5)	1484(11)	1246(28)	1528(237)	1201(48)	1594(109)	1397(81)
CO	77.1(2.4)	62.2(10.4)	193(7)	229(98)	347(3)	95.4(27.0)	58.3(23.3)
CH_4	2.29(0.01)	1.63(0.50)	6.10(2.08)	11.9(9.0)	13.5(1.8)	5.19(2.50)	2.90(1.92)
NH_3	0.934(0.106)	0.183(0.057)	2.16(0.25)	1.35(0.94)	1.82(0.35)	1.68(0.65)	0.948(0.650)
C_2H_2	1.07(0.07)	0.183(0.048)	9.92E-2(2.45E-3)	0.167(0.061)	0.194(0.061)	1.13(0.30)	0.231(0.085)
HCN	0.225(0.000)	-	1.73(0.55)	3.62(0.43)	5.60(2.73)	0.654(0.335)	0.360(0.144)
C_2H_4	2.19(0.01)	0.448(0.011)	0.796(0.280)	1.11(0.63)	1.57(0.64)	4.40(1.98)	1.08(0.42)
HCHO	1.35(0.01)	0.427(0.053)	1.40(0.36)	1.56(0.70)	1.78(1.25)	3.58(1.38)	1.15(0.54)
NO	1.45(0.26)	0.886(0.041)	-	1.42(0.00)	0.585	1.45(0.35)	1.90(0.28)
CH_3OH	0.788(0.132)	0.354(0.181)	0.736(0.349)	3.834(0.972)	3.42(3.57)	3.33(1.83)	1.14(1.21)
HCl	-	8.24E-2(5.69E-2)	-	-	7.45E-03	6.20E-2(2.55E-2)	0.427(0.287)
C_3H_6	0.495(0.000)	-	0.485	1.353(0.829)	1.42(0.50)	1.33(0.38)	0.457(0.305)
HCOOH	0.259(0.025)	5.92E-2(2.07E-2)	0.391(0.054)	0.537(0.048)	0.428(0.327)	0.957(0.450)	0.305(0.404)
NO_2	0.774(1.086)	0.819(0.589)	-	2.32	1.25(0.00)	2.33(0.68)	1.66(0.25)
HONO	1.05(0.11)	-	0.174	-	0.811(0.000)	0.887(0.168)	0.320(0.118)
CH_3COOH	1.47(0.53)	0.643(0.245)	1.82(1.34)	7.45(3.57)	8.22(8.19)	5.56(3.49)	1.91(1.98)
$C_2H_4O_2$	-	-	-	-	-	0.844(0.703)	1.28(1.33)
SO_2	-	-	-	-	4.26	0.888(0.273)	1.27(0.35)
C_4H_4O	0.131(0.026)	5.69E-2(2.97E-2)	0.861(0.042)	1.01(0.04)	2.32(2.07)	0.407(0.304)	0.230(0.351)
PTR-TOF-MS species							
Formula	Manzanita CA (1) EF	Millet Ghana (1) EF	Peat Canadian (1) EF	Peat IN (2) EF	NC Peat (1) EF	Ponderosa pine (1) EF	Rice Straw (2) EF
C_3H_4	0.365(0.070)	-	-	-	-	0.716(0.252)	0.462(0.330)
C_2H_3N	-	1.92E-2(9.07E-3)	0.346(0.096)	0.639(0.192)	0.818(0.244)	0.204(0.116)	2.11E-1(8.45E-2)

C_2H_2O	0.594(0.037)	0.246(0.113)	0.831(0.136)	1.44(0.51)	2.00(2.08)	2.08(1.11)	1.23(1.18)
C_2H_4O	0.694(0.043)	0.313(0.098)	1.47(0.49)	1.52(0.16)	1.91(1.32)	2.71(1.06)	1.76(1.23)
C_4H_2	7.97E-3(1.84E-3)	3.01E-04	1.01E-3(0.00E0)	3.75E-03	3.18E-03	4.11E-3(1.92E-3)	2.32E-3(2.75E-3)
C_4H_4	6.36E-2(3.27E-3)	1.09E-2(2.23E-3)	2.60E-2(1.39E-2)	2.43E-2(5.22E-3)	3.54E-2(2.47E-2)	8.47E-2(5.00E-2)	3.16E-2(2.73E-2)
C_3H_2O	3.70E-2(5.70E-3)	6.53E-3(3.72E-3)	-	-	9.57E-02	7.92E-2(4.63E-2)	2.98E-2(2.41E-2)
C_4H_6	0.261(0.025)	4.15E-2(1.91E-2)	0.113(0.041)	0.279(0.111)	0.388(0.144)	0.465(0.272)	0.136(0.088)
C3H4O	0.455(0.036)	0.128(0.053)	0.312(0.107)	0.192(0.033)	0.315(0.223)	1.06(0.52)	0.530(0.405)
C_4H_8	0.219(0.127)	6.72E-2(0.00E0)	0.249(0.024)	1.07(0.56)	0.916(0.335)	0.524(0.300)	0.105(0.037)
C_3H_6O	0.310(0.041)	0.157(0.071)	0.672(0.180)	1.40(0.01)	1.29(0.90)	0.821(0.491)	0.510(0.274)
C_2H_6S	1.65E-2(1.07E-3)	-	-	-	8.80E-02	2.64E-2(8.55E-3)	-
C_5H_6	0.118(0.003)	1.99E-2(4.81E-3)	3.72E-2(1.86E-2)	6.69E-2(2.68E-2)	7.85E-02	0.281(0.172)	0.059(0.039)
C_3O_2	-	-	-	-	-	2.78E-03	-
C_5H_8	0.745(0.210)	5.74E-2(4.02E-2)	0.247(0.059)	1.16(0.38)	1.54(0.84)	1.53(1.02)	0.194(0.099)
C_4H_6O	0.242(0.005)	7.66E-2(3.20E-2)	0.289(0.158)	0.251(0.038)	0.364(0.268)	0.615(0.351)	0.413(0.336)
$C_3H_4O_2$	0.161(0.000)	4.71E-2(2.17E-2)	0.291(0.132)	0.185(0.040)	0.210(0.180)	0.458(0.265)	0.293(0.254)
C_4H_8O	5.24E-2(2.35E-3)	4.76E-2(2.24E-2)	0.201(0.049)	0.657(0.134)	0.764(0.594)	0.214(0.137)	0.198(0.166)
$C_3H_6O_2$	-	0.178(0.073)	0.274(0.114)	0.424(0.137)	0.552(0.545)	0.974(0.683)	1.10(1.22)
C_6H_6	0.753(0.029)	0.171(0.014)	0.435(0.034)	0.784(0.346)	1.12(0.35)	1.29(0.91)	0.284(0.115)
C_5H_4O	0.107(0.005)	4.15E-2(2.44E-2)	0.108(0.034)	9.33E-2(2.15E-2)	4.25E-02	0.371(0.206)	0.191(0.203)
C_5H_6O	0.157(0.007)	6.47E-2(3.07E-2)	0.438(0.238)	0.423(0.089)	0.640(0.508)	0.477(0.296)	0.346(0.341)
C_6H_{10}	8.01E-2(2.27E-2)	9.75E-3(9.78E-3)	3.99E-2(3.24E-3)	0.178(0.090)	0.180	0.133(0.066)	2.00E-2(8.08E-3)
$C_4H_4O_2$	0.207(0.011)	5.29E-2(2.48E-2)	0.816(0.396)	0.537(0.077)	0.210	0.877(0.437)	0.425(0.484)
C_5H_8O	6.51E-2(4.82E-4)	2.76E-2(1.26E-2)	0.133(0.081)	0.184(0.013)	0.130	0.257(0.138)	0.136(0.109)
$C_4H_6O_2$	0.203(0.012)	0.125(0.058)	0.337(0.150)	0.399(0.092)	0.150	0.756(0.398)	0.705(0.774)
$C_4H_8O_2$	3.78E-2(5.39E-3)	2.76E-2(1.23E-2)	7.36E-2(5.80E-3)	0.181(0.002)	7.53E-02	0.123(0.079)	0.145(0.181)
C_7H_6	4.42E-2(6.60E-3)	5.56E-3(3.17E-3)	2.00E-2(0.00E0)	9.39E-02	6.43E-02	7.29E-2(3.78E-2)	2.07E-2(1.80E-2)
C_7H_8	0.52(0.08)	6.84E-2(3.07E-2)	0.168(0.019)	0.601(0.206)	0.790(0.221)	2.99(2.15)	0.248(0.127)
C_6H_6O	0.351(0.006)	0.137(0.070)	0.411(0.394)	0.658(0.082)	0.421	0.916(0.457)	0.405(0.328)
$C_5H_4O_2$	0.405(0.026)	9.37E-2(4.27E-2)	2.325(0.872)	2.25(0.57)	1.25	1.13(0.59)	0.551(0.491)
$C_5H_6O_2$	0.228(0.006)	6.85E-2(3.55E-2)	0.536(0.335)	0.355(0.021)	0.189	0.820(0.424)	0.563(0.671)
$C_5H_8O_2$	6.41E-2(6.21E-4)	2.84E-2(1.56E-2)	0.120(0.044)	0.208(0.005)	0.113	0.246(0.139)	0.182(0.220)
C_8H_6	-	-	-	-	-	0.230	0.321(0.326)
C_8H_8	8.67E-2(2.00E-3)	1.49E-2(1.58E-4)	3.34E-2(1.97E-3)	1.13E-1(4.66E-2)	0.119	0.231(0.170)	4.25E-2(2.60E-2)
C_7H_6O	8.09E-2(6.54E-3)	1.88E-2(5.43E-3)	3.14E-2(7.57E-3)	8.07E-2(7.34E-3)	5.81E-02	0.176(0.083)	5.13E-2(3.36E-2)
C_8H_{10}	0.119(0.008)	2.86E-2(1.09E-2)	8.09E-2(3.25E-2)	0.532(0.273)	0.485(0.098)	0.389(0.293)	8.49E-2(6.27E-2)
$C_6H_4O_2$	0.950(0.002)	-	-	-	-	0.184(0.080)	5.27E-2(5.25E-2)
$C_6H_6O_2$	0.835(0.015)	4.24E-2(2.04E-2)	0.934(0.610)	0.853(0.222)	0.338	0.908(0.384)	0.341(0.379)
$C_7H_{10}O$	1.66E-2(5.06E-3)	3.30E-2(1.56E-2)	6.03E-2(0.00E0)	0.218	0.146	0.167(0.109)	0.137(0.121)
$C_5H_4O_3$	6.15E-2(1.96E-3)	8.64E-3(7.16E-4)	0.249(0.135)	0.245(0.028)	0.114	0.211(0.125)	4.64E-2(5.11E-2)
$C_6H_8O_2$	8.80E-2(5.13E-3)	4.50E-2(1.98E-2)	0.243(0.170)	0.212(0.000)	0.121	0.514(0.259)	0.374(0.472)
$C_5H_6O_3$	0.117(0.006)	1.63E-2(8.12E-3)	0.467(0.296)	0.248(0.125)	5.99E-02	0.475(0.257)	0.250(0.305)
C_9H_8	-	-	4.21E-2(0.00E0)	4.78E-02	3.23E-02	0.268	-
C_8H_6O	2.73E-2(5.70E-4)	1.02E-2(2.07E-3)	2.65E-2(1.40E-2)	3.72E-2(1.03E-2)	3.20E-02	6.36E-2(3.13E-2)	3.15E-2(2.19E-2)

C_9H_{10}	4.46E-2(3.98E-3)	6.69E-3(1.68E-3)	1.53E-2(7.02E-3)	0.102(0.052)	0.102	0.143(0.109)	2.55E-2(1.84E-2)
C_8H_8O	0.111(0.007)	0.102(0.043)	6.95E-2(4.14E-2)	0.136(0.014)	0.123	0.321(0.164)	0.329(0.341)
C_9H_{12}	3.69E-2(6.70E-3)	2.26E-2(1.11E-2)	4.75E-2(1.47E-2)	0.315(0.161)	0.325(0.097)	0.230(0.187)	4.71E-2(2.77E-2)
$C_7H_6O_2$	5.82E-2(3.84E-3)	2.10E-2(9.23E-3)	5.54E-2(3.41E-2)	0.284(0.043)	3.11E-02	0.190(0.080)	5.15E-2(5.08E-2)
$C_8H_{10}O$	2.06E-2(1.69E-3)	5.62E-2(3.08E-2)	0.122(0.101)	0.261(0.114)	0.241	0.166(0.094)	0.227(0.234)
$C_7H_8O_2$	5.23E-2(6.79E-3)	5.03E-2(1.96E-2)	0.185(0.047)	0.878(0.157)	0.227	0.552(0.275)	0.391(0.509)
$C_6H_6O_3$	0.125(0.007)	1.69E-2(1.06E-2)	0.456(0.248)	0.377(0.040)	0.136	0.566(0.199)	0.129(0.151)
$C_{10}H_8$	0.145(0.015)	3.30E-2(8.53E-5)	0.216(0.000)	0.236	0.161(0.033)	0.242(0.124)	0.134(0.190)
$C_{10}H_{10}$	-	-	2.90E-2(0.00E0)	3.32E-02	0.164	6.50E-2(3.95E-2)	3.95E-2(3.24E-2)
$C_{10}H_{16}$	7.86E-2(2.82E-3)	1.78E-2(3.99E-3)	5.47E-2(1.85E-2)	0.196(0.064)	0.225(0.058)	0.226(0.161)	5.01E-2(3.41E-2)
$C_{11}H_{10}$	5.50E-2(9.49E-4)	-	-	-		0.112(0.043)	0.120(0.125)

PTR-TOF-MS Extended Analysis
Species

Formula	Manzanita CA (1) EF	Millet Ghana (1) EF	Peat Canadian (1) EF	Peat IN (2) EF	NC Peat (1) EF	Ponderosa pine (1) EF	Rice Straw (2) EF
C_2H_7N	9.82E-03	1.28E-02	-	-	-	6.90E-02	5.32E-2(8.98E-3)
CH_4S	1.59E-02	2.69E-03	2.92E-04	5.39E-2(6.72E-2)	5.36E-03	3.91E-02	2.22E-2(7.08E-3)
C_2H_5NO	-	-	3.86	2.54(2.36)	2.55	-	7.99E-02
C_3H_9N	3.74E-03	1.41E-03	-	-	-	9.97E-03	3.39E-2(3.55E-2)
C_5H_4	1.02E-02	1.34E-04	7.09E-02	0.107(0.126)	0.218	1.53E-02	8.01E-3(3.79E-3)
C_5H_{10}	2.52E-02	8.65E-03	0.585	0.316(0.200)	0.240	0.118	2.45E-2(5.57E-3)
C_6H_{12}	5.03E-03	1.78E-03	0.666	0.393(0.458)	0.421	5.61E-02	1.02E-2(2.45E-3)
$C_5H_{10}O$	-	-	2.48E-02	0.123(0.112)	2.93E-02	-	-
C_4H_9NO	-	1.27E-02	1.27E-02	6.85E-2(9.27E-2)	2.12E-03	6.36E-02	3.16E-2(1.81E-2)
$C_3H_4O_3$	1.90E-03	9.78E-04	0.110	0.103(0.143)	0.110	2.13E-02	3.12E-3(1.14E-3)
$C_4H_{11}NO$	-	-	-	-	-	-	1.84E-2(1.12E-2)
C_6H_4O	8.08E-03	7.28E-04	0.125	0.291(0.395)	0.541	1.02E-02	6.18E-03
C_7H_{10}	0.163	3.94E-02	4.64	1.962(2.498)	3.19	0.416	0.211(0.144)
C_6H_8O	0.129	6.01E-02	-	0.145	0.133	0.251	0.174(0.231)
C_7H_{12}	4.39E-02	6.56E-03	0.169	0.302(0.098)	0.180	0.115	0.271
$C_6H_{10}O$	2.82E-02	-	9.91E-02	0.157	8.32E-02	-	-
$C_4H_4O_3$	2.54E-02	2.25E-03	0.110	0.190(0.075)	0.156	0.130	4.73E-2(5.25E-2)
$C_4H_6O_3$	6.23E-02	2.37E-02	6.31E-02	0.158(0.178)	9.81E-02	0.204	7.35E-2(6.26E-2)
$C_5H_{10}O_2$	2.60E-02	9.09E-03	5.91E-02	0.224(0.021)	0.166	4.87E-02	2.80E-2(1.76E-3)
C_7H_5N	3.41E-02	-	-	-	-	-	-
C_7H_8O	0.198	6.80E-02	2.64E-02	0.259(0.167)	0.124	0.277	0.227(0.101)
C_8H_{12}	5.94E-02	-	1.32	0.743(0.899)	0.844	-	-
C_8H_{14}	-	1.78E-03	0.455	0.362(0.241)	0.307	4.43E-02	4.93E-03
$C_6H_{10}O_2$	-	-	-	-	-	-	3.62E-02
$C_5H_8O_3$	7.89E-02	5.53E-02	5.16E-02	3.58E-2(1.01E-2)	3.67E-02	0.286	1.82E-1(8.32E-2)
$C_6H_{12}O_2$	2.77E-02	-	4.14E-02	9.26E-2(2.30E-2)	7.85E-02	-	-
C_9H_{14}	6.54E-02	7.45E-03	4.62E-03	0.193(0.113)	0.189	0.137	9.62E-03
$C_6H_4O_3$	5.88E-02	1.27E-02	0.176	0.137(0.017)	7.40E-02	0.192	8.97E-2(1.97E-2)

$C_7H_{10}O_2$	5.72E-02	2.01E-02	-	-	-	0.111	8.38E-2(5.14E-2)
C_9H_8O	-	-	-	-	-	-	-
$C_8H_6O_2$	2.08E-02	5.53E-03	1.31E-02	4.38E-02	2.41E-02	3.17E-02	2.27E-2(8.77E-3)
$C_9H_{10}O$	2.55E-02	1.32E-02	1.61E-02	8.95E-02	7.62E-02	8.59E-02	3.84E-2(1.29E-2)
$C_{10}H_{14}$	4.87E-02	4.83E-03	8.21E-03	0.274(0.006)	0.210	0.171	0.020(0.018)
$C_8H_8O_2$	4.87E-02	1.46E-02	4.48E-02	0.127(0.029)	5.87E-02	9.33E-02	6.82E-2(1.61E-2)
$C_9H_{12}O$	-	-	2.16E-02	0.114(0.051)	0.115	-	-
$C_7H_6O_3$	2.16E-02	6.03E-03	0.106	0.317(0.319)	0.201	0.103	4.32E-2(1.35E-2)
$C_8H_{10}O_2$	3.49E-02	2.02E-02	-	0.216	-	0.220	8.08E-2(4.18E-2)
$C_7H_8O_3$	1.48E-02	6.00E-03	4.41E-02	0.185(0.022)	8.76E-02	7.63E-02	2.37E-2(1.10E-2)
$C_8H_{12}O_2$	1.56E-02	7.91E-03	-	-	-	3.47E-02	2.57E-2(1.38E-2)
$C_{10}H_8O$	6.85E-02	8.21E-03	0.301	0.295(0.058)	0.397	0.256	4.51E-2(1.69E-2)
$C_{11}H_{13}$	5.87E-02	1.01E-02	4.54E-02	0.291	0.237	0.106	-
$C_{10}H_{10}O$	3.97E-02	1.60E-02	3.67E-02	0.127	0.109	8.98E-02	4.72E-2(1.76E-2)
$C_{11}H_{14}$	-	-	7.14E-03	0.165	0.153	-	-
$C_9H_8O_2$	3.14E-02	7.35E-03	4.65E-02	0.148(0.002)	8.42E-02	5.68E-02	3.74E-2(8.75E-3)
$C_{10}H_{12}O$	-	-	-	-	-	-	3.74E-02
$C_{11}H_{16}$	4.71E-02	1.53E-02	2.83E-02	0.269	0.221	0.271	-
$C_9H_{10}O_2$	2.94E-02	3.59E-02	6.32E-02	0.297	0.156	0.304	1.50E-1(6.55E-2)
$C_{11}H_{18}$	3.24E-02	-	-	-	-	-	-
$C_8H_{10}O_3$	6.96E-02	2.34E-02	4.37E-02	0.286(0.090)	8.70E-02	4.83E-02	6.33E-2(2.44E-2)
$C_{10}H_{12}O_2$	-	-	-	-	-	-	5.86E-02

Table S3. Continued

Fuel type (number of fires)	Sawgrass (12) EF	Sugar Cane (2) EF	Wheat Straw Conv. (4) EF	Wheat Straw Organic (6) EF	Wiregrass (7) EF
MCE	0.959(0.004)	0.922(0.011)	0.959(0.003)	0.956(0.014)	0.968(0.004)
OP-FTIR species					
CO_2	1599(12)	1288(53)	1454(58)	1486(36)	1650(9)
CO	43.8(4.0)	69.5(7.5)	39.1(3.8)	43.7(13.6)	34.2(4.5)
CH_4	0.911(0.465)	2.99(0.67)	1.36(0.45)	1.74(0.76)	0.584(0.188)
NH_3	0.138(0.084)	1.15(0.01)	0.207(0.139)	0.231(0.203)	0.152(0.096)
C_2H_2	0.192(0.049)	0.802(0.177)	0.192(0.066)	0.134(0.032)	0.103(0.025)
HCN	0.258(0.043)	0.455(0.096)	0.100(0.013)	0.123(0.040)	9.65E-2(1.04E-2)
C_2H_4	0.429(0.174)	2.03(0.41)	0.601(0.157)	0.542(0.100)	0.280(0.052)
HCHO	0.372(0.135)	3.58(0.95)	0.831(0.358)	1.15(0.30)	0.358(0.079)
NO	2.00(0.20)	1.03(0.15)	1.21(0.16)	1.19(0.18)	1.85(0.09)
CH_3OH	0.166(0.101)	1.94(0.62)	0.483(0.237)	1.14(0.64)	0.139(0.056)
HCl	1.72(0.34)	9.93E-2(3.51E-2)	0.470(0.518)	0.721(0.115)	6.60E-2(3.21E-2)
C_3H_6	0.141(0.109)	0.682(0.163)	0.178(0.057)	0.225(0.083)	6.98E-2(3.80E-2)
HCOOH	4.85E-2(2.92E-2)	1.11(0.61)	6.19E-2(2.11E-2)	0.196(0.067)	4.84E-2(1.83E-2)

NO_2	0.955(0.194)	1.48(0.04)	1.07(0.19)	1.45(0.60)	0.658(0.259)
HONO	0.180(0.054)	0.613(0.090)	0.176(0.049)	0.183(0.009)	0.210(0.042)
CH_3COOH	0.499(0.327)	6.08(2.48)	0.653(0.283)	2.49(1.47)	0.364(0.119)
$C_2H_4O_2$	0.141(0.055)	4.81(2.39)	0.428(0.000)	0.254(0.158)	0.182(0.065)
SO_2	1.82(0.09)	0.840(0.000)	0.735(0.147)	1.11(0.35)	1.00(0.09)
C_4H_4O	7.97E-2(2.82E-2)	0.227(0.033)	6.37E-2(3.36E-2)	0.163(0.074)	4.37E-2(1.77E-2)

PTR-TOF-MS species

Formula	Sawgrass SC (1) EF	Sugar Cane LA(2) EF	Wheat Straw Conv (1) EF	Wheat Straw Organic (1) EF	Wiregrass (1) EF
C_3H_4	6.41E-2(3.63E-2)	-	-	0.202(0.044)	3.64E-2(1.43E-2)
C_2H_3N	5.10E-2(1.56E-2)	0.251(0.046)	5.20E-2(2.15E-2)	4.63E-2(2.38E-2)	1.82E-2(9.80E-3)
C_2H_2O	0.230(0.287)	3.99(1.64)	0.310(0.163)	0.850(0.452)	0.210(0.132)
C_2H_4O	0.391(0.465)	4.33(1.37)	0.610(0.323)	0.910(0.416)	0.298(0.178)
C_4H_2	6.87E-4(2.84E-4)	4.90E-3(1.54E-3)	5.17E-4(2.84E-4)	7.28E-4(2.03E-4)	3.09E-4(1.10E-4)
C_4H_4	6.78E-3(2.33E-3)	9.81E-2(3.59E-2)	1.19E-2(4.77E-3)	2.12E-2(8.58E-3)	5.88E-3(1.35E-3)
C_3H_2O	7.24E-3(3.04E-3)	-	1.24E-2(6.11E-3)	2.50E-2(1.22E-2)	5.28E-3(1.20E-3)
C_4H_6	2.71E-2(1.49E-2)	0.288(0.091)	5.16E-2(2.23E-2)	6.72E-2(2.63E-2)	1.84E-2(5.46E-3)
C3H4O	0.105(0.058)	1.47(0.47)	0.256(0.141)	0.347(0.126)	0.100(0.031)
C_4H_8	2.83E-2(3.10E-2)	0.218(0.064)	4.67E-2(3.10E-2)	3.99E-2(2.34E-2)	1.75E-2(1.03E-2)
C_3H_6O	9.28E-2(6.68E-2)	0.973(0.304)	0.218(0.107)	0.329(0.167)	5.96E-2(1.11E-2)
C_2H_6S	4.35E-3(2.58E-3)	-	-	2.60E-2(1.01E-2)	3.02E-03
C_5H_6	1.37E-2(6.23E-3)	0.129(0.040)	0.022(0.009)	2.61E-2(1.03E-2)	8.23E-3(2.24E-3)
C_3O_2	6.54E-4(1.01E-4)	-	1.35E-3(1.27E-4)	3.18E-04	-
C_5H_8	4.10E-2(2.98E-2)	0.372(0.116)	7.47E-2(4.16E-2)	8.09E-2(3.90E-2)	1.94E-2(7.37E-3)
C_4H_6O	7.61E-2(4.85E-2)	0.837(0.281)	0.143(0.075)	0.253(0.128)	5.10E-2(1.94E-2)
$C_3H_4O_2$	4.47E-2(2.75E-2)	1.01(0.41)	9.22E-2(5.15E-2)	0.226(0.115)	4.55E-2(1.34E-2)
C_4H_8O	1.95E-2(1.53E-2)	0.356(0.180)	6.10E-2(2.93E-2)	0.136(0.059)	1.26E-2(6.88E-3)
$C_3H_6O_2$	4.09E-2(2.08E-2)	2.10(0.88)	0.207(0.124)	0.369(0.192)	7.06E-2(4.26E-2)
C_6H_6	0.161(0.047)	0.398(0.087)	0.142(0.040)	0.112(0.028)	7.24E-2(1.89E-2)
C_5H_4O	2.13E-2(1.07E-2)	0.358(0.134)	6.69E-2(4.00E-2)	0.136(0.072)	2.37E-2(1.10E-2)
C_5H_6O	4.01E-2(3.01E-2)	0.612(0.226)	0.100(0.055)	0.235(0.152)	2.97E-2(1.27E-2)
C_6H_{10}	4.16E-3(2.91E-3)	4.52E-2(1.28E-2)	9.93E-3(6.34E-3)	1.09E-2(9.19E-3)	2.73E-3(5.28E-4)
$C_4H_4O_2$	6.17E-2(4.34E-2)	1.24(0.51)	0.126(0.083)	0.370(0.233)	5.50E-2(2.16E-2)
C_5H_8O	1.82E-2(1.49E-2)	0.220(0.075)	4.54E-2(2.56E-2)	6.93E-2(3.47E-2)	1.28E-2(6.22E-3)
$C_4H_6O_2$	5.38E-2(4.11E-2)	1.47(0.58)	0.173(0.105)	0.409(0.246)	6.89E-2(2.70E-2)
$C_4H_8O_2$	7.75E-3(6.28E-3)	0.264(0.115)	2.86E-2(1.55E-2)	7.46E-2(4.46E-2)	1.12E-2(5.25E-3)
C_7H_6	3.81E-3(1.39E-3)	5.18E-2(2.13E-2)	4.93E-3(1.96E-3)	9.27E-3(5.11E-3)	2.27E-3(6.96E-4)
C_7H_8	5.39E-2(2.81E-2)	0.449(0.134)	8.98E-2(4.58E-2)	0.101(0.030)	3.13E-2(9.17E-3)
C_6H_6O	0.105(0.051)	0.550(0.157)	9.35E-2(4.16E-2)	0.132(0.068)	4.31E-2(1.59E-2)
$C_5H_4O_2$	0.175(0.123)	1.48(0.57)	0.277(0.194)	0.674(0.464)	7.67E-2(2.94E-2)
$C_5H_6O_2$	6.19E-2(5.50E-2)	1.43(0.61)	0.113(0.071)	0.387(0.259)	5.71E-2(2.56E-2)
$C_5H_8O_2$	1.49E-2(1.21E-2)	0.324(0.131)	3.87E-2(2.22E-2)	0.118(0.076)	1.82E-2(8.22E-3)

C_8H_6	-	-	-	-	1.14E-2(3.95E-3)
C_8H_8	1.49E-2(5.16E-3)	8.59E-2(2.32E-2)	1.57E-2(5.64E-3)	1.41E-2(6.27E-3)	7.68E-3(2.38E-3)
C_7H_6O	1.74E-2(3.95E-3)	9.89E-2(2.19E-2)	2.49E-2(1.03E-2)	2.55E-2(9.04E-3)	9.97E-3(2.08E-3)
C_8H_{10}	1.48E-2(7.83E-3)	0.117(0.037)	2.74E-2(1.27E-2)	3.75E-2(2.04E-2)	8.06E-3(2.83E-3)
$C_6H_4O_2$	1.33E-2(5.89E-3)	-	2.33E-2(3.52E-3)	0.104(0.050)	7.26E-3(1.78E-3)
$C_6H_6O_2$	5.84E-2(5.09E-2)	0.653(0.279)	7.88E-2(4.60E-2)	0.243(0.179)	0.029(0.014)
$C_7H_{10}O$	9.34E-3(7.44E-3)	0.181(0.069)	2.22E-2(1.83E-2)	5.75E-2(3.02E-2)	7.42E-3(3.74E-3)
$C_5H_4O_3$	1.23E-2(7.70E-3)	0.418(0.260)	1.36E-2(7.95E-3)	6.90E-2(4.65E-2)	7.10E-3(2.78E-3)
$C_6H_8O_2$	2.16E-2(2.05E-2)	0.628(0.281)	5.68E-2(3.44E-2)	0.169(0.113)	2.52E-2(1.25E-2)
$C_5H_6O_3$	5.40E-2(4.25E-2)	0.978(0.514)	4.17E-2(3.13E-2)	0.200(0.132)	3.36E-2(1.13E-2)
C_9H_8	9.93E-3(4.78E-3)	-	1.40E-02	5.43E-2(2.93E-2)	-
C_8H_6O	9.34E-3(2.40E-3)	6.13E-2(2.00E-2)	1.06E-2(4.07E-3)	1.60E-2(7.85E-3)	4.71E-3(1.21E-3)
C_9H_{10}	5.40E-3(2.35E-3)	3.74E-2(1.15E-2)	7.60E-3(2.70E-3)	8.93E-3(3.18E-3)	2.73E-3(9.05E-4)
C_8H_8O	7.97E-2(5.16E-2)	1.09(0.44)	5.53E-2(3.42E-2)	7.40E-2(3.97E-2)	4.56E-2(1.57E-2)
C_9H_{12}	6.45E-3(3.96E-3)	0.115(0.041)	1.71E-2(9.99E-3)	1.82E-2(7.13E-3)	5.21E-3(3.04E-3)
$C_7H_6O_2$	1.70E-2(6.71E-3)	0.187(0.066)	2.45E-2(1.43E-2)	4.46E-2(3.04E-2)	9.56E-3(2.88E-3)
$C_8H_{10}O$	2.41E-2(1.62E-2)	0.246(0.086)	3.85E-2(2.08E-2)	5.80E-2(3.23E-2)	1.45E-2(9.59E-3)
$C_7H_8O_2$	2.29E-2(2.16E-2)	0.579(0.231)	6.90E-2(4.49E-2)	0.201(0.138)	2.58E-2(1.32E-2)
$C_6H_6O_3$	2.72E-2(2.82E-2)	0.464(0.252)	3.10E-2(1.66E-2)	0.194(0.171)	1.53E-2(7.82E-3)
$C_{10}H_8$	2.71E-2(8.28E-3)	9.32E-2(3.02E-2)	3.24E-2(1.43E-2)	3.80E-2(1.73E-2)	1.74E-2(4.29E-3)
$C_{10}H_{10}$	-	4.46E-2(1.74E-2)	3.23E-03	4.83E-03	3.77E-3(1.19E-3)
$C_{10}H_{16}$	1.26E-2(5.64E-3)	7.77E-2(2.26E-2)	1.70E-2(6.44E-3)	2.08E-2(1.01E-2)	6.40E-3(2.06E-3)
$C_{11}H_{10}$	1.01E-2(3.15E-3)		-	5.03E-02	4.62E-3(1.52E-3)

PTR-TOF-MS Extended Analysis Species

Formula	Sawgrass SC (1) EF	Sugar Cane LA(2) EF	Wheat Straw Conv (1) EF	Wheat Straw Organic (1) EF	Wiregrass (1) EF
C_2H_7N	1.48E-02	7.95E-2(1.04E-1)	7.66E-03	3.17E-02	-
CH_4S	9.51E-04	3.83E-2(3.39E-2)	1.99E-03	7.64E-03	1.74E-03
C_2H_5NO	-	-	-	-	-
C_3H_9N	1.00E-02	8.25E-2(1.12E-1)	2.80E-03	2.72E-02	6.92E-03
C_5H_4	5.82E-04	1.23E-2(1.34E-2)	6.00E-04	3.54E-03	1.24E-03
C_5H_{10}	3.75E-03	3.13E-2(2.84E-2)	6.96E-03	2.46E-02	4.84E-03
C_6H_{12}	1.72E-03	1.24E-2(1.09E-2)	-	9.58E-03	2.55E-03
$C_5H_{10}O$	-	-	-	-	-
C_4H_9NO	3.80E-03	0.182(0.000)	6.22E-03	3.80E-02	8.20E-03
$C_3H_4O_3$	1.06E-03	1.78E-2(2.18E-2)	8.06E-04	4.14E-03	1.65E-03
$C_4H_{11}NO$	-	5.31E-2(0.00E0)	-	9.13E-03	-
C_6H_4O	5.72E-04	8.17E-3(6.57E-3)	-	1.56E-02	4.07E-03
C_7H_{10}	1.61E-02	0.820(1.114)	1.49E-02	0.523	1.03E-02
C_6H_8O	2.06E-02	4.08E-2(2.42E-2)	1.87E-02	1.30E-02	1.51E-02
C_7H_{12}	2.69E-03	0.820(1.145)	8.29E-03	0.291	7.28E-03
$C_6H_{10}O$	-	1.25E-2(0.00E0)	-	-	-

$C_4H_4O_3$	1.87E-03	0.186(0.254)	1.85E-03	8.63E-02	4.24E-03
$C_4H_6O_3$	7.24E-03	5.60E-2(2.67E-2)	7.29E-03	1.03E-02	2.07E-02
$C_5H_{10}O_2$	-	7.76E-3(0.00E0)	2.92E-03	-	-
C_7H_5N	-	2.76E-2(0.00E0)	-	-	-
C_7H_8O	4.96E-02	0.211(0.188)	2.24E-02	7.65E-02	1.95E-02
C_8H_{12}	-	1.44E-2(0.00E0)	-	-	-
C_8H_{14}	1.43E-04	8.02E-3(3.86E-3)	4.26E-03	1.00E-02	4.61E-03
$C_6H_{10}O_2$	-	-	5.92E-03	-	-
$C_5H_8O_3$	8.81E-03	0.421(0.524)	1.13E-02	0.138	2.06E-02
$C_6H_{12}O_2$	-	4.84E-3(0.00E0)	-	-	-
C_9H_{14}	5.25E-03	1.85E-2(1.11E-2)	3.80E-03	7.93E-03	3.63E-03
$C_6H_4O_3$	5.57E-03	0.191(0.250)	3.25E-03	0.128	8.18E-03
$C_7H_{10}O_2$	2.25E-03	0.115(0.136)	5.79E-03	3.64E-02	6.05E-03
C_9H_8O	-	-	-	-	-
$C_8H_6O_2$	-	4.23E-2(5.03E-2)	2.23E-03	1.64E-02	-
$C_9H_{10}O$	1.18E-02	4.77E-2(4.75E-2)	4.01E-03	1.34E-02	6.90E-03
$C_{10}H_{14}$	-	1.27E-2(6.90E-3)	-	4.51E-03	-
$C_8H_8O_2$	5.35E-03	0.166(0.204)	1.04E-03	5.42E-02	5.75E-03
$C_9H_{12}O$	5.13E-03	-	8.95E-03	-	2.92E-03
$C_7H_6O_3$	1.83E-03	0.119(0.154)	2.86E-03	5.21E-02	5.01E-03
$C_8H_{10}O_2$	3.15E-03	0.132(0.159)	6.19E-03	5.13E-02	9.43E-03
$C_7H_8O_3$	1.56E-03	5.89E-2(7.27E-2)	2.04E-03	1.65E-02	3.29E-03
$C_8H_{12}O_2$	-	3.46E-2(4.16E-2)	1.84E-03	1.17E-02	-
$C_{10}H_8O$	6.11E-03	0.139(0.175)	5.13E-03	4.00E-02	5.52E-03
$C_{11}H_{13}$	-	7.58E-3(0.00E0)	3.75E-03	-	-
$C_{10}H_{10}O$	9.50E-03	5.90E-2(5.93E-2)	5.44E-03	2.06E-02	3.81E-03
$C_{11}H_{14}$	-	-	-	-	-
$C_9H_8O_2$	7.96E-03	7.22E-2(8.12E-2)	-	2.78E-02	6.38E-03
$C_{10}H_{12}O$	-	-	-	-	-
$C_{11}H_{16}$	-	1.01E-2(0.00E0)	-	-	-
$C_9H_{10}O_2$	6.10E-03	0.307(0.358)	1.05E-02	0.103	2.19E-02
$C_{11}H_{18}$	-	4.51E-3(0.00E0)	-	-	-
$C_8H_{10}O_3$	-	0.120(0.146)	6.29E-03	5.54E-02	-
$C_{10}H_{12}O_2$	-	-	-	-	-

Table S3. Continued

Fuel type (number of fires)	Trash (2) EF	Tires Shredded (1) EF	Cook Envirofit Rocket G3300 (3) EF	Cook Ezystove (2) EF	Cook 3 Stone (3) EF
MCE	0.973(0.006)	0.961	0.975(0.010)	0.968(0.024)	0.968(0.004)
OP-FTIR species					
CO_2	1780(32)	2807	1633(43)	1569(112)	1611(30)
CO	31.3(6.8)	73.5	26.5(10.0)	32.8(23.5)	34.3(4.9)
CH_4	0.795(0.198)	1.43	0.814(0.548)	1.51(1.56)	1.30(0.05)
NH_3	6.21E-02	-	1.44E-2(1.19E-2)	0.121(0.145)	1.41E-2(1.23E-2)
C_2H_2	0.325(0.103)	1.293	0.454(0.693)	0.324(0.128)	0.627(0.376)
HCN	5.30E-2(6.34E-2)	0.353	0.042962	-	-
C_2H_4	0.977(0.048)	1.33	0.333(0.428)	0.518(0.443)	0.594(0.375)
HCHO	0.915(0.468)	-	0.321(0.162)	0.605(0.288)	0.455(0.199)
NO	0.518(0.085)	3.32	0.470(0.182)	0.790(0.322)	0.331(0.092)
CH_3OH	0.167(0.081)	-	0.350(0.254)	0.786(0.028)	0.550(0.438)
HCl	0.797(1.000)	-	-	-	-
C_3H_6	0.638(0.046)	-	-	0.0118079	8.49E-2(3.89E-2)
HCOOH	4.45E-2(3.11E-2)	7.25E-02	0.118(0.070)	0.185(0.082)	0.166(0.143)
NO_2	0.767(0.393)	2.48	1.06(0.11)	1.56(0.00)	1.15(0.29)
HONO	0.240(0.124)	1.47	0.660045	-	0.302(0.176)
CH_3COOH	-	1.22	1.23(0.72)	2.47(0.71)	2.39(2.49)
$C_2H_4O_2$	0.658(0.817)	-	0.182432	0.107169	0.122(0.040)
SO_2	0.892	27.1	-	-	0.519056
C_4H_4O	0.117(0.048)	2.13E-02	4.50E-2(3.11E-2)	6.78E-2(7.33E-2)	6.13E-2(4.34E-2)

PTR-TOF-MS species

Formula	Trash (1) EF	Tires Shredded (1) EF	Cook Envirofit Rocket G3300 (3) EF	Cook Ezystove (2) EF	Cook 3 Stone (3) EF
C_3H_4	-	0.617	-	-	-
C_2H_3N	1.94E-2(1.17E-2)	8.46E-02	1.18E-3(9.66E-4)	1.43E-2(1.81E-2)	5.50E-3(1.24E-3)
C_2H_2O	0.359(0.246)	0.229	0.256(0.179)	0.628(0.188)	0.356(0.364)
C_2H_4O	0.782(0.463)	0.331	0.180(0.203)	0.367(0.148)	0.213(0.118)
C_4H_2	2.05E-3(8.82E-5)	3.03E-02	0.000276712	0.0022931	4.39E-3(3.32E-3)
C_4H_4	1.99E-2(5.50E-3)	0.1684759	4.32E-3(1.64E-3)	1.70E-2(7.18E-3)	2.14E-2(1.22E-2)
C_3H_2O	-	1.99E-02	-	-	-
C_4H_6	0.112(0.007)	0.321	1.59E-2(5.20E-3)	4.04E-2(7.66E-3)	3.50E-2(1.01E-2)
C3H4O	0.230(0.096)	0.203	6.70E-2(5.36E-2)	0.173(0.106)	9.20E-2(3.58E-2)
C_4H_8	0.192(0.033)	0.731	2.94E-2(5.93E-3)	3.01E-2(1.85E-2)	6.59E-2(3.97E-2)
C_3H_6O	0.112	-	4.58E-2(2.65E-2)	0.217(0.168)	-
C_2H_6S	-	-	-	-	-
C_5H_6	3.37E-2(2.10E-3)	0.267	4.63E-3(2.62E-3)	2.48E-2(1.83E-2)	3.37E-2(2.58E-2)

C_3O_2	2.66E-04		-	-	-
C_5H_8	0.199(0.043)	1.072555	0.0359824	0.0164446	3.89E-2(2.08E-2)
C_4H_6O	0.140(0.062)	0.111	3.89E-2(2.74E-2)	0.118(0.065)	5.70E-2(3.02E-2)
$C_3H_4O_2$	0.124(0.083)	3.79E-02	4.32E-2(3.23E-2)	7.65E-2(5.78E-3)	4.75E-2(2.80E-2)
C_4H_8O	3.75E-2(5.60E-3)	8.50E-03	1.32E-2(9.97E-3)	8.27E-2(7.63E-2)	2.16E-2(1.34E-2)
$C_3H_6O_2$	0.211(0.160)	-	0.109(0.096)	0.296(0.092)	0.129(0.098)
C_6H_6	0.328(0.063)	8.68	4.82E-2(1.34E-2)	0.203(0.216)	0.692(0.720)
C_5H_4O	5.17E-2(3.70E-2)	6.46E-02	2.75E-2(2.28E-2)	0.105(0.008)	4.27E-2(3.24E-2)
C_5H_6O	8.95E-2(3.43E-2)	5.27E-02	3.75E-2(2.77E-2)	0.125(0.037)	5.93E-2(3.71E-2)
C_6H_{10}	4.10E-2(1.88E-2)	7.46E-02	5.56E-3(1.85E-3)	0.0092146	5.95E-3(1.55E-3)
$C_4H_4O_2$	0.166(0.133)	7.78E-02	4.91E-2(3.41E-2)	0.132(0.048)	5.57E-2(4.54E-2)
C_5H_8O	4.19E-2(1.71E-2)	4.01E-02	1.68E-2(1.19E-2)	4.95E-2(2.65E-2)	2.42E-2(1.39E-2)
$C_4H_6O_2$	0.128(0.078)	2.39E-02	8.23E-2(6.55E-2)	0.227(0.058)	0.109(0.081)
$C_4H_8O_2$	2.19E-2(1.21E-2)	-	1.40E-2(7.97E-3)	5.61E-2(1.26E-2)	2.34E-2(2.28E-2)
C_7H_6	1.33E-2(2.59E-3)	8.56E-02	2.63E-3(2.98E-5)	3.91E-3(3.02E-3)	1.00E-2(8.37E-3)
C_7H_8	0.150(0.048)	0.569	0.117(0.154)	5.57E-2(3.63E-2)	7.79E-2(8.34E-2)
C_6H_6O	5.78E-2(1.66E-3)	0.464	1.55E-2(8.57E-3)	0.135(0.164)	7.08E-2(2.28E-2)
$C_5H_4O_2$	0.180(0.117)	6.16E-02	0.135(0.107)	0.345(0.170)	0.249(0.278)
$C_5H_6O_2$	0.143(0.106)	3.18E-02	3.12E-2(0.00E0)	-	7.76E-2(6.39E-2)
$C_5H_8O_2$	4.22E-2(2.94E-2)	1.30E-03	2.75E-2(1.82E-2)	8.66E-2(2.31E-2)	4.21E-2(4.14E-2)
C_8H_6	-	0.227	-	-	6.34E-2(2.86E-2)
C_8H_8	0.383(0.144)	0.746	4.32E-3(1.45E-3)	1.92E-2(1.65E-2)	6.29E-2(8.20E-2)
C_7H_6O	5.11E-2(1.06E-2)	0.368	4.34E-3(1.79E-3)	2.17E-2(2.29E-2)	3.06E-2(2.74E-2)
C_8H_{10}	4.29E-2(1.57E-2)	0.504	7.78E-3(7.04E-3)	2.74E-2(2.96E-2)	7.10E-2(1.02E-1)
$C_6H_4O_2$	-	4.76E-02	-	-	-
$C_6H_6O_2$	0.075(0.042)	4.47E-02	3.09E-2(1.74E-2)	8.83E-2(8.57E-4)	5.02E-2(3.46E-2)
$C_7H_{10}O$	2.25E-2(6.33E-3)	2.38E-03	7.55E-3(6.46E-3)	5.36E-2(4.27E-2)	1.10E-2(6.33E-3)
$C_5H_4O_3$	4.24E-2(3.68E-2)	1.19E-02	8.21E-3(3.17E-3)	1.83E-2(1.03E-2)	8.84E-3(6.54E-3)
$C_6H_8O_2$	5.54E-2(3.22E-2)	1.58E-02	2.64E-2(1.92E-2)	8.13E-2(4.47E-3)	3.98E-2(2.96E-2)
$C_5H_6O_3$	0.070(0.055)	-	1.96E-2(1.08E-2)	5.30E-2(3.81E-2)	3.23E-2(3.64E-2)
C_9H_8	9.67E-02	-	0.0197692	-	0.104(0.071)
C_8H_6O	1.10E-2(1.11E-3)	0.101	1.99E-3(1.34E-3)	9.26E-3(1.22E-2)	1.23E-2(6.91E-3)
C_9H_{10}	2.15E-2(9.52E-3)	0.198	2.29E-3(1.01E-3)	7.99E-3(7.52E-3)	2.64E-2(3.84E-2)
C_8H_8O	2.53E-2(2.11E-3)	0.102	3.33E-3(2.05E-3)	9.23E-2(1.24E-1)	1.78E-2(1.14E-2)
C_9H_{12}	1.57E-2(4.74E-3)	0.147	4.41E-3(6.46E-3)	2.13E-2(2.67E-2)	1.88E-2(2.49E-2)
$C_7H_6O_2$	2.06E-2(6.16E-3)	0.103	4.34E-3(1.18E-3)	2.70E-2(1.99E-2)	1.32E-2(7.14E-4)
$C_8H_{10}O$	1.74E-2(8.71E-4)	1.58E-02	6.96E-3(5.37E-3)	7.28E-2(8.94E-2)	1.52E-2(5.81E-3)
$C_7H_8O_2$	4.05E-2(2.30E-2)	1.14E-02	2.91E-2(2.41E-2)	8.55E-2(3.79E-2)	4.02E-2(2.72E-2)
$C_6H_6O_3$	9.37E-2(8.19E-2)	-	1.49E-2(6.23E-3)	3.25E-2(8.83E-3)	2.00E-2(1.43E-2)
$C_{10}H_8$	5.92E-02	2.77	2.58E-2(1.64E-2)	4.82E-2(9.50E-3)	0.279(0.339)
$C_{10}H_{10}$	-	0.142	-	-	2.66E-2(3.31E-2)
$C_{10}H_{16}$	3.00E-2(1.21E-2)	0.555	3.70E-3(2.91E-3)	1.61E-2(2.01E-2)	5.28E-2(6.90E-2)
$C_{11}H_{10}$	-	0.493	-	-	-

PTR-TOF-MS Extended Analysis Species

Formula	Trash (1) EF	Tires Shredded (1) EF	Cook Envirofit Rocket G3300 (3) EF	Cook Ezystove (2) EF	Cook 3 Stone (3) EF
C_2H_7N	8.23E-03		0.001357095	0.010189931	0.013394404
CH_4S	1.99E-03		0.00126465	0.00176495	0.002649792
C_2H_5NO	-		-	0.010675276	0.010853526
C_3H_9N	8.51E-04		-	-	-
C_5H_4	2.05E-03		-	-	-
C_5H_{10}	7.25E-02		2.16382E-05	0.007722238	0.006148992
C_6H_{12}	4.90E-02		-	0.002820348	0.001143917
$C_5H_{10}O$	-		-	-	-
C_4H_9NO	6.66E-03		0.007383919	0.01565163	0.022347977
$C_3H_4O_3$	1.22E-03		-	0.001422656	0.000390765
$C_4H_{11}NO$	-		-	-	-
C_6H_4O	-		-	0.004581214	0.018725745
C_7H_{10}	5.23E-02		0.003321212	0.006646942	0.012755995
C_6H_8O	3.19E-02		-	-	-
C_7H_{12}	6.22E-02		0.000756882	0.02552336	0.034509122
$C_6H_{10}O$	1.25E-02		-	-	-
$C_4H_4O_3$	4.32E-03		0.001273022	0.009282984	0.006364288
$C_4H_6O_3$	2.31E-02		0.014544569	0.037958186	0.05723266
$C_5H_{10}O_2$	7.70E-03		-	-	-
C_7H_5N	-		-	-	-
C_7H_8O	7.51E-03		0.001640728	0.012059809	0.033091845
C_8H_{12}	5.39E-02		0.003826944	0.005497219	0.005388368
C_8H_{14}	-		-	-	0.002034644
$C_6H_{10}O_2$	-		-	-	-
$C_5H_8O_3$	9.70E-03		0.008566051	0.051225979	0.079851267
$C_6H_{12}O_2$	2.56E-02		-	0.00385558	0.007010837
C_9H_{14}	2.74E-02		-	0.002496594	0.005300344
$C_6H_4O_3$	9.70E-03		0.00472459	0.016834314	0.026063674
$C_7H_{10}O_2$	-		0.00212055	0.01107822	0.018600782
C_9H_8O	-		-	-	-
$C_8H_6O_2$	4.99E-03		0.000957476	0.001325727	0.004451757
$C_9H_{10}O$	3.74E-03		0.001771154	0.004214834	0.007025028
$C_{10}H_{14}$	1.14E-02		-	-	0.00175423
$C_8H_8O_2$	4.37E-03		0.002143527	0.008390181	0.018552922
$C_9H_{12}O$	-		-	-	-
$C_7H_6O_3$	1.33E-02		0.002502763	0.006221881	0.014721563
$C_8H_{10}O_2$	3.69E-03		0.007016489	0.022333445	0.033423231
$C_7H_8O_3$	1.24E-02		-	0.012894996	0.020883085
$C_8H_{12}O_2$	-		-	-	-

$C_{10}H_8O$	8.45E-03	0.001688903	0.007430579	0.016183878
$C_{11}H_{13}$	3.90E-02	-	-	-
$C_{10}H_{10}O$	-	0.001590815	0.005618523	0.009103636
$C_{11}H_{14}$	-	-	-	-
$C_9H_8O_2$	3.74E-03	-	-	-
$C_{10}H_{12}O$	-	-	-	-
$C_{11}H_{16}$	1.29E-02	-	-	-
$C_9H_{10}O_2$	5.10E-03	0.003272317	0.015556551	0.027374466
$C_{11}H_{18}$	1.33E-02	-	-	-
$C_8H_{10}O_3$	-	0.009450812	0.041551239	0.077254981
$C_{10}H_{12}O_2$	-	0.003775361	0.014218819	0.036741984

Table S4. Emission factors (g/kg) for common fire-types adjusted to improve laboratory representation of real-world biomass burning emissions.

Protonated m/z	Formula	EF Savanna grasses (18)[a]	EF Crop Residue (19) (food fuels)[a]	EF Peat (6) avg,stdev	EF Chaparral (8) avg,stdev	EF Coniferous Canopy (14) avg,stdev	EF Open Cooking adjusted (3[b], 1[b])	EF Rocket cookstoves (5) avg,stdev	EF Gasifier Cookstove (1)
	MCE	0.938	0.925	0.767(0.074)	0.927(0.017)	0.933(0.032)	0.927	0.972(0.015)	0.984063
	CO_2	-	-	1325.1(192.3)	1656.0(50.6)	1656.6(112.0)	-	1607.6(72.6)	1679.9
	CO	-	-	256.1(84.7)	82.7(18.9)	74.2(32.5)	-	29.1(14.2)	17.31
	CH_4	2.27(1.32)	3.49(2.19)	10.5(5.5)	3.10(1.35)	3.69(2.61)	4.86(0.20)	1.09(0.95)	0.374
18.034	NH_3	0.689(0.651)	1.10(1.05)	1.78(0.59)	0.992(0.285)	1.20(0.79)	7.88E-2(6.90E-2)	5.71E-2(9.36E-2)	1.12E-02
	C_2H_2	0.250(0.103)	0.331(0.277)	0.153(0.058)	1.16(0.59)	0.887(0.424)	0.602(0.361)	0.402(0.499)	0.158
28.018	HCN	0.329(0.081)	0.381(0.259)	3.65(2.14)	0.343(0.208)	0.457(0.344)	0.221(0.005)	0.043	-
	C_2H_4	1.14(0.69)	1.34(0.80)	1.16(0.55)	2.52(1.34)	3.20(2.12)	2.21(1.40)	0.407(0.388)	0.156
31.018	HCHO	2.52(1.63)	1.93(1.32)	1.58(0.68)	1.66(0.80)	2.53(1.67)	1.70(0.74)	0.435(0.241)	0.206
	NO	2.93(0.65)	1.44(0.42)	1.00(0.59)	1.81(0.49)	1.89(0.76)	0.319(0.089)	0.598(0.271)	0.606
33.033	CH_3OH	1.19(1.00)	1.87(1.53)	2.66(2.24)	0.942(0.375)	2.22(1.90)	2.05(1.63)	0.524(0.300)	8.71E-02
	HCl	0.236(0.054)	0.472(0.320)	7.45E-03	0.028	0.071(0.040)	-		-
43.054	C_3H_6	0.347(0.104)	0.576(0.415)	1.21(0.63)	0.571(0.282)	0.956(0.551)	0.317(0.145)	0.012	5.98E-03
47.013	HCOOH	0.335(0.224)	0.633(0.846)	0.452(0.165)	0.192(0.082)	0.646(0.513)	0.620(0.533)	0.145(0.074)	5.00E-02
	NO_2	1.99(0.36)	1.65(0.47)	1.79(0.76)	0.874(0.546)	2.18(0.67)	1.11(0.28)	1.23(0.30)	1.657
	HONO	0.360(0.069)	0.395(0.221)	0.493(0.450)	0.783(0.268)	0.679(0.277)	0.291(0.169)	0.660	-
61.028	CH_3COOH	3.96(2.57)	3.88(3.64)	5.83(5.11)	1.63(0.67)	3.69(3.46)	8.90(9.27)	1.85(0.92)	7.59E-02
	$C_2H_4O_2$	0.181(0.199)	2.29(3.04)		0.136(0.058)	0.660(0.589)	0.455(0.149)	0.145(0.053)	0.261
	SO_2	1.75(0.52)	1.06(0.36)	4.26	0.550(0.243)	0.983(0.235)	0.498		-
69.033	C_4H_4O	0.392(0.277)	0.355(0.445)	1.40(1.17)	0.168(0.098)	0.276(0.275)	0.228(0.162)	5.41E-2(4.45E-2)	1.80E-02
41.039	C_3H_4	-	0.340(0.250)		0.344(0.055)	0.716(0.252)	-		-
42.034	C_2H_3N	0.152(0.138)	0.225(0.173)	0.601(0.258)	8.65E-2(3.26E-2)	0.132(0.111)	2.05E-2(4.63E-3)	6.45E-03(1.16E-02)	6.29E-04
43.018	C_2H_2O	1.87(1.89)	2.29(2.51)	1.42(1.09)	0.741(0.389)	1.42(1.17)	1.33(1.35)	0.405(0.257)	9.54E-02
45.033	C_2H_4O	2.38(2.26)	2.68(2.42)	1.63(0.67)	0.957(0.452)	1.87(1.31)	0.792(0.439)	0.255(0.191)	0.130
51.023	C_4H_2	1.69E-3(1.43E-3)	3.63E-3(4.51E-3)	2.65E-03(1.45E-03)	4.74E-03(2.80E-03)	3.49E-03(2.02E-03)	1.64E-2(1.24E-2)	1.62E-03(1.68E-03)	6.63E-04
53.039	C_4H_4	5.08E-2(4.98E-2)	5.59E-2(5.55E-2)	2.86E-02(1.40E-02)	4.87E-2(1.92E-2)	6.18E-02(4.80E-02)	7.99E-2(4.56E-2)	9.40E-03(7.91E-03)	3.96E-03
55.018	C_3H_2O	6.88E-2(6.34E-2)	4.22E-2(3.20E-2)	0.096	2.60E-2(1.17E-2)	6.31E-02(4.34E-02)	-		-
55.054	C_4H_6	0.141(0.127)	0.191(0.156)	0.260(0.149)	0.205(0.078)	0.330(0.264)	3.37E-2(9.67E-3)	2.82E-2(1.51E-2)	9.53E-03
57.033	C3H4O	0.865(0.806)	0.875(0.764)	0.273(0.128)	0.456(0.193)	0.739(0.554)	0.343(0.133)	0.109(0.087)	3.95E-02

57.070	C_4H_8	0.106(0.082)	0.134(0.100)	0.744(0.486)	0.167(0.096)	0.346(0.309)	0.245(0.148)	2.98E-2(1.12E-2)	3.85E-02
59.049	C_3H_6O	0.579(0.477)	0.884(0.611)	1.12(0.54)	0.302(0.137)	0.686(0.578)	-	0.131(0.139)	5.31E-02
63.026	C_2H_6S	2.53E-2(1.77E-2)	6.80E-2(2.64E-2)	0.0879776	1.47E-2(6.19E-3)	2.64E-02(8.55E-03)	-		-
67.054	C_5H_6	5.22E-2(4.50E-2)	8.29E-2(7.14E-2)	5.74E-02(2.50E-02)	0.102(0.036)	0.190(0.164)	0.126(0.096)	1.27E-2(1.45E-2)	5.67E-03
68.997	C_3O_2	-	4.64E-3(2.78E-3)			2.78E-03	-	8.95E-04(5.89E-04)	3.87E-04
69.070	C_5H_8	0.154(0.111)	0.220(0.170)	0.983(0.726)	0.536(0.234)	1.03(0.97)	0.145(0.077)	2.62E-2(1.38E-2)	1.94E-02
71.049	C_4H_6O	0.570(0.550)	0.607(0.515)	0.301(0.149)	0.233(0.099)	0.429(0.349)	0.213(0.112)	7.06E-2(5.74E-2)	2.07E-02
73.028	$C_3H_4O_2$	0.642(0.596)	0.554(0.582)	0.229(0.113)	0.148(0.064)	0.332(0.262)	0.177(0.104)	5.65E-2(2.94E-2)	2.80E-02
73.065	C_4H_8O	0.140(0.129)	0.290(0.243)	0.540(0.383)	0.066(0.026)	0.145(0.132)	8.04E-2(4.98E-2)	4.10E-2(5.43E-2)	5.88E-03
75.044	$C_3H_6O_2$	0.856(1.029)	1.69(2.03)	0.417(0.285)	0.191(0.073)	0.563(0.600)	0.480(0.367)	0.184(0.131)	3.84E-02
79.054	C_6H_6	0.235(0.161)	0.301(0.177)	0.779(0.376)	0.795(0.359)	0.946(0.800)	2.58(2.68)	0.110(0.138)	8.01E-02
81.033	C_5H_4O	0.204(0.205)	0.303(0.280)	8.89E-02(3.36E-02)	0.103(0.024)	0.231(0.216)	0.159(0.121)	5.84E-2(4.56E-2)	8.78E-03
83.049	C_5H_6O	0.418(0.402)	0.532(0.492)	0.500(0.276)	0.139(0.051)	0.323(0.290)	0.221(0.138)	7.25E-2(5.50E-2)	1.19E-02
83.086	C_6H_{10}	2.82E-2(2.30E-2)	3.57E-2(2.71E-2)	0.123(0.088)	4.49E-2(2.77E-2)	8.81E-02(7.02E-02)	2.22E-2(5.78E-3)	6.78E-03(2.48E-03)	2.11E-03
85.028	$C_4H_4O_2$	0.839(0.839)	0.820(0.858)	0.583(0.322)	0.199(0.054)	0.545(0.493)	0.208(0.169)	8.23E-2(5.67E-2)	2.85E-02
85.065	C_5H_8O	0.153(0.146)	0.186(0.157)	0.153(0.050)	7.26E-2(1.93E-2)	0.167(0.143)	9.02E-2(5.18E-2)	2.99E-2(2.38E-2)	3.82E-03
87.044	$C_4H_6O_2$	0.651(0.643)	1.15(1.21)	0.324(0.135)	0.219(0.059)	0.477(0.428)	0.41(0.30)	0.140(0.096)	2.50E-02
89.060	$C_4H_8O_2$	0.110(0.113)	0.233(0.276)	0.117(0.059)	3.79E-2(6.94E-3)	7.72E-02(7.70E-02)	8.72E-2(8.50E-2)	3.08E-2(2.45E-2)	3.24E-03
91.054	C_7H_6	1.98E-2(1.72E-2)	3.28E-2(3.51E-2)	5.94E-02(3.72E-02)	3.46E-2(1.14E-2)	5.39E-02(3.81E-02)	3.73E-2(3.12E-2)	3.27E-03(1.89E-03)	1.75E-03
93.070	C_7H_8	0.174(0.141)	0.296(0.228)	0.520(0.316)	0.416(0.172)	2.42(1.92)	0.290(0.311)	8.61E-2(9.79E-2)	2.24E-02
95.049	C_6H_6O	0.273(0.242)	0.494(0.480)	0.512(0.242)	0.322(0.120)	0.566(0.514)	0.264(0.085)	6.35E-2(1.05E-1)	1.89E-02
97.028	$C_5H_4O_2$	1.58(1.52)	1.03(0.86)	2.08(0.70)	0.316(0.086)	0.713(0.635)	0.926(1.037)	0.219(0.161)	3.20E-02
99.044	$C_5H_6O_2$	0.864(0.914)	1.02(1.15)	0.394(0.222)	0.212(0.060)	0.512(0.466)	0.289(0.238)	0.0312236	-
101.060	$C_5H_8O_2$	0.199(0.204)	0.295(0.322)	0.154(0.054)	6.65E-2(1.37E-2)	0.156(0.144)	0.157(0.154)	5.11E-2(3.67E-2)	5.78E-03
103.054	C_8H_6	-	0.254(0.257)		6.23E-2(5.95E-3)	0.230	0.236(0.107)		-
105.070	C_8H_8	3.04E-2(2.43E-2)	5.63E-2(4.91E-2)	8.25E-02(5.06E-02)	9.07E-2(3.84E-2)	0.152(0.151)	0.234(0.306)	1.03E-2(1.16E-2)	4.52E-03
107.049	C_7H_6O	4.92E-2(3.92E-2)	7.02E-2(5.19E-2)	5.65E-02(2.52E-02)	8.73E-2(3.57E-2)	0.120(0.088)	0.114(0.102)	1.13E-2(1.49E-2)	4.99E-03
107.086	C_8H_{10}	4.73E-2(3.71E-2)	0.107(0.088)	0.366(0.257)	0.114(0.045)	0.285(0.255)	0.265(0.380)	1.56E-2(1.90E-2)	5.27E-03
109.028	$C_6H_4O_2$	2.33E-3(1.16E-3)	6.98E-2(5.67E-2)		0.576(0.322)	0.184(0.080)	-		-
111.044	$C_6H_6O_2$	0.464(0.465)	0.548(0.559)	0.782(0.411)	0.495(0.292)	0.545(0.495)	0.187(0.129)	5.39E-2(3.38E-2)	1.09E-02
111.080	$C_7H_{10}O$	0.106(0.091)	0.177(0.167)	0.141(0.079)	2.75E-2(9.99E-3)	0.109(0.102)	4.12E-2(2.36E-2)	2.60E-2(3.34E-2)	1.51E-03
113.023	$C_5H_4O_3$	0.209(0.202)	0.166(0.269)	0.220(0.091)	5.65E-2(1.85E-2)	0.137(0.126)	3.29E-2(2.44E-2)	1.22E-2(7.87E-3)	5.53E-03
113.060	$C_6H_8O_2$	0.305(0.371)	0.557(0.693)	0.206(0.099)	9.03E-2(2.04E-2)	0.295(0.292)	0.148(0.110)	4.84E-2(3.31E-2)	5.75E-03

115.039	$C_5H_6O_3$	0.769(1.159)	0.523(0.682)	0.298(0.235)	0.105(0.030)	0.275(0.275)	0.120(0.136)	3.30E-2(2.75E-2)	0.0184
117.070	C_9H_8	2.44E-2(1.67E-2)	0.118(0.090)	0.041(0.008)		0.268	0.386(0.265)	0.020	
119.049	C_8H_6O	2.99E-2(2.55E-2)	4.35E-2(3.62E-2)	3.19E-02(1.02E-02)	3.16E-2(1.28E-2)	4.34E-02(3.27E-02)	4.58E-2(2.57E-2)	4.90E-03(7.34E-03)	2.16E-03
119.086	C_9H_{10}	1.47E-2(1.17E-2)	3.09E-2(2.70E-2)	0.067(0.054)	4.32E-2(1.54E-2)	9.47E-02(9.50E-02)	9.82E-2(1.43E-1)	4.57E-03(4.94E-03)	1.95E-03
121.065	C_8H_8O	0.254(0.245)	0.574(0.832)	0.107(0.041)	0.123(0.058)	0.211(0.174)	6.62E-2(4.25E-2)	3.89E-2(7.87E-2)	3.27E-03
121.101	C_9H_{12}	4.19E-2(3.60E-2)	6.58E-2(6.11E-2)	0.229(0.164)	3.98E-2(9.29E-3)	0.168(0.160)	7.01E-2(9.27E-2)	1.12E-2(1.69E-2)	3.24E-03
123.044	$C_7H_6O_2$	6.59E-2(5.66E-2)	0.106(0.109)	0.142(0.133)	5.89E-2(2.81E-2)	0.120(0.099)	4.92E-2(2.66E-3)	1.34E-2(1.59E-2)	5.40E-03
123.080	$C_8H_{10}O$	0.133(0.126)	0.275(0.336)	0.201(0.105)	3.97E-2(1.42E-2)	0.112(0.092)	5.67E-2(2.17E-2)	3.33E-2(5.76E-2)	2.78E-03
125.060	$C_7H_8O_2$	0.291(0.330)	0.578(0.701)	0.471(0.381)	7.75E-2(2.76E-2)	0.323(0.307)	0.150(0.101)	5.17E-2(4.01E-2)	7.61E-03
127.039	$C_6H_6O_3$	0.361(0.427)	0.296(0.332)	0.360(0.182)	8.51E-2(3.75E-2)	0.331(0.288)	7.45E-2(5.31E-2)	2.19E-2(1.15E-2)	1.00E-02
129.070	$C_{10}H_8$	0.136(0.151)	0.164(0.245)	0.194(0.043)	0.138(0.048)	0.183(0.125)	1.04(1.26)	3.47E-2(1.76E-2)	1.53E-02
131.086	$C_{10}H_{10}$	4.14E-2(4.66E-2)	4.01E-2(3.53E-2)	7.55E-02(7.70E-02)	2.41E-2(1.39E-2)	4.63E-02(3.43E-02)	9.90E-2(1.23E-1)		-
137.132	$C_{10}H_{16}$	3.11E-2(2.43E-2)	6.35E-2(5.12E-2)	0.159(0.091)	7.55E-2(3.28E-2)	0.163(0.143)	0.197(0.257)	8.64E-03(1.23E-02)	4.46E-03
143.086	$C_{11}H_{10}$	-	8.80E-2(8.59E-2)		5.31E-2(1.37E-2)	0.112(0.043)	-		-

Protonated m/z	**Formula**	**EF Savanna grasses (3)[a]**	**EF Crop Residue (6) (food fuels)[a]**	**EF Peat (4) avg,stdev**	**EF Chaparral (2) avg,stdev**	**EF Coniferous Canopy (3) avg,stdev**	**EF Open Cooking Fires (1)[b]**	**EF Rocket cookstoves (2) avg,stdev**	**EF Gasifier Cookstove (0)**
46.065	C_2H_7N	1.51E-2(6.98E-3)	8.44E-2(9.04E-2)		1.39E-2(5.83E-3)	2.79E-02(3.55E-02)	5.07E-02	5.77E-3(6.25E-3)	-
49.011	CH_4S	1.71E-2(1.65E-2)	3.84E-2(3.82E-2)	2.84E-2(4.88E-2)	9.29E-3(9.32E-3)	1.80E-02(1.91E-02)	1.00E-02	1.51E-3(3.54E-4)	-
60.044	C_2H_5NO	-	-	2.87(1.52)	-	-	4.11E-02	1.07E-02	-
60.081	C_3H_9N	4.41E-2(3.41E-2)	7.85E-2(1.10E-1)	-	2.99E-3(1.07E-3)	5.09E-03(4.74E-03)	-	-	-
65.039	C_5H_4	1.32E-2(7.66E-3)	1.29E-2(1.35E-2)	0.126(0.097)	6.89E-3(4.64E-3)	7.96E-03(7.15E-03)	-	-	-
71.086	C_5H_{10}	1.95E-2(1.05E-2)	3.27E-2(2.16E-2)	0.364(0.190)	2.23E-2(4.12E-3)	5.69E-02(5.43E-02)	2.33E-02	3.87E-3(5.45E-3)	-
85.101	C_6H_{12}	1.43E-2(7.42E-3)	1.30E-2(6.86E-3)	0.468(0.296)	5.03E-03	3.69E-02(2.72E-02)	4.33E-03	2.82E-03	-
87.080	$C_5H_{10}O$	-	-	7.49E-2(8.50E-2)	-	-	-	-	-
88.076	C_4H_9NO	6.64E-2(2.80E-2)	0.116(0.143)	3.80E-2(6.42E-2)	1.06E-02	3.42E-02(4.15E-02)	8.46E-02	1.15E-2(5.85E-3)	-
89.023	$C_3H_4O_3$	7.60E-3(2.20E-3)	1.57E-2(2.52E-2)	0.106(0.083)	1.59E-3(4.37E-4)	9.40E-03(1.08E-02)	1.48E-03	1.42E-03	-
90.091	$C_4H_{11}NO$	3.65E-3(2.33E-3)	3.94E-2(3.25E-2)	-	-	-	-	-	-
93.033	C_6H_4O	1.47E-2(9.34E-3)	8.50E-3(5.01E-3)	0.312(0.285)	8.08E-03	6.48E-03(5.22E-03)	7.09E-02	4.58E-03	-
95.086	C_7H_{10}	6.34E-2(2.29E-2)	0.741(1.039)	2.94(1.92)	0.100(0.088)	0.249(0.186)	4.83E-02	4.98E-3(2.35E-3)	-
97.065	C_6H_8O	0.150(0.043)	9.81E-2(1.64E-1)	0.139(0.009)	7.95E-2(7.02E-2)	0.122(0.118)	-	-	-
97.101	C_7H_{12}	1.56E-2(1.00E-2)	0.842(1.292)	0.238(0.093)	2.67E-2(2.43E-2)	5.40E-02(5.52E-02)	0.131	1.31E-2(1.75E-2)	-
99.080	$C_6H_{10}O$	-	-	0.113(0.039)	2.82E-02	0.0241	-	-	-
101.023	$C_4H_4O_3$	6.30E-2(2.31E-2)	0.168(0.254)	0.162(0.058)	1.50E-2(1.48E-2)	5.06E-02(6.94E-02)	2.41E-02	5.28E-3(5.66E-3)	-

103.039	$C_4H_6O_3$	0.139(0.044)	7.08E-2(6.55E-2)	0.119(0.113)	4.25E-2(2.81E-2)	9.23E-02(1.00E-01)	0.217	2.63E-2(1.66E-2)	-
103.075	$C_5H_{10}O_2$	4.43E-3(2.45E-3)	2.16E-2(1.72E-2)	0.168(0.079)	1.80E-2(1.14E-2)	2.41E-02(2.18E-02)	-	-	-
104.049	C_7H_5N	-	-	-	3.41E-02	2.31E-02	-	-	-
109.065	C_7H_8O	8.60E-2(1.35E-2)	0.249(0.201)	0.167(0.149)	1.19E-1(1.12E-1)	0.144(0.123)	0.125	6.85E-3(7.37E-3)	-
109.101	C_8H_{12}	-	-	0.913(0.588)	5.94E-02	0.139	2.04E-02	4.66E-3(1.18E-3)	-
111.117	C_8H_{14}	1.91E-2(1.21E-2)	7.95E-3(3.47E-3)	0.371(0.152)	5.28E-03	2.19E-02(1.98E-02)	7.70E-03	-	-
115.075	$C_6H_{10}O_2$	-	-	-	9.64E-03	4.70E-03	-	-	-
117.055	$C_5H_8O_3$	0.191(0.074)	0.414(0.529)	3.99E-2(9.70E-3)	5.68E-2(3.13E-2)	0.125(0.141)	0.302	2.99E-2(3.02E-2)	-
117.091	$C_6H_{12}O_2$	-	-	7.63E-2(2.76E-2)	2.77E-02	1.57E-02	2.65E-02	3.86E-03	-
123.117	C_9H_{14}	1.78E-2(5.93E-3)	1.81E-2(1.33E-2)	0.145(0.114)	3.69E-2(4.03E-2)	8.43E-02(6.35E-02)	2.01E-02	2.50E-03	-
125.023	$C_6H_4O_3$	0.101(0.030)	0.186(0.214)	0.131(0.043)	3.19E-2(3.80E-2)	7.74E-02(1.01E-01)	9.86E-02	1.08E-2(8.56E-3)	-
127.075	$C_7H_{10}O_2$	1.45E-2(0.00E0)	0.126(0.135)	-	3.24E-2(3.51E-2)	5.02E-02(5.48E-02)	7.04E-02	6.60E-3(6.33E-3)	-
133.065	C_9H_8O	7.80E-3(1.52E-3)	-	-	-	-	-	-	-
135.044	$C_8H_6O_2$	3.82E-3(1.27E-3)	4.18E-2(4.66E-2)	2.70E-2(1.55E-2)	1.29E-2(1.11E-2)	1.55E-02(1.48E-02)	1.68E-02	1.14E-3(2.60E-4)	-
135.080	$C_9H_{10}O$	2.23E-2(1.04E-2)	5.21E-2(4.73E-2)	6.06E-2(3.91E-2)	1.60E-2(1.34E-2)	4.19E-02(3.96E-02)	2.66E-02	2.99E-3(1.73E-3)	-
135.117	$C_{10}H_{14}$	2.06E-3(7.17E-6)	1.72E-2(1.44E-2)	0.191(0.126)	4.87E-02	0.140(0.045)	6.64E-03	-	-
137.060	$C_8H_8O_2$	3.97E-2(8.44E-3)	0.159(0.206)	8.94E-2(4.69E-2)	2.68E-2(3.10E-2)	5.15E-02(4.25E-02)	7.02E-02	5.27E-3(4.42E-3)	-
137.096	$C_9H_{12}O$	6.87E-3(0.00E0)	-	9.10E-2(5.48E-2)	1.36E-02	8.31E-03	-	-	-
139.039	$C_7H_6O_3$	3.37E-2(1.17E-2)	0.113(0.148)	0.235(0.210)	1.29E-2(1.23E-2)	4.53E-02(5.16E-02)	5.57E-02	4.36E-3(2.63E-3)	-
139.075	$C_8H_{10}O_2$	9.97E-2(3.07E-2)	0.138(0.151)	0.216051177	2.29E-2(1.70E-2)	9.52E-02(1.11E-01)	0.126	1.47E-2(1.08E-2)	-
141.055	$C_7H_8O_3$	4.91E-2(1.75E-2)	5.73E-2(7.55E-2)	0.125(0.072)	1.02E-2(6.60E-3)	3.15E-02(3.92E-02)	7.90E-02	1.29E-02	-
141.091	$C_8H_{12}O_2$	-	3.80E-2(4.00E-2)	-	9.87E-3(8.08E-3)	1.67E-02(1.66E-02)	-	-	-
145.065	$C_{10}H_8O$	0.218(0.076)	0.131(0.185)	0.322(0.060)	3.91E-2(4.16E-2)	0.106(0.132)	6.12E-02	4.56E-3(4.06E-3)	-
145.101	$C_{11}H_{13}$	-	8.08E-3(3.86E-3)	0.191(0.129)	3.44E-2(3.43E-2)	5.01E-02(4.98E-02)	-	-	-
147.080	$C_{10}H_{10}O$	3.25E-2(7.97E-3)	6.42E-2(5.70E-2)	9.10E-2(4.79E-2)	2.64E-2(1.88E-2)	4.44E-02(4.10E-02)	3.44E-02	3.60E-3(2.85E-3)	-
147.117	$C_{11}H_{14}$	-	-	0.108(0.088)	-	-	-	-	-
149.060	$C_9H_8O_2$	3.73E-2(9.72E-3)	7.06E-2(6.58E-2)	0.107(0.050)	3.14E-02	4.05E-02(2.31E-02)	-	-	-
149.096	$C_{10}H_{12}O$	-	-	-	-	-	-	-	-
149.132	$C_{11}H_{16}$	-	-	0.173(0.127)	4.71E-02	0.167(0.147)	-	-	-
151.075	$C_9H_{10}O_2$	0.122(0.037)	0.306(0.358)	0.172(0.118)	2.10E-2(1.19E-2)	0.134(0.152)	0.104	9.41E-3(8.69E-3)	-
151.148	$C_{11}H_{18}$	-	-	-	3.24E-02	-	-	-	-
155.070	$C_8H_{10}O_3$	1.29E-2(5.71E-3)	0.121(0.134)	0.175(0.138)	4.77E-2(3.09E-2)	2.58E-02(2.03E-02)	0.292	2.55E-2(2.27E-2)	-
165.091	$C_{10}H_{12}O_2$	-	-	-	-	-	0.139	9.00E-3(7.38E-3)	-

note: values in parenthesis following fuel-type indicate the number of fires included in adjustment procedure or during averaging

a-Laboratory EF adjusted using the MCE plot based approach described in Stockwell et al. (2014)

b-The EF of smoldering NMOCs adjusted based on their ratio to CH_4 and the flaming compounds adjusted based on their ratio to CO_2

Table S5. Molecular formulas and likely identities of masses detected by full PTR-TOF-MS scans

Assignment	Protonated m/z	Formula	Compound	Secondary compounds / Alternative assignments
Confirmed	18.034	NH_3	Ammonia	
Confirmed	28.018	HCN	Hydrogen Cyanide	
Confirmed	31.018	HCHO	Formaldehyde	
Confirmed	33.033	CH_3OH	Methanol	
Confirmed	41.039	C_3H_4	Propyne[1]	
Confirmed	42.034	C_2H_3N	Acetonitirile	
Confirmed	43.018	C_2H_2O	Ketene Fragments	
Confirmed	43.054	C_3H_6	Propene	
Tentative	44.049	C_2H_5N	Ethenamine[6]	
Confirmed	45.033	C_2H_4O	Acetaldehyde	
Tentative	46.065	C_2H_7N	Dimethylamine[6,15,18]; Ethylamine[6,15,18]	
Confirmed	47.013	HCOOH	Formic acid	
Tentative	49.011	CH_4S	Methanethiol	
Confirmed	51.023	C_4H_2	1,3-Butadiyne	
Confirmed	53.039	C_4H_4	Butenyne	
Confirmed	54.034	C_3H_3N	Acrylonitirile[1,12]	
Tentative	55.018	C_3H_2O	2-Propynal	Propadienal; Cyclopropenone
Confirmed	55.054	C_4H_6	1,3-Butadiene	(~10%) : 1,2-Butadiene; 1-Butyne; 2-Butyne
Confirmed	56.049	C_3H_5N	Propanenitrile[12]	
Confirmed	57.033	C3H4O	Acrolein	
Confirmed	57.070	C_4H_8	1-Butene	2-Methylpropene; trans-Butene; cis-Butene
Confirmed	59.049	C_3H_6O	Acetone	Propanal (~10%)
Tentative	60.044	C_2H_5NO	Acetamide[6,3]	
Tentative	60.081	C_3H_9N	Trimethylamine[6,15,17]	Propanamine[6]
Confirmed	61.028	$C_2H_4O_2$	Acetic Acid	Glycolaldehyde (10-50%); Methylformate
Confirmed	63.026	C_2H_6S	Dimethyl Sulfide[1]	
Tentative	65.039	C_5H_4	1,3-Pentadiyne	
Confirmed	67.054	C_5H_6	1,3-Cyclopentadiene	Pentenyne isomers
Confirmed	68.049	C_4H_5N	Pyrrole[7,12]	Minor contribution from nitriles: Methacrylonitrile; 2 & 3-Butenenitrile
Confirmed	68.997	C_3O_2	Carbon suboxide	
Confirmed	69.033	C_4H_4O	Furan	
Confirmed	69.070	C_5H_8	Isoprene	(~10-20%) : Cyclopentene; trans-1,3-Pentadiene; cis-1,3-Pentadiene
Confirmed	71.049	C_4H_6O	Methyl Vinyl Ketone, Crotonaldehyde, Methacrolein (~50, 30, 20%)	
Confirmed	71.086	C_5H_{10}	Assorted HCs[20]	
Tentative	73.028	$C_3H_4O_2$	Methylglyoxal[2]	
Confirmed	73.065	C_4H_8O	Methyl Ethyl Ketone	(~25%) : 2-Methylpropanal; n-Butanal; Tetrahydrofuran
Confirmed	75.044	$C_3H_6O_2$	Hydroxyacetone[5,8]	Methyl acetate; Ethyl formate
Confirmed	79.054	C_6H_6	Benzene	
Confirmed	80.049	C_5H_5N	Pyridine[7,12,14,20]	

Tentative	81.033	C_5H_4O	2,4-Cyclopentadiene-1-one	
Confirmed	82.065	C_5H_7N	Methylpyrroles[7]	Minor contribution from nitriles: 2-Methylene-Butanenitrile; 3-Methyl-3-Butenenitrile[7]
Confirmed	83.049	C_5H_6O	2-Methylfuran[9,19,20]	3-Methylfuran; Cyclopentenone[2]
Confirmed	83.086	C_6H_{10}	Assorted HCs[20]	
Tentative	85.028	$C_4H_4O_2$	2-Furanone[2,8,14,16]	
Confirmed	85.065	C_5H_8O	Pentenone[20]	Cyclopentanone; 2-Methyl-2-Butenal
Confirmed	85.101	C_6H_{12}	Assorted HCs[20]	
Confirmed	87.044	$C_4H_6O_2$	2,3-Butanedione[12]	(20-50%) Methyl Acrylate; Vinyl acetate; 2,3-Dihydro-1,4-Dioxin
Confirmed	87.080	$C_5H_{10}O$	Pentanone[20]	2-Methylbutanal; 3-Methyl-2-Butanone; Pentanal
Tentative	88.076	C_4H_9NO	Assorted Amides[6]	Dimethylacetamide; N-ethylacetamide, 2-methylpropanamide, Butanamide; Morpholine
Unknown	89.023	$C_3H_4O_3$	Unknown	
Tentative	89.060	$C_4H_8O_2$	Ethyl acetate[14]	1-Hydroxy-2-Butanone[14]; Butyric acid[9,14]; Methyl Propanoate[20]
Tentative	90.091	$C_4H_{11}NO$	Assorted Amines[6]	Dimethylethanolamine[6]
Unknown	91.054	C_7H_6	Unknown	
Unknown	93.033	C_6H_4O	Unknown	
Confirmed	93.070	C_7H_8	Toluene	(<5%) Heptadiyne isomer
Confirmed	95.049	C_6H_6O	Phenol	
Unknown	95.086	C_7H_{10}	Unknown	
Confirmed	97.028	$C_5H_4O_2$	2-Furaldehyde (furfural)[2,8,9,13,14,19]	3-Furaldehyde; Cyclopentenedione[20]
Confirmed	97.065	C_6H_8O	2,5-Dimethylfuran[19,20]	2-Ethylfuran[20]; 2-Methylcyclopentenone[13,14,16]
Confirmed	97.101	C_7H_{12}	Assorted HCs[20]	
Tentative	99.044	$C_5H_6O_2$	2-Furan Methanol (furfuryl alcohol)[13,14,16]	Methyl Furanone[19;] Hydroxy-Cyclopentenone[2,8]
Unknown	99.080	$C_6H_{10}O$	Unknown	
Unknown	101.023	$C_4H_4O_3$	Unknown	
Unknown	101.060	$C_5H_8O_2$	Unknown	Methyl Methacrylate[20]; 2,3-Pentanedione[19]
Tentative	103.039	$C_4H_6O_3$	Methyl pyruvate[8]	Hydroxyoxobutanal[19]
Confirmed	103.054	C_8H_6	Ethynyl Benzene (phenylacetylene)	
Unknown	103.075	$C_5H_{10}O_2$	Unknown	
Tentative	104.049	C_7H_5N	Benzonitrile[7]	
Confirmed	105.070	C_8H_8	Styrene	
Confirmed	107.049	C_7H_6O	Benzaldehyde[20]	
Confirmed	107.086	C_8H_{10}	Xylenes	Ethylbenzene (~20%)
Unknown	109.028	$C_6H_4O_2$	Unknown	
Tentative	109.065	C_7H_8O	Cresols (Methylphenols)[2,4,10,13,14,16]	
Unknown	109.101	C_8H_{12}	Unknown	
Tentative	111.044	$C_6H_6O_2$	Catechol (Benzenediols)[8,10,13,16,19,21]; Methylfurfural[11,14,16,19]	
Unknown	111.080	$C_7H_{10}O$	Unknown	
Unknown	111.117	C_8H_{14}	Unknown	
Unknown	113.023	$C_5H_4O_3$	Unknown	
Tentative	113.060	$C_6H_8O_2$	2-Hydroxy-3-Methyl-2-Cyclopentenone[8,14]	
Unknown	115.039	$C_5H_6O_3$	Unknown	
Unknown	115.075	$C_6H_{10}O_2$	Unknown	

Unknown	117.055	$C_5H_8O_3$	Unknown	
Unknown	117.070	C_9H_8	Unknown	
Unknown	117.091	$C_6H_{12}O_2$	Unknown	
Confirmed	119.049	C_8H_6O	Benzofuran[20]	
Confirmed	119.086	C_9H_{10}	Assorted HCs[20]	
Tentative	121.065	C_8H_8O	Vinylphenol[4]	3-Methylbenzaldehyde[7]; Acetophenone[7]; Benzenacetaldehyde[7]
Confirmed	121.101	C_9H_{12}	Trimethylbenzene; Assorted HCs[20]	
Tentative	123.044	$C_7H_6O_2$	Salicylaldehyde[7,11]	
Tentative	123.080	$C_8H_{10}O$	Xylenol (2,5-Dimethyl phenol)[7,13]	4-Ethylphenol[4,14]
Unknown	123.117	C_9H_{14}	Unknown	
Unknown	125.023	$C_6H_4O_3$	Unknown	
Tentative	125.060	$C_7H_8O_2$	Guaiacol (2-Methoxyphenol)[2,4,8,10,13,14,16]	
Tentative	127.039	$C_6H_6O_3$	Hydroxymethylfurfural[8,13,14]	2-Hydroxy-3-Ethyl-2-Cyclopentenone[14]
Unknown	127.075	$C_7H_{10}O_2$	Unknown	
Confirmed	129.070	$C_{10}H_8$	Naphthalene[20]	
Tentative	131.086	$C_{10}H_{10}$	Assorted HCs[20] inc. Dihydronaphthalene	
Tentative	133.065	C_9H_8O	Assorted HCs[20] inc. Methylbenzofurans	
Unknown	135.044	$C_8H_6O_2$	Unknown	
Unknown	135.080	$C_9H_{10}O$	Unknown	
Confirmed	135.117	$C_{10}H_{14}$	p-Cymene[20]	Assorted HCs[20]
Unknown	137.060	$C_8H_8O_2$	Unknown	
Unknown	137.096	$C_9H_{12}O$	Unknown	
Confirmed	137.132	$C_{10}H_{16}$	Terpenes (α-Pinene)	
Unknown	139.039	$C_7H_6O_3$	Unknown	
Tentative	139.075	$C_8H_{10}O_2$	Creosol (4-Methylguaiacol)[4,8,9,10,14,16]	
Tentative	141.055	$C_7H_8O_3$	3-Methoxycatechol (3-Methoxy-1,2-Benzenediol)[10]	
Unknown	141.091	$C_8H_{12}O_2$	Unknown	
Tentative	143.086	$C_{11}H_{10}$	Methyl-Naphthalenes[7]	
Unknown	145.065	$C_{10}H_8O$	Unknown	
Unknown	145.101	$C_{11}H_{13}$	Unknown	
Unknown	147.080	$C_{10}H_{10}O$	Unknown	
Unknown	147.117	$C_{11}H_{14}$	Unknown	
Unknown	149.060	$C_9H_8O_2$	Unknown	
Unknown	149.096	$C_{10}H_{12}O$	Unknown	
Unknown	149.132	$C_{11}H_{16}$	Unknown	
Tentative	151.075	$C_9H_{10}O_2$	4-Vinylguaiacol (2-Methoxy-6-Vinylphenol)[4,8,9,10]	
Unknown	151.148	$C_{11}H_{18}$	Unknown	
Unknown	153.070	$C_{12}H_8$	Unknown	
Tentative	155.070	$C_8H_{10}O_3$	Syringol[2,4,8,10,13,14]	
Tentative	165.091	$C_{10}H_{12}O_2$	Eugenol[8,10] / Isoeugenol[11]	

References are as follows: 1-Akagi et al., 2013; 2-Azeez et al., 2011; 3-Barnes et al., 2010; 4-Bocchini et al., 1997; 5- Christian et al., 2003; 6-Ge et al., 2011; 7-Hatch et al., 2014; 8-Heigenmoser et al., 2013; 9-Ingemarrsson et al., 1998; 10-Jiang et al., 2010; 11-Jordon and Seen, 2005;

12-Karl et al., 2007; 13-Li et al., 2013; 14-Liu et al., 2012; 15-Lobert et al., 1991; 16-Pittman Jr. et al., 2012; 17-Rehbein et al., 2011; 18-Schade and Crutzen, 1995; 19-Simmleit and Schulten, 1989; 20-Yokelson et al., 2013a; 21-Veres et al., 2010

Table S6. Emission factors (g/kg) for individual motorbikes pre- and post-service

Compound	**EF Pre-service** Hero Honda CBZ 1	**EF Post-service** Hero Honda CBZ 1	**EF Pre-service** Hero Honda CBZ 2	**EF Post-service** Hero Honda CBZ 2	**EF Pre-Service** Bajaj Pulsar	**EF Post-Service-** Bajaj Pulsar	**EF Pre-Service** Bajaj Discover	**EF Post-Service-** Bajaj Discover	**EF Pre-Service** Honda Aviator scooter	**EF Post-Service** Honda Aviator scooter	**EF Hero** Honda Splender
Method	FTIR	FTIR	FTIR	FTIR	FTIR+WAS	FTIR	FTIR	FTIR	FTIR	FTIR	FTIR
MCE	0.589	0.559	0.749	0.747	0.598	0.432	0.288	0.445	0.870	0.821	0.774
Carbon Dioxide (CO_2)	1753	1683	2267	2281	1732	1283	822	1313	2656	2518	2330
Carbon Monoxide (CO)	779	845	483	491	741	1074	1294	1044	253	350	433
Methane (CH_4)	8.76	7.19	4.14	3.57	4.54	8.26	19.6	13.2	1.00	1.45	2.85
Acetylene (C_2H_2)	13.1	9.39	6.35	3.35	7.06	9.26	30.2	16.1	1.70	1.30	4.56
Ethylene (C_2H_4)	13.0	9.12	10.2	9.10	15.7	18.5	18.3	12.0	8.59	8.24	15.7
Propylene (C_3H_6)	2.88	2.01	2.76	1.85	4.24	4.38	4.01	2.41	2.70	2.22	5.38
Formaldehyde (HCHO)	bdl	bdl	bdl	bdl	bdl	bdl	bdl	bdl	0.548	0.535	bdl
Methanol (CH_3OH)	bdl	bdl	bdl	bdl	bdl	bdl	bdl	bdl	bdl	bdl	bdl
Formic Acid (HCOOH)	6.67E-02	7.26E-02	8.50E-02	3.85E-02	bdl	bdl	bdl	bdl	0.136	6.74E-02	bdl
Acetic Acid (CH_3COOH)	bdl	bdl	bdl	bdl	bdl	bdl	bdl	bdl	bdl	bdl	bdl
Glycolaldehyde ($C_2H_4O_2$)	bdl	bdl	bdl	bdl	bdl	bdl	bdl	bdl	bdl	bdl	bdl
Furan (C_4H_4O)	bdl	bdl	bdl	bdl	bdl	bdl	bdl	bdl	bdl	bdl	bdl
Hydroxyacetone ($C_3H_6O_2$)	0.543	4.05	1.43	1.56	0.644	1.85	0.174	2.03	7.73	2.55	0.861
Phenol (C_6H_5OH)	5.56	3.37	3.86	1.36	3.44	3.46	10.4	6.42	0.895	0.513	2.53
1,3-Butadiene (C_4H_6)	1.20	0.918	1.01	0.819	2.04	2.041	1.51	1.47	0.714	0.712	2.57
Isoprene (C_5H_8)	bdl	bdl	bdl	bdl	bdl	bdl	bdl	bdl	bdl	bdl	bdl
Ammonia (NH_3)	9.73E-02	bdl	0.110	1.60E-02	8.40E-02	bdl	0.161	4.81E-02	bdl	bdl	5.55E-02
Hydrogen Cyanide (HCN)	0.851	0.646	0.803	0.511	0.955	0.922	1.40	0.634	0.20	bdl	0.355
Nitrous Acid (HONO)	bdl	bdl	bdl	bdl	bdl	bdl	bdl	bdl	bdl	bdl	bdl
Sulfur Dioxide (SO_2)	bdl	bdl	bdl	bdl	bdl	bdl	bdl	bdl	bdl	bdl	bdl
Hydrogen Fluoride (HF)	bdl	bdl	bdl	bdl	bdl	bdl	bdl	bdl	bdl	bdl	bdl
Hydrogen chloride (HCl)	bdl	bdl	bdl	bdl	bdl	bdl	bdl	bdl	bdl	bdl	bdl
Nitric Oxide (NO)	4.59	0.744	3.38	2.18	5.74	2.38	0.718	2.75	0.260	1.42	1.46
Nitrogen Dioxide (NO_2)	bdl	bdl	bdl	bdl	bdl	bdl	bdl	bdl	bdl	bdl	bdl
Carbonyl sulfide (OCS)	nm	nm	nm	nm	1.02E-02	nm	nm	nm	nm	nm	nm
DMS (C_2H_6S)	nm	nm	nm	nm	4.94E-03	nm	nm	nm	nm	nm	nm
Chloromethane (CH_3Cl)	nm	nm	nm	nm	-	nm	nm	nm	nm	nm	nm
Bromomethane (CH_3Br)	nm	nm	nm	nm	-	nm	nm	nm	nm	nm	nm
Methyl iodide (CH_3I)	nm	nm	nm	nm	4.81E-06	nm	nm	nm	nm	nm	nm
1,2-Dichloroethene ($C_2H_2Cl_2$)	nm	nm	nm	nm	9.34E-04	nm	nm	nm	nm	nm	nm

Methyl nitrate (CH_3NO_3)	nm	nm	nm	nm	1.39E-02	nm	nm	nm	nm	nm	nm
Ethane (C_2H_6)	nm	nm	nm	nm	0.948	nm	nm	nm	nm	nm	nm
Propane (C_3H_8)	nm	nm	nm	nm	0.178	nm	nm	nm	nm	nm	nm
i-Butane (C_4H_{10})	nm	nm	nm	nm	0.218	nm	nm	nm	nm	nm	nm
n-Butane (C_4H_{10})	nm	nm	nm	nm	0.251	nm	nm	nm	nm	nm	nm
1-Butene (C_4H_8)	nm	nm	nm	nm	0.619	nm	nm	nm	nm	nm	nm
i-Butene (C_4H_8)	nm	nm	nm	nm	0.576	nm	nm	nm	nm	nm	nm
trans-2-Butene (C_4H_8)	nm	nm	nm	nm	0.227	nm	nm	nm	nm	nm	nm
cis-2-Butene (C_4H_8)	nm	nm	nm	nm	0.147	nm	nm	nm	nm	nm	nm
i-Pentane (C_5H_{12})	nm	nm	nm	nm	1.96	nm	nm	nm	nm	nm	nm
n-Pentane (C_5H_{12})	nm	nm	nm	nm	0.585	nm	nm	nm	nm	nm	nm
1-Pentene (C_5H_{10})	nm	nm	nm	nm	0.201	nm	nm	nm	nm	nm	nm
trans-2-Pentene (C_5H_{10})	nm	nm	nm	nm	0.278	nm	nm	nm	nm	nm	nm
cis-2-Pentene (C_5H_{10})	nm	nm	nm	nm	0.130	nm	nm	nm	nm	nm	nm
3-Methyl-1-butene (C_5H_{10})	nm	nm	nm	nm	7.71E-02	nm	nm	nm	nm	nm	nm
1,2-Propadiene (C_3H_4)	nm	nm	nm	nm	0.299	nm	nm	nm	nm	nm	nm
Propyne (C_3H_4)	nm	nm	nm	nm	0.412	nm	nm	nm	nm	nm	nm
1-Butyne (C_4H_6)	nm	nm	nm	nm	3.48E-02	nm	nm	nm	nm	nm	nm
2-Butyne (C_4H_6)	nm	nm	nm	nm	3.40E-02	nm	nm	nm	nm	nm	nm
n-Hexane (C_6H_{14})	nm	nm	nm	nm	0.490	nm	nm	nm	nm	nm	nm
n-Heptane (C_7H_{16})	nm	nm	nm	nm	0.580	nm	nm	nm	nm	nm	nm
n-Octane (C_8H_{18})	nm	nm	nm	nm	0.482	nm	nm	nm	nm	nm	nm
n-Nonane (C_9H_{20})	nm	nm	nm	nm	0.227	nm	nm	nm	nm	nm	nm
n-Decane ($C_{10}H_{22)}$	nm	nm	nm	nm	9.59E-02	nm	nm	nm	nm	nm	nm
2,3-Dimethylbutane (C_6H_{14})	nm	nm	nm	nm	0.279	nm	nm	nm	nm	nm	nm
2-Methylpentane (C_6H_{14})	nm	nm	nm	nm	0.754	nm	nm	nm	nm	nm	nm
3-Methylpentane (C_6H_{14})	nm	nm	nm	nm	0.441	nm	nm	nm	nm	nm	nm
2,2,4-Trimethylpentane (C_8H_{18})	nm	nm	nm	nm	0.215	nm	nm	nm	nm	nm	nm
Cyclopentane (C_5H_{10})	nm	nm	nm	nm	0.117	nm	nm	nm	nm	nm	nm
Cyclohexane (C_6H_{12})	nm	nm	nm	nm	0.536	nm	nm	nm	nm	nm	nm
Methylcyclohexane (C_7H_{14})	nm	nm	nm	nm	0.387	nm	nm	nm	nm	nm	nm
Benzene (C_6H_6)	nm	nm	nm	nm	2.10	nm	nm	nm	nm	nm	nm
Toluene (C_7H_8)	nm	nm	nm	nm	5.29	nm	nm	nm	nm	nm	nm
Ethylbenzene (C_8H_{10})	nm	nm	nm	nm	1.36	nm	nm	nm	nm	nm	nm
m/p-Xylene (C_8H_{10})	nm	nm	nm	nm	4.76	nm	nm	nm	nm	nm	nm
o-Xylene (C_8H_{10})	nm	nm	nm	nm	1.63	nm	nm	nm	nm	nm	nm
Styrene (C_8H_8)	nm	nm	nm	nm	0.131	nm	nm	nm	nm	nm	nm

i-Propylbenzene (C_9H_{12})	nm	nm	nm	nm	5.64E-02	nm	nm	nm	nm	nm	nm
n-Propylbenzene (C_9H_{12})	nm	nm	nm	nm	0.178	nm	nm	nm	nm	nm	nm
3-Ethyltoluene (C_9H_{12})	nm	nm	nm	nm	0.940	nm	nm	nm	nm	nm	nm
4-Ethyltoluene (C_9H_{12})	nm	nm	nm	nm	0.442	nm	nm	nm	nm	nm	nm
2-Ethyltoluene (C_9H_{12})	nm	nm	nm	nm	0.274	nm	nm	nm	nm	nm	nm
1,3,5-Trimethylbenzene (C_9H_{12})	nm	nm	nm	nm	0.389	nm	nm	nm	nm	nm	nm
1,2,4-Trimethylbenzene (C_9H_{12})	nm	nm	nm	nm	0.929	nm	nm	nm	nm	nm	nm
1,2,3-Trimethylbenzene (C_9H_{12})	nm	nm	nm	nm	0.259	nm	nm	nm	nm	nm	nm
alpha-Pinene ($C_{10}H_{16}$)	nm	nm	nm	nm	5.35E-03	nm	nm	nm	nm	nm	nm
beta-Pinene ($C_{10}H_{16}$)	nm	nm	nm	nm	bdl	nm	nm	nm	nm	nm	nm
Ethanol (C_2H_6O)	nm	nm	nm	nm	0.211	nm	nm	nm	nm	nm	nm
Acetaldehyde (C_2H_4O)	nm	nm	nm	nm	0.817	nm	nm	nm	nm	nm	nm
Acetone (C_3H_6O)	nm	nm	nm	nm	1.11	nm	nm	nm	nm	nm	nm
Butanal (C_4H_8O)	nm	nm	nm	nm	6.22E-02	nm	nm	nm	nm	nm	nm
Butanone (C_4H_8O)	nm	nm	nm	nm	2.32E-03	nm	nm	nm	nm	nm	nm

Table S7. The average emission factors (g/kg) for agricultural diesel irrigation pumps sampled by FTIR and WAS-only EFs for a likely gasoline-powered irrigation pump

Compound (Formula)	**EF Agricultural pumps** Avg (stdev)	**EF surface water pump-** likely gasoline powered
Method	FTIR	WAS
Date	23-Apr	6-Jun
MCE	0.992	0.337
Carbon Dioxide (CO_2)	3132(41)	999
Carbon Monoxide (CO)	16.7(13.2)	1253
Methane (CH_4)	2.61(1.69)	10.3
Acetylene (C_2H_2)	0.246(0.237)	16.6
Ethylene (C_2H_4)	3.42(2.75)	6.10
Propylene (C_3H_6)	1.14(1.01)	3.01
Formaldehyde (HCHO)	0.280(0.320)	nm
Methanol (CH_3OH)	2.08E-2(2.13E-2)	0.143
Formic Acid (HCOOH)	bdl	nm
Acetic Acid (CH_3COOH)	bdl	nm
Glycolaldehyde ($C_2H_4O_2$)	bdl	nm
Furan (C_4H_4O)	bdl	nm
Hydroxyacetone ($C_3H_6O_2$)	bdl	nm
Phenol (C_6H_5OH)	0.283(0.235)	nm
1,3-Butadiene (C_4H_6)	0.501(0.435)	1.01
Isoprene (C_5H_8)	1.74E-2(2.69E-3)	0.518
Ammonia (NH_3)	5.29E-3(5.62E-3)	nm
Hydrogen Cyanide (HCN)	0.118(0.099)	nm
Nitrous Acid (HONO)	0.347(0.001)	nm
Sulfur Dioxide (SO_2)	bdl	nm
Hydrogen Fluoride (HF)	bdl	nm
Hydrogen chloride (HCl)	bdl	nm
Nitric Oxide (NO)	10.6(7.5)	nm
Nitrogen Dioxide (NO_2)	1.69(0.70)	nm
Carbonyl sulfide (OCS)	nm	8.61E-02
DMS (C_2H_6S)	nm	3.51E-04
Chloromethane (CH_3Cl)	nm	-
Bromomethane (CH_3Br)	nm	-
Methyl iodide (CH_3I)	nm	1.17E-05
1,2-Dichloroethene ($C_2H_2Cl_2$)	nm	1.43E-03
Methyl nitrate (CH_3NO_3)	nm	4.88E-04
Ethane (C_2H_6)	nm	0.550
Propane (C_3H_8)	nm	8.64E-02
i-Butane (C_4H_{10})	nm	8.08E-03
n-Butane (C_4H_{10})	nm	1.45E-02
1-Butene (C_4H_8)	nm	0.693
i-Butene (C_4H_8)	nm	0.511
trans-2-Butene (C_4H_8)	nm	0.128
cis-2-Butene (C_4H_8)	nm	0.098
i-Pentane (C_5H_{12})	nm	0.105
n-Pentane (C_5H_{12})	nm	3.31E-02
1-Pentene (C_5H_{10})	nm	0.300

trans-2-Pentene (C_5H_{10})	nm	8.48E-02
cis-2-Pentene (C_5H_{10})	nm	4.62E-02
3-Methyl-1-butene (C_5H_{10})	nm	8.41E-02
1,2-Propadiene (C_3H_4)	nm	0.151
Propyne (C_3H_4)	nm	0.230
1-Butyne (C_4H_6)	nm	1.87E-02
2-Butyne (C_4H_6)	nm	2.39E-02
n-Hexane (C_6H_{14})	nm	1.37E-02
n-Heptane (C_7H_{16})	nm	5.54E-02
n-Octane (C_8H_{18})	nm	0.134
n-Nonane (C_9H_{20})	nm	0.539
n-Decane ($C_{10}H_{22)}$	nm	0.802
2,3-Dimethylbutane (C_6H_{14})	nm	1.19E-02
2-Methylpentane (C_6H_{14})	nm	2.38E-02
3-Methylpentane (C_6H_{14})	nm	bdl
2,2,4-Trimethylpentane (C_8H_{18})	nm	bdl
Cyclopentane (C_5H_{10})	nm	4.33E-03
Cyclohexane (C_6H_{12})	nm	3.35E-02
Methylcyclohexane (C_7H_{14})	nm	6.87E-02
Benzene (C_6H_6)	nm	1.21
Toluene (C_7H_8)	nm	0.593
Ethylbenzene (C_8H_{10})	nm	0.224
m/p-Xylene (C_8H_{10})	nm	0.761
o-Xylene (C_8H_{10})	nm	0.453
Styrene (C_8H_8)	nm	0.171
i-Propylbenzene (C_9H_{12})	nm	2.44E-02
n-Propylbenzene (C_9H_{12})	nm	4.22E-02
3-Ethyltoluene (C_9H_{12})	nm	0.180
4-Ethyltoluene (C_9H_{12})	nm	9.08E-02
2-Ethyltoluene (C_9H_{12})	nm	8.45E-02
1,3,5-Trimethylbenzene (C_9H_{12})	nm	0.137
1,2,4-Trimethylbenzene (C_9H_{12})	nm	0.291
1,2,3-Trimethylbenzene (C_9H_{12})	nm	0.151
alpha-Pinene ($C_{10}H_{16}$)	nm	bdl
beta-Pinene ($C_{10}H_{16}$)	nm	bdl
Ethanol (C_2H_6O)	nm	7.83E-02
Acetaldehyde (C_2H_4O)	nm	0.111
Acetone (C_3H_6O)	nm	0.111
Butanal (C_4H_8O)	nm	7.87E-03
Butanone (C_4H_8O)	nm	2.38E-02

Note: "bdl" indicates below the detection limit; "-" indicates concentrations were not greater than background; "nm" indicates not measured

C-fractions: Gasoline (0.85), Diesel (0.87): source is *Kirchstetter et al.* (1999)

Table S8. Emission factors (g/kg) for all cooking fires

Stove type	**EF 1-pot traditional mudstove** hw-Shorea robusta (Sāl) + 1 other species	**EF 1-pot traditional mudstove** hw- Melia azedarach (Bakaino)	**EF 1-pot traditional mudstove**	**EF Chimney stove**	**EF Envirotek stove**	**EF Forced draft stove**	**EF 3-stone cooking fire**	**EF 1-pot traditional mudstove**
Fuel type	hw	hw	hw	hw	hw	hw	hw	d
Lab/Field Measurement	Field	Field	Lab	Lab	Lab	Lab	Lab	Field
Method	FTIR+WAS	FTIR	FTIR + WAS	FTIR	FTIR	FTIR	FTIR	FTIR
Date Measured	22-Apr	21-Apr	16-Apr	16-Apr	16-Apr	16-Apr	16-Apr	22-Apr
C-fraction[a]	45	45	45	45	45	45	45	35
MCE	0.933	0.914	0.966	0.983	0.984	0.975	0.955	0.908
Carbon Dioxide (CO_2)	1474	1451	1561	1614	1612	1600	1546	1094
Carbon Monoxide (CO)	67.7	86.8	35.2	17.4	17.1	25.6	46.5	70.9
Methane (CH_4)	3.46	6.86	2.06	0.728	0.400	0.498	3.25	6.06
Acetylene (C_2H_2)	0.927	1.16	0.681	0.243	0.136	0.272	0.344	1.09
Ethylene (C_2H_4)	2.53	2.82	1.65	0.452	0.230	0.477	0.816	5.33
Propylene (C_3H_6)	0.394	0.850	0.222	0.116	4.10E-02	6.79E-02	0.317	1.28
Formaldehyde (HCHO)	0.963	1.756	1.05	0.275	0.151	0.452	1.54	2.00
Methanol (CH_3OH)	1.24	2.71	0.728	0.145	0.242	0.252	1.22	2.28
Formic Acid (HCOOH)	9.41E-02	0.147	9.33E-02	3.27E-02	6.95E-02	5.89E-02	1.52E-01	0.252
Acetic Acid (CH_3COOH)	2.16	2.78	1.90	0.398	0.806	0.470	1.81	2.63
Glycolaldehyde ($C_2H_4O_2$)	7.16E-02	0.380	bdl	1.18E-02	0.170	bdl	1.65E-01	0.738
Furan (C_4H_4O)	0.228	0.269	bdl	bdl	4.53E-02	bdl	0.143	0.568
Hydroxyacetone ($C_3H_6O_2$)	1.14	1.30	0.509	0.06	5.31E-02	bdl	0.84	2.73
Phenol (C_6H_5OH)	0.425	0.328	0.280	0.038	bdl	0.119	0.335	1.17
1,3-Butadiene (C_4H_6)	0.256	0.376	0.150	0.056	0.015	0.103	4.68E-02	0.733
Isoprene (C_5H_8)	5.74E-02	bdl	1.03E-02	9.09E-03	bdl	2.35E-02	bdl	0.284
Ammonia (NH_3)	0.508	0.267	8.49E-04	bdl	6.918	bdl	bdl	2.26
Hydrogen Cyanide (HCN)	0.459	0.627	0.345	bdl	4.52E-02	0.215	0.177	1.84
Nitrous Acid (HONO)	0.504	0.517	0.423	0.158	4.73E-02	0.192	0.412	0.113
Sulfur Dioxide (SO_2)	bdl	bdl	bdl	bdl	bdl	bdl	bdl	bdl
Hydrogen Fluoride (HF)	bdl	bdl	bdl	bdl	bdl	bdl	bdl	bdl
Hydrogen chloride (HCl)	bdl	1.86E-02	bdl	8.96E-03	bdl	bdl	0.1391348	bdl
Nitric Oxide (NO)	1.76	0.705	3.63	0.528	2.07	1.21	0.645	1.74
Nitrogen Dioxide (NO_2)	0.377	0.212	1.049	0.617	0.212	0.439	0.778	0.931
Carbonyl sulfide (OCS)	2.69E-02	nm	4.22E-03	nm	nm	nm	nm	nm
DMS (C_2H_6S)	0.510	nm	5.06E-04	nm	nm	nm	nm	nm
Chloromethane (CH_3Cl)	1.22E-02	nm	1.40E-02	nm	nm	nm	nm	nm
Bromomethane (CH_3Br)	7.74E-04	nm	1.39E-04	nm	nm	nm	nm	nm
Methyl iodide (CH_3I)	4.48E-05	nm	8.06E-05	nm	nm	nm	nm	nm
1,2-Dichloroethene ($C_2H_2Cl_2$)	1.45E-04	nm	4.11E-05	nm	nm	nm	nm	nm
Methyl nitrate (CH_3NO_3)	1.10E-02	nm	1.16E-03	nm	nm	nm	nm	nm
Ethane (C_2H_6)	7.43E-02	nm	9.86E-02	nm	nm	nm	nm	nm

Propane (C_3H_8)	0.301	nm	4.10E-02	nm	nm	nm	nm	nm
i-Butane (C_4H_{10})	0.744	nm	2.70E-02	nm	nm	nm	nm	nm
n-Butane (C_4H_{10})	2.16	nm	2.78E-02	nm	nm	nm	nm	nm
1-Butene (C_4H_8)	1.36	nm	3.47E-02	nm	nm	nm	nm	nm
i-Butene (C_4H_8)	1.63	nm	2.37E-02	nm	nm	nm	nm	nm
trans-2-Butene (C_4H_8)	0.110	nm	1.02E-02	nm	nm	nm	nm	nm
cis-2-Butene (C_4H_8)	8.88E-02	nm	8.58E-03	nm	nm	nm	nm	nm
i-Pentane (C_5H_{12})	7.46E-02	nm	3.88E-02	nm	nm	nm	nm	nm
n-Pentane (C_5H_{12})	9.62E-03	nm	1.36E-02	nm	nm	nm	nm	nm
1-Pentene (C_5H_{10})	7.63E-03	nm	8.35E-03	nm	nm	nm	nm	nm
trans-2-Pentene (C_5H_{10})	4.61E-03	nm	6.54E-03	nm	nm	nm	nm	nm
cis-2-Pentene (C_5H_{10})	bdl	nm	3.47E-03	nm	nm	nm	nm	nm
3-Methyl-1-butene (C_5H_{10})	3.34E-03	nm	4.61E-03	nm	nm	nm	nm	nm
1,2-Propadiene (C_3H_4)	1.57E-02	nm	1.24E-02	nm	nm	nm	nm	nm
Propyne (C_3H_4)	4.21E-02	nm	3.42E-02	nm	nm	nm	nm	nm
1-Butyne (C_4H_6)	1.61E-02	nm	3.78E-03	nm	nm	nm	nm	nm
2-Butyne (C_4H_6)	1.49E-02	nm	2.24E-03	nm	nm	nm	nm	nm
n-Hexane (C_6H_{14})	-	nm	7.41E-03	nm	nm	nm	nm	nm
n-Heptane (C_7H_{16})	5.27E-04	nm	7.87E-03	nm	nm	nm	nm	nm
n-Octane (C_8H_{18})	bdl	nm	6.98E-03	nm	nm	nm	nm	nm
n-Nonane (C_9H_{20})	3.47E-03	nm	3.76E-02	nm	nm	nm	nm	nm
n-Decane ($C_{10}H_{22)}$	1.08E-03	nm	5.48E-02	nm	nm	nm	nm	nm
2,3-Dimethylbutane (C_6H_{14})	2.39E-02	nm	2.97E-03	nm	nm	nm	nm	nm
2-Methylpentane (C_6H_{14})	8.38E-04	nm	7.60E-03	nm	nm	nm	nm	nm
3-Methylpentane (C_6H_{14})	2.11E-03	nm	4.59E-03	nm	nm	nm	nm	nm
2,2,4-Trimethylpentane (C_8H_{18})	bdl	nm	bdl	nm	nm	nm	nm	nm
Cyclopentane (C_5H_{10})	bdl	nm	1.62E-03	nm	nm	nm	nm	nm
Cyclohexane (C_6H_{12})	bdl	nm	4.62E-03	nm	nm	nm	nm	nm
Methylcyclohexane (C_7H_{14})	bdl	nm	6.49E-03	nm	nm	nm	nm	nm
Benzene (C_6H_6)	0.912	nm	0.472	nm	nm	nm	nm	nm
Toluene (C_7H_8)	0.129	nm	0.142	nm	nm	nm	nm	nm
Ethylbenzene (C_8H_{10})	1.18E-02	nm	2.87E-02	nm	nm	nm	nm	nm
m/p-Xylene (C_8H_{10})	3.92E-02	nm	6.09E-02	nm	nm	nm	nm	nm
o-Xylene (C_8H_{10})	8.79E-03	nm	2.79E-02	nm	nm	nm	nm	nm
Styrene (C_8H_8)	3.98E-02	nm	5.38E-02	nm	nm	nm	nm	nm
i-Propylbenzene (C_9H_{12})	2.88E-02	nm	2.08E-03	nm	nm	nm	nm	nm
n-Propylbenzene (C_9H_{12})	2.90E-02	nm	2.67E-03	nm	nm	nm	nm	nm
3-Ethyltoluene (C_9H_{12})	3.00E-02	nm	8.95E-03	nm	nm	nm	nm	nm
4-Ethyltoluene (C_9H_{12})	2.92E-02	nm	4.92E-03	nm	nm	nm	nm	nm
2-Ethyltoluene (C_9H_{12})	2.92E-02	nm	5.14E-03	nm	nm	nm	nm	nm
1,3,5-Trimethylbenzene (C_9H_{12})	-	nm	8.56E-03	nm	nm	nm	nm	nm
1,2,4-Trimethylbenzene (C_9H_{12})	8.48E-04	nm	1.36E-02	nm	nm	nm	nm	nm

1,2,3-Trimethylbenzene (C_9H_{12})	-	nm	8.63E-03	nm	nm	nm	nm	nm
alpha-Pinene ($C_{10}H_{16}$)	3.66E-02	nm	1.50E-03	nm	nm	nm	nm	nm
beta-Pinene ($C_{10}H_{16}$)	4.67E-02	nm	bdl	nm	nm	nm	nm	nm
Ethanol (C_2H_6O)	0.140	nm	4.65E-02	nm	nm	nm	nm	nm
Acetaldehyde (C_2H_4O)	0.797	nm	0.114	nm	nm	nm	nm	nm
Acetone (C_3H_6O)	0.705	nm	0.137	nm	nm	nm	nm	nm
Butanal (C_4H_8O)	1.27E-02	nm	1.54E-03	nm	nm	nm	nm	nm
Butanone (C_4H_8O)	0.434	nm	1.21E-02	nm	nm	nm	nm	nm
BC	0.310	0.131	0.323	0.169	0.676	0.107	0.098	6.40E-02
BrC	12.572	4.618	0.806	0.770	1.661	0.858	1.223	6.71
EF Babs 405 (m^2/kg)	15.425	5.863	4.074	2.478	8.515	1.932	2.191	7.23
EF Bscat 405 (m2/kg)	57.225	23.520	3.299	4.000	4.053	6.356	9.458	45.4
EF Babs 870 (m2/kg)	1.466	0.623	1.529	0.802	3.206	0.508	0.462	0.304
EF Bscat 870 (m2/kg)	1.878	1.148	0.502	1.083	0.495	0.688	1.125	0.693
EF Babs 405 just BrC (m2/kg)	12.276	4.525	0.790	0.754	1.628	0.841	1.198	6.57
EF Babs 405 just BC (m2/kg)	3.149	1.337	3.284	1.723	6.887	1.091	0.993	0.652
SSA 870	0.562	0.648	0.247	0.574	0.134	0.575	0.709	0.695
SSA 405	0.788	0.800	0.447	0.618	0.322	0.767	0.812	0.863
AAE	3.078	2.933	1.282	1.475	1.277	1.747	2.035	4.15

Table S8. Continued

Stove type	**EF 1-pot traditional mudstove**	**EF 3-stone cooking fire**	**EF 1-pot traditional mudstove**	**EF 1-pot traditional mudstove**	**EF 1-pot traditional mudstove**	**EFChimney stove**	**EF Chimney stove**	**EF Envirotek stove**
Fuel type	d	d	d+hw for ignition	hw+d	d+t	d+hw	d+t	d+hw
Lab/Field Measurement	Lab	Lab	Field	Lab	Lab	Lab	Lab	Lab
Method	FTIR+WAS	FTIR	FTIR+WAS	FTIR+WAS	FTIR+WAS	FTIR	FTIR	FTIR
Date Measured	16-Apr	16-Apr	22-Apr	16-Apr	16-Apr	16-Apr	16-Apr	16-Apr
C-fraction[a]	0.35	0.35	0.4	0.4	0.4	0.4	0.4	0.4
MCE	0.956	0.964	0.912	0.976	0.980	0.965	0.957	0.971
Carbon Dioxide (CO_2)	1193	1208	1221	1410	1423	1398	1377	1404
Carbon Monoxide (CO)	35.0	28.5	75.1	22.4	18.4	32.1	39.1	26.3
Methane (CH_4)	1.37	1.23	7.35	1.75	1.32	1.69	1.55	1.79
Acetylene (C_2H_2)	0.199	0.183	1.03	0.316	0.567	0.469	0.283	0.461
Ethylene (C_2H_4)	0.736	0.793	5.70	0.819	8.44E-02	1.32	0.849	1.04
Propylene (C_3H_6)	0.355	0.431	1.13	0.203	0.204	0.326	0.308	0.274
Formaldehyde (HCHO)	0.569	0.864	1.54	0.271	9.35E-02	0.473	0.500	0.413
Methanol (CH_3OH)	0.312	0.720	2.23	0.159	0.329	0.223	0.520	0.325
Formic Acid (HCOOH)	6.05E-02	0.162	0.145	2.91E-02	4.45E-02	5.44E-02	4.92E-02	4.97E-02
Acetic Acid (CH_3COOH)	3.32	2.34	2.59	1.10	0.755	0.789	1.23	0.580
Glycolaldehyde ($C_2H_4O_2$)	bdl	0.130	0.213	bdl	8.51E-02	bdl	bdl	bdl
Furan (C_4H_4O)	0.148	0.138	0.312	2.94E-02	3.96E-02	7.62E-02	8.29E-02	3.72E-02

Hydroxyacetone ($C_3H_6O_2$)	0.719	1.27	1.11	0.215	0.256	8.09E-02	0.145	9.28E-02
Phenol (C_6H_5OH)	0.290	0.212	0.762	0.156	4.45E-02	8.50E-02	7.74E-02	0.225
1,3-Butadiene (C_4H_6)	7.37E-02	0.1033215	0.621	8.19E-02	9.66E-02	0.165	0.105	0.105
Isoprene (C_5H_8)	0.226	1.05E-02	7.98E-02	5.76E-02	2.49E-03	1.06E-02	bdl	3.29E-03
Ammonia (NH_3)	0.391	0.412	3.46	8.99E-02	6.96E-02	6.46E-03	5.72E-03	5.01E-03
Hydrogen Cyanide (HCN)	0.459	0.738	1.26	0.438	0.165	bdl	4.33	0.486
Nitrous Acid (HONO)	0.285	0.392	0.279	0.258	0.179	0.294	0.350	0.193
Sulfur Dioxide (SO_2)	bdl	bdl	bdl	bdl	bdl	bdl	bdl	bdl
Hydrogen Fluoride (HF)	bdl	bdl	bdl	bdl	bdl	bdl	bdl	bdl
Hydrogen chloride (HCl)	3.67E-02	1.21E-02	1.53E-02	1.05E-02	6.52E-02	4.90E-03	4.06E-03	bdl
Nitric Oxide (NO)	3.47	3.59	1.23	3.32	3.35	3.08	2.65	2.88
Nitrogen Dioxide (NO_2)	1.017	1.60	0.248	0.887	0.872	0.896	0.912	0.504
Carbonyl sulfide (OCS)	4.81E-02	nm	6.09E-02	1.72E-02	5.31E-03	nm	nm	nm
DMS (C_2H_6S)	4.97E-03	nm	2.31E-02	2.14E-04	1.65E-04	nm	nm	nm
Chloromethane (CH_3Cl)	0.550	nm	0.521	0.164	4.22E-02	nm	nm	nm
Bromomethane (CH_3Br)	6.57E-04	nm	7.47E-03	2.30E-04	7.87E-05	nm	nm	nm
Methyl iodide (CH_3I)	1.16E-04	nm	3.13E-04	5.09E-05	2.94E-05	nm	nm	nm
1,2-Dichloroethene ($C_2H_2Cl_2$)	1.02E-03	nm	-	2.53E-04	1.70E-04	nm	nm	nm
Methyl nitrate (CH_3NO_3)	5.82E-03	nm	8.61E-04	7.47E-03	2.93E-03	nm	nm	nm
Ethane (C_2H_6)	0.264	nm	0.863	6.05E-02	8.66E-02	nm	nm	nm
Propane (C_3H_8)	0.114	nm	0.360	3.15E-02	2.07E-02	nm	nm	nm
i-Butane (C_4H_{10})	6.24E-02	nm	0.126	9.08E-03	5.44E-03	nm	nm	nm
n-Butane (C_4H_{10})	7.23E-02	nm	0.222	1.27E-02	7.23E-03	nm	nm	nm
1-Butene (C_4H_8)	0.130	nm	0.166	3.84E-02	2.22E-02	nm	nm	nm
i-Butene (C_4H_8)	7.08E-02	nm	0.217	1.97E-02	1.14E-02	nm	nm	nm
trans-2-Butene (C_4H_8)	2.95E-02	nm	0.158	8.91E-03	6.50E-03	nm	nm	nm
cis-2-Butene (C_4H_8)	2.34E-02	nm	9.09E-02	6.52E-03	4.64E-03	nm	nm	nm
i-Pentane (C_5H_{12})	0.110	nm	1.08	1.21E-02	1.02E-02	nm	nm	nm
n-Pentane (C_5H_{12})	2.10E-03	nm	0.370	6.13E-03	9.21E-04	nm	nm	nm
1-Pentene (C_5H_{10})	4.69E-02	nm	0.108	1.53E-02	5.61E-03	nm	nm	nm
trans-2-Pentene (C_5H_{10})	1.86E-02	nm	0.140	4.93E-03	4.00E-03	nm	nm	nm
cis-2-Pentene (C_5H_{10})	9.45E-03	nm	5.67E-02	2.31E-03	1.99E-03	nm	nm	nm
3-Methyl-1-butene (C_5H_{10})	1.65E-02	nm	3.10E-02	4.95E-03	2.85E-03	nm	nm	nm
1,2-Propadiene (C_3H_4)	2.45E-02	nm	2.37E-02	7.43E-03	4.90E-03	nm	nm	nm
Propyne (C_3H_4)	5.79E-02	nm	6.12E-02	2.17E-02	1.43E-02	nm	nm	nm
1-Butyne (C_4H_6)	6.69E-03	nm	1.32E-02	2.53E-03	1.75E-03	nm	nm	nm
2-Butyne (C_4H_6)	5.14E-03	nm	1.21E-02	1.18E-03	9.64E-04	nm	nm	nm
n-Hexane (C_6H_{14})	2.37E-02	nm	0.466	4.00E-03	2.43E-03	nm	nm	nm
n-Heptane (C_7H_{16})	1.33E-02	nm	0.163	3.50E-03	9.97E-04	nm	nm	nm
n-Octane (C_8H_{18})	8.35E-03	nm	5.46E-02	1.80E-03	3.22E-04	nm	nm	nm
n-Nonane (C_9H_{20})	1.33E-02	nm	2.88E-02	6.83E-03	2.58E-03	nm	nm	nm
n-Decane ($C_{10}H_{22)}$	1.55E-02	nm	1.86E-02	1.14E-02	2.19E-03	nm	nm	nm
2,3-Dimethylbutane (C_6H_{14})	7.82E-03	nm	0.186	1.07E-03	7.64E-04	nm	nm	nm

2-Methylpentane (C_6H_{14})	1.96E-02	nm	0.367	2.65E-03	1.88E-03	nm	nm	nm
3-Methylpentane (C_6H_{14})	1.19E-02	nm	0.252	bdl	8.71E-04	nm	nm	nm
2,2,4-Trimethylpentane (C_8H_{18})	9.05E-03	nm	0.157	2.54E-03	bdl	nm	nm	nm
Cyclopentane (C_5H_{10})	4.05E-03	nm	0.271	6.34E-04	3.72E-04	nm	nm	nm
Cyclohexane (C_6H_{12})	8.88E-03	nm	0.404	9.25E-04	bdl	nm	nm	nm
Methylcyclohexane (C_7H_{14})	4.03E-03	nm	7.57E-02	8.17E-04	1.30E-04	nm	nm	nm
Benzene (C_6H_6)	0.468	nm	1.64	0.256	0.117	nm	nm	nm
Toluene (C_7H_8)	0.266	nm	1.22	8.23E-02	4.43E-02	nm	nm	nm
Ethylbenzene (C_8H_{10})	6.26E-02	nm	0.426	1.91E-02	1.23E-02	nm	nm	nm
m/p-Xylene (C_8H_{10})	8.07E-02	nm	0.809	2.77E-02	1.84E-02	nm	nm	nm
o-Xylene (C_8H_{10})	3.48E-02	nm	0.287	1.30E-02	8.00E-03	nm	nm	nm
Styrene (C_8H_8)	3.91E-02	nm	0.320	5.46E-04	1.90E-04	nm	nm	nm
i-Propylbenzene (C_9H_{12})	1.82E-03	nm	2.86E-02	8.70E-04	4.98E-04	nm	nm	nm
n-Propylbenzene (C_9H_{12})	4.24E-03	nm	4.12E-02	1.61E-03	7.67E-04	nm	nm	nm
3-Ethyltoluene (C_9H_{12})	8.06E-03	nm	7.29E-02	3.89E-03	2.14E-03	nm	nm	nm
4-Ethyltoluene (C_9H_{12})	4.81E-03	nm	4.81E-02	2.47E-03	1.40E-03	nm	nm	nm
2-Ethyltoluene (C_9H_{12})	5.00E-03	nm	4.33E-02	2.21E-03	1.18E-03	nm	nm	nm
1,3,5-Trimethylbenzene (C_9H_{12})	2.47E-03	nm	2.38E-02	2.40E-03	8.24E-04	nm	nm	nm
1,2,4-Trimethylbenzene (C_9H_{12})	5.64E-03	nm	5.08E-02	4.06E-03	2.25E-03	nm	nm	nm
1,2,3-Trimethylbenzene (C_9H_{12})	4.18E-03	nm	2.64E-02	3.01E-03	9.16E-04	nm	nm	nm
alpha-Pinene ($C_{10}H_{16}$)	7.78E-04	nm	0.692	5.18E-04	bdl	nm	nm	nm
beta-Pinene ($C_{10}H_{16}$)	bdl	nm	0.471	bdl	bdl	nm	nm	nm
Ethanol (C_2H_6O)	3.01E-02	nm	0.980	1.07E-02	7.80E-03	nm	nm	nm
Acetaldehyde (C_2H_4O)	0.622	nm	0.724	0.220	9.28E-02	nm	nm	nm
Acetone (C_3H_6O)	0.389	nm	1.36	0.946	0.113	nm	nm	nm
Butanal (C_4H_8O)	1.43E-02	nm	3.85E-02	3.44E-03	3.03E-03	nm	nm	nm
Butanone (C_4H_8O)	6.95E-02	nm	0.185	2.52E-02	1.54E-02	nm	nm	nm
BC	5.79E-02	1.05E-01	nm	8.19E-02	8.64E-02	0.181	0.130	0.491
BrC	1.076	7.60	nm	1.20	2.07	2.23	2.59	7.12
EF Babs 405 (m^2/kg)	1.64	8.52	nm	2.01	2.91	4.03	3.86	11.975495
EF Bscat 405 (m2/kg)	16.6	136	nm	5.06	18.0	17.5	41.4	42.3
EF Babs 870 (m2/kg)	0.275	0.499	nm	0.388	0.410	0.856	0.616	2.33
EF Bscat 870 (m2/kg)	2.44	12.2	nm	0.749	1.75	1.27	3.96	4.45
EF Babs 405 just BrC (m2/kg)	1.055	7.45	nm	1.18	2.03	2.19	2.54	6.98
EF Babs 405 just BC (m2/kg)	0.590	1.07	nm	0.833	0.880	1.84	1.32	5.00
SSA 870	0.899	0.961	nm	0.659	0.810	0.597	0.865	0.657
SSA 405	0.910	0.941	nm	0.715	0.861	0.813	0.915	0.779
AAE	2.34	3.71	nm	2.15	2.56	2.03	2.40	2.14

Table S8. Continued

Stove type	EF 1-pot traditional mudstove	EF 3-stone cooking fire	EF 1-pot traditional mudstove	EF 1-pot traditional mudstove	EF 1-pot traditional mudstove	EFChimney stove	EF Chimney stove	EF Envirotek stove
Fuel type	d	d	d+hw for ignition	hw+d	d+t	d+hw	d+t	d+hw
Lab/Field Measurement	Lab	Lab	Field	Lab	Lab	Lab	Lab	Lab
Method	FTIR+WAS	FTIR	FTIR+WAS	FTIR+WAS	FTIR+WAS	FTIR	FTIR	FTIR
Date Measured	16-Apr	16-Apr	22-Apr	16-Apr	16-Apr	16-Apr	16-Apr	16-Apr
C-fraction[a]	0.35	0.35	0.4	0.4	0.4	0.4	0.4	0.4
MCE	0.956	0.964	0.912	0.976	0.980	0.965	0.957	0.971
Carbon Dioxide (CO_2)	1193	1208	1221	1410	1423	1398	1377	1404
Carbon Monoxide (CO)	35.0	28.5	75.1	22.4	18.4	32.1	39.1	26.3
Methane (CH_4)	1.37	1.23	7.35	1.75	1.32	1.69	1.55	1.79
Acetylene (C_2H_2)	0.199	0.183	1.03	0.316	0.567	0.469	0.283	0.461
Ethylene (C_2H_4)	0.736	0.793	5.70	0.819	8.44E-02	1.32	0.849	1.04
Propylene (C_3H_6)	0.355	0.431	1.13	0.203	0.204	0.326	0.308	0.274
Formaldehyde (HCHO)	0.569	0.864	1.54	0.271	9.35E-02	0.473	0.500	0.413
Methanol (CH_3OH)	0.312	0.720	2.23	0.159	0.329	0.223	0.520	0.325
Formic Acid (HCOOH)	6.05E-02	0.162	0.145	2.91E-02	4.45E-02	5.44E-02	4.92E-02	4.97E-02
Acetic Acid (CH_3COOH)	3.32	2.34	2.59	1.10	0.755	0.789	1.23	0.580
Glycolaldehyde ($C_2H_4O_2$)	bdl	0.130	0.213	bdl	8.51E-02	bdl	bdl	bdl
Furan (C_4H_4O)	0.148	0.138	0.312	2.94E-02	3.96E-02	7.62E-02	8.29E-02	3.72E-02
Hydroxyacetone ($C_3H_6O_2$)	0.719	1.27	1.11	0.215	0.256	8.09E-02	0.145	9.28E-02
Phenol (C_6H_5OH)	0.290	0.212	0.762	0.156	4.45E-02	8.50E-02	7.74E-02	0.225
1,3-Butadiene (C_4H_6)	7.37E-02	0.1033215	0.621	8.19E-02	9.66E-02	0.165	0.105	0.105
Isoprene (C_5H_8)	0.226	1.05E-02	7.98E-02	5.76E-02	2.49E-03	1.06E-02	bdl	3.29E-03
Ammonia (NH_3)	0.391	0.412	3.46	8.99E-02	6.96E-02	6.46E-03	5.72E-03	5.01E-03
Hydrogen Cyanide (HCN)	0.459	0.738	1.26	0.438	0.165	bdl	4.33	0.486
Nitrous Acid (HONO)	0.285	0.392	0.279	0.258	0.179	0.294	0.350	0.193
Sulfur Dioxide (SO_2)	bdl	bdl	bdl	bdl	bdl	bdl	bdl	bdl
Hydrogen Fluoride (HF)	bdl	bdl	bdl	bdl	bdl	bdl	bdl	bdl
Hydrogen chloride (HCl)	3.67E-02	1.21E-02	1.53E-02	1.05E-02	6.52E-02	4.90E-03	4.06E-03	bdl
Nitric Oxide (NO)	3.47	3.59	1.23	3.32	3.35	3.08	2.65	2.88
Nitrogen Dioxide (NO_2)	1.017	1.60	0.248	0.887	0.872	0.896	0.912	0.504
Carbonyl sulfide (OCS)	4.81E-02	nm	6.09E-02	1.72E-02	5.31E-03	nm	nm	nm
DMS (C_2H_6S)	4.97E-03	nm	2.31E-02	2.14E-04	1.65E-04	nm	nm	nm
Chloromethane (CH_3Cl)	0.550	nm	0.521	0.164	4.22E-02	nm	nm	nm
Bromomethane (CH_3Br)	6.57E-04	nm	7.47E-03	2.30E-04	7.87E-05	nm	nm	nm
Methyl iodide (CH_3I)	1.16E-04	nm	3.13E-04	5.09E-05	2.94E-05	nm	nm	nm
1,2-Dichloroethene ($C_2H_2Cl_2$)	1.02E-03	nm	-	2.53E-04	1.70E-04	nm	nm	nm
Methyl nitrate (CH_3NO_3)	5.82E-03	nm	8.61E-04	7.47E-03	2.93E-03	nm	nm	nm
Ethane (C_2H_6)	0.264	nm	0.863	6.05E-02	8.66E-02	nm	nm	nm
Propane (C_3H_8)	0.114	nm	0.360	3.15E-02	2.07E-02	nm	nm	nm

i-Butane (C_4H_{10})	6.24E-02	nm	0.126	9.08E-03	5.44E-03	nm	nm	nm
n-Butane (C_4H_{10})	7.23E-02	nm	0.222	1.27E-02	7.23E-03	nm	nm	nm
1-Butene (C_4H_8)	0.130	nm	0.166	3.84E-02	2.22E-02	nm	nm	nm
i-Butene (C_4H_8)	7.08E-02	nm	0.217	1.97E-02	1.14E-02	nm	nm	nm
trans-2-Butene (C_4H_8)	2.95E-02	nm	0.158	8.91E-03	6.50E-03	nm	nm	nm
cis-2-Butene (C_4H_8)	2.34E-02	nm	9.09E-02	6.52E-03	4.64E-03	nm	nm	nm
i-Pentane (C_5H_{12})	0.110	nm	1.08	1.21E-02	1.02E-02	nm	nm	nm
n-Pentane (C_5H_{12})	2.10E-03	nm	0.370	6.13E-03	9.21E-04	nm	nm	nm
1-Pentene (C_5H_{10})	4.69E-02	nm	0.108	1.53E-02	5.61E-03	nm	nm	nm
trans-2-Pentene (C_5H_{10})	1.86E-02	nm	0.140	4.93E-03	4.00E-03	nm	nm	nm
cis-2-Pentene (C_5H_{10})	9.45E-03	nm	5.67E-02	2.31E-03	1.99E-03	nm	nm	nm
3-Methyl-1-butene (C_5H_{10})	1.65E-02	nm	3.10E-02	4.95E-03	2.85E-03	nm	nm	nm
1,2-Propadiene (C_3H_4)	2.45E-02	nm	2.37E-02	7.43E-03	4.90E-03	nm	nm	nm
Propyne (C_3H_4)	5.79E-02	nm	6.12E-02	2.17E-02	1.43E-02	nm	nm	nm
1-Butyne (C_4H_6)	6.69E-03	nm	1.32E-02	2.53E-03	1.75E-03	nm	nm	nm
2-Butyne (C_4H_6)	5.14E-03	nm	1.21E-02	1.18E-03	9.64E-04	nm	nm	nm
n-Hexane (C_6H_{14})	2.37E-02	nm	0.466	4.00E-03	2.43E-03	nm	nm	nm
n-Heptane (C_7H_{16})	1.33E-02	nm	0.163	3.50E-03	9.97E-04	nm	nm	nm
n-Octane (C_8H_{18})	8.35E-03	nm	5.46E-02	1.80E-03	3.22E-04	nm	nm	nm
n-Nonane (C_9H_{20})	1.33E-02	nm	2.88E-02	6.83E-03	2.58E-03	nm	nm	nm
n-Decane ($C_{10}H_{22)}$	1.55E-02	nm	1.86E-02	1.14E-02	2.19E-03	nm	nm	nm
2,3-Dimethylbutane (C_6H_{14})	7.82E-03	nm	0.186	1.07E-03	7.64E-04	nm	nm	nm
2-Methylpentane (C_6H_{14})	1.96E-02	nm	0.367	2.65E-03	1.88E-03	nm	nm	nm
3-Methylpentane (C_6H_{14})	1.19E-02	nm	0.252	bdl	8.71E-04	nm	nm	nm
2,2,4-Trimethylpentane (C_8H_{18})	9.05E-03	nm	0.157	2.54E-03	bdl	nm	nm	nm
Cyclopentane (C_5H_{10})	4.05E-03	nm	0.271	6.34E-04	3.72E-04	nm	nm	nm
Cyclohexane (C_6H_{12})	8.88E-03	nm	0.404	9.25E-04	bdl	nm	nm	nm
Methylcyclohexane (C_7H_{14})	4.03E-03	nm	7.57E-02	8.17E-04	1.30E-04	nm	nm	nm
Benzene (C_6H_6)	0.468	nm	1.64	0.256	0.117	nm	nm	nm
Toluene (C_7H_8)	0.266	nm	1.22	8.23E-02	4.43E-02	nm	nm	nm
Ethylbenzene (C_8H_{10})	6.26E-02	nm	0.426	1.91E-02	1.23E-02	nm	nm	nm
m/p-Xylene (C_8H_{10})	8.07E-02	nm	0.809	2.77E-02	1.84E-02	nm	nm	nm
o-Xylene (C_8H_{10})	3.48E-02	nm	0.287	1.30E-02	8.00E-03	nm	nm	nm
Styrene (C_8H_8)	3.91E-02	nm	0.320	5.46E-04	1.90E-04	nm	nm	nm
i-Propylbenzene (C_9H_{12})	1.82E-03	nm	2.86E-02	8.70E-04	4.98E-04	nm	nm	nm
n-Propylbenzene (C_9H_{12})	4.24E-03	nm	4.12E-02	1.61E-03	7.67E-04	nm	nm	nm
3-Ethyltoluene (C_9H_{12})	8.06E-03	nm	7.29E-02	3.89E-03	2.14E-03	nm	nm	nm
4-Ethyltoluene (C_9H_{12})	4.81E-03	nm	4.81E-02	2.47E-03	1.40E-03	nm	nm	nm
2-Ethyltoluene (C_9H_{12})	5.00E-03	nm	4.33E-02	2.21E-03	1.18E-03	nm	nm	nm
1,3,5-Trimethylbenzene (C_9H_{12})	2.47E-03	nm	2.38E-02	2.40E-03	8.24E-04	nm	nm	nm
1,2,4-Trimethylbenzene (C_9H_{12})	5.64E-03	nm	5.08E-02	4.06E-03	2.25E-03	nm	nm	nm
1,2,3-Trimethylbenzene (C_9H_{12})	4.18E-03	nm	2.64E-02	3.01E-03	9.16E-04	nm	nm	nm

alpha-Pinene ($C_{10}H_{16}$)	7.78E-04	nm	0.692	5.18E-04	bdl	nm	nm	nm
beta-Pinene ($C_{10}H_{16}$)	bdl	nm	0.471	bdl	bdl	nm	nm	nm
Ethanol (C_2H_6O)	3.01E-02	nm	0.980	1.07E-02	7.80E-03	nm	nm	nm
Acetaldehyde (C_2H_4O)	0.622	nm	0.724	0.220	9.28E-02	nm	nm	nm
Acetone (C_3H_6O)	0.389	nm	1.36	0.946	0.113	nm	nm	nm
Butanal (C_4H_8O)	1.43E-02	nm	3.85E-02	3.44E-03	3.03E-03	nm	nm	nm
Butanone (C_4H_8O)	6.95E-02	nm	0.185	2.52E-02	1.54E-02	nm	nm	nm
BC	5.79E-02	1.05E-01	nm	8.19E-02	8.64E-02	0.181	0.130	0.491
BrC	1.076	7.60	nm	1.20	2.07	2.23	2.59	7.12
EF Babs 405 (m^2/kg)	1.64	8.52	nm	2.01	2.91	4.03	3.86	12.0
EF Bscat 405 (m2/kg)	16.6	136	nm	5.06	18.0	17.5	41.4	42.3
EF Babs 870 (m2/kg)	0.275	0.499	nm	0.388	0.410	0.856	0.616	2.33
EF Bscat 870 (m2/kg)	2.44	12.2	nm	0.749	1.75	1.27	3.96	4.45
EF Babs 405 just BrC (m2/kg)	1.055	7.45	nm	1.18	2.03	2.19	2.54	6.98
EF Babs 405 just BC (m2/kg)	0.590	1.07	nm	0.833	0.880	1.84	1.32	5.00
SSA 870	0.899	0.961	nm	0.659	0.810	0.597	0.865	0.657
SSA 405	0.910	0.941	nm	0.715	0.861	0.813	0.915	0.779
AAE	2.34	3.71	nm	2.15	2.56	2.03	2.40	2.14